SIMULATION AND MODEL VERIFICATION OF AGRICULTURAL TRACTOR OVERTURNS

A Thesis

Presented to the Faculty of the Graduate School

of Cornell University for the Degree of

Doctor of Philosophy

by

Denny Cecil Davis

August 1973

Gerald E. Rehkugler

SIMULATION AND MODEL VERIFICATION
OF AGRICULTURAL TRACTOR OVERTURNS

Denny Cecil Davis, Ph.D.
Cornell University 1973

Each year about 500 people are killed in tractor overturning accidents in the United States, usually when the tractor operator is pinned and crushed beneath the tractor. Realization that tractor overturns can not always be prevented has led to the development of roll-over protection structures (ROPS) to protect the tractor operator from serious injury or death in the event of an accidental overturn.

With the advent of the ROPS has come the need for testing the structures to assure the tractor operator that he will be protected during a tractor overturn. Many tests have been devised to simulate the loading conditions which the protective structure would be expected to encounter during an overturn, but controversies over the relative severity of the various tests and the severity of each test relative to accidental overturns in practice continue to prevent universal acceptance of any one testing procedure. An improved understanding of tractor motions during overturns is required before the ROPS loading conditions for that overturn may be defined.

A mathematical model is proposed to define the dynamics of a wide-front-end tractor during overturning motions. The model describes the tractor with ten degrees of freedom - six for the tractor body, one each for the rear wheels, one for the front end, and one for the engine rotation - yielding twenty first order ordinary differential equations.

This model uses Euler parameters of the finite angle of rotation to describe the rotational motion of the tractor body, thus allowing large angles of rotation while eliminating problems of equation stability. Engine dynamics, rear wheel coupling, clutching features, and terrain-enveloping tire characteristics make the model adaptable to many overturning situations.

Verification of the mathematical model is provided by comparisons between tractor motions predicted by the mathematical model and those observed during 1/12 scale-model tractor overturns. Ten experimental side overturns of an unpowered tractor were recorded on high-speed film. Replications of two different overturn tests provided evidence that the repeatability of the experimental overturns is more than adequate to justify their use in verifying the mathematical model.

A digital computer program was used to implement the mathematical model and simulate two of those overturns which were analyzed experimentally. Comparisons between the experimental and simulation paths of four tractor-body-fixed reference points throughout the overturns demonstrated the accuracy of the mathematical model in predicting the overturning motion of tractors. The computer program is presented and documented for use by interested researchers.

The digital computer program provides capabilities for conducting parameter studies to determine the effects of tractor and terrain conditions on the overturning motions of wide-front-end or tricycle-type wheel tractors. Energy and momentum information supplied by the program also provides capabilities for examining the energy levels which must be dissipated by roll-over protection structures. The inclusion of external force specification features may encourage future work in the comparison of ROPS testing procedures which restrain or do not restrain the tractor during loading.

BIOGRAPHICAL SKETCH

Denny Cecil Davis was born in Toppenish, Washington, on December 21, 1944. He obtained his undergraduate education at Washington State University, receiving a Bachelor of Science degree in Agricultural Engineering with Distinction in June 1967. He obtained his graduate education at Cornell University, receiving a Master of Science degree in Agricultural Engineering in September 1969.

Mr. Davis is a member of the Alpha Zeta, Omicron Delta Kappa, Phi Kappa Phi, Sigma Tau, and Tau Beta Pi honor societies and a student member of the American Society of Agricultural Engineers. During his graduate study he was the recipient of the National Defense Education Act Title IV Fellowship and the National Science Foundation Graduate Fellowship.

He was married to Irma Mary Friesen on March 18, 1972.

ACKNOWLEDGEMENTS

The author wishes to express his appreciation to his Special Committee - Professors G.E. Rehkugler, J.F. Booker, and R.H. Rand - for their guidance during his doctoral program at Cornell. Special thanks go to his Committee Chairman, Dr. Rehkugler, whose personal interest, encouragement, and inspiration extended beyond the academic realm.

The author expresses his appreciation to the Office of Education, U.S. Department of Health, Education, and Welfare and to the National Science Foundation for their fellowship support during his graduate program. Thanks also go the the Department of Agricultural Engineering at Cornell University and the Cornell Research Grants Committee for financial assistance in the author's research. Some of his computation was done at the New York State Veterinary College Computer Facility which is supported by NIH grant RR326.

The author expresses his appreciation to those faculty and staff in the Department of Agricultural Engineering too numerous to mention, who contributed their time and efforts to assist him in his research. Special personal thanks go to Professor D.C. Ludington, former graduate student B. Derrell McLendon, and others who prayerfully led the author into a personal relationship with their Lord and Saviour, Jesus Christ, thereby changing and enriching his life.

The author also wishes to thank his wife, Irma, for her continuous and exhaustive support in conducting his research and preparing his dissertation.

TABLE OF CONTENTS

Page

LIST OF TABLES

LIST OF FIGURES

Figure Page

Figure		Page

Figure		Page

CHAPTER I

INTRODUCTION

1.1. Background

Each year between 800 and 1000 people are killed in tractor accidents in the United States. Two-thirds of these deaths occur in accidents involving tractor overturns, usually when the tractor operator is pinned and crushed beneath the tractor. Approximately 75 per cent of the overturn fatalities result from side overturns, 25 percent from rear overturns, and a negligible number from front overturns. (Volpe, 1971)

The earliest attempts to protect the tractor operator from overturns were the development of devices to shut off the tractor engine or disengage the clutch when elevation of the front end caused the tractor body to reach a "dangerous angle" relative to the horizontal plane. More recently a phase plane analysis has provided a more accurate definition of tractor rearward overturning stability in terms of the tractor inclination and its angular velocity (Mitchell, et al., 1970). The expense of required sensing devices, the lack of instrumentation reliability when exposed to field conditions for long periods of time, and the inability of existing techniques to predict and prevent side overturns has turned attention away from preventing overturns. Instead, engineering efforts have been directed toward protecting the tractor operator in the event of an accidental overturn.

The first significant work in the development and testing of operator roll-over protection structures (ROPS)* for agricultural tractors was conducted in Sweden in 1954 (Möberg, 1964). Identical frames of varying strength were constructed and tested under laboratory and field conditions to determine the strength required to withstand field overturns and to define appropriate laboratory tests which would result in the same degree of frame deformation as that experienced in the field. A series of laboratory tests designed to be equivalent to the field overturns incorporated pendulum impacts from the rear and the side followed by a static vertical compression load. The pendulum energies and compression load were empirical functions of the tractor weight.

Many European countries, Australia, New Zealand, and the United States have conducted their own testing programs and developed their own test standards for ROPS (Nordström, 1970). By 1970, seven of the European countries had laws detailing mandatory use of protective cabs or frames on agricultural tractors. The United States, New Zealand, and Australia are developing legislation which may make the use of ROPS compulsory throughout their respective nations. Standardization of testing procedures between countries has been attempted by organizations such as the International Organization for Standardization (ISO) and the Organization for Economic Cooperation and Development (OECD). The OECD test code has been defined and accepted

---

*Roll-over protection structures may be either frames or cabs which are deisgned to protect a tractor operator in the event of a tractor overturn during normal operating conditions.

by the Nordic countries, but the ISO continues to consider different proposals for the testing of roll-over protection structures.

A comparison of ROPS testing procedures used by the testing agencies of various countries shows a variety of impact tests, static load tests, and field overturn tests, and differing criteria for allowable deformations used in evaluating the performance of the protective frame or cab. Each testing procedure is regarded as a method for evaluating the performance of the protective structure as it responds to the loading conditions of a reasonably severe overturn accident. Because a ROPS must protect the tractor operator from the injurious consequences of an unplanned tractor overturn, the definition of a reasonably severe tractor overturn is supremely important.

Manufacturers of roll-over protection structures in the United States, through repeated overturns of instrumented tractors with ROPS, have identified overturn situations which they consider reasonably severe. They have also identified alternative non-overturn tests which are designed to subject the ROPS to energy levels comparable to those expected during actual field overturns. The energy levels established for these alternative tests are expressed as empirical functions of the tractor weight (when ballasted to specified levels) without regard to any other tractor characteristics.

Intense controversies continue to occur over the relative severities of field overturn and non-overturn tests and over the adequacy of the standard ROPS testing procedures in the United States (Jensen, 1970; Steinbruegge, 1971; Baker, et al., 1972; Jensen, 1973). A better understanding of tractor overturn motions and the effect of tractor and terrain parameter values on the tractor overturning motion is required before test engineers may be assured that they have defined a reasonably severe overturn for a tractor under normal operating conditions. A theoretical basis for establishing the test atandards for roll-over protection structures is conspicuously absent and obviously needed to provide credibility to and improve acceptance of ROPS testing procedures.

1.2. Objectives

The general objective of this thesis is to develop a method for studying tractor overturns under repeatable conditions, so that overturn severity may be described more precisely in terms of tractor and terrain characteristics. This should provide a more accurate definition of a reasonably severe tractor overturn, or possibly, an equivalent alternative test.

The general objective is to be met through the following detailed objectives:

1. To develop a mathematical model of a wide-front-end tractor traversing a general terrain and undergoing complete overturns.
2. To verify the mathematical tractor model with scale model tests:
   a. By developing an experimental method for studying the motion of a scale model tractor during overturns, and
   b. By comparing the paths of particular points on the tractor during simulated and actual overturns.

3. To identify energy levels and orientations of tractors during overturns by simulating tractor overturns with the mathematical model.

CHAPTER II

REVIEW OF LITERATURE

2.1. Tractor Overturn Protection

The magnitude of the tractor overturn problem has been acknowledged by engineers around the world for many years. Sweden was the first country to initiate extensive tractor overturn studies in 1954 (Möberg, 1964). Field and laboratory tests provided the experience used in defining a set of laboratory based tests for evaluating tractor roll-over protection structures (ROPS). Ten years of use of ROPS on tractors in Sweden has provided documentation for the success of the Swedish tests and laws in reducing fatalities from tractor overturns (Nordström, 1970).

The Swedish ROPS tests - a pendulum blow from the rear, one from the side, and a static vertical load from the top - are run in sequence on the same ROPS to simulate conditions occurring during a tractor overturn. The pendulum energy levels were adjusted to produce damage to the protective structure which was comparable to that occurring in an actual field overturn. Other European countries, following the example of Sweden, have tested ROPS and established similar standard testing procedures. Use of roll-over protection structures has become mandatory on farm tractors in Sweden (1959), Norway (1964), Iceland (1966), Denmark (1967), Finland (1969), West Germany (1970), and England (1970) (Nordström, 1970).

New Zealand developed an interim test procedure to control the manufacture and sale of roll-over protection structures while they accumulated engineering data for developing their own tests (Watson, 1967). The interim tests included features of the Swedish and Norwegian tests. Watson detailed differences in the Swedish, Norwegian, and British tests showing the discrepancies in engineers' opinions regarding what constitutes a sufficiently severe test and acceptable performance criteria.

The need for operator protection in Australia has caused roll-over protection structure testing to be standardized there also (Baillie, 1971). Compulsory use of ROPS in Australia is expected when sufficient testing experience has been gained.

The first test standards for ROPS in the United States were parterned after the Swedish tests, but included modifications found necessary through experience (Bucher, 1966; Hansen, 1966). Standard tests in the U.S. today include a side overturn, a rear overturn, and either a static or dynamic laboratory test (ASAE Agricultural Engineer's Yearbook, 1972). The static loading test and the dynamic pendulum impact test have energy levels defined as empirical functions of the tractor weight when ballasted according to the tractor horsepower. Not only do these empirical relationships differ from those defined for the Swedish pendulum test, but the definitions of the tractor weights also differ. The larger and more powerful tractors used in the U.S. also require the U.S. test specifications to fit a wider range of tractor weights than that found in Europe. A sample of popular U.S. tractors has shown the U.S. test energy requirements to be twelve per cent less than those specified by the Swedish energy equations (Jensen, 1970). Arndt (1971) presents an extensive review of the early ROPS development and steps leading to the acceptance of voluntary test standards for ROPS in the United States.

The adequacy of the American Society of Agricultural Engineers (ASAE) and the Society of Automotive Engineers (SAE) test standards for wheel tractor ROPS have been vigorously debated as federal legislation threatens to replace previously voluntary use and testing of ROPS with mandatory regulations (Volpe, 1971). Points of particular emphasis have been the disputed need for tractor overturn tests (Stevenson, 1970; Floyd, 1971; Hensen, 1971) and conflicting results between pendulum test results and tractor overturn results (Jensen, 1970; Steinbruegge, 1971). Proposed changes to the ASAE test standards eliminate the requirement for tractor overturns if energy levels used in the laboratory tests are increased by fifteen per cent (Hahn, 1973).

The unanswered questions in testing ROPS continue to be:

1. What energy levels and velocities of impact do the various parts of the ROPS see in a tractor overturn?
2. Can pendulum impacts or static tests simulate the overturn load conditions?

Watson (1967) discussed the theory of plastic bending as it applies to energy absorption in ROPS. Klose (1969) discussed the effects of ROPS mountings and relative stiffness of the soil and ROPS on the energy absorption characteristics of the ROPS. Others (Macarus, 1971; U.S. Steel, 1971) have developed elastic and plastic structural analysis theory for designing ROPS when design loads are specified, but this again assumes that overturn loadings are well defined.

A rigorous analysis of tractor motions throughout a general overturning situation has not been reported to the best knowledge of the author. Watson (1967) derived the kinetic energy for a tractor tipping sideways down a slope or off a bank. He showed the importance of the rear wheel in absorbing energy as the center of tractor rotation is shifted by the impact of the side of the wheel onto the ground during the roll. Tractor side-rolls off a bank were shown to be more severe to ROPS than those down a uniform slope because of the wheel impact would not occur in some bank overturn situations. Watson also emphasized the point of impact as an important factor in determining the proportion of the tractor energy to be absorbed by the ROPS. Maximum energy would be absorbed by the ROPS when the impact point is near the center of percussion for the tractor-ROPS system. A similar discussion of energy absorption in general impact situations was given by Bickford (1968).

Poor repeatability of tractor overturn tests prevents the accumulation of parametric data to define energies involved in overturn, points of ROPS impact, and impact velocities. This has caused the adoption of controlled overturns for certain tests where comparative data was required for tractors (Möberg, 1964) and for automobiles (Wilson, et al., 1972), but it has not provided data for defining the conditions surrounding actual tractor overturns in the field.

Baker, et al. (1972) presented an engineering analysis of thirty-six tractor overturn accidents in an attempt to define the energy of the tractor at the time of overturn. An estimate of the tractor speed and orientiation at the instant of instability was used to calculate the kinetic energy of the tractor and its potential energy gain as the center of mass reached its final elevation. The total energy calculated for the tractors was much greater than pendulum energies specified for testing ROPS on the same tractors. Jensen (1973) was quick to point out that only part of this tractor energy is absorbed by the ROPS.

The question of energy levels incident to the ROPS in a tractor overturn has not been answered satisfactorily by the studies found in the literature. Two possibilities for controlled parametric studies of tractor overturns to obtain the desired information are:

1. Physical model studies using similitude principles.
2. Mathematical modelling of tractor overturns using digital computer simulations.

The latter approach was chosen because computer simulations provide the greatest repeatability and the easiest control of parameters. The following sections present developments in mathematical modeling of vehicles which are pertinent to this study.

2.2. Mathematical Modelling of Vehicles

The concern of engineers for the stability of tractors under normal farming conditions has existed for many years (McKibben, 1927; McCormick, 1941; Worthington, 1949; Sack, 1956). The kinematic and dynamic analyses of that time, however, were primarily directed toward defining the factors which determined stable and unstable operating conditions.

Raney, et al. (1961) and Barger, et al. (1963) analyzed the tractor as a vibrating system having, respectively, three and two degrees of freedom. They developed the dynamic equations of motion for the tractor and identified the corresponding natural frequencies of vibration. The major objective was to define the tractor steady-state response to terrain undulations in terms of measured tractor characteristics.

Steady-state tractor motions on sidehills also have been studied. Pershing, et al. (1964) defined the equilibrium tractive forces and orientation of a tractor following a prescribed path on a sidehill, and later (Pershing, 1971) developed a similar analysis for a four-wheel drive articulated vehicle. Stability of the vehicle operating conditions was included. A study of tractor motions directly uphill identified those tractor characteristics which influence tractive ability and stability under these operating conditions (Gilfillan, 1970).

A number of mathematical models have been developed to describe the motions of automobiles and military vehicles in response to general terrain inputs or prescribed accident conditions. McWilliams, et al. (1960) modelled a vehicle with four degrees of freedom in an analog computer analysis of the vehicle suspension. His vehicle chassis equations defined only vertical and pitch motions. Chenchanna (1969) modelled the vehicle, engine, and passenger motions in one direction as he used the analog computer to study passenger sensitivity to statistically defined road profiles.

Ford, et al. (1969) modelled an automobile for two-dimensional roll motion studies. He then validated his model by comparisons with actual auto side rolls as initiated by a ramp and curved-rail test site. The mathematical model of Sharp, et al. (1969) included additional vehicle degrees of freedom, but vehicle motions were restricted to small amplitudes to maintain a linear model. This model allowed the chassis motion six degrees of freedom while using Euler angles to define its orientation. The terrain inputs were transmitted to the vehicle through rigid wheels.

Highly sophisticated mathematical models of automobiles for handling and accident studies have been reported by McHenry, et al. (1968) and McHenry (1969). These models provided six degrees of freedom to the chassis in addition to two for the rear axle, one each for the front wheels, and one for steering. Because large rotational motions of the automobile were to be modelled, a method of indexing and redefining the Euler angles was used to avoid the unstable range for certain rotations near ninety degrees. Detailed suspension features, braking options, and inertial coupling of the drive wheels provided added versatility to the model.

McHenry, et al. also provided options to specify the tire-road interaction as a point-contact model or as an enveloping-tire model. The friction circle concept was used to define the relationship between the maximum lateral and circumferential tire forces. Validation tests were conducted to compare the vehicle response to that obtained from digital computer simulations of the mathematically modelled vehicle traversing roads having conditions described in tabular form.

R. Smith (1965) modelled a track traversing terrains described by Fourier series coefficients. His truck model included bounce, pitch, and roll motions for the chassis plus bounce and roll motions for both front and rear axles. Suspension features were defined by tabular spring and shock absorber data with different loading and unloading characteristics. The tire-terrain interactions were defined as a wheel rolling radius which was a function of the interaction forces and the soil-tire characteristics, but which did not allow the wheel to leave the ground. The vehicle forward motion was restricted to a constant speed. Verification tests showed good correlation between the predicted and measured vehicle motions while traversing a controlled terrain.

Schuring, et al. (1969) developed a sophisticated model for a military vehicle travelling over soft soil or a rough terrain. The vehicle hull motion was described by six degrees of freedom using Euler angles for the rotational coordinates. Suspension options included anti-dive, anti-squat, and anti-roll devices and solid axle or independent suspension features. Shock sbsorbers and springs were described by tabulated data. Although many tire-terrain models were described, only point-contact models were incorporated into the vehicle model. No tests for verifying the vehicle model were reported.

R. Smith (1967) applied the modelling methods reported in his previous work to studies of agricultural vehicles crossing visco-elastic fields. (The term "viscoelastic" identified the surfaces as those dissipating energy as they yielded to tire loads.) The tire and ground force-response properties were defined as composite values for the particular tire and ground condition. The mathematical model for the vehicle was verified and then used to obtain vehicle reactions and responses to various terrains. The suspension reactions were then used as input to a second digital computer program which performed structural analysis for designing the vehicle frame components.

Mathematical models of farm tractors have been developed primarily for studies of tractor stability or vehicle ride conditions. Huang, et al. (1964) developed a tractor model for evaluating an elastic wheel mounting as a possible ride improvement mechanism. This model was limited to small amplitude displacements within a vertical plane; its purpose was not to accurately model the tractor but to provide comparative evaluation of ride characteristics for changes in the wheel parameters.

Models for rearward overturning of tractors have been developed by several researchers. Mitchell, et al. (1970) developed a single differential equation model for tractor rotation about the rear axle from which a phase plane analysis defined stable and unstable regions of operation. Circuitry to disengage the clutch when the unstable conditions were detected was designed and tested. The model assumed constant rear axle torque while neglecting both translational accelerations of the tractor center of mass and rotational accelerations of the rear wheels. The overturn predictions and control were therefore limited to conditions when the rear wheels were wedged and could not rotate.

Goering, et al. (1967) developed the first model which would simulate tractor rear overturns due to rapid clutch engagement or to slower engagement with a large drawbar load. This model was limited to motion in a vertical plane. The tire-ground interaction was represented by a parallel spring and dashpot combination in the radial direction but by traction-slip data in the circumferential direction.

The model also included a transmission final drive, a clutch, and an engine. The engine simulator, however, was replaced by torque-time data when difficulties in the analog simulation of the model arose.

Koch, et al. (1970) conducted rear overturn tests with a full-sized tractor to verify the rear overturn model developed by Goering, et al. The methods used to determine the tractor center of mass and moments of inertia and to determine traction-slip data were described. The mathematical model for rear overturns produced highly reliable predictions of the tractor behavior.

D. Smith, et al. (1970) modelled rearward tractor overturns in two parts. The vertical displacement, horizontal (forward) displacement, and pitch of the tractor chassis were described by equations written at the tractor center of mass while the front tires contacted the ground, but these motions were described by equations written at the rear axle when the front wheels were off the ground. All motion was limited to a vertical plane normal to the rear axle and passing through the tractor center of mass. The model also contained a modified version of Goering's power train simulator to include inertial effects of the engine and drive train, rear wheel coupling, and engine torque variations. Bilinear relationships were used to describe the speed-torque characteristics of the engine and the slip-torque characteristics of the clutch. The tire-terrain interaction was described radially by a parallel combination of a spring and dashpot on a rigid surface and circumferentially by a gross traction coefficient expressed mathematically as an exponential function of the wheel slip (Persson, 1967). Two tractor overturns were conducted to verify the overturn model.

Grevis-James, et al. (1971) also developed a rear overturn model for a tractor restricted to motion in a vertical plane normal to the ground surface. The equation developed to describe dynamic equilibrium between the tractor chassis and rear wheels included translational accelerations of the chassis, rotational accelerations of the chassis and rear wheels, drawbar loads, rolling resistance, and engine torque. The final model, however, assumed that the rear wheels were restrained and the chassis translational accelerations were negligible. The final model defined the rotational motion of the chassis in terms of the engine power output and clutch power dissipation when the clutch was being engaged, and in terms of the engine inertia, engine torque-speed characteristics, and the chassis inertia properties after the clutch was fully engaged. Verification tests emphasized the role that energy storage in the flywheel and drive train play in response to sudden clutch engagement.

Mathematical models of wheel tractors in lateral motion have been developed to study tractor stability and handling behavior. Pershing, et al. (1969) described the motion of a wide-front-end tractor by nine degrees of freedom - six for the chassis, one each for the rear wheel rotations, and one for the front-end rotation. All motions were defined as the deviation from the steady-state condition and were limited to small amplitudes. The equations of motion were derived using kinetic, potential, and dissipative energy functions of the coordinates in the Langrange equation formulation.

Pershing's model was developed primarily to study the time domain response of tractors operating on sidehills when they encounter terrain irregularities. The tire-terrain interactions were described by linear spring and dashpot forces in response to tire motions relative to the terrain surface. The terrain was assumed nondeformable while the tire location was defined by single point contact with the terrain.

Observations of a tractor operating on a sidehill and encountering a sine bump at the uphill rear tire were used to verify Pershing's tractor model. A three-degree-of-freedom model for the tractor proved very inferior to the nine-degree-of-freedom model in predicting the tractor responses. The small-amplitude-oscillation assumption of this model makes it unfit for simulating tractor side overturns.

Unruh (1969) developed a mathematical model of an articulated vehicle operating on a uniform rigid slope. The model had six degrees of freedom for the articulated body (the steering angle was not a degree of freedom) plus one degree of freedom for roll of the rear axle. The tire characteristics were modelled by a parallel combination of springs and dashpots in three mutually perpendicular directions. The equations of motion, derived by considering constraints at the axle pin, were made linear by limiting all coordinates to small amplitude oscillation. Unruh defined the static stability of the vehicle by varying the slope of the ground surface and the orientation of the vehicle on the surface while observing the tire forces normal to the ground surface; a zero force denoted a statically unstable condition. Dynamic analysis of the vehicle included identification of the vehicle's undamped natural frequencies and mode shapes and also simulation of the vehicle motions on an analog computer.

Wolken, et al. (1972) used a mathematical model similar to Pershing's to evaluate operator ride characteristics of wide-front-end tractors traversing statistically defined terrain profiles. Bilinear springs and linearly viscous dashpots were used to describe tire-terrain interactions in which separation of the tire from the terrain was permitted. Random data techniques were used to analyze the chassis motion in parametric studies of vehicle speed, tire spring rate, and moments of inertia. Once again, the small-amplitude-angular-rotation limitation prevents this model from predicting tractor motion during overturns.

D. Smith, et al. (1971) developed a two-part mathematical model to describe the side overturn motion of wide-front-end and tricycle-type wheel tractors. Three dimensional vector techniques were used to derive differential equations expressing the tractor angular acceleration about a tip axis in terms of the tractor geometry, inertial forces, side slopes, and ground disturbances. The inertial forces were calculated after assuming a history of the acceleration of a point on the tip axis about which rotation of the tractor center of mass occurred. Two stages of tipping were analyzed for the wide-front-end tractor - initial tipping of the chassis about the front pin, and after the rotation limit at the front pin had been reached, tipping of the chassis and front end about an axis connecting the two tire-ground contact points about which rotation would occur. Smith's model was not developed for close prediction of the actual overturning motion but rather for analysis of those factors which influence lateral overturning.

Larson, et al. (1971) developed the first mathematical model designed specifically to simulate sideways tractor overturns and to predict when they would occur. This model described a tricycle-type wheel tractor by six chassis degrees of freedom plus one degree of freedom each for the rear wheels. The chassis orientation was defined by Euler angles, giving the roll, pitch, and yaw rotations. Restricting assumptions used were: rigid ground surface, no external loads on the tractor, and constant engine torque with no drive-line inertia. A wagon-tongue steering technique was used to provide steering corrections to keep the tractor on a desired path.

The tire forces were defined by three mutually perpendicular force components - normal to the ground plane, in the ground plane parallel to the direction of vehicle travel, and in the ground plane perpendicular to the direction of travel. The radial tire forces were modelled as the reactions of parallel spring and dashpot combinations making point contact with the ground surface below the wheel center. Spring characteristics were described by a bilinear representation of the static force-deformation curves of the tires while damping forces were defined by the viscous damping coefficients reported by Pershing, et al. (1969) and Raney, et al. (1961).

Tire forces parallel to the tractor direction of travel included both traction and rolling resistance forces defined by the product of their respective coefficients and the tire force normal to the ground surface. Larson defined the coefficient of traction as an exponential function of the wheel slip using data reported by Persson (1967). The coefficient of rolling resistance was defined as a linear function of the wheel slip angle based upon data reported by Schwanghart (1968) for unpowered tires.

The tire forces perpendicular to the tractor direction of travel included forces sufficient to keep the tractor from sliding down the sideslope plus side forces due to tire slip angles. The coefficients of lateral force due to slip angles were determined by linearizations of data reported by Schwanghart (1968) for unpowered wheels, and by Krick (1970) for slip angle and wheel slip effects on powered wheels.

Larson conducted field tests and digital computer simulations of a tractor operating at different speeds on a side slope while encountering a sinusoidal bump at the rear tire on the uphill side. The simulations predicted overturns for less severe conditions than those observed in the field tests. The tire forces were thought to be the cause of this discrepancy. Larson's tractor model did not allow a general analysis of tractor motions in which skidding or pitch angles near ninety degrees would occur.

D. Smith (1972) modified Larson's mathematical model of a tricycle-type tractor to study the handling behavior of this type tractor to step changes in the steering angle. This model included inertial coupling of the rear drive wheels (with significant drive train inertia) plus a power train simulator developed previously (D. Smith, et al., 1970) to provide torque and speed variations to the rear wheels. A friction ellipse concept was used to define the effects of the tractive force on the lateral force obtainable at the drive wheels. Simulations of a tractor responding to step steering changes while travelling on a flat rigid terrain provided results which, on a qualitative basis, were very good.

The wheel tractor simulations developed to date have been based upon assumptions or limitations which have made them too restrictive for use in performing a general parametric study of tractor overturns. The model used by D. Smith (1972) most nearly provided the desired flexibility; however, it also contained some restrictions which were undesirable for the proposed overturn analyses. Restrictions which must be overcome are:

1. The use of Euler angles limits the pitch angle to magnitudes less than ninety degrees.
2. The model could be used for only tricycle-type tractor simulations.
3. The tire radial forces, defined by a point-contact model, could not be defined adequately for travel on an irregular terrain.
4. The empirical data used in the tractor-terrain model need to be determined carefully for the specific tractor and terrain situation of interest.

The following section reviews other works that provide insight into overcoming some of the restrictions listed above.

2.3. Additional Modelling Considerations

Shortcomings of the reported mathematical models for wheel tractors lie principally in defining the rotational equations of motion and in accurately representing the tire-terrain interface. McHenry, et al. (1968) described a procedure which was used to overcome the large angle stability problem that sometimes occurred when Euler angles were used to define the vehicle orientation. This method included an indexing and a redefining of the vehicle-fixed coordinate axes whenever the pitch angle magnitude was greater than seventy degrees. This was done to avoid the region near a ninety degree pitch angle, a value at which the orientation becomes undefined.

An alternative method for defining the rigid body orientations without encountering conditions of undefined equations is to define the orientations in terms of Euler parameters of the vector of finite rotation (Deprit, 1970). Four Euler parameters (not to be confused with Euler angles) uniquely define the orientation of a rigid body in terms of the direction cosines for the principal axes of that body expressed in the inertial reference frame directions. Four differential equations for the Euler parameters replace the three which would have been used for the Euler angles, but the simplicity of use and stability of the equations make utilization of Euler parameters advantageous when large rotations of rigid bodies may be expected during the simulations.

The principal moments of inertia and principal axes for a rigid body are defined as the eigenvalues and eigenvectors, respectively, of the inertia matrix for that rigid body (Greenwood, 1965, p. 305). Thus, if the inertia matrix is defined in body-fixed axes directions, the eigenvectors define the orientation of the principal axes relative to the body-fixed axes. Eigenvalues of a square matrix may be determined by using quadratic root searching techniques to obtain the roots of the characteristic polynomial of the matrix (Conte, 1965). The eigenvectors are then obtained by substituting the eigenvalues, one at a time, into the matrix equation which defined the eigenvalue problem originally (Greenwood, 1965, p. 305).

The use of principal moments of inertia in the differential equations for the derivatives of the angular velocities eliminates the product of inertia terms and thus results in a simplification of these equations. Use of principal moments of inertia and principal axes therefore leads to improvement in the differential equations for both angular orientation and angular velocities.

The tire-terrain interface may be improved for irregular terrain surfaces by changing either the terrain surface representation or the tire model to provide tire enveloping characteristics. Thompson, et al. (1970) showed that step terrain changes could be represented as combinations of quadratic and linear curves to enable a point-contact tire model to respond as a real tire does to the step change. This method would be impractical for situations where terrains were to be changed frequently or where the vehicle might approach the terrain features from different directions in different simulations.

A tire-terrain interface which may be most practical in a general simulation situation where irregular surfaces occur was used by McHenry, et al. (1968). This desirable interface was provided by an enveloping tire model described in detail by Albert (1961). The model represented the tire by evenly-spaced radial springs which sensed radial tire deflections over incremental lengths of the tire circumference and collectively defined one equivalent contact point from which the radial deflection and force were defined, and at which an equivalent ground plane was defined. The equivalent ground plane then was used in defining the lateral and circumferential forces on the tire. Although this model redefines the terrain and uses a point-contact representation for the tire, it is not detrimentally affected by changing the direction from which the tire approaches an obstacle.

Generality of a mathematical model can best be maintained by formulating the model in a way that allows the addition or subtraction of degrees of freedom with relative ease (Bartz, 1972). Non-Lagrangian techniques in which all constraint forces are identified provide this versatility. Formulation in this manner will most readily allow external forces to be applied to any part of the vehicle and allow transition between a wide-front-end tractor and a tricycle-type tractor. This transition actually is the same as that which takes place when the front-end rotation of a wide-front-end tractor reaches its limit relative to the tractor chassis. Thus the provision for this rotation limit may be seen as a provision for both wide-front-end and tricycle-type tractors in the same model.

CHAPTER III

DEVELOPMENT OF THEORY

The behavior of a tractor while traversing a general terrain requires the theory of rigid body dynamics for its description. The tractor dynamics can be described by considering the dynamics of its various component parts and the constraints between these parts.

The proposed tractor model consists of the following entities, each having its own dynamic characteristics

1) the tractor body or chassis,
2) the tractor front end, including the front wheels,
3) the left rear wheel,
4) the right rear wheel,
5) the engine.

Ten degrees of freedom for the tractor are assigned to the various components as shown in Table 3-1.

TABLE 3-1. Tractor Degrees of Freedom

	translational	rotational
tractor body	3	3
front end	0	1
left rear wheel	0	1
right rear wheel	0	1
engine	0	1
	3	7

The following assumptions have been made in the development of dynamic equations of motion for the proposed tractor model.

1. The front end is free to rotate about the connecting pin without transmitting torque in the pin-axis direction until the rotation reaches a set limit.
2. Steering motions of the front wheels do not significantly change the inertial properties of the front end.
3. The rotational inertia of the front wheels about their axles is not significant.
4. The tractor differential gears transmit torque equally to both rear wheels.
5. The tractor front end has a plane of symmetry passing through the center of mass of the front end while perpendicular to the transverse axis of the front end.
6. A plane of symmetry exists for each of the rear wheels and for the tractor body.
7. A single "ground-contact point," through which the ground forces act, may be defined for each tire.
8. The ground surface is nondeformable.
9. The effects of engine angular momentum on the tractor motion are insignificant.

The tractor motion is dependent upon the external forces which act upon the component parts of the tractor. In addition to ground forces acting on the tires, gravitational and externally applied forces (e.g., drawbar forces) are often influential in determining the tractor motion, so all are considered in this tractor model. Upon applying the appropriate constraints existing between the component parts of the tractor, a combined set of differential equations is obtained to describe the motion of the tractor as it traverses a specified terrain.

A coordinate system fixed in the inertial reference frame is used to define the position of the tractor at all times. All other coordinate systems used in the development of the tractor model can be related to the inertial directions as follows.

$$\underline{e}_B = A_{BI}\ \underline{e}_I \tag{3-1}$$

where $\underline{e}_I$ is the right-hand triad of unit vectors fixed in the inertial reference frame having $\underline{e}_{I_3}$ defined vertically down,

$\underline{e}_B$ is the right-hand triad of unit vectors whose orientation is being defined, and

A_{BI} is a 3-by-3 matrix of direction cosines defining the orientation of vectors $\underline{e}_B$ in terms of the $\underline{e}_I$ unit vectors.

The variables used in developing the mathematical model of the wide-front-end tractor have a basic pattern in their notation. The notation used in defining the variable type is shown in Table 3-2 while the bodies being referred to are defined in Table 3-3 and the coordinate system is defined in Table 3-4.

TABLE 3-2. Variable Types

Variable	Definition
$\underline{X}_{\alpha\beta}$	absolute position of point α expressed in β coordinates, in.
$\underline{V}_{\alpha\beta}$	absolute velocity of point α expressed in β coordinates, in/sec.
$\underline{R}_{\alpha\gamma\beta}$	position of point α relative to point γ expressed in β coordinates, in.
$\underline{\omega}_{\alpha\beta}$	absolute angular velocity of body α expressed in β coordinates, rad/sec.
$\theta_{\alpha\beta}$	angular rotation of body α expressed in β coordinate direction, rad.
$I_{\alpha\beta}$	mass moments of inertia and products of inertia for body α measured about the center of mass and expressed in terms of β axis directions, lb-in-sec^2.
m_α	mass of body α, lb-sec^2/in.
$\underline{e}_\alpha$	unit vectors of the α coordinate system
$A_{\alpha\gamma}$	direction cosines defining the attitude of the $\underline{e}_\alpha$ unit vectors in terms of the $\underline{e}_\gamma$ unit vector directions
$\underline{F}_{\alpha\beta}$	force acting on the α body expressed in β coordinates, lb.
$\underline{F}_{\alpha\gamma\beta}$	force acting on the α body due to interaction with the γ body expressed in β coordinates, lb.
$\underline{M}_{\alpha\beta}$	moment acting on the α body about its center of mass expressed in β coordinates, in-lb.
$\underline{M}_{\alpha\gamma\beta}$	moment acting on the α body as applied at the γ point of interaction expressed in β coordinates, in-lb.
$\underline{W}_{\alpha\beta}$	weight force on the α body expressed in β coordinates, lb

NOTE: Underscores indicate vector quantities while additional numerical subscripts indicate specific components of vectors; a dot over the variable indicates the derivative of that variable with respect to time.

TABLE 3-3. Bodies and Points Referenced by Variable Notation

α,γ	Definition of body or point
B	tractor body or its center of mass
L	left rear wheel or its center of mass
R	right rear wheel or its center of mass
F	tractor front end or its center of mass
P	tractor front pin
W	a wheel or its center of mass
C	wheel center
G	ground
E	external source
WG	wheel-ground contact point
A	axle
S	front end "stop"

TABLE 3-4. Coordinate Systems Denoted by Variable Notation

β	Coordinate system
I	inertial reference frame
T	tractor-body axes
P	principal axes of the tractor body
F	tractor front-end axes
W	wheel axes

Examples of the notation given in Tables 3-2 through 3-4 are:

a. $\underline{X}_{LI}$ is the inertial (I) reference frame vector defining the absolute position (X) of the left rear wheel center of mass (L) .

b. $\underline{R}_{PBI}$ is the vector defining the relative position (R) of the front pin (P) with respect to the tractor-body center of mass (B) while expressed in inertial coordinate components (I) .

c. $\underline{R}_{PBP}$ is the same vector as defined in (b), but now it is expressed in the component directions of the tractor-body principal axes (P rather than I).

d. $\underline{V}_{WGI}$ is the vector defining the absolute velocity (V) of the wheel-ground contact point (WG) expressed in inertial component directions (I) .

e. $\underline{W}_{FI}$ is the weight force vector (W) for the tractor front end expressed in inertial component directions (I) .

3.1. The Tractor Body

The tractor body is considered separate from the rear wheels and the front end. A coordinate system fixed in the tractor body is used to define the orientation of the body at any time. (See Figure 3-1.) The origin of this coordinate system is located at the body's center of mass while the axes directions, $\underline{e}_{T_1}$, $\underline{e}_{T_2}$, and $\underline{e}_{T_3}$ are respectively, parallel to the front-end axis of rotation (positive forward), parallel to the rear axle (positive to the driver's right side), and the direction of the vector cross product $\underline{e}_{T_1} \times \underline{e}_{T_2}$ (positive down).

The motion of the tractor body is defined in terms of positions and orientations in the inertial coordinate system. The equations of motion for the translational degrees of freedom are obtained directly from a summation of forces acting upon the body as given by equations 3-2 and 3-3. The translational velocities and the total force are related by

$$\dot{\underline{V}}_{BI} = \frac{1}{m_B} \underline{F}_{BI} \qquad (3\text{-}2)$$

while the translational positions and velocities are related by

$$\dot{\underline{X}}_{BI} = \underline{V}_{BI} \ . \qquad (3\text{-}3)$$

The rotational equilibrium conditions for a rigid body having three rotational degrees of freedom require three equations defining the derivatives of the angular velocities plus others defining the derivatives of orientation parameters. The derivatives of the angular velocities can be expressed as three independent relationships only when the principal coordinates of the rigid body are used in writing the equations. These principal coordinates of the tractor body are defined as the triad of unit vectors whose origin is at the body center of mass while the axes are coincident with the axes of the body's principal mass moments of inertia.

Determination of principal axes and principal moments of inertia for a body is an eigenvalue - eigenvector problem such as

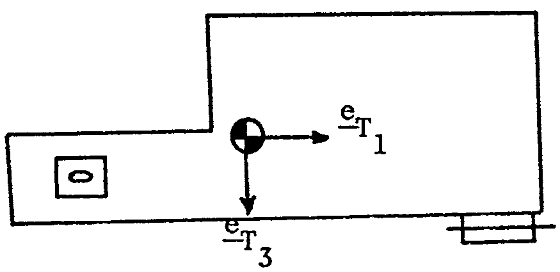

Side View

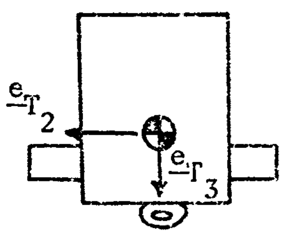

Front View

Figure 3-1. The Tractor-Body Coordinate Axes.

described in many numerical methods textbooks (Conte, 1965; Greenwood, 1965). The mass moments of inertia and products of inertia define the inertia matrix of the rigid body. When the inertia matrix is defined for the tractor-axes directions, the principal moment of inertia matrix is the diagonal matrix consisting of the eigenvalues of the tractor-axes moment of inertia matrix, which is also the matrix obtained from equation 3-4.

$$I_{BP} = A_{TP}^{-1}\, I_{BT}\, A_{TP} \tag{3-4}$$

where I_{BP} is the 3-by-3 diagonal matrix whose three nonzero elements are the eigenvalues of matrix I_{BT}, lb-in-sec^2,

A_{TP} is the 3-by-3 matrix of eigenvectors corresponding to the eigenvalues of matrix I_{BT}, dimensionless,

I_{BT} is the mass moment of inertia matrix for the tractor body defined for the tractor-axes directions, lb-in-sec^2.

The matrix A_{TP} is also the matrix of direction cosines defining the orientation of the tractor axes in terms of the principal-axes directions. The inverse of matrix A_{TP}, A_{TP}^{-1}, is also the transpose of matrix A_{TP} which is now designated as matrix A_{PT}, the matrix of direction cosines defining the orientation of the principal axes in terms of the tractor-axes directions. Thus the principal-axes directions may be defined in terms of tractor-axes directions as

$$\underline{e}_P = A_{PT}\, \underline{e}_T\,. \tag{3-5}$$

where $\underline{e}_P$ is the triad of principal axes, or in terms of inertial-coordinate directions as

$$\underline{e}_P = A_{PT} A_{TI} \underline{e}_I \ . \tag{3-6}$$

This relationship can be simplified to

$$\underline{e}_P = A_{PI} \underline{e}_I \tag{3-7}$$

where A_{PI} is the 3-by-3 matrix of direction cosines defining the orientation of the principal-axes directions in terms of the inertial-coordinate directions; it is the matrix product of A_{PT} premultiplied to A_{TI} .

The three simultaneous equations for the time derivatives of the principal angular velocities of the tractor body are derived from Euler's equations of motion (Greenwood, 1965, p. 365).

$$\dot{\omega}_{BP_1} = \frac{1}{I_{BP_{11}}} [M_{BP_1} - \omega_{BP_2}\omega_{BP_3}(I_{BP_{33}} - I_{BP_{22}})] \tag{3-8}$$

$$\dot{\omega}_{BP_2} = \frac{1}{I_{BP_{22}}} [M_{BP_2} - \omega_{BP_1}\omega_{BP_3}(I_{BP_{11}} - I_{BP_{33}})] \tag{3-9}$$

$$\dot{\omega}_{BP_3} = \frac{1}{I_{BP_{33}}} [M_{BP_3} - \omega_{BP_1}\omega_{BP_2}(I_{BP_{22}} - I_{BP_{11}})] \tag{3-10}$$

where $\dot{\omega}_{BP_1}$, $\dot{\omega}_{BP_2}$, $\dot{\omega}_{BP_3}$ are the time derivatives of the angular velocities about the $\underline{e}_{P_1}$, $\underline{e}_{P_2}$, and $\underline{e}_{P_3}$ principal axes, respectively, rad/sec^2.

Because finite rotations are not vector quantities, the angular velocities can not be integrated directly to obtain the orientation of the tractor body. Euler angles (Greenwood, 1965) have been used widely in engineering applications where the "heading angle," "attitude angle," and "bank angle" are meaningful parameters. However, these angles become undefined whenever the attitude angle (or pitch angle) approaches ±90°.

Some researchers (McHenry, <u>et al.</u>, 1968) have used a method of continually redefining the body-fixed coordinate system to control the magnitude of the Euler angles when large rotations are expected, but this method will not be used here.

Direction cosines can be obtained directly from the integration of nine simultaneous differential equations. However, this increase in the required number of equations is excessive.

Euler parameters (Deprit, 1970) are four functions of the direction cosines which can be obtained directly from integrations. Their reduction in the required number of differential equations from nine (when direction cosines are used) to four when Euler parameters are used, their stability for all orientations, and the fact that they are normalized parameters make Euler parameters desirable for describing the orientation of the tractor body.

Recalling that the direction cosines defining the orientation of the tractor-body principal axes are (in expanded form) defined by

$$\begin{Bmatrix} \underline{e}_{P_1} \\ \underline{e}_{P_2} \\ \underline{e}_{P_3} \end{Bmatrix} = \begin{bmatrix} A_{PI_{11}} & A_{PI_{12}} & A_{PI_{13}} \\ A_{PI_{21}} & A_{PI_{22}} & A_{PI_{23}} \\ A_{PI_{31}} & A_{PI_{32}} & A_{PI_{33}} \end{bmatrix} \begin{Bmatrix} \underline{e}_{I_1} \\ \underline{e}_{I_2} \\ \underline{e}_{I_3} \end{Bmatrix} \qquad (3\text{-}11)$$

where the $A_{PI_{ij}}$ are the direction cosines, the Euler parameters are then defined as

$$\lambda_0 = [(A_{PI_{11}} + A_{PI_{22}} + A_{PI_{33}} + 1)/4]^{1/2} \tag{3-12}$$

$$\lambda_1 = (A_{PI_{23}} - A_{PI_{32}})/4\lambda_0 \tag{3-13}$$

$$\lambda_2 = (A_{PI_{31}} - A_{PI_{13}})/4\lambda_0 \tag{3-14}$$

$$\lambda_3 = (A_{PI_{12}} - A_{PI_{21}})/4\lambda_0 \tag{3-15}$$

where λ_0, λ_1, λ_2, and λ_3 are the Euler parameters, dimensionless.

Equations 3-16 through 3-19 define the relationships of the Euler parameter derivatives with respect to time to the principal angular velocities and the Euler parameters of the body.

$$\dot{\lambda}_0 = \frac{1}{2}(-\omega_{BP_1}\lambda_1 - \omega_{BP_2}\lambda_2 - \omega_{BP_3}\lambda_3) \tag{3-16}$$

$$\dot{\lambda}_1 = \frac{1}{2}(\omega_{BP_1}\lambda_0 - \omega_{BP_2}\lambda_3 + \omega_{BP_3}\lambda_2) \tag{3-17}$$

$$\dot{\lambda}_2 = \frac{1}{2}(\omega_{BP_2}\lambda_0 - \omega_{BP_3}\lambda_1 + \omega_{BP_1}\lambda_3) \tag{3-18}$$

$$\dot{\lambda}_3 = \frac{1}{2}(\omega_{BP_3}\lambda_0 - \omega_{BP_1}\lambda_2 + \omega_{BP_2}\lambda_1) \tag{3-19}$$

Thus, integration of equations 3-16 through 3-19 yields the Euler parameters at any given time. The direction cosines can then be obtained by relationships which are inverse to equations 3-12 through 3-15. These relationships are

$$A_{PI_{11}} = \lambda_0^2 + \lambda_1^2 - \lambda_2^2 - \lambda_3^2 \tag{3-20}$$

$$A_{PI_{12}} = 2(\lambda_1\lambda_2 + \lambda_0\lambda_3) \tag{3-21}$$

$$A_{PI_{13}} = 2(\lambda_1\lambda_3 - \lambda_0\lambda_2) \tag{3-22}$$

$$A_{PI_{21}} = 2(\lambda_1\lambda_2 - \lambda_0\lambda_3) \tag{3-23}$$

$$A_{PI_{22}} = \lambda_0^2 + \lambda_2^2 - \lambda_3^2 - \lambda_1^2 \tag{3-24}$$

$$A_{PI_{23}} = 2(\lambda_2\lambda_3 + \lambda_0\lambda_1) \tag{3-25}$$

$$A_{PI_{31}} = 2(\lambda_3\lambda_1 + \lambda_0\lambda_2) \tag{3-26}$$

$$A_{PI_{32}} = 2(\lambda_2\lambda_3 - \lambda_0\lambda_1) \tag{3-27}$$

$$A_{PI_{33}} = \lambda_0^2 + \lambda_3^2 - \lambda_1^2 - \lambda_2^2 \tag{3-28}$$

The total moment reaction acting upon the tractor body about its center of mass and the total force reaction acting on this body are composed of the tractor body weight, reactions at the left rear and right rear axles, reactions at the front pin, and external reactions applied directly to the tractor body. (See Figure 3-2.) These relationships are

$$\underline{F}_{BI} = \underline{W}_{BI} - \underline{F}_{FPI} - \underline{F}_{LAI} - \underline{F}_{RAI} + \underline{F}_{BEI} \tag{3-30}$$

and

$$\begin{aligned} \underline{M}_{BP} = &- \underline{M}_{FPP} + \underline{R}_{PBP} \times (-\underline{F}_{FPP}) - \underline{M}_{LAP} - \underline{M}_{RAP} \\ &+ \underline{R}_{LBP} \times (-\underline{F}_{LAP}) + \underline{R}_{RBP} \times (-\underline{F}_{RAP}) + \underline{M}_{BEP} \end{aligned} \tag{3-31}$$

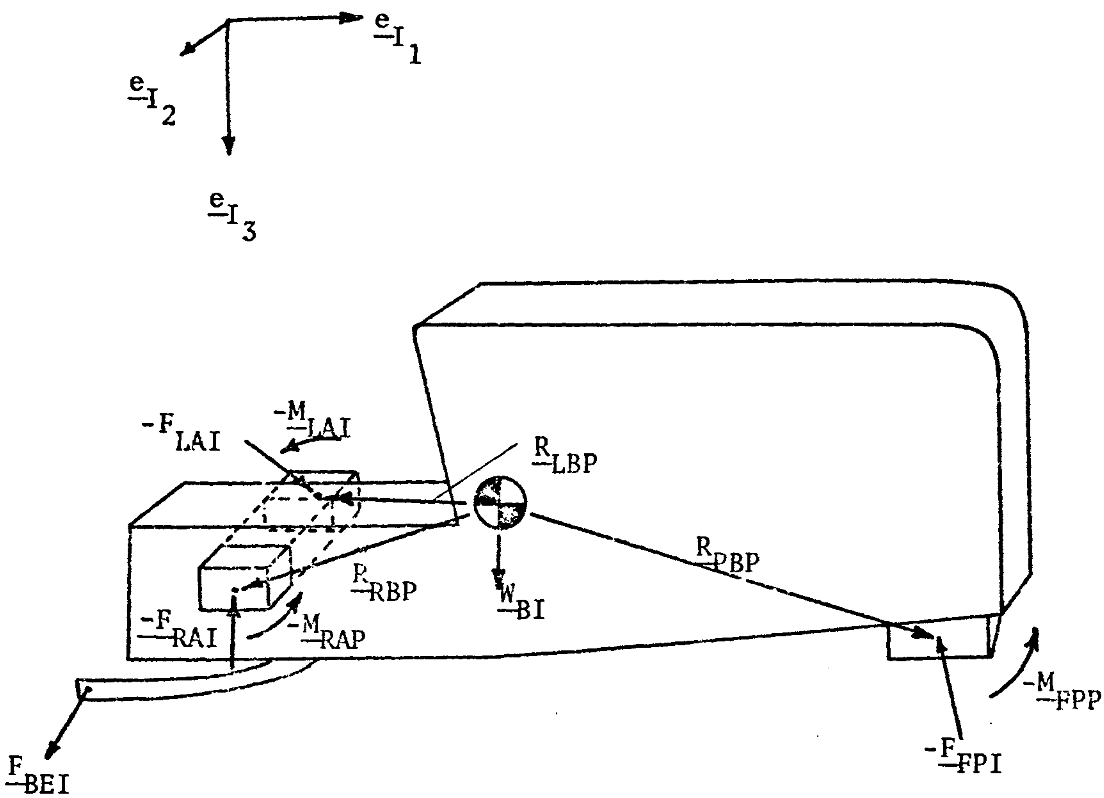

Figure 3-2. Free Body Diagram of the Tractor Body.

Substitution of equations 3-30 and 3-31 into equations 3-2 and 3-8 through 3-10 yields the translational and rotational differential equations for the tractor body in terms of the reactions on the body

$$\dot{\underline{V}}_{BI} = \frac{1}{m_B} (\underline{W}_{BI} - \underline{F}_{FPI} - \underline{F}_{LAI} - \underline{F}_{RAI} + \underline{F}_{BEI}) \tag{3-32}$$

and

$$\begin{aligned} \dot{\omega}_{BP_i} = \frac{-1}{I_{BP_{ii}}} [& M_{FPP_i} + (\underline{R}_{PBP} \times \underline{F}_{FPP})_i + M_{LAP_i} + M_{RAP_i} \\ & + (\underline{R}_{LBP} \times \underline{F}_{LAP})_i + (\underline{R}_{RBP} \times \underline{F}_{RAP})_i - M_{BEP_i} \\ & + (I_{BP_{jj}} - I_{BP_{kk}}) \omega_{BP_j} \omega_{BP_k}] \end{aligned} \tag{3-33}$$

where

$i = 1,2,3$ and

$j = 3$, $k = 2$ when $i = 1$

$j = 1$, $k = 3$ when $i = 2$

$j = 2$, $k = 1$ when $i = 3$.

3.2. The Rear Wheels

The rear wheels are constrained to move with the tractor body in all degrees of freedom except rotation about the rear axle. Thus each rear wheel has one degree of freedom - rotation in the $\underline{e}_{T_2}$ axis direction of the tractor.

The tractor body has a plane of symmetry perpendicular to the $\underline{e}_{T_2}$ axis and through the body center of mass; thus the $\underline{e}_{T_2}$ axis is a principal axis of that body. By similar reasoning the axis parallel to $\underline{e}_{T_2}$ is a principal axis of the rear wheels. Because the rear wheels are radially symmetric about the axle, any two axes which are normal to the axle and to one another are also principal axes of the rear wheels. For the above reasons and to simplify notation, the coordinate axes used in defining the rear wheel motions are the principal-axes directions of the tractor body. The origin for the rear wheel rotational equations, however, is the center of mass of the appropriate wheel.

The two rear wheel rotations are coupled to one another by the differential gears. If the $\underline{e}_{P_2}$ direction is the rear axle direction and R_2 is the differential speed ratio, then the drive-line speed ω_d is given by

$$\omega_d = \frac{1}{2} R_2 \left[(\omega_{LP_2} - \omega_{BP_2}) + (\omega_{RP_2} - \omega_{BP_2}) \right] . \qquad (3\text{-}34)$$

The kinetic energy of rotation for the rear wheel and drive train is given as

$$KE = \frac{1}{2} I_{LP_{22}} \omega_{LP_2}^2 + \frac{1}{2} I_{RP_{22}} \omega_{RP_2}^2 + \frac{1}{2} I_d \omega_d^2 , \qquad (3\text{-}35)$$

where I_d is the mass moment of inertia for the drive line, differential gears, and transmission as seen at the drive line, lb-in-sec^2, and

KE is the kinetic energy, in-lb.

Substitution of equation 3-34 into 3-35 and the use of Lagrange's equations yields the following two differential equations.

$$I_{LP_{22}}\dot{\omega}_{LP_2} + \frac{1}{4} I_d R_2^2 (\dot{\omega}_{LP_2} + \dot{\omega}_{RP_2}) = M_{LAP_2} + M_{LGP_2} \qquad (3\text{-}36)$$

$\dot{\omega}_{RP_2}$

and

$$I_{RP_{22}}\dot{\omega}_{RP_2} + \frac{1}{4} I_d R_2^2 (\dot{\omega}_{RP_2} + \dot{\omega}_{LP_2}) = M_{RAP_2} + M_{RGP_2} \; . \qquad (3\text{-}37)$$

$\dot{\omega}_{RP_2}$

Assuming that the differential gears transmit torque equally to each of the rear wheels (in the $-\underline{e}_{P_2}$ direction), the drive-line wheel torque relationship is

$$M_{LAP_2} = M_{RAP_2} = -\frac{1}{2} R_2 T_d \; . \qquad (3\text{-}38)$$

Also assuming that the rear wheel inertias are equal,

$$I_{RP_{22}} = I_{LP_{22}} \qquad (3\text{-}39)$$

and

$$m_R = m_L \; . \qquad (3\text{-}40)$$

The two equations of motion for the rear wheel rotational velocities about the axle are obtained by solving the equations 3-36 and 3-37 for $\dot{\omega}_{LP_2}$ and $\dot{\omega}_{RP_2}$.

$$\dot{\omega}_{LP_2} = [(- \frac{1}{2} R_2 T_d + M_{LGP_2})(I_{RP_{22}} + \frac{1}{4} R_2^2 I_d) - (- \frac{1}{2} R_2 T_d + M_{RGP_2})(\frac{1}{4} R_2^2 I_d)]/(I_{RP_{22}}^2 + \frac{1}{2} R_2^2 I_d I_{RP_{22}}) \tag{3-41}$$

and

$$\dot{\omega}_{RP_2} = [(- \frac{1}{2} R_2 T_d + M_{RGP_2})(I_{RP_{22}} + \frac{1}{4} R_2^2 I_d) - (- \frac{1}{2} R_2 T_d + M_{LGP_2})(\frac{1}{4} R_2^2 I_d)]/(I_{RP_{22}}^2 + \frac{1}{2} R_2^2 I_d I_{RP_{22}}) \tag{3-42}$$

Because $\underline{\omega}_{LP}$ and $\underline{\omega}_{RP}$ are absolute angular velocities, the angular rotation of the rear wheels about the axles can be obtained directly from integration of these angular velocities. Thus, the differential equations for the rear wheel rotations are

$$\dot{\theta}_{LP_2} = \omega_{LP_2} \tag{3-43}$$

and

$$\dot{\theta}_{RP_2} = \omega_{RP_2} \tag{3-44}$$

The constraints placed upon the rear wheels are expressed in equations 3-45 through 3-52.

$$\omega_{LP_1} = \omega_{RP_1} = \omega_{BP_1} \tag{3-45}$$

$$\omega_{LP_3} = \omega_{RP_3} = \omega_{BP_3} \tag{3-46}$$

$$\dot{\omega}_{LP_1} = \dot{\omega}_{RP_1} = \dot{\omega}_{BP_1} \tag{3-47}$$

$$\dot{\omega}_{LP_3} = \dot{\omega}_{RP_3} = \dot{\omega}_{BP_3} \tag{3-48}$$

$$\underline{V}_{LI} = \underline{V}_{BI} + (\underline{\omega}_{BI} \times \underline{R}_{LBI}) \tag{3-49}$$

$$\underline{V}_{RI} = \underline{V}_{BI} + (\underline{\omega}_{BI} \times \underline{R}_{RBI}) \tag{3-50}$$

$$\dot{\underline{V}}_{LI} = \dot{\underline{V}}_{BI} + (\dot{\underline{\omega}}_{BI} \times \underline{R}_{LBI}) + \underline{\omega}_{BI} \times (\underline{\omega}_{BI} \times \underline{R}_{LBI}) \tag{3-51}$$

$$\dot{\underline{V}}_{RI} = \dot{\underline{V}}_{BI} + (\dot{\underline{\omega}}_{BI} \times \underline{R}_{RBI}) + \underline{\omega}_{BI} \times (\underline{\omega}_{BI} \times \underline{R}_{RBI}) \tag{3-52}$$

The reactions between the rear wheels and the tractor body are based upon the above-cited constraints and the corresponding differential equations of motion for the constrained degrees of freedom. The equations relating the rear wheel rotations and the constraint forces are

$$M_{LP_1} = I_{LP_{11}}\dot{\omega}_{LP_1} + (I_{LP_{33}} - I_{LP_{22}})\omega_{LP_2}\omega_{LP_3} \tag{3-53}$$

$$M_{RP_1} = I_{RP_{11}}\dot{\omega}_{RP_1} + (I_{RP_{33}} - I_{RP_{22}})\omega_{RP_2}\omega_{RP_3} \tag{3-54}$$

$$M_{LP_3} = I_{LP_{33}}\dot{\omega}_{LP_3} + (I_{LP_{22}} - I_{LP_{11}})\omega_{LP_1}\omega_{LP_2} \tag{3-55}$$

and

$$M_{RP_3} = I_{RP_{33}}\dot{\omega}_{RP_3} + (I_{RP_{22}} - I_{RP_{11}})\omega_{RP_1}\omega_{RP_2} \tag{3-56}$$

The total moments acting on the left and right wheels, $\underline{M}_{LP}$ and $\underline{M}_{RP}$, are the resultants of the ground reactions and the axle reactions, thus

$$\underline{M}_{LP} = \underline{M}_{LGP} + \underline{M}_{LAP} \tag{3-57}$$

$$\underline{M}_{RP} = \underline{M}_{RGP} + \underline{M}_{RAP} \tag{3-58}$$

Combining equations 3-53 through 3-56 with equations 3-57 and 3-58, the following relationships result for the axle moment reactions:

$$M_{LAP_1} = I_{LP_{11}}\dot{\omega}_{LP_1} + (I_{LP_{33}} - I_{LP_{22}})\omega_{LP_2}\omega_{LP_3} - M_{LGP_1} \tag{3-59}$$

$$M_{RAP_1} = I_{RP_{11}}\dot{\omega}_{RP_1} + (I_{RP_{33}} - I_{RP_{22}})\omega_{RP_2}\omega_{RP_3} - M_{RGP_1} \tag{3-60}$$

$$M_{LAP_3} = I_{LP_{33}}\dot{\omega}_{LP_3} + (I_{LP_{22}} - I_{LP_{11}})\omega_{LP_1}\omega_{LP_2} - M_{LGP_3} \tag{3-61}$$

and

$$M_{RAP_3} = I_{RP_{33}}\dot{\omega}_{RP_3} + (I_{RP_{22}} - I_{RP_{11}})\omega_{RP_1}\omega_{RP_2} - M_{RGP_3} \; . \tag{3-62}$$

The relationships for the forces acting at the axle are similarly obtained by combining the translational differential equations of motion for the rear wheels with the appropriate constraints. The translational differential equations for the rear wheel centers of mass are thus

$$\underline{F}_{LI} = m_R\dot{\underline{V}}_{LI} \tag{3-63}$$

and

$$\underline{F}_{RI} = m_R\dot{\underline{V}}_{RI} \; . \tag{3-64}$$

The total forces acting on the rear wheels include the ground forces, the axle forces, and the gravitational forces,

$$\underline{F}_{LI} = \underline{F}_{LGI} + \underline{F}_{LAI} + \underline{W}_{LI} \tag{3-65}$$

and

$$\underline{F}_{RI} = \underline{F}_{RGI} + \underline{F}_{RAI} + \underline{W}_{RI} \; . \tag{3-66}$$

Combination of equations 3-63 and 3-64 with equations 3-65 and 3-66 yields expressions for the forces at the axles in terms of the wheel center-of-mass accelerations, the ground forces, and the gravitational forces,

$$\underline{F}_{LAI} = m_R\dot{\underline{V}}_{LI} - \underline{F}_{LGI} - \underline{W}_{LI} \tag{3-67}$$

and

$$\underline{F}_{RAI} = m_R\dot{\underline{V}}_{RI} - \underline{F}_{RGI} - \underline{W}_{RI} \tag{3-68}$$

3.3. The Tractor Front End

The tractor front end is defined as that portion of the tractor which rotates about the front pin of a wide-front-end tractor. The pin axis is assumed to be parallel to the number one tractor axis, $\underline{e}_{T_1}$. The front end has one degree of freedom, rotation relative to the tractor body about the front pin axis.

The dynamic equations of motion for the front end are written about the center of mass of the front end. A set of coordinate axes (called the front-end axes and denoted by the subscript F) are defined such that $\underline{e}_{F_1}$ is parallel to the front pin (positive forward), $\underline{e}_{F_2}$ is parallel to the transverse framework of the front end (positive to the right), and $\underline{e}_{F_3}$ is the direction of the vector cross product of $\underline{e}_{F_1}$ and $\underline{e}_{F_2}$ (positive down). (See Figure 3-3).

Because the tractor front end is symmetric about the plane

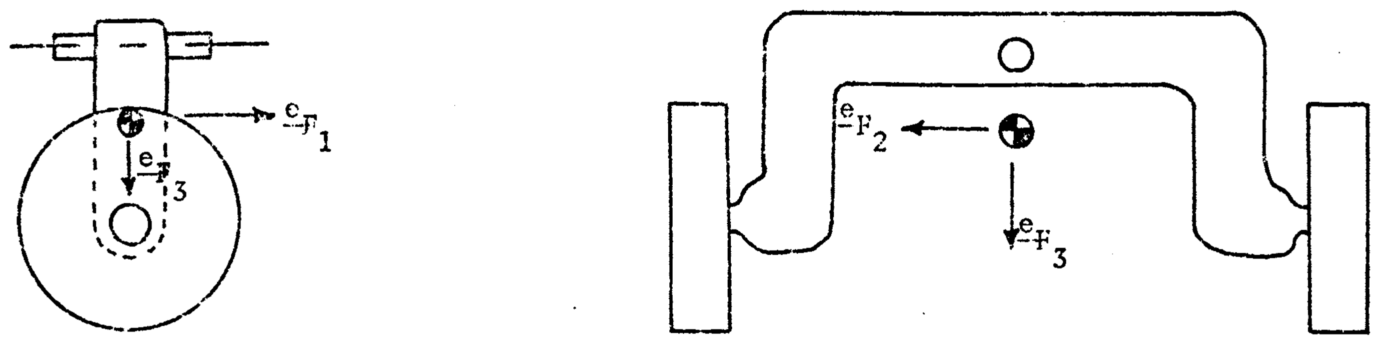

View from Right Side　　　　Front View

Figure 3-3. The Coordinate Directions for the Tractor Front End.

perpendicular to unit vector $\underline{e}_{F_2}$ and passing through the center of mass, the only nonzero products of inertia in the front end mass moment of inertia matrix are $I_{FF_{13}}$ and $I_{FF_{31}}$ which are equal to one another. This results in a rotational equation of motion about the front end center of mass and parallel to the pin axis which is simplified from the general equation about an axis that is not a principal axis.

$$\dot{\omega}_{FF_1} = \frac{1}{I_{FF_{11}}} [-I_{FF_{13}}(\dot{\omega}_{FF_3} + \omega_{FF_1}\omega_{FF_2}) - (I_{FF_{33}} - I_{FF_{22}})\omega_{FF_2}\omega_{FF_3} + M_{FF_1}] \quad (3\text{-}69)$$

The angular rotation about the $\underline{e}_{F_1}$ axis can be obtained directly from integration of the angular velocity about that axis, ω_{FF_1}, but a more meaningful parameter is the relative angular position between the tractor body and the front end. Defining θ_{FF_1} as the angle of front-end rotation about the front pin relative to the tractor body, θ_{FF_1} can be obtained by integrating the equation,

$$\dot{\theta}_{FF_1} = \omega_{FF_1} - \omega_{BF_1} . \quad (3\text{-}70)$$

The motion constraints applied to the tractor front end by the front pin are:

$$\omega_{FF_2} = \omega_{BF_2} \tag{3-71}$$

$$\omega_{FF_3} = \omega_{BF_3} \tag{3-72}$$

$$\dot{\omega}_{FF_2} = \dot{\omega}_{BF_2} \tag{3-73}$$

$$\dot{\omega}_{FF_3} = \dot{\omega}_{BF_3} \tag{3-74}$$

$$\underline{V}_{FI} = \underline{V}_{BI} + (\underline{\omega}_{BI} \times \underline{R}_{PBI}) + (\underline{\omega}_{FI} \times \underline{R}_{FPI}) \tag{3-75}$$

and

$$\dot{\underline{V}}_{FI} = \dot{\underline{V}}_{BI} + (\dot{\underline{\omega}}_{BI} \times \underline{R}_{PBI}) + \underline{\omega}_{BI} \times (\underline{\omega}_{BI} \times \underline{R}_{PBI})$$
$$+ (\dot{\underline{\omega}}_{FI} \times \underline{R}_{FPI}) + \underline{\omega}_{FI} \times (\underline{\omega}_{FI} \times \underline{R}_{FPI}) \, . \tag{3-76}$$

The differential equations for front-end rotation in the constrained directions can be used to obtain relationships for the constraining forces and moments. Rearrangement of the equations of motion for the constrained component directions yields the two pin moments and the pin forces,

$$M_{FF_2} = I_{FF_2}\dot{\omega}_{FF_2} + (I_{FF_{11}} - I_{FF_{33}})\omega_{FF_1}\omega_{FF_3}$$
$$+ I_{FF_{13}}(\omega^2_{FF_3} - \omega^2_{FF_1}) \, , \tag{3-77}$$

$$M_{FF_3} = I_{FF_{33}}\dot{\omega}_{FF_3} + I_{FF_{13}}(\dot{\omega}_{FF_1} - \omega_{FF_2}\omega_{FF_3})$$
$$+ (I_{FF_{22}} - I_{FF_{11}})\omega_{FF_1}\omega_{FF_2} \, , \tag{3-78}$$

and

$$\underline{F}_{FI} = m_F\dot{\underline{V}}_{FI} \tag{3-79}$$

The total moment reaction about the front-end center of mass and the total force acting upon the front end are composed of pin reactions, ground reactions, and the front-end weight,

$$\underline{M}_{FF} = \underline{M}_{FPF} + \underline{M}_{FGF} - (\underline{R}_{FPF} \times \underline{F}_{FPF}) \tag{3-80}$$

and

$$\underline{F}_{FI} = \underline{F}_{FPI} + \underline{F}_{FGI} + \underline{W}_{FI} \ . \tag{3-81}$$

The front pin reactions are obtained from combinations of equations 3-77 through 3-79 with equations 3-80 and 3-81, and are given by

$$\underline{F}_{FPI} = m_F \underline{\dot{V}}_{FI} - \underline{F}_{FGI} - \underline{W}_{FI} \tag{3-82}$$

$$\begin{aligned} M_{FPF_2} &= I_{FF_{22}} \dot{\omega}_{FF_2} + (I_{FF_{11}} - I_{FF_{33}}) \omega_{FF_1} \omega_{FF_3} \\ &\quad + I_{FF_{13}} (\omega^2_{FF_3} - \omega^2_{FF_1}) - M_{FGF_2} + (\underline{R}_{FPF} \times \underline{F}_{FPF})_2 \ , \end{aligned} \tag{3-83}$$

and

$$\begin{aligned} M_{FPF_3} &= I_{FF_{33}} \dot{\omega}_{FF_3} + I_{FF_{13}} (\dot{\omega}_{FF_1} - \omega_{FF_2} \omega_{FF_3}) \\ &\quad + (I_{FF_{22}} - I_{FF_{11}}) \omega_{FF_1} \omega_{FF_2} - M_{FGF_3} \\ &\quad + (\underline{R}_{FPF} \times \underline{F}_{FPF})_3 \ . \end{aligned} \tag{3-84}$$

3.4. Tire-Ground Interaction

The tire-ground interaction is determined from the position and velocity of a thin, radially-deformable wheel relative to a locally-planar, rigid ground surface. The tire is assumed to contact the ground surface at a single point (the "ground-contact point") while all ground reactions occur at this point. Because the ground surface beneath the wheel may be irregular (i.e., not identified by a single plane), two different tire models may be used to determine the tire-ground interaction. When the ground is irregular, an enveloping-tire model redefines the ground surface to conform to the locally-planar assumption cited above.

A ground scanning technique is used to define the state of the local terrain and thus select the appropriate tire model for a given tire location. The following section describes the ground-scanning process.

3.4.1. Selecting the Appropriate Tire Model

Each time that the tire-ground interaction is to be determined, the appropriate tire model must be chosen to fit the ground surface conditions. If the ground surface is identified as a single plane beneath the wheel, the ground is called "smooth" and the point-contact tire model of Section 3.4.3 is used. Otherwise, the surface is "irregular" and the enveloping-tire model of Section 3.4.2 is used to redefine the local terrain to fit the planar requirement.

The ground surface is checked at three points beneath the wheel to determine if the surface is smooth or irregular. If all three points locate regions of the ground surface which are part of the same plane, the ground is smooth; otherwise, the ground is irregular. The three ground points are those points vertically above or below three corresponding points defined on the wheel circumference. These circumferential points are defined by wheel-coordinate directions from the wheel center - one in the "down" direction, one forty-five degrees "ahead" of down, and one forty-five degrees "behind" down. Figure 3-4 shows the points and notation used in scanning the ground surface.

The ground elevations and ground normal vectors at the three ground points provide the necessary information for determining whether or not they lie on the same plane. The three points are on the same plane only if the ground normal vectors at the three points are parallel to one another and the vectors connecting the three points are perpendicular to the common ground normal vector. The first condition expressed mathematically is

$$\underline{U}_{GI} \cdot \underline{U}_{GPI_a} = 1 \ , \tag{3-85}$$

and

$$\underline{U}_{GI} \cdot \underline{U}_{GPI_b} = 1 \ , \tag{3-86}$$

where

$\underline{U}_{GI}$ is the ground normal vector for the "down" point,

$\underline{U}_{GPI_a}$ is the ground normal vector for the "ahead" point, and

$\underline{U}_{GPI_b}$ is the ground normal vector for the "behind" point.

The second condition for points common to a single plane may be expressed

$$(\underline{X}_{P1I} - \underline{X}_{WGI}) \cdot \underline{U}_{GI} = 0 \tag{3-87}$$

and

$$(\underline{X}_{P2I} - \underline{X}_{WGI}) \cdot \underline{U}_{GI} = 0 \ , \tag{3-88}$$

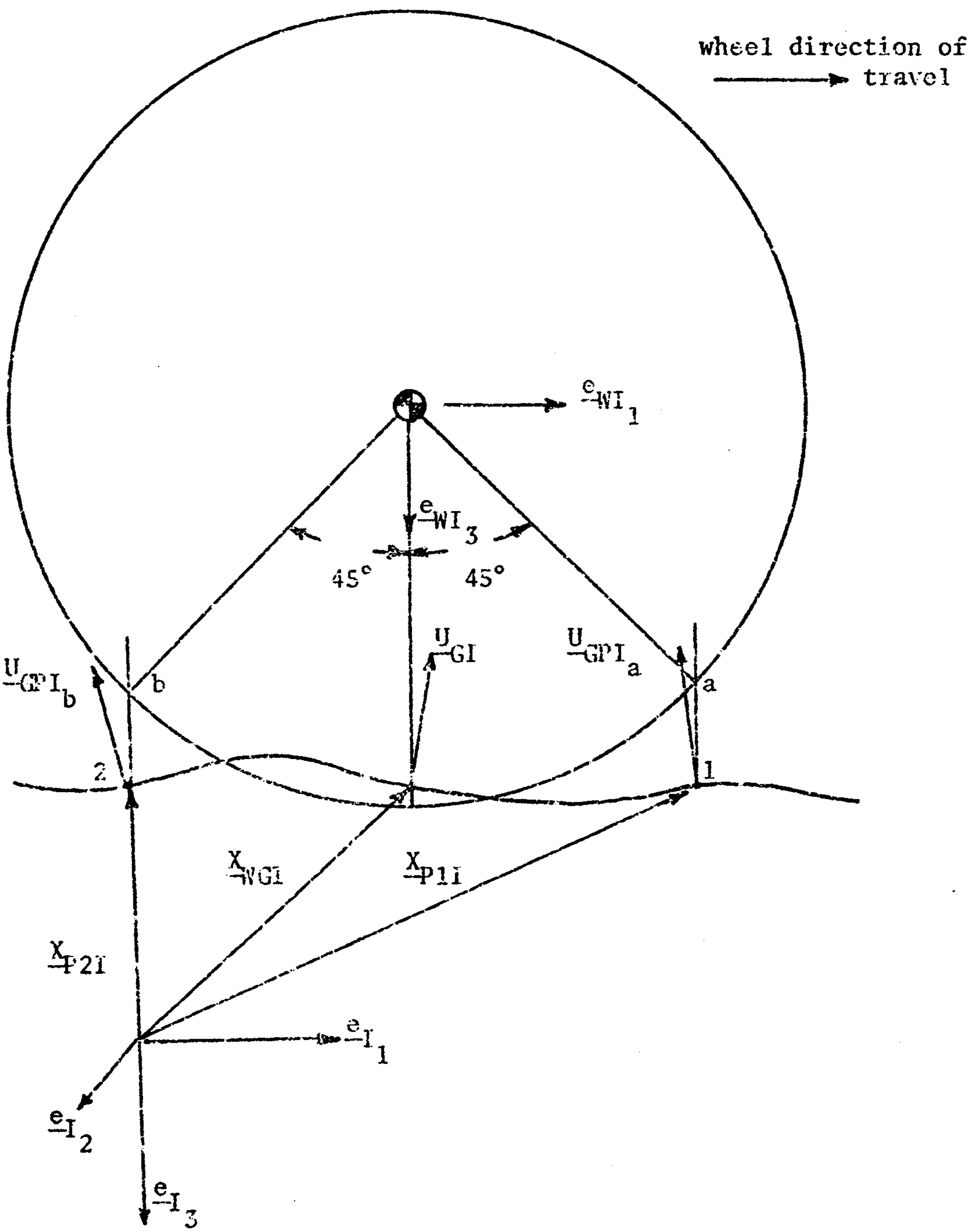

Figure 3-4. Tire Scanning the Ground Surface.

where

$\underline{X}_{WGI}$ is the location of the ground point "below" the wheel center,

$\underline{X}_{P1I}$ is the location of the ground point "ahead" of the wheel center, and

$\underline{X}_{P2I}$ is the location of the ground point "behind" the wheel center.

All the above conditions must be checked before a ground surface is identified as smooth, but as soon as one of these conditions is not satisfied, the ground has been identified as irregular.

3.4.2. The Enveloping-Tire Model

The enveloping-tire model envelopes an irregular ground surface and defines an "equivalent ground plane" for the region of the ground surface contacted by the tire. The enveloping features of the tire are provided by a radial-spring concept described by Albert (1961); however, specific details in the determination of radial spring deflections and force magnitudes have been modified to improve calculation efficiency and adapt the model to tabulated tire force data.

Equivalence of the irregular surface and the "equivalent ground plane" is defined by the following constraints:

1. The radial tire force direction must reflect the sum effect of incremental radial tire deformations at points of tire-ground contact.
2. The radial tire force magnitude must reflect the total displaced volume (or, displaced area for a thin wheel)

of the tire.

3. The equivalent ground plane must displace the same tire volume as does the irregular surface.

4. The equivalent ground plane orientation must conform to both the regional ground orientation (reflected by the radial force direction) and the orientation of the actual ground surface at the newly defined ground-contact point.

The radial spring tire model used to envelope the irregular ground surface is shown in Figure 3-5. Radial springs are spaced at 5 degree increments both behind and ahead of the "down" wheel-axis direction to encompass the wheel segments 40 degrees ahead to 40 degrees behind the $\underline{e}_{WI_3}$ direction. Each radial spring may intersect the ground surface and thus be deflected radially by the rigid ground surface.

Because the ground elevation is defined for each pair of coordinates in a horizontal plane, the generally non-vertical radial spring moves over generally different ground elevations as it is compressed. Thus the point of spring-ground intersection must be determined by either an iterative method or an approximate interpolation method. Albert (1961) used an iterative method, shortening the spring incrementally until intersection was detected, but a linear interpolation method was chosen here to limit the number of calculation steps.

The point of radial spring-ground surface intersection is defined by the following procedure:

1. Determine the ground elevation vertically above or below

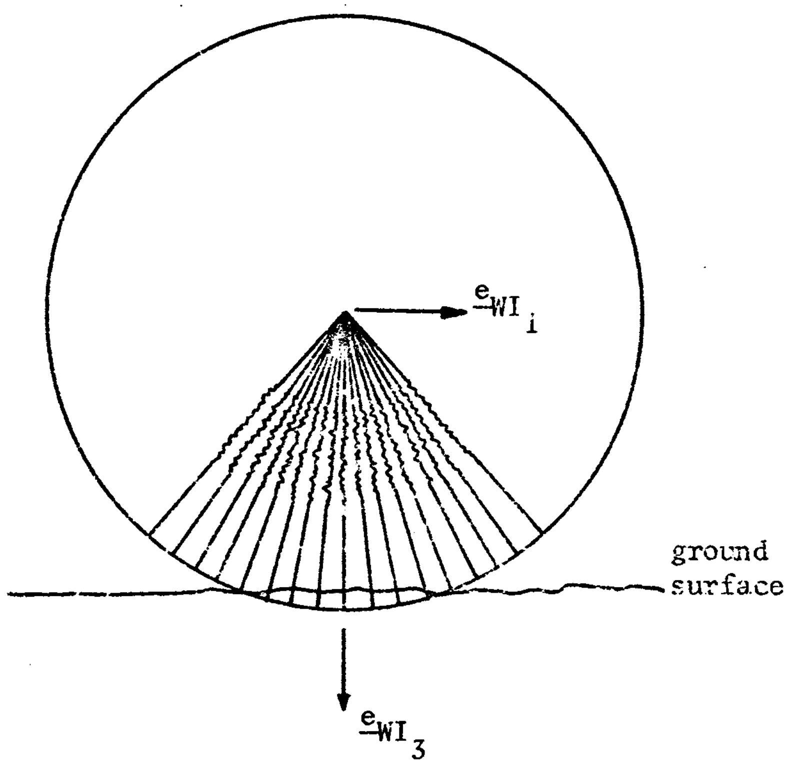

Figure 3-5. Radial-Spring Tire Model.

the end of the undeflected radial spring.

2. Determine the ground elevation vertically above or below the end of the radial spring when deflected a predetermined amount.

3. Use linear interpolation to define the total spring deflection required to make the elevation difference between the spring end and the ground surface equal to zero.

The radial spring deflection is defined by the similar triangles shown in Figure 3-6 and expressed mathematically as

$$dr_2 = \frac{E_o}{E_0 - E_1} dr_1 \,, \tag{3-89}$$

where

dr_1 is the trial spring deflection used in item (2) above, in,

E_o is the difference between the ground elevation and the spring-end elevation when the radial spring is undeflected, in,

E_1 is the difference between the ground elevation and the spring-end elevation when the radial spring is deflected the trial value (dr_1), in, and

dr_2 is the spring deflection at which the linear interpolation predicts intersection of the spring and ground surface, in.

The ground elevation for the undeflected spring position (0) is that at point (a), the elevation for the trial-deflection position

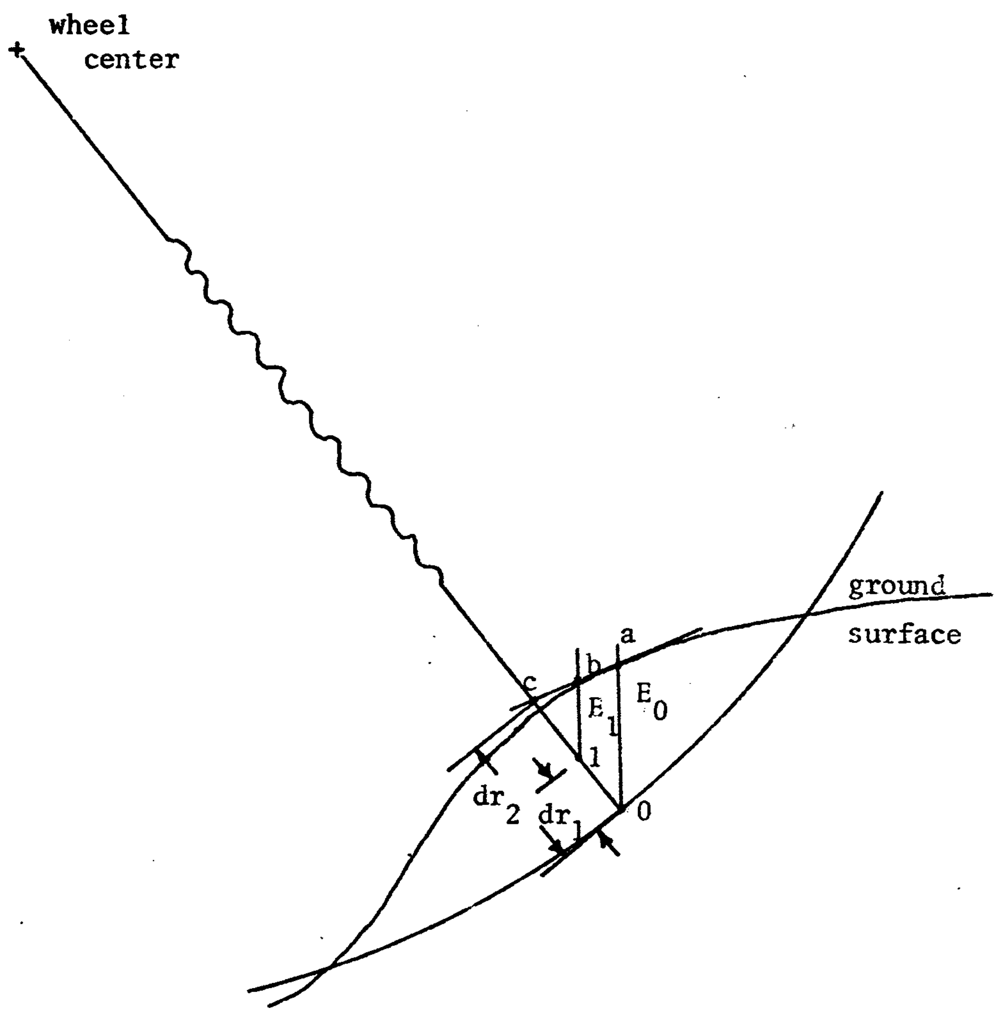

Figure 3-6. Determination of the Radial Spring Deflection.

(1) is that at (b), and the interpolated elevation for equal elevation of the spring end and ground is that at point (c).

The experimentally-measured radial force-deflection relationships for tires on flat, rigid surfaces assume that the maximum radial tire deflection is given by

$$d_{max} = r(1 - \cos \frac{\theta_T}{2}) \tag{3-90}$$

and individual radial deflections at an angle from this maximum deflection line are given by

$$d = r \left[1 - \left(\frac{\cos \frac{\theta_T}{2}}{\cos \phi} \right) \right] . \tag{3-91}$$

where

- r is the undeflected tire radius, in,
- θ_T is the angle within which the tire is radially deformed on the rigid, flat surface, rad,
- ϕ is the angle from the perpendicular bisector of the contact-patch arc to the radial line of interest, rad,
- d is the radial deflection of the tire along the line defined by ϕ , in, and
- d_{max} is the maximum radial tire deflection for the tire on a flat, rigid surface when the arc of the contact patch is θ_T , in.

The deflection relationships are shown in Figure 3-7. Because the experimental force-deflection data are tabulations of radial tire force vs. d_{max} , this data can be used only indirectly in defining the

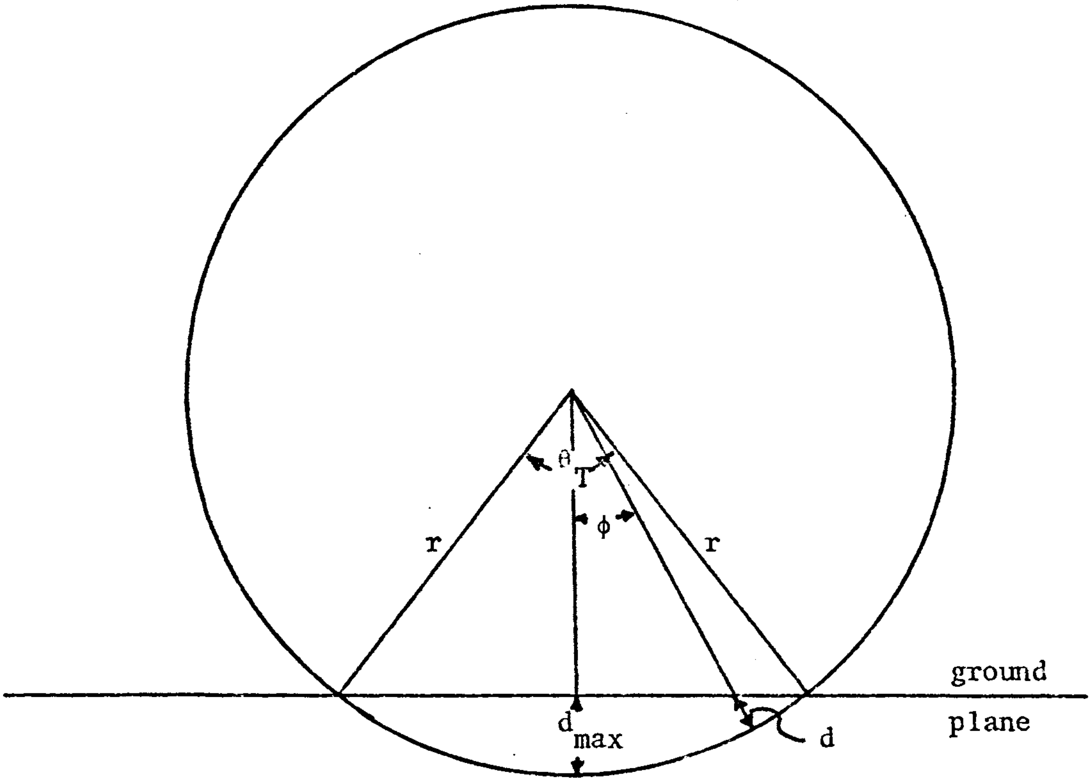

Figure 3-7. Radial Tire Deflection on a Rigid, Flat Surface.

radial tire force due to deformation by an irregular ground surface.

The direction of the radial tire force when the tire is on an irregular ground surface is defined by the direction of the resultant of the individual radial force vectors associated with each of the radial spring deflections. Because the actual force associated with the deflection of one incremental segment of the tire circumference is not known, the individual deflections are "weighted" by the force-deflection curve for the tire. Thus, because the incremental deflections are "weighted" and summed to obtain a resultant force, the direction of the resultant redial force is realistic but the magnitude is not. The line-of-action for the radial tire force is parallel to the resultant radial force vector while passing through the wheel center.

The magnitude of the resultant radial tire force is determined by the tire area displaced by the irregular ground surface and the force-area relationship for the tire on a flat, rigid surface. The displaced tire area when the tire is on a rigid, flat surface with a contact patch arc of θ_T radians is

$$A_S = \frac{1}{2} r^2 (\theta_T - \sin \theta_T) \ , \tag{3-92}$$

where

A_S is the displaced area on the smooth surface, in^2.

The total arc of the contact patch for a tire on an irregular surface may be approximated by the summation of incremental arcs for the deflected segments,

$$\theta_T = \sum_{i=1}^{N} \Delta\theta_i = N\Delta\theta \tag{3-93}$$

and the displaced tire area may be approximated by summing the incremental areas of the deflected segments,

$$A_T = \sum_{i=1}^{N} (r\,d_i - \frac{1}{2}\,d_i^2)\Delta\theta \tag{3-94}$$

where

A_T is the total tire area displaced by the irregular ground surface over N deflected incremental arcs (each of $\Delta\theta$ radians), in^2, and

θ_T is the total contact arc defined by the sum of N deflected arcs (each of $\Delta\theta$ radians), rad.

Because the areas A_S and A_T are calculated for the same arc of contact, an equivalent deflection is defined from the ratio of these two areas and the maximum deflection associated with A_S,

$$d_e = \frac{A_S}{A_T}\,d_{max}\ , \tag{3-95}$$

where

d_e is the equivalent deflection for the tire on the irregular ground surface, in, and

d_{max} is the deflection defined in equation 3-90, in.

The equivalent deflection defines the maximum deflection for the tire on the equivalent ground plane; therefore, it also defines the ground-contact point for the tire on the equivalent ground plane. The radial tire force magnitude is obtained directly from the tire force-deflection data and this equivalent deflection value. Figure 3-8 shows the tire on an irregular surface with the equivalent ground plane superimposed.

The line-of-intersection for the wheel and equivalent ground plane is that line in the ground plane passing through the equivalent ground-contact point while being perpendicular to the resultant radial tire force vector. The orientation of the equivalent ground plane is determined by the following procedure:

1. Determine the ground normal vector for the original ground surface vertically above or below the equivalent ground-contact point.
2. Temporarily define the equivalent ground plane as that plane which has the normal vector of (1) while passing through the equivalent ground-contact point.
3, Rotate the ground plane about an axis, passing through the ground-contact point and parallel to the axle of the wheel, until the ground plane intersects the wheel at the line in the wheel plane which is perpendicular to the resultant radial force vector.

The equivalent ground plane now includes all the features required for the calculation of the remaining tire reactions in the same manner as is done for a tire on a smooth ground surface. These remaining tire reactions are discussed in Section 3.4.4.

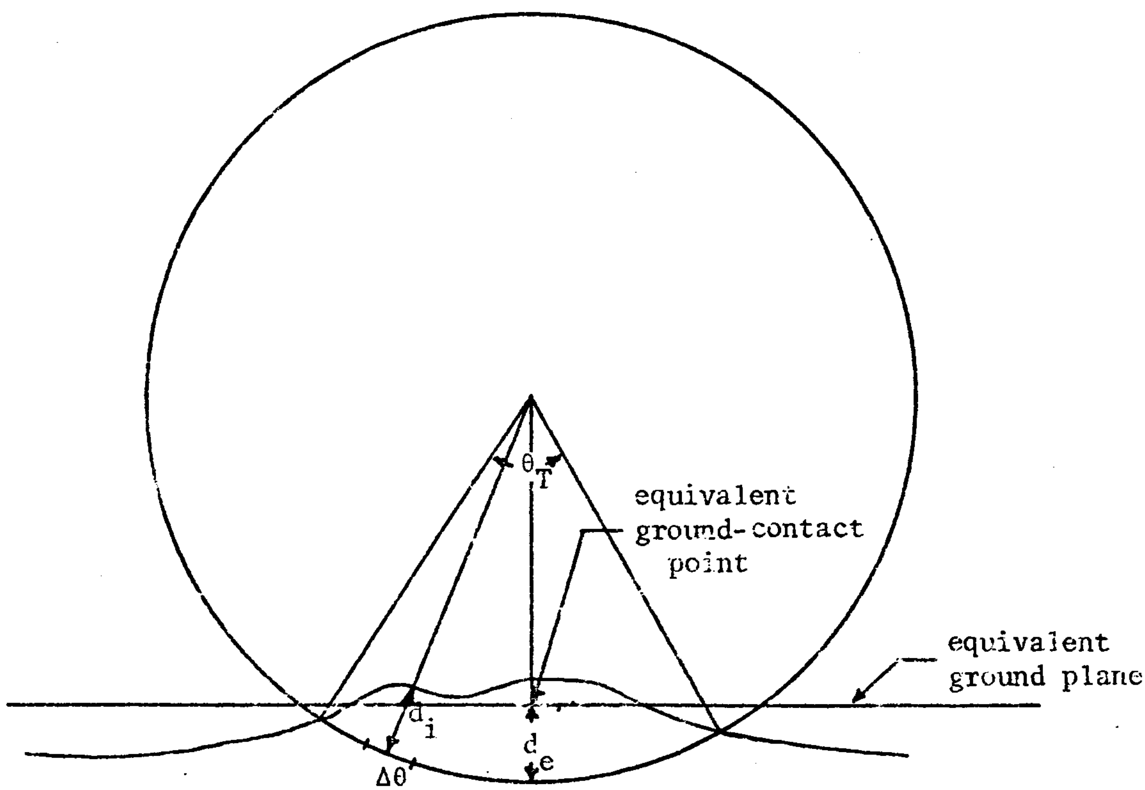

Figure 3-8. Radial Tire Deflection on an Irregular Ground Surface.

3.4.3. The Point-Contact Tire Model

The point-contact tire model is used to define the tire-ground interactions when the ground surface is planar in the region of the tire contact patch. This model is used to define the radial tire force, the lateral tire force, and the circumferential tire forces; however, only the radial force derivation is discussed in this section. Because the lateral and circumferential tire forces are defined in the same manner whether the ground surface was initially smooth or if the initially irregular surface was redefined as an equivalent plane (in Section 3.4.2), the derivations of these forces are presented in Section 3.4.4.

The point-contact tire model is based upon the definition of a single point of wheel-ground contact, the "ground-contact point," through which all the tire-ground forces act. Because this single-point contact does not allow the tire to sense the ground conditions at the other points within the tire contact patch, its use is limited to ground surfaces which satisfy the following conditions:

1. The surface in the path of the wheel has no step changes in its elevation or slope.
2. The wave length of the ground surface is at least three times the tire-ground contact patch length (Albert, 1961).
3. The elevation and slope of the ground surface within the tire-ground contact patch may be defined by the plane tangent to the ground surface at the "ground-contact point."

The ground-contact point is defined as the point-of-intersection for the following three planes:

1. the wheel plane,
2. the ground surface plane, and
3. the plane which passes through the wheel center while also containing in it the normal vectors of the wheel plane and the ground plane.

The unit normal vectors for these three planes in terms of the inertial-coordinate directions are, respectively, $\underline{U}_{WI}$, $\underline{U}_{GI}$, and $\underline{U}_{WGI}$, where

$$\underline{U}_{WGI} = \underline{U}_{GI} \times \underline{U}_{WI} \ . \qquad (3\text{-}96)$$

The unit vector $\underline{U}_{WGI}$ is parallel to the line-of-intersection for the wheel plane and the ground plane. Figure 3-9 shows the three planes, the corresponding unit normal vectors, and the ground-contact point.

The point-of-intersection for three planes is determined by solving simultaneously the three equations of those three planes for the coordinates of their common point. The equation for each plane is defined by equating to zero the expression for the dot product of the plane's normal vector and a second vector which lies in the plane. In each case the line in the plane of interest is defined to be the line from a known point in the plane to the unknown location of the ground-contact point.

If $\underline{X}_{WGI}$ is the ground-contact point location and $\underline{X}_{CI}$ defines the wheel center location, the equation for the wheel plane is obtained from

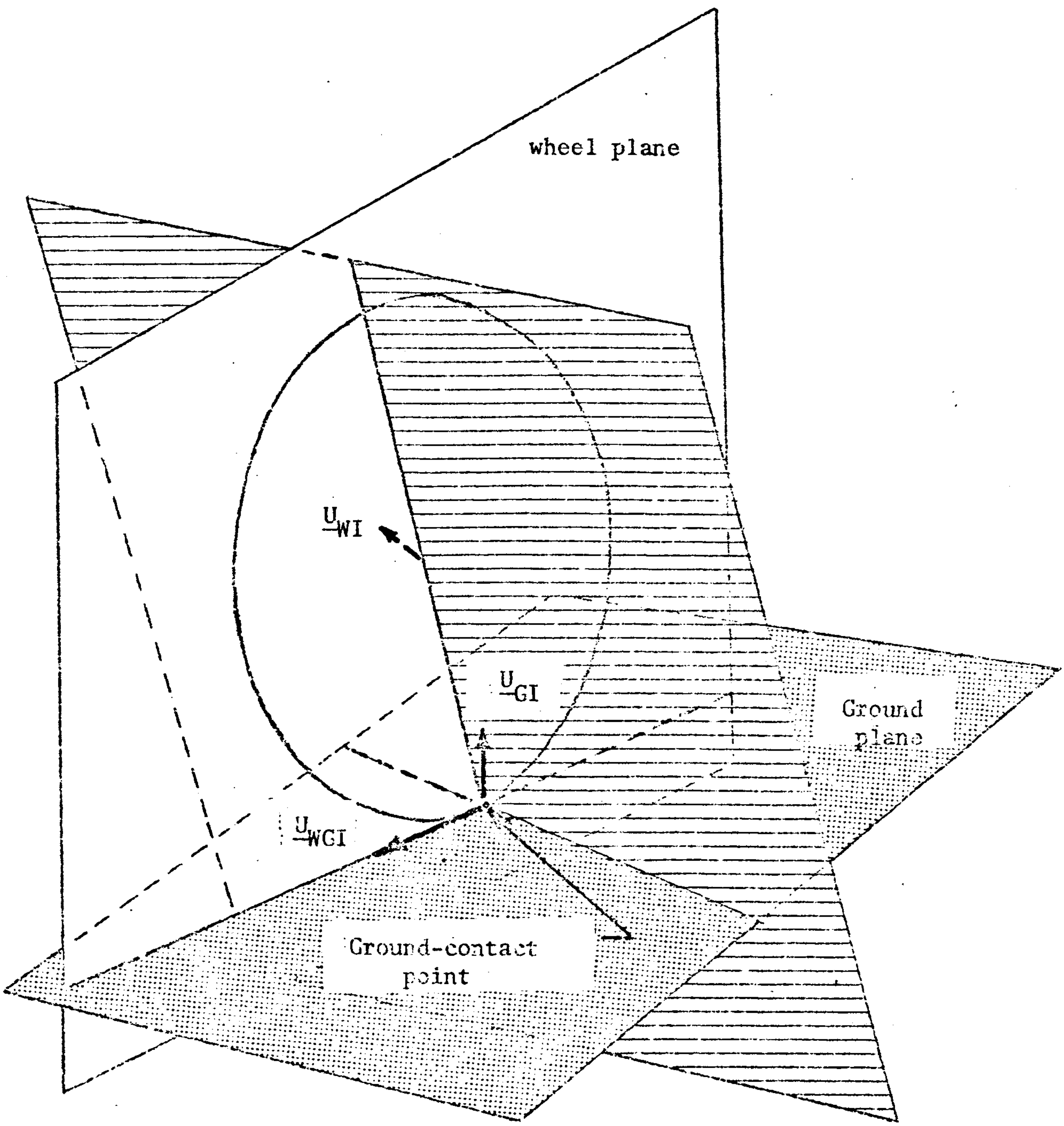

Figure 3-9. Definition of the Ground-Contact Point.

$$(\underline{X}_{WGI} - \underline{X}_{CI}) \cdot \underline{U}_{WI} = 0 \; . \tag{3-97}$$

If $\underline{X}_{GI}$ defines the location of a point on the ground surface in the region of the ground-contact point (assumed to be in the same ground plane), the ground plane equation is obtained from

$$(\underline{X}_{WGI} - \underline{X}_{GI}) \cdot \underline{U}_{GI} = 0 \; . \tag{3-98}$$

The third plane is defined by the dot product

$$(\underline{X}_{WGI} - \underline{X}_{CI}) \cdot \underline{U}_{WGI} = 0 \; . \tag{3-99}$$

Simultaneous consideration of the expanded form of equations 3-97 through 3-99 yields the following matrix equation including the unknown ground-contact point location, $\underline{X}_{WGI}$.

$$\begin{bmatrix} U_{WI_1} & U_{WI_2} & U_{WI_3} \\ U_{GI_1} & U_{GI_2} & U_{GI_3} \\ U_{WGI_1} & U_{WGI_2} & U_{WGI_3} \end{bmatrix} \begin{Bmatrix} X_{WGI_1} \\ X_{WGI_2} \\ X_{WGI_3} \end{Bmatrix} = \begin{Bmatrix} \underline{X}_{CI} \cdot \underline{U}_{WI} \\ \underline{X}_{GI} \cdot \underline{U}_{GI} \\ \underline{X}_{CI} \cdot \underline{U}_{WGI} \end{Bmatrix} \; . \tag{3-100}$$

Solution of equation 3-100 for the ground-contact point, $\underline{X}_{WCI}$, can be accomplished easily by use of Cramer's rule or some other method for solving sets of linear equations (Conte, 1965).

The vector from the wheel center to the ground-contact point is defined by

$$\underline{R}_{WGCI} = \underline{X}_{WGI} - \underline{X}_{CI} \; . \tag{3-101}$$

The radial tire deflection is the difference between the undeflected radius, r , and the length of the deflected-radius vector, $\underline{R}_{WGCI}$,

$$d = r - \left|\underline{R}_{WGCI}\right| . \tag{3-102}$$

Thus the radial tire force is determined from the tabulated force-deflection data for this tire and the specific deflection value, d . The remaining tire-ground reactions are obtained in the same manner whether the ground surface was initially planar or if it was initially irregular and then redefined as an equivalent ground plane. The derivations of these reactions are presented in Section 3.4.4.

3.4.4. Tire-Ground Interactions Common to Both Tire Models.

Once the tire-ground contact point and the ground plane beneath the tire have been defined, the tire reactions are independent of any ground irregularities which actually may be present beneath the tire. The tire may be represented as a parallel combination of a nonlinear spring and a linearly viscous dashpot between the wheel center and the ground-contact point. Thus, the radial component of the total tire-ground reaction is defined by the position and velocity of the wheel center relative to the ground-contact point.

The radial tire force may be expressed as the sum of the spring and dashpot reactions in the $\underline{U}_{RI}$ direction,

$$F_r = - F_s - F_d \tag{3-103}$$

where

F_s is the spring force, lb,

F_d is the dashpot force, lb, and

F_r is the total radial tire force, lb.

The spring force is defined by the tabulated force-deflection data for the tire on a flat, rigid surface with the specific tire deflection value, d , derived in the appropriate Section 3.4.2 or 3.4.3. The damping force has a non-zero value only when the tire deflection is greater than zero and decreasing.

$$F_d = C_d(\underline{V}_{CI} \cdot \underline{U}_{RI}) \quad \text{when} \begin{cases} d > 0 \text{ , and} \\ \underline{V}_{CI} \cdot \underline{U}_{RI} < 0 \end{cases} \tag{3-104}$$

or

$$F_d = 0 \quad \text{when} \begin{cases} d \leq 0 \text{ , or} \\ \underline{V}_{CI} \cdot \underline{U}_{RI} \geq 0 \end{cases} \tag{3-105}$$

where

C_d is the tire viscous damping coefficient, lb-sec/in,

$\underline{U}_{RI}$ is the unit vector directed from the wheel center to the ground-contact point, and

$\underline{V}_{CI}$ is the velocity of the wheel center, in/sec.

The velocity of the wheel center is determined differently for front and rear wheels:

For rear wheels -

$$\underline{V}_{CI} = \underline{V}_{BI} + \underline{\omega}_{BI} \times \underline{R}_{CBI} \tag{3-106}$$

For front wheels -

$$\underline{V}_{CI} = \underline{V}_{BI} + \underline{\omega}_{BI} \times \underline{R}_{PBI} + \underline{\omega}_{FI} \times \underline{R}_{CPI} \ . \tag{3-107}$$

Complete definition of the tire-ground reaction includes rolling resistance, traction, and lateral forces in addition to the radial component of the total tire force. Figure 3-10 shows the unit vectors used to define both the relative wheel-ground orientation and the directions of the tire force components to be discussed. The radial force is defined in the $\underline{U}_{RI}$ direction, the normal (to the ground) force in the $\underline{U}_{GI}$ direction, the lateral force in the $\underline{U}_{LI}$ direction, while the traction and rolling resistance forces are defined in the $\underline{U}_{WGI}$ direction.

The circumferential tire unit vector, $\underline{U}_{WGI}$, (defined by equation 3-96) is parallel to both the wheel plane and the ground plane and thus defines the direction of the line-of-intersection for these two planes. The lateral force unit vector, $\underline{U}_{LI}$, also parallel to the ground plane, is defined by the cross product of the circumferential force unit vector and the ground normal vector,

$$\underline{U}_{LI} = \underline{U}_{WGI} \times \underline{U}_{GI} \; . \tag{3-108}$$

Because $\underline{U}_{GI}$, $\underline{U}_{WGI}$, and $\underline{U}_{LI}$ are mutually perpendicular unit vectors, and because the tire forces are frequently defined as functions of the normal (to the ground) force component, the total tire-ground force is defined as

$$\underline{F}_{WGI} = F_n \underline{U}_{GI} + F_c \underline{U}_{WGI} + F_\ell \underline{U}_{LI} \; , \tag{3-109}$$

where

F_n is the normal (to the ground) force, lb,

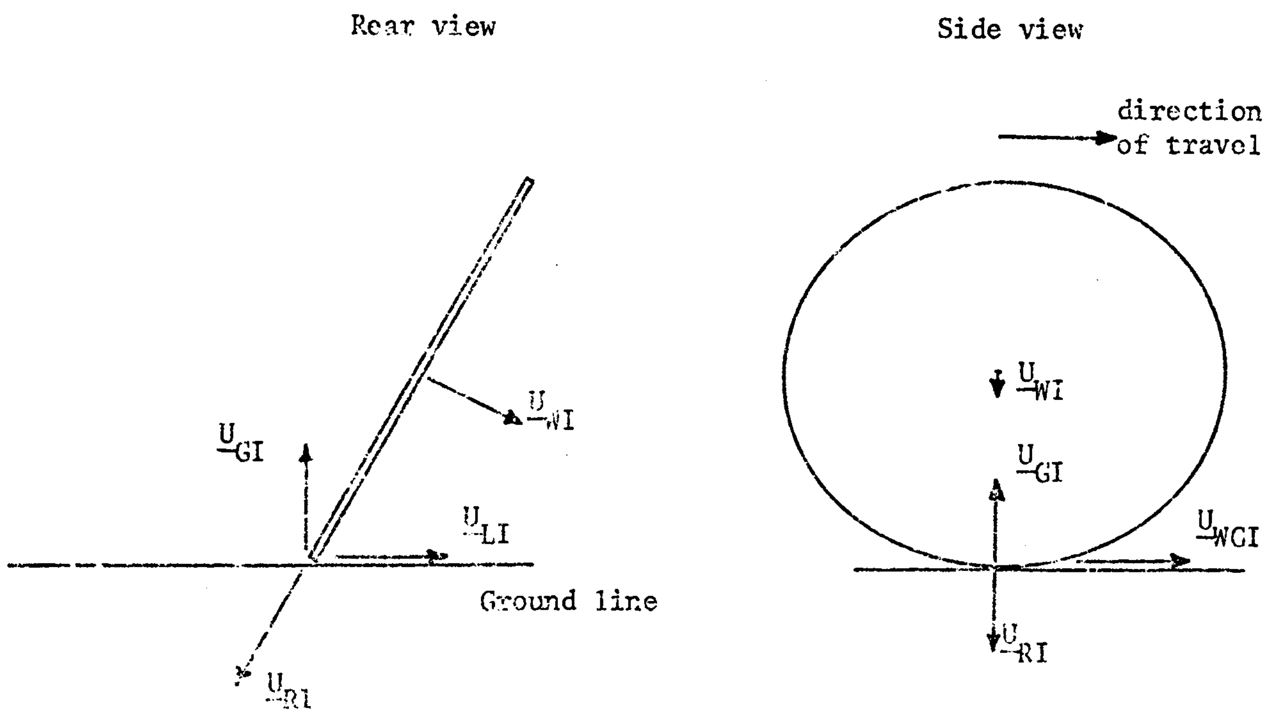

Figure 3-10. Unit Vector Directions Used in Defining the Tire Forces.

F_c is the circumferential (traction and rolling resistance) force, lb.

F_ℓ is the lateral (in the ground plane) force, lb, and

$\underline{F}_{WGI}$ is the vector sum of the mutually-perpendicular force components, lb.

Because the total tire-ground force acts at the ground-contact point, the moment of this force at the wheel center is defined by the vector cross product,

$$\underline{M}_{WGI} = \underline{R}_{WGCI} \times \underline{F}_{WGI} , \qquad (3\text{-}110)$$

where

$\underline{R}_{WGCI}$ is the vector in the $\underline{U}_{RI}$ direction from the wheel center to the ground-contact point, in.

A consideration of equation 3-109 and Figure 3-10 reveals the following:

1. The radial force component, the normal force component, and the lateral force component lie in the same plane so only two are independent forces.
2. The normal force component is used in defining the total tire-ground reaction while the radial force component is not.
3. The radial force component can be determined directly from the position and velocity of the tire relative to the ground surface, but the normal force depends upon other factors as well.

4. Only the normal force and the radial force may have components perpendicular to the ground plane.

Empirical data for lateral and circumferential tire forces relate these forces to the normal force by coefficients such as

$$F_\ell = S_\ell F_n \tag{3-111}$$

and

$$F_c = S_c F_n \tag{3-112}$$

where

S_ℓ is the lateral force coefficient, and

S_c is the circumferential force coefficient, usually expressed as separate rolling resistance and traction coefficients.

Thus only the normal force remains to be defined from the radial tire force.

Both the normal and radial tire forces act to support the tire on the ground surface while the lateral and circumferential forces act only in the ground plane. Thus the component of the radial tire force which acts perpendicular to the ground surface must be the normal tire force. Expressed in terms of the unit vectors shown in Figure 3-10, the normal force is

$$F_n = F_r(\underline{U}_{Ri} \cdot \underline{U}_{GI}) \ . \tag{3-113}$$

As seen in Figure 3-10, the circumferential force direction is perpendicular to the radial force direction. The circumferential force is defined by equation 3-112 after the normal force and the appropriate circumferential force coefficients are determined.

Because the circumferential force may be only rolling resistance for an undriven wheel or both traction and rolling resistance for a driven wheel, the circumferential force coefficient is defined as these two parts:

For driven wheels -

$$S_c = C_t + C_f \qquad (3\text{-}114)$$

For undriven wheels -

$$S_c = C_r \qquad (3\text{-}115)$$

where

C_t is the coefficient of gross traction, and

C_r is the coefficient of rolling resistance.

The coefficient of rolling resistance is defined impirically as a linear function of the tire slip angle, while the sign depends upon the direction of wheel motion

$$C_r = - \mathrm{SIGN}(\underline{V}_{CI} \cdot \underline{U}_{WGI})(a + b\theta_s) \qquad (3\text{-}116)$$

where

$\mathrm{SIGN}(\underline{V}_{CI} \cdot \underline{U}_{WGI})$ means "the sign of" the quantity inside the parenthesis,

θ_s is the slip angle, degrees, and

a and b are empirical constants determined for the specific tire-ground conditions.

The slip angle is defined as the angle between the velocity vector for the ground-contact point and the wheel forward direction (given by $\underline{U}_{WGI}$) while the sign of the slip angle is defined positive for motion to the right of the wheel plane.

$$\theta_s = \mathrm{SIGN}(\underline{V}_{WGI} \cdot \underline{U}_{LI}) \arccos \left| \frac{|\underline{V}_{WGI} \cdot \underline{U}_{WGI}|}{|\underline{V}_{WGI}|} \right| \qquad (3\text{-}117)$$

where

$\underline{V}_{WGI}$ is the velocity of the wheel-ground contact point, in/sec.

The velocity of the wheel-ground contact point is defined by assuming that the ground-contact point will retain its position relative to the wheel center,

$$\underline{V}_{WGI} = \underline{V}_{CI} + \underline{\omega}_{WI} \times \underline{R}_{WGCI} , \qquad (3\text{-}118)$$

where

$\underline{V}_{CI}$ is the wheel center velocity defined by the appropriate equation (3-106 or 3-105), in/sec, and

$\underline{\omega}_{WI}$ is the angular velocity of the wheel, instantaneously fixed to the axle, being either the tractor body angular velocity (for a rear wheel) or the front-end angular velocity (for a front wheel), rad/sec.

The coefficient of gross traction, C_t , for driven wheels is defined empirically as a function of the wheel slip, S_w . The wheel slip is defined as

$$S_w = 1 - \frac{\underline{V}_{CI} \cdot \underline{U}_{WGI}}{|\underline{R}_{WGCI}| \omega_{WW_2}} \qquad (3\text{-}119)$$

where

ω_{WW_2} is the component of the wheel angular velocity which is parallel to the axle, rad/sec.

Lateral tire force coefficients are functions of only the tire slip angle for undriven wheels but functions of both slip angle and tractive force for driven wheels. For both driven and undriven wheels the lateral force coefficients are values related empirically to the slip angle, while for driven wheels this coefficient is reduced by a factor which depends upon the tractive force. Thus if C_ℓ is an empirical coefficient obtained for the given slip angle, the lateral force coefficient is:

For driven wheels -

$$S_1 = - C_\ell C_f \text{ SIGN } (\theta_s) \tag{3-120}$$

For undriven wheels -

$$S_1 = - C_\ell \text{ SIGN } (\theta_s) \tag{3-121}$$

where

C_f is the factor dependent upon the traction force.

Using the friction ellipse concept for lateral force definition, this factor becomes

$$C_f = 1 - \left(\frac{C_t}{C_{t\ max}} \right)^2 \tag{3-122}$$

where

$C_{t\ max}$ is the maximum value that the coefficient of traction can attain.

Thus the maximum lateral force coefficient, S_ℓ , is obtained when the traction force is zero.

3-5. The Tractor Engine

The tractor model includes an engine, clutch, transmission, and differential whose characteristics also influence the response of the tractor to terrain and external force disturbances. The tractor throttle setting and transmission gear ratio are assumed to remain fixed throughout the simulation period.

The engine torque-speed characteristics are defined by a single torque-speed curve obtained for the engine at the specified throttle setting. Figure 3-11 shows a typical torque-speed curve. For a given engine speed the output torque is uniquely defined, but when a particular torque is specified, an additional condition stating whether the engine speed is above or below the speed of maximum torque must be provided to obtain a unique engine speed.

The engine speed ω_e changes when a torque imbalance exists between the torque at the clutch, T_c , and the engine torque, T_e . The equation defining the engine speed equilibrium is

$$\dot{\omega}_e = (T_e - T_c)/I_e \tag{3-123}$$

where

I_e is the mass moment of inertia of the rotating engine parts as seen at the flywheel.

The clutch characteristics affecting the tractor dynamic

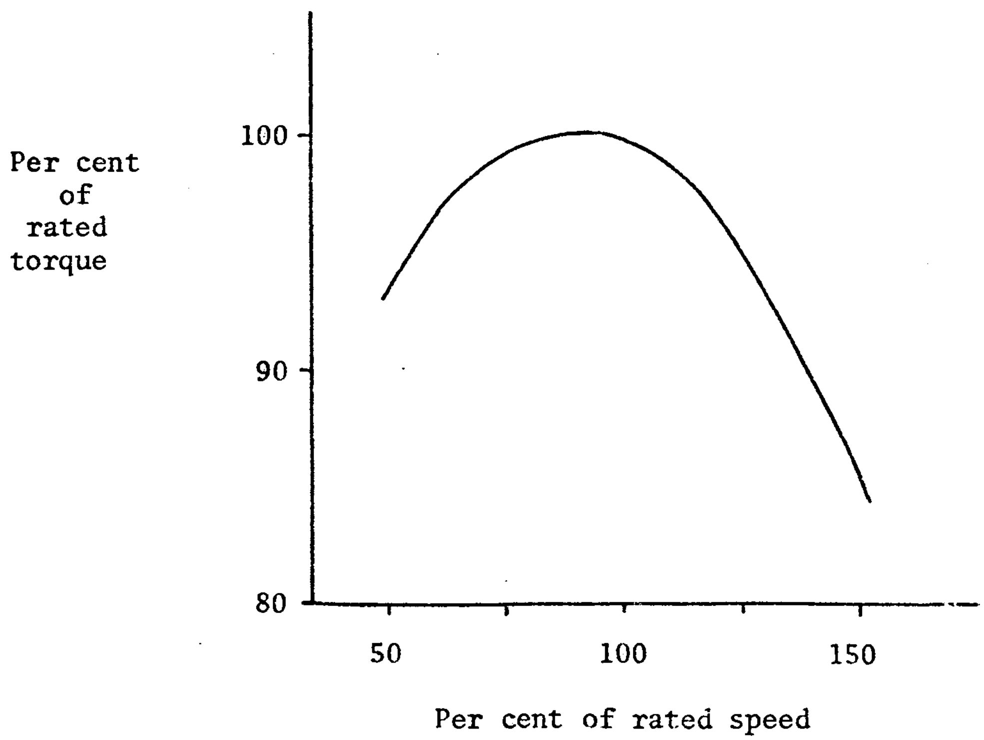

Figure 3-11. Typical Engine Torque-Speed Relationship.

response may be summarized by the torque-slip curve for the clutch. Figure 3-12 shows a typical torque-slip curve for a tractor clutch. Each torque defines a unique slip, but each slip does not define a unique torque so again there is ambiguity in this curve. The clutch slip, σ_c , is defined as

$$\sigma_c = 1 - \frac{\omega_e}{\omega_c} \tag{3-124}$$

where

ω_c is the clutch rotational speed, rad/sec.

The transmission speed ratio R_1 defines the drive-line speed in terms of the clutch speed,

$$\omega_d = \frac{\omega_c}{R_1} \tag{3-125}$$

where

ω_d is the drive-line rotational speed, rad/sec.

If the transmission efficiency is designated as E , then the drive-line torque, T_d , is given by

$$T_d = E\ R_1 T_c\ . \tag{3-126}$$

3.6. The Total Tractor Model

The mathematical model for a wide-front-end tractor is constructed from the differential equations of motion for the component

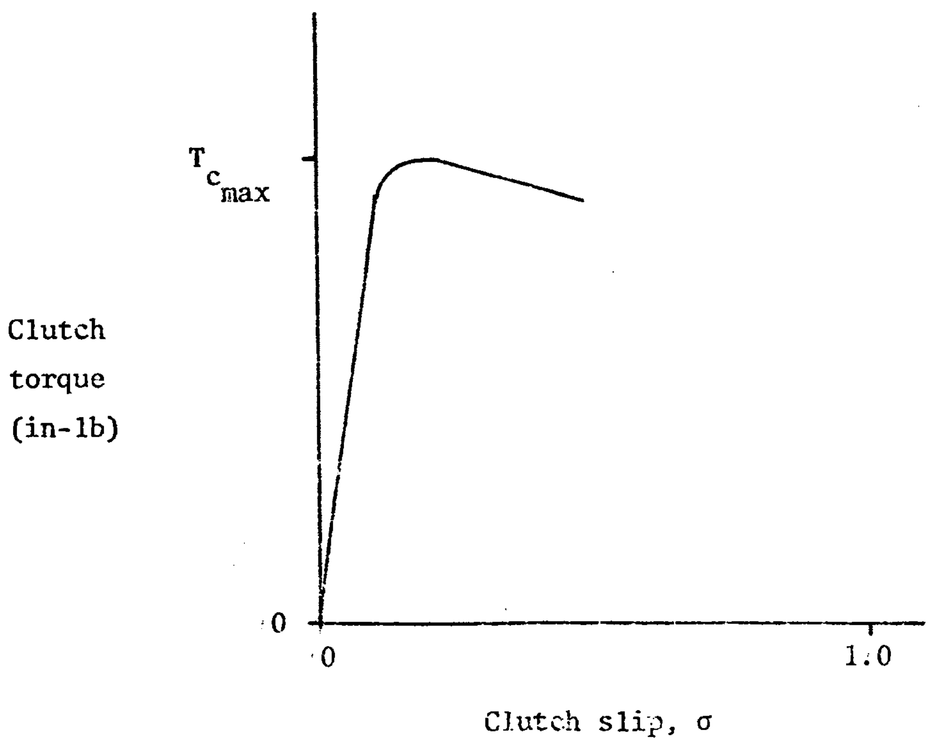

Figure 3-12. Typical Clutch Torque-Slip Relationship (from Goering, et al., 1967).

parts of the tractor, subject to the appropriate motion constraints. The ten degrees of freedom for the tractor (given in Table 3-1) require twenty first-order differential equations to define the dynamic state of the tractor. These twenty state variables and the number of the equation which defines the derivative of each are listed in Table 3-5.

After all the motion constraints have been applied to the differential equations, the twenty resulting simultaneous equations are seen to be functions of ground forces, gravitational forces, external forces, positions, and other velocities and accelerations. Many of the velocities and accelerations which are the derivatives of the state variables are non-linear functions of one another making the explicit expression of each an insurmountable task. Digital simulation of the tractor motion, however, requires explicit expression of the derivative of each state variable so integration of each may be performed to obtain the desired solution.

The following two classifications for the state variables are proposed to aid in obtaining an explicit expression for each of the state-variable derivatives:

1. acceleration-independent derivatives - those which can be expressed as explicit functions that do not contain rotational or translational accelerations, and
2. acceleration-dependent derivatives - those which when expressed as explicit functions do contain rotational or translational accelerations in their expression.

The relative influence of external reactions upon the accelerations

TABLE 3-5. Variables Whose Derivatives are Defined in the Differential Equations of Motion.

Tractor component	Variable(s)	Translational	Rotational	Equation(s)
Tractor body				
	$\underline{V}_{BI}$	3*	0	3-32
	$\underline{\omega}_{BP}$	0	3*	3-33
	$\underline{X}_{BI}$	3	0	3-3
	$\lambda_0, \lambda_1, \lambda_2, \lambda_3$	0	4	3-16 through 3-19
Tractor front end				
	ω_{FF_1}	0	1*	3-69
	θ_{FF_1}	0	1	3-70
Left rear wheel				
	ω_{LP_2}	0	1*	3-41
	θ_{LP_2}	0	1	3-43
Right rear wheel				
	ω_{RP_2}	0	1*	3-42
	θ_{RP_2}	0	1	3-44
Engine				
	ω_e	0	1*	3-123
		6	14	

*Derivatives of these variables are accelerations or functions of accelerations.

and velocities of a body suggest that maximum care should be used in evaluating the acceleration-dependent derivatives. Accelerations are the direct result of applied forces and moments so they reflect abrupt changes in these reactions. Velocities, however, are quantities obtained from the integration of accelerations, so they reflect little of the abrupt reaction variations. The following procedure is proposed to provide preferential treatment to the highest-order (acceleration-dependent) derivatives:

1. Identify those derivatives which are acceleration-dependent and those which are acceleration-independent. (The asterisk (*) in Table 3-5 denotes the acceleration-dependent derivatives.)
2. Evaluate the acceleration-independent derivatives for the present time interval by using the positions and velocities which are defined by integrations over the previous time interval (or, by initial conditions, for the first integration step).
3. Evaluate the acceleration-dependent derivatives using the newly-calculated velocities.

Of the ten acceleration-dependent derivatives, only three - ω_{LP_2}, ω_{RP_2}, and ω_e - are expressed as functions which do not include other accelerations. The remaining seven acceleration-dependent derivatives are functions of one another. Thus the evaluation of the acceleration-dependent derivatives (step 3) can be accomplished in part by directly evaluating the explicit expressions for the three derivatives. The remaining seven derivatives must be determined from a set of seven simultaneous equations defining the coupled state of these derivatives. The seven coupled accelerations are expressed by the following matrix equation:

$$\begin{bmatrix} B_{11} & B_{12} & B_{13} & B_{14} & B_{15} & B_{16} & B_{17} \\ B_{21} & B_{22} & B_{23} & B_{24} & B_{25} & B_{26} & B_{27} \\ B_{31} & B_{32} & B_{33} & B_{34} & B_{35} & B_{36} & B_{37} \\ B_{41} & B_{42} & B_{43} & B_{44} & B_{45} & B_{46} & B_{47} \\ B_{51} & B_{52} & B_{53} & B_{54} & B_{55} & B_{56} & B_{57} \\ B_{61} & B_{62} & B_{63} & B_{64} & B_{65} & B_{66} & B_{67} \\ B_{71} & B_{72} & B_{73} & B_{74} & B_{75} & B_{76} & B_{77} \end{bmatrix} \begin{Bmatrix} X_1 \\ X_2 \\ X_3 \\ X_4 \\ X_5 \\ X_6 \\ X_7 \end{Bmatrix} = \begin{Bmatrix} C_1 \\ C_2 \\ C_3 \\ C_4 \\ C_5 \\ C_6 \\ C_7 \end{Bmatrix} \tag{3-127}$$

where

B_{ij} are coupling coefficients between the accelerations,

C_i are constants, and

X_i are the accelerations.

The coupling coefficients and constants of equation 3-127 are evaluated using the positions and velocities at the particular time of interest, so they change with time and actually are not constant. The accelerations can be obtained by using standard methods for solving linear equations. The coupling coefficients, constants, and accelerations, together with the exhaustive derivations of these are presented in Appendix A.

Evaluation of all the derivatives listed in Table 5 is accomplished by evaluating the ten acceleration-independent derivatives, the ground and external forces, then the seven coupled and three uncoupled acceleration-dependent derivatives. This then provides twenty derivatives which may be integrated simultaneously over one incremental time step. Successive derivative evaluations and integrations produce the record of the tractor state variables over the desired time interval. The complexity of the derivative evaluations and integration steps require the use of a digital computer to perform the necessary calculations. Appendix C provides a detailed description of the digital computer program developed to produce the desired tractor simulations.

3.7. Limitations to Front-End Rotation

Rotational motion of the tractor front end about the front pin is not restrained by the tractor body until the front end strikes a "stop" between it and the tractor body. Thus the "stop" interaction needs to be considered only when the front-end rotation exceeds a certain magnitude, i.e., when

$$\left|\theta_{FF_1}\right| \geq \theta_{max} \tag{3-128}$$

where

θ_{max} is the rotation limit for the tractor front end relative to the tractor body (about the $\underline{e}_{F_1}$ axis), rad.

The discussion of this section is limited to conditions in which equation 3-128 is satisfied.

The "stop" transmits the reaction between the tractor body and the front end necessary to cause the rotations of these two tractor parts to conform to one another while they remain in contact. During the traversing of irregular terrains, the relative angular velocity of the front end and tractor body may differ greatly; thus as the rotation limit is encountered, the "stop" must transmit large reactions while deforming minimally to cause the angular accelerations and decelerations necessary for the two tractor parts to reach the state of coincident rotation. Although both energy storage and energy dissipating characteristics are desirable for this "stop" material, judicious use of these properties must be exercised in the mathematical model of the "stop" to minimize shock loadings and maintain the accuracy of the mathematical simulations.

Modelling the "stop" with only energy-storage characteristics could allow unwanted oscillations to persist in the simulation, but the addition of velocity-dependent energy dissipation characteristics adversely increases the shock load when impact occurs. Thus, a modification from the frequently-used parallel spring-dashpot system is proposed. The proposed "stop" representation provides purely energy storage (elastic) properties during the compression-phase but both elastic and viscous damping properties during the relaxation phase of the "stop" deformation. The "stop" reaction is thereby reduced in magnitude and smoothed while also dissipating enough energy to minimize oscillations without adversely compromising the over-all accuracy of the tractor simulation.

The "stop" reaction is defined to be equal and opposite forces applied to both the front end and the tractor body at the point S shown in Figure 3-12. The location of the point S is, relative to the front-end center of mass,

$$\underline{R}_{SFI} = - \underline{R}_{FPI} - \ell_S \mathrm{SIGN}(\theta_{FF_1}) \underline{e}_{F_2} \qquad (3\text{-}129)$$

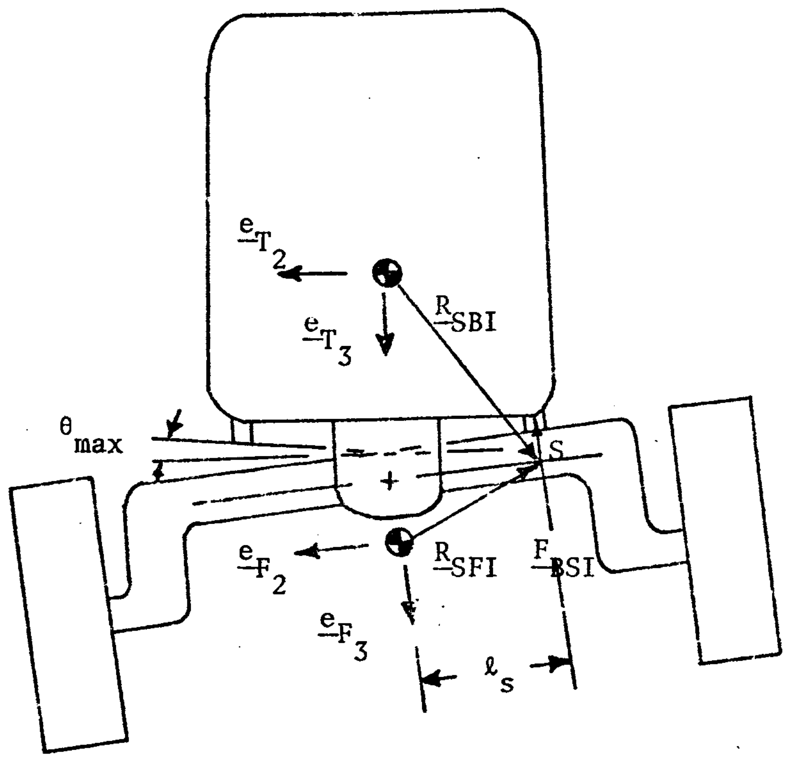

Figure 3-13. Notation Used to Define Reactions When the Tractor Front End is Against a "Stop".

and, relative to the tractor-body center of mass,

$$\underline{R}_{SBI} = R_{PBI} - \ell_S \mathrm{SIGN}(\theta_{FF_1})\underline{e}_{F_2} \tag{3-130}$$

where

ℓ_S is the distance from the front pin to the line-of-action (parallel to $\underline{e}_{F_3}$) for the "stop" force measured in the $\underline{e}_{F_2}$ direction, in.

The "stop" force, defined to act parallel to the $\underline{e}_{F_3}$ axis through the point S, is always compressive into the tractor body and into the front end.

When the stop is being increasingly compressed, i.e., if

$$(\omega_{FF_1} - \omega_{BF_1})\mathrm{SIGN}(\theta_{FF_1}) \geq 0 . \tag{3-131}$$

then

$$F_S = k_S \ell_S [|\theta_{FF_1}| - \theta_{max}] \tag{3-132}$$

where

k_S is the spring stiffness of the "stop," lb/in.

When the "stop" is being unloaded, i.e., if

$$(\omega_{FF_1} - \omega_{BF_1})\mathrm{SIGN}(\theta_{FF_1}) < 0 , \tag{3-133}$$

then

$$F_S = k_S \ell_S [|\theta_{FF_1}| - \theta_{max}]$$

$$+ c_S \ell_S (\omega_{FF_1} - \omega_{BF_1}) \mathrm{SIGN}(\theta_{FF_1}) \,, \qquad (3\text{-}134)$$

where

c_S is the viscous damping coefficient for the "stop" during unloading, lb-sec/in.

The reactions due to the "stop" are summarized for the tractor body as the force

$$\underline{F}_{BSI} = - F_S \underline{e}_{F_3} \qquad (3\text{-}135)$$

and the moment about the tractor-body center of mass

$$\underline{M}_{BSI} = \underline{R}_{SBI} \times \underline{F}_{BSI} \,. \qquad (3\text{-}136)$$

The reactions due to the "stop" for the front end are the force

$$\underline{F}_{FSI} = F_S \underline{e}_{F_3} \qquad (3\text{-}137)$$

and the moment about the front-end center of mass

$$\underline{M}_{FSI} = \underline{R}_{SFI} \times \underline{F}_{FSI} \qquad (3\text{-}138)$$

These reactions may be applied as inputs to the front end or tractor body in the same manner as external reactions or ground reactions are applied to bodies.

CHAPTER IV

EXPERIMENTAL PROCEDURE

Verification of the mathematical model of a wide-front-end tractor requires observation of an actual tractor under the conditions for which the mathematical model is proposed. As an alternative to full-sized tractor overturns a scale-model test was used for the mathematical model verification. This procedure is justified in that the actual parameters of the scale model are measured and used in the simulations that are to be verified by the scale-model tests.

4.1. The Physical Tractor Model

A commercially available* toy Ford "8000" tractor was purchased and modified for the physical model tests. The tractor was an approximate 1/12 scale model of die cast aluminum having front wheel steering and a front end which rotates about the front pin as required. Figure 4-1 shows the tractor model as it was prior to modification and in the modified state. The tractor was not powered.

Modifications of the tractor model made to increase the similarity between the full-sized tractor and the scale-model tractor and to improve the control of overturn tests are listed below.

---

*Part number 900-6841, manufactured by The ERTL Company, Dyersville, Iowa 52040, a subsidiary of Victor Comptometer Corporation.

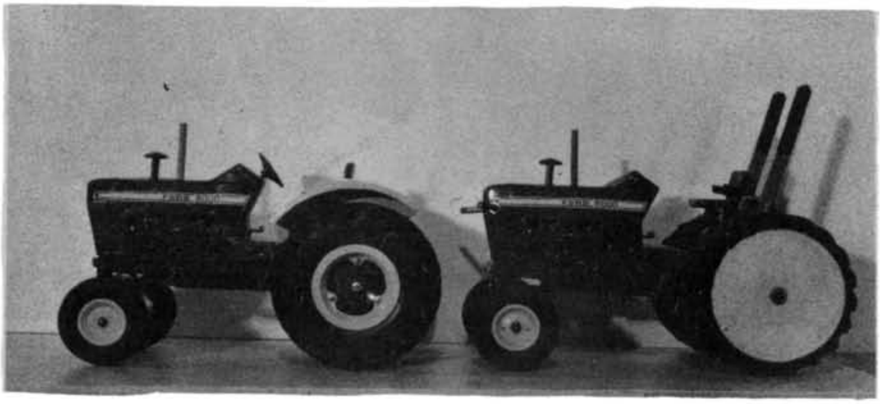

Figure 4-1. The Scale-Model Tractor Before and After Modification.

1. Rebuilt rear wheels.

   The rear wheels of the purchased tractor were not symmetric about a plane passing through their centers of mass. The wheels, therefore, were removed from the rims, cut to yield symmetric tires, and mounted on symmetric rims.

2. Rebuilt tractor front end.

   The tractor front end was disassembled and reconstructed to eliminate excessively loose joints. The front pin joint was reamed and fit with bushings to provide free motion about the desired axis of rotation. The front wheels were also reamed and fit with bushings. New steering knuckles were made to improve the steering-axis joints and to provide a method for locking the front wheels in a fixed position. Screw admustments were added to allow desired front-end rotation limits to be set.

3. Increased tractor mass.

   The tractor mass was increased by fastening a molded lead piece inside the hollow tractor chassis. This increased the total tractor weight from 4.4 lb to 6.4 lb after all modifications, a weight appropriate for a model of the unballasted Ford 8000 tractor.*

4. Defined reference points.

   Four reference points on the tractor were defined to aid in observation of the tractor motion. These points were established by extending steel arms from the tractor body and pointing them

---

*The proper weight for a 1/12 scale model should be $(1/2)^3$ or 1/1728 of the full-sized tractor weight. Thus 6.4 lb is appropriate for 1/12 scale of an 11,000 (i.e., 1728 × 6.4) lb tractor.

so that their ends were readily identifiable points throughout the expected tractor overturns. Two points were extended sideways and forward from the front of the tractor body while two others were extended upward and slightly rearward from the rear axle similar to the orientation of many two-post overturn protection frames.

The coordinate axes of the tractor body (the tractor-axes directions) were defined:

$\underline{e}_{T_1}$ - forward, parallel to the front pin axis

$\underline{e}_{T_2}$ - to the driver's right, parallel to the rear axle

$\underline{e}_{T_3}$ - down, perpendicular to $\underline{e}_{T_1}$ and $\underline{e}_{T_2}$.

The origin of this coordinate system was the tractor-body center of mass, to be differentiated from the total tractor center of mass. The tractor motion, its orientation, and the location of points on the tractor body were defined by using the tractor-axes coordinates and the tractor-body center of mass.

4.2. The Overturn Test Course

The terrain chosen for use in the model overturn tests was an approximate 1/12 scale model of the terrain specified by the American Society of Agricultural Engineers (Standard S306.2) and by the Society of Automotive Engineers (Standard J334) for side overturns

(ASAE Agricultural Engineer's Yearbook, 1972). Dimensions of the test course are defined in Figure 4-2.

The scale-model test course was constructed of 3/4 inch plywood while all surfaces over which the tractor wheels rolled were covered with 100-grit sandpaper* to provide uniform surface characteristics. All other terrain surfaces were painted contrasting colors to aid in the visual identification of terrain details.

An inertial coordinate system was defined fixed in the test setting with the $\underline{e}_{I_1}$ axis parallel to the ramp, the $\underline{e}_{I_2}$ axis perpendicular to and to the right of the ramp (as approaching to climb the ramp), and the $\underline{e}_{I_3}$ axis vertically down. The origin was chosen so that the $\underline{e}_{I_2}$ axis defines the base of the ramp incline and the $\underline{e}_{I_1}$ axis defines the path of travel for the tractor centerline as it approaches the ramp with the right rear wheel on the ramp centerline. The inertial coordinates are shown in Figure 4-2.

Two vertical planes of black-on-white one-inch-square grid lines were erected to establish reference lines for defining tractor positions. One plane of grid lines was erected parallel to the $\underline{e}_{I_1}$ and $\underline{e}_{I_3}$ axes to define positions in the $\underline{e}_{I_1}$ and $\underline{e}_{I_3}$ directions while the second plane was oriented parallel to the $\underline{e}_{I_2}$ and $\underline{e}_{I_3}$ axes to define positions in the $\underline{e}_{I_2}$ direction.

---

*100 grit X265F Carborundum Aloxite industrial cloth in 6-inch wide by 48-inch perpheral length belts.

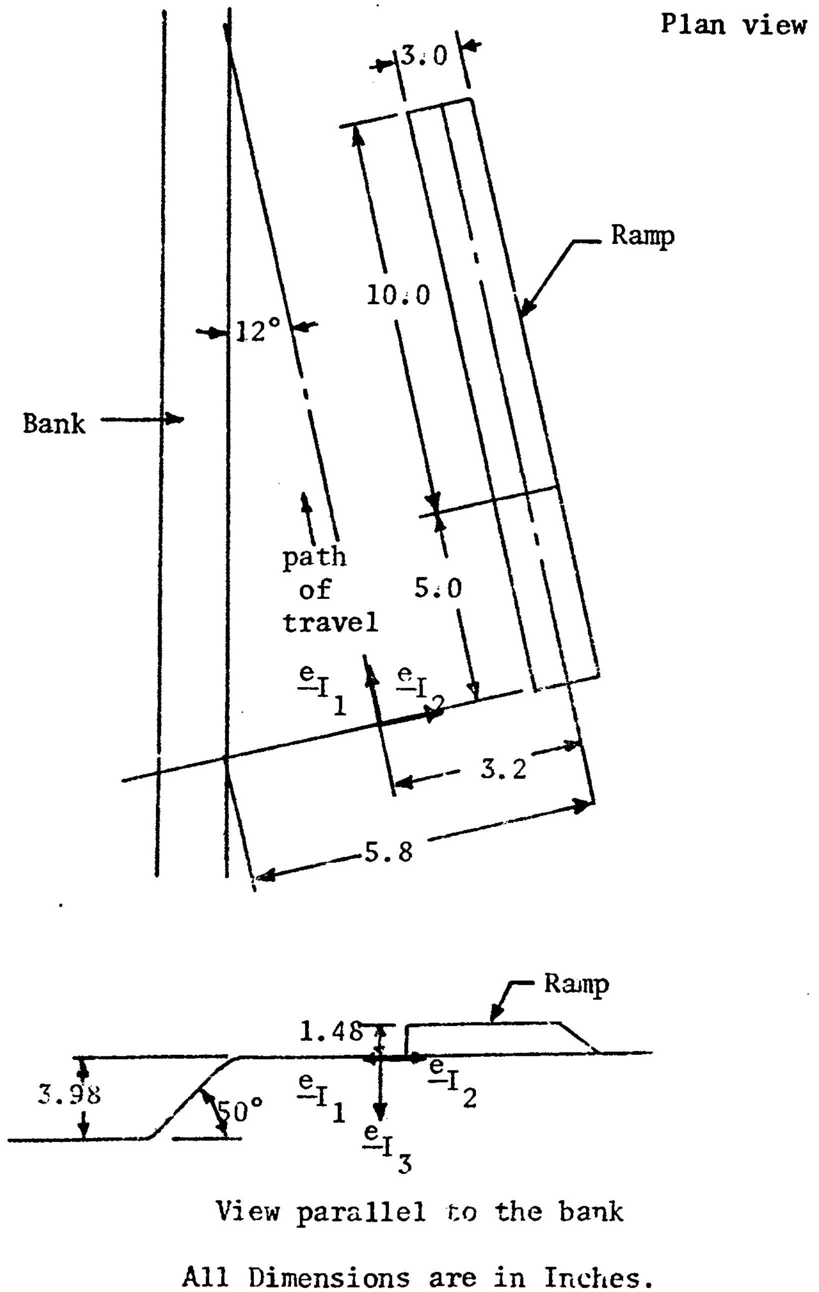

Figure 4-2. The Scale-Model Overturn Test Course.

4.3. Measurement of Physical Model Parameters

A complete description of the dynamic characteristics of the scale-model tractor was required before any mathematical model simulations could be conducted. Pertinent properties included the mass (or weight) of the component tractor parts, centers of mass, mass moments and products of inertia, location of attachment points between components, location of other pertinent points, and tire characteristics. Because the scale model was not powered, characteristics of the engine, clutch, transmission, differential, and the coefficient of traction were not required, and, therefore were not measured. Further simulation of powered vehicles would require measurement of these parameters.

4.3.1. Geometric and Inertia Properties

All geometric descriptions of the tractor were defined in terms of the coordinate system of that component. In all cases the origin of the coordinate system was at the center of mass for that component. Thus the center of mass for each component part was located prior to establishing the coordinates of other points on that part.

The center of mass was located by a method of suspension. After suspending the component part at least three times (by a different point each time) and noting the force line-of-action each time, the center of mass was defined as the point-of-intersection for the force lines-of-action.

The tractor-body coordinate system was established with its origin at the body center of mass and its axes directions forward parallel to the front pin, to the driver's right, and down as defined in Section 4.1. The location of the front pin, the rear wheel centers of mass, the four reference points (defined in Section 4.1), and other points of interest were defined in terms of tractor-axes coordinates.

The front-end coordinate system was established with its origin at the front-end center of mass and its axes directions parallel to those of the tractor body when the front-end rotation was zero. The locations of the front pin, the effective point of spindle rotation, and the orientation of the steering axis were defined from the front-end coordinate-axes directions. Dimensions of tractor parts and important point locations are given in Table 4-1.

The mass of each tractor component was calculated from its weight. A ten-pound maximum weight single-platform scale provided weights to the nearest hundredth of a pound. Because the units used in the mathematical model were pounds, inches, and seconds, the local gravitational acceleration used in calculating the masses was 386 in/sec^2.

The mass moments of inertia and products of inertia were measured by a trifilar pendulum method. (Phelan, 1967, p. 149). The trifilar pendulum was constructed of a 12 by 12 by 1 inch styrofoam platform suspended by three 34-inch long, 24-gage copper wires. The wires were fastened at the corners of an equilateral triangle at both the top and the bottom ends. Each triangle was inscribed in a 5.50-inch radius circle; the center of the bottom circle was the platform center of mass.

TABLE 4-1. Dimensions and Point Locations for the 1/12 Scale Model Tractor.

Radius rear wheel, in	2.75		
Radius front wheel, in	1.50		
Effective length front axle, in	0.90		
Tractor-axes vectors, in, from mass center to:			
	$\underline{e}_{T_1}$	$\underline{e}_{T_2}$	$\underline{e}_{T_3}$
Left rear wheel center	-2.80	-3.20	1.35
Right rear wheel center	-2.80	3.20	1.35
Front pin	5.65	0.00	1.75
Left rear reference point	-4.23	-1.52	-5.90
Right rear reference point	-4.23	1.43	-5.90
Left front reference point	6.87	-3.35	-0.90
Right front reference point	7.20	3.35	-0.90
Front-end-axes vectors, in, from mass center to:			
Front pin	0.00	0.00	-0.90
Turning point - L.F. spindle	0.00	-1.80	0.35
Turning point - R.F. spindle	0.00	1.85	0.35

The mass moments of inertia of a body were determined by placing the body center of mass over the platform center of mass with the axis about which the inertia property was to be measured aligned vertically (joining the triangle centroids). Figure 4-3 shows the tractor body on the platform of the trifilar pendulum. Small amplitude oscillation about the vertical axis was induced and the period of oscillation was measured. Then the mass moment of inertia for the body was determined by subtracting the mass moment of inertia for the platform from that for the composite (body and platform). The relationship used in determining the mass moments of inertia was

$$I = \frac{W\, r^2 T^2}{4\pi^2 \ell} \tag{4-1}$$

where

I = mass moment of inertia for the platform or platform and body, lb-in-sec^2,

W = weight of the oscillating platform or platform and body, lb.

r = distance from platform center of mass to the support wires, in

T = period of oscillation for the platform or platform and body, sec, and

ℓ = length of the supporting wires, in.

The tractor body and the tractor front end required the determination of one product of inertia for each because each body had a

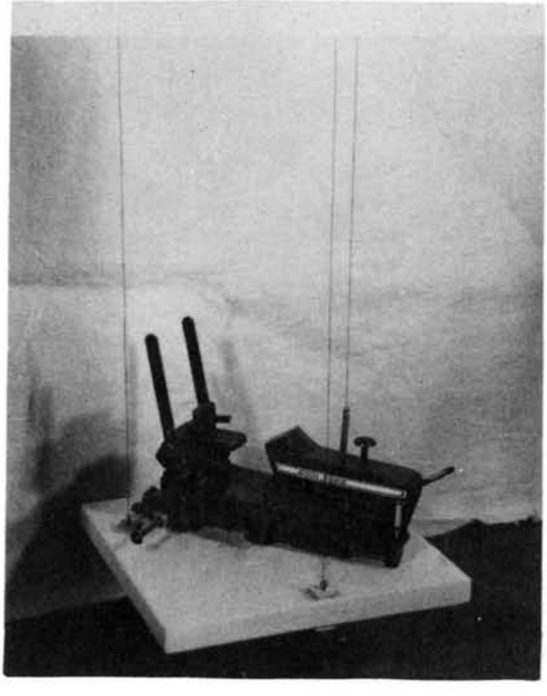

Figure 4-3. Scale-Model Tractor Body on the Trifilar Pendulum Platform.

plane of symmetry making the $\underline{e}_{T_2}$ and $\underline{e}_{F_2}$ axes principal axes. The $I_{BT_{13}} = I_{BT_{31}}$ and the $I_{FF_{13}} = I_{FF_{31}}$ products of inertia were nonzero, thus causing measurement of an extra moment of inertia for each of these two bodies.

If α is the angle of rotation (about the $\underline{e}_{T_2}$ axis, the axis normal to a plane of symmetry) from the $\underline{e}_{T_1}$ axis to a second axis $\underline{e}_{T_A}$, then the moment of inertia measured by oscillations about the $\underline{e}_{T_A}$ axis is given by Greenwood (1965, p. 315) as

$$I_{BT_A} = I_{BT_{11}} \cos^2\alpha + I_{BT_{33}} \sin^2\alpha - I_{BT_{13}} \sin 2\alpha \ . \tag{4-2}$$

Solving for the product of inertia, $I_{BT_{13}}$, yields

$$I_{BT_{13}} = \frac{I_{BT_{11}} \cos^2\alpha + I_{BT_{33}} \sin^2\alpha - I_{BT_A}}{\sin 2\alpha} \tag{4-3}$$

where

$I_{BT_{13}}$ is the product of inertia (equal to $I_{BT_{31}}$), lb-in-sec^2,

$I_{BT_{11}}$ is the mass moment of inertia measured about the $\underline{e}_{T_1}$ axis, lb-in-sec^2,

$I_{BT_{33}}$ is the mass moment of inertia measured about the $\underline{e}_{T_3}$ axis, lb-in-sec^2,

I_{BT_A} is the moment of inertia measured about the $\underline{e}_{T_A}$ axis, lb-in-sec^2, and

α is the angle of rotation (about the $\underline{e}_{T_2}$ axis) from the $\underline{e}_{T_1}$ axis to the $\underline{e}_{T_A}$ axis.

Thus the products of inertia for both the tractor body and the tractor front end were determined by measuring the mass moment of inertia about an appropriate axis and calculating the product of inertia from equation 4-3. The inertia properties of the scale-model tractor components are summarized in Table 4-2.

TABLE 4-2. Weight and Inertia Properties for the 1/12 Scale Model Tractor Components

	Tractor Body	Tractor Front end	Rear Wheel
Weight, lb	3.69	0.76	0.985
Moments of inertia, lb-in-sec^2			
I_{11}	0.0260	0.0128	0.00825
I_{22}	0.0840	0.00391	0.0132
I_{33}	0.0788	0.0125	0.00825
$I_{31} = I_{13}$	-0.000447	-0.00136	0.0
All other I_{ij}	0.0	0.0	0.0
$j = 1,2,3;\ i = 1,2,3$			

4.3.2. Tractor Tire Characteristics

Description of the scale-model tractor required a definition of the forces acting upon the tires in terms of the position and velocity of the tire relative to the ground surface. Because the tractor was unpowered, the gross coefficient of traction for the rear tires was not required, thus the empirical relationships necessary for description of the front and rear tires were of the same types. Those relationships which were determined experimentally for the tires are listed below.

1. Radial tire force (lb) as a function of the radial tire deflection (in),
2. Circumferential rolling resistance (lb) as a function of tire normal force (lb) and tire slip angle (degrees),
3. Lateral tire force (lb) as a function of tire normal force (lb) and tire slip angle (degrees), and
4. Viscous damping coefficient (lb-sec/in) for radial deflection.

The tire radial force-deflection relationship was determined by deflecting each tire at a constant rate on an Instron Tester. Because the loading head moved at a constant rate and the chart paper of the plotter (integral with the testing machine) moved at a constant rate, the desired force-deflection relationships were obtained directly from the chart records.

The radial force-deflection tests were conducted on each tire while the tire was clamped by an axle to a yoke as shown in Figure 4-4. The loading head advanced two-hundredths of an inch per minute

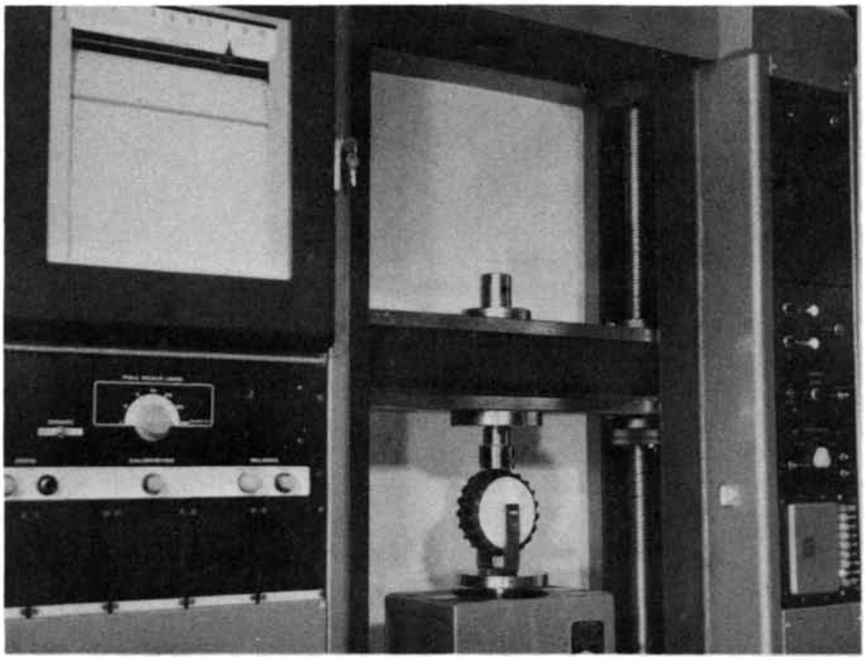

Figure 4-4. Measuring the Tire Radial Force-Deflection Characteristics with the Instron Tester.

as it loaded the tire periphery while the yoke transmitted the force to the load cell beneath the tire. By zeroing the chart pen prior to contact between the loading head and the tire, the force-deflection curve was obtained directly on the chart.

Two radial force-deflection replications were conducted for each tire. The curves of Figure 4-5 show the averages obtained for the four loadings of front tires and the four loadings of rear tires.

The tire circumferential and lateral force relationships were determined from measurements of the circumferential and axial forces derived from the apparatus shown in Figure 4-6. The front or rear tire was held in place and allowed to rotate freely on a shaft as the sandpaper surface moved beneath the tire. The normal force acting on the tire was varied by adding or subtracting weights stacked above the outer yoke, while turning this yoke about a vertical axis relative to the direction of sandpaper travel provided the desired variation in tire slip angle.

The circumferential force acting at the point of tire-sandpaper contact was determined indirectly by measuring the force required to prevent the inner yoke (through which the axle passed) from rotating relative to the outer yoke about a horizontal axis. A cantilever beam mounted on the outer yoke restrained the inner yoke and provided a force indication through four SR-4 strain gages cemented onto the beam. A four-arm strain bridge amplifier provided a voltage signal proportional to the circumferential force. This signal was then amplified by a strip chart recorder amplifier to provide a direct reading of the force which would have been required at the axle

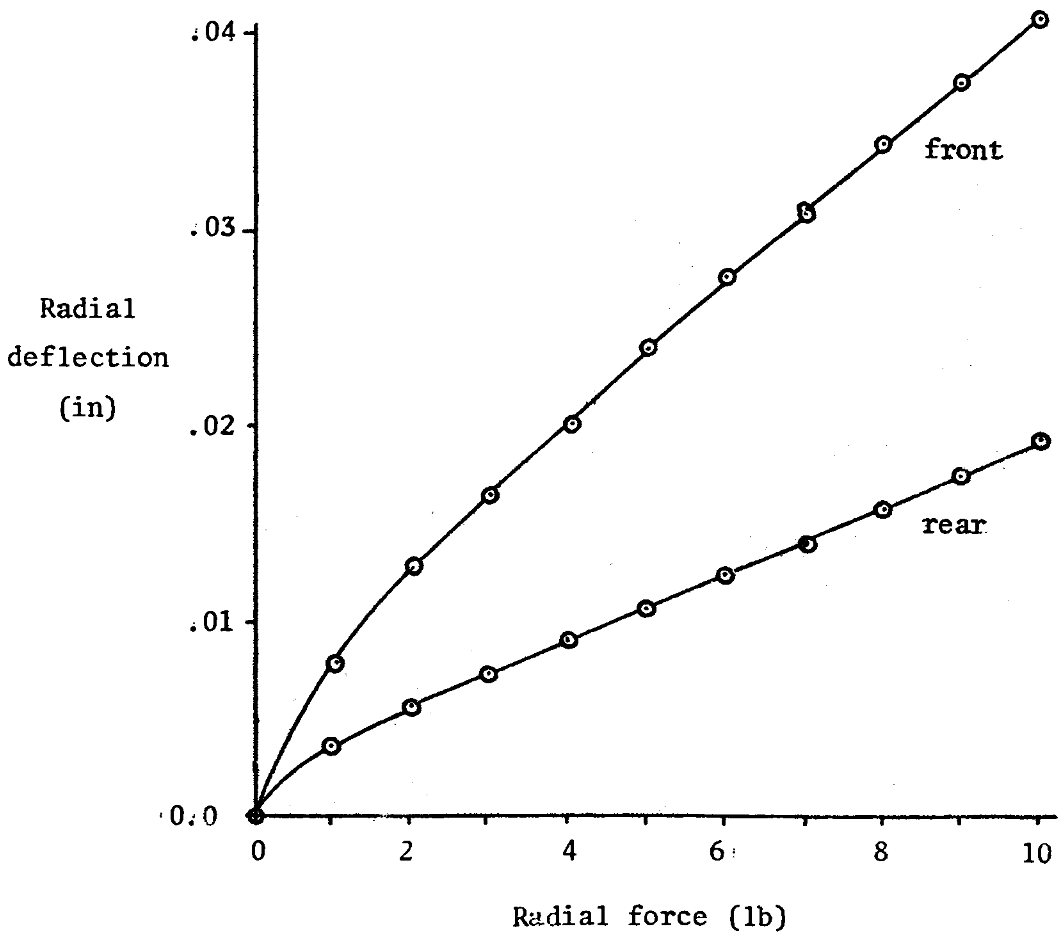

Figure 4-5. Tire Radial Force-Deflection Curves.

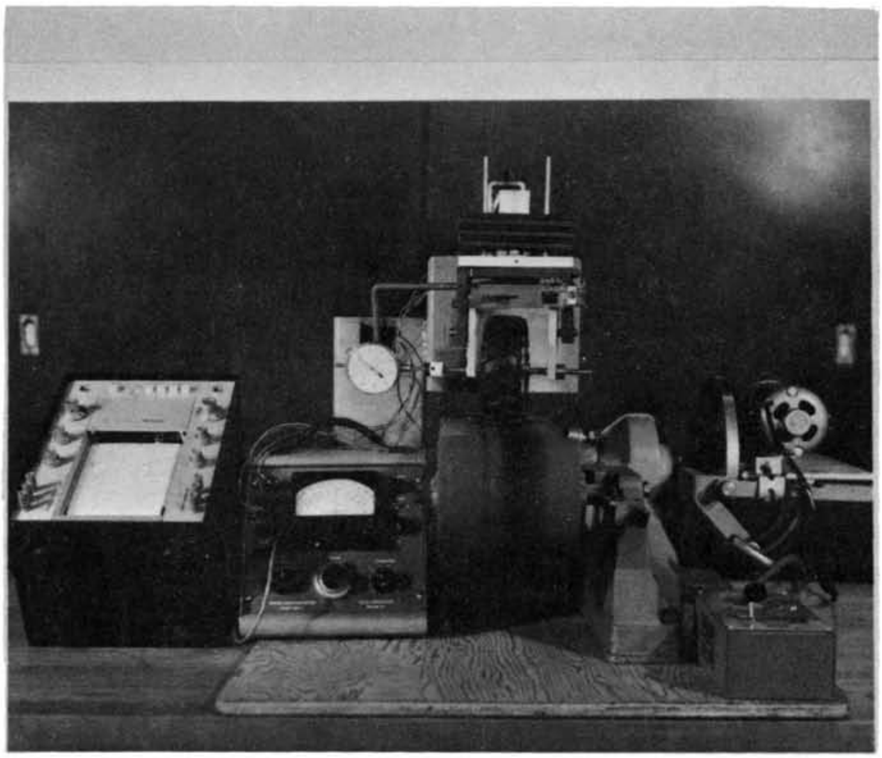

Figure 4-6. The Apparatus Used in Measuring the Tire Circumferential and Lateral Force Characteristics.

(in the circumferential direction) to produce the same strain bridge output. Details of the equipment and procedure for obtaining the circumferential force are presented in Appendix B.

The circumferential force data required by the mathematical model of the tractor is the tire rolling resistance coefficient as a linear function of the slip angle (in degrees). Figure 4-7 shows the plot of rear wheel rolling resistance coefficients while Figure 4-8 shows the plot of front wheel rolling resistance coefficients as functions of the slip angle. The least squares linear curves for each set of data (also plotted in these figures) are presented in Table 4-3.

The apparatus shown in Figure 4-6 also provided an indirect measurement of the lateral tire force. The dial gage shown indicated the axial displacement of the wheel and axle against a compression spring. Thus the dial gage reading was calibrated to yield a measure of the axial force acting on the tire from which the lateral tire force was derived. Details of the lateral force derivation and tabulated data are presented in Appendix B.

The lateral tire force plotted as a function of the normal force with selected values of the tire slip angle as a parameter is shown for the rear tires in Figure 4-9 and for the front tires in Figure 4-10. The mathematical model of the tractor requires a lateral force coefficient (as given by the slopes of these curves) to define the lateral force for any given tire slip angle, thus the lateral tire force data for each measured slip angle were fit by the method of least squares to equations of the form

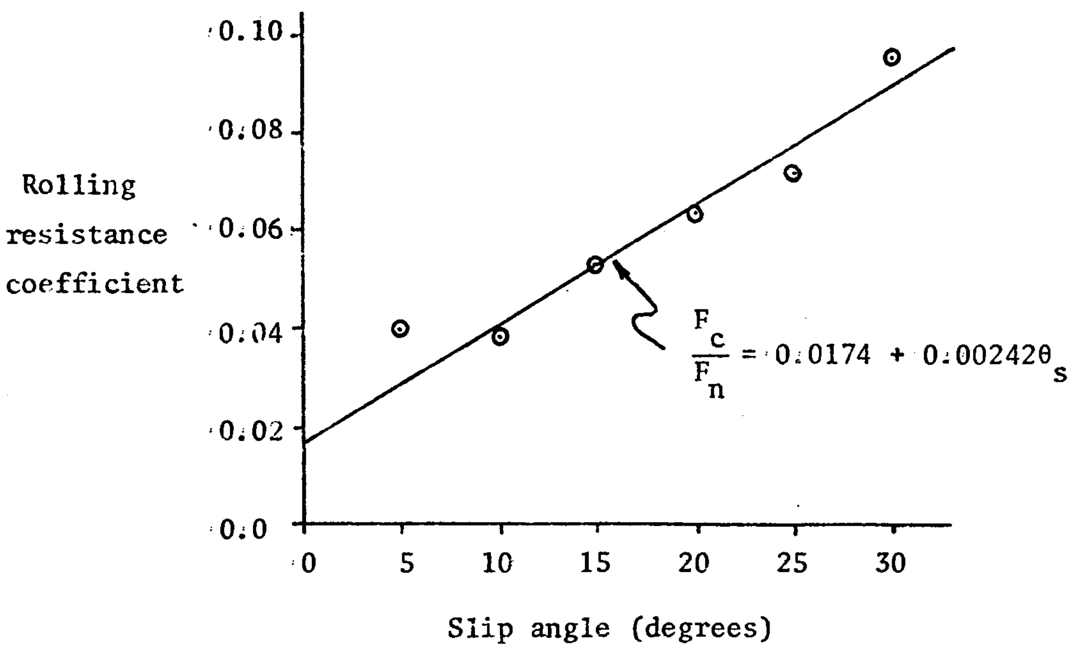

Figure 4-7. Rear Tire Rolling Resistance Coefficients as a Function of the Slip Angle.

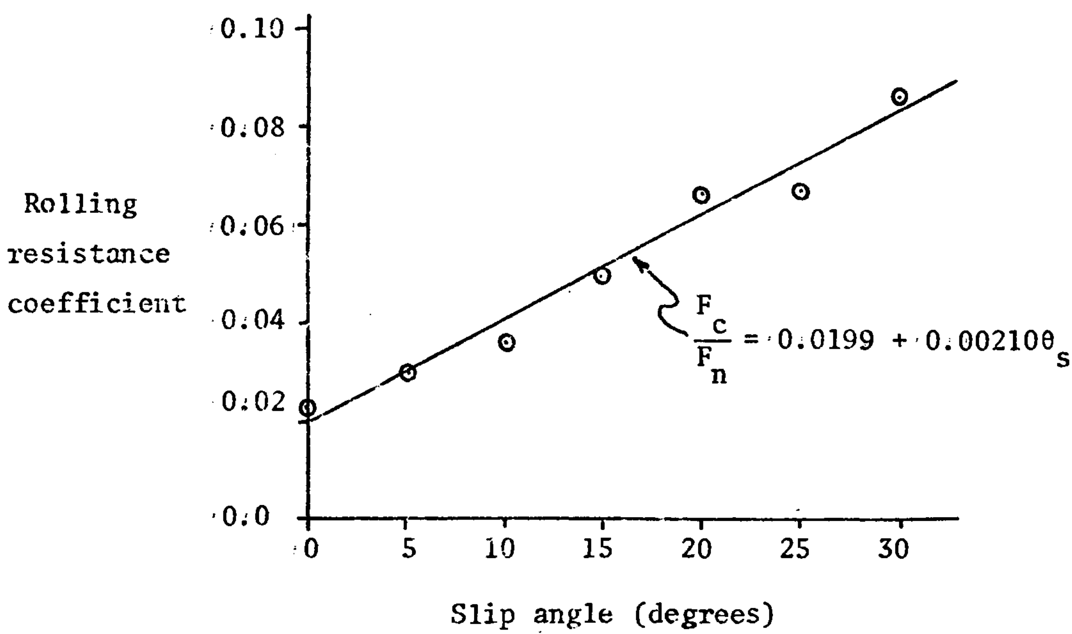

Figure 4-8. Front Tire Rolling Resistance Coefficients as a Function of the Slip Angle.

TABLE 4-3. Rolling Resistance Coefficients for Scale-Model Tractor Tires.

Equation form*: $\frac{F_c}{F_n} = a + b\theta_s$

	a	b	r
Rear tires	0.0174	0.00242	0.972
Front tires	0.0199	0.00210	0.986

$\frac{F_c}{F_n}$ = coefficient of rolling resistance

θ_s = tire slip angle, degrees

$$F_\ell = S_\ell F_n \qquad (4\text{-}4)$$

where

F_ℓ is the lateral force, lb,

F_n is normal force, lb, and

S_ℓ is the lateral force coefficient defined for the particular tire and slip angle.

The lateral force coefficients are presented for both the front and rear tires in Table 4-4.

The tire radial damping force was defined in Section 3.4.4. as

$$F_d = C_d(\underline{V}_{CI} \cdot \underline{U}_{RI}) \quad \text{for} \begin{cases} \underline{V}_{CI} \cdot \underline{U}_{RI} < 0 \\ d > 0 \;. \end{cases} \qquad (4\text{-}5)$$

where

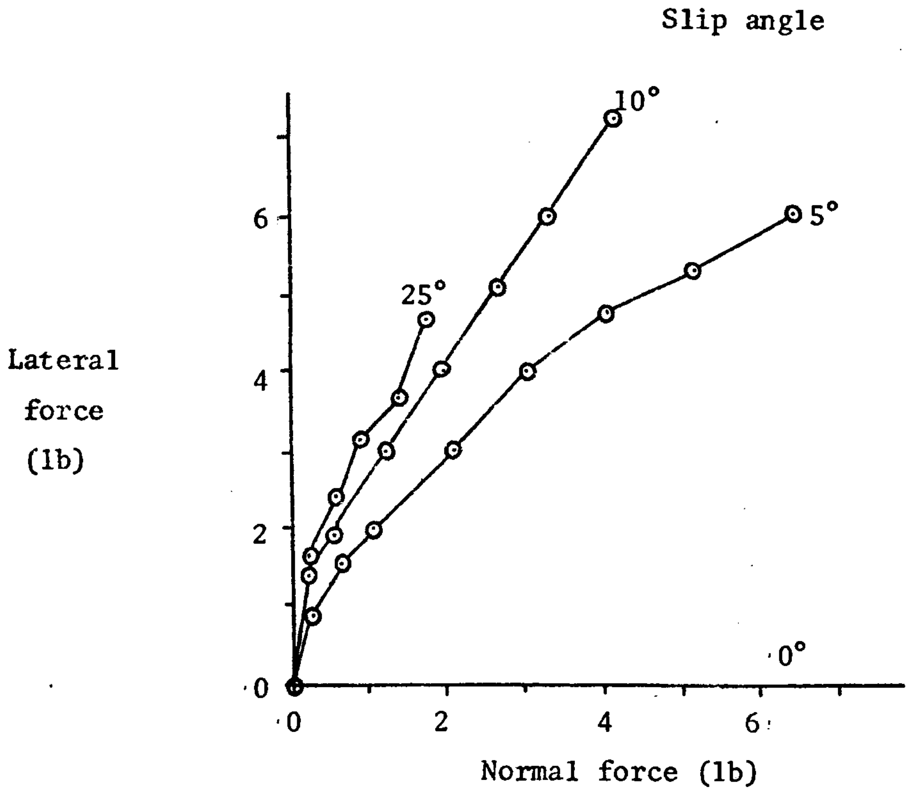

Figure 4-9. Rear Tire Lateral Force as Functions of the Tire Normal Force.

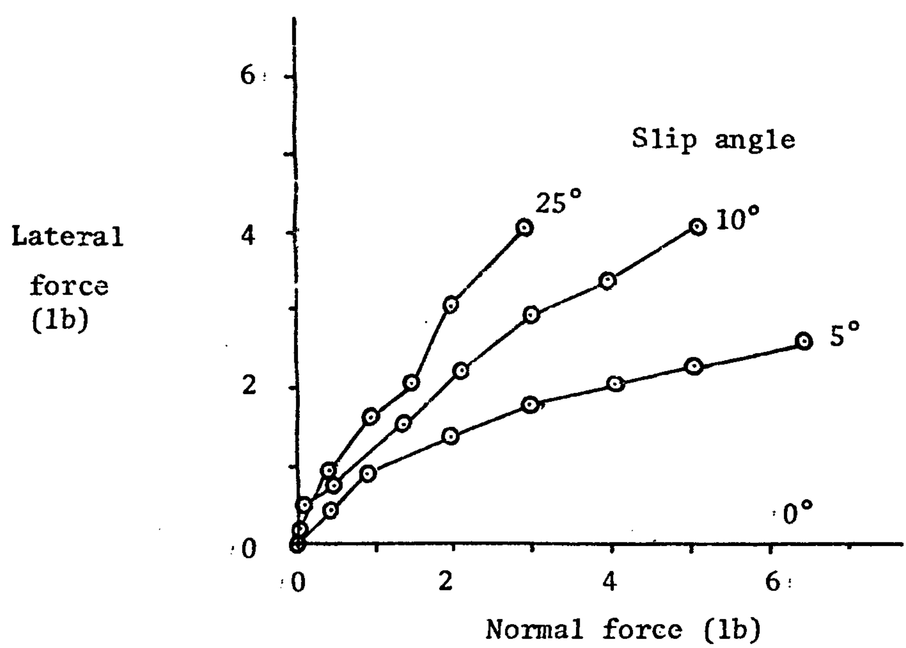

Figure 4-10. Front Tire Lateral Force as Functions of the Tire Normal Force.

TABLE 4-4. Lateral Force Coefficients for Scale-Model Tractor Tires.

	Slip angle (degrees)	Lateral force coefficient (F_ℓ/F_n)	r
Rear tires	5	1.07	0.986
	10	1.85	0.991
	15	2.22	0.983
	20	2.59	0.981
	25	2.87	0.985
	30	3.39	0.952
Front tires	5	0.466	0.979
	10	0.863	0.989
	15	1.27	0.995
	20	1.44	0.999
	25	1.65	0.999
	30	1.65	0.999
	40	2.14	0.985

F_d is the radial damping force, lb,

C_d is the viscous damping coefficient, lb-sec/in,

$(\underline{V}_{CI} \cdot \underline{U}_{RI})$ is the component of the wheel center velocity that is radial away from the wheel center, in/sec, and

d is the tire radial deflection, in.

Thus the tire damping characteristic is defined by the damping coefficient C_d

The tire radial damping coefficients were measured by recording simultaneously on an oscilloscope screen the acceleration of the tire and the acceleration of a vibrating surface against which the tire rested. The phase angle between the sinusoidal tire and surface accelerations provided a damping ratio for the tire from which the damping coefficient could be determined. Figure 4-11 shows the physical arrangement used in exciting the tire and in recording the accelerations. A detailed description of the equipment and procedure used in measuring the tire damping is presented in Appendix B. Table 4-5 presents those tire radial damping coefficients determined for the scale-model tractor tires.

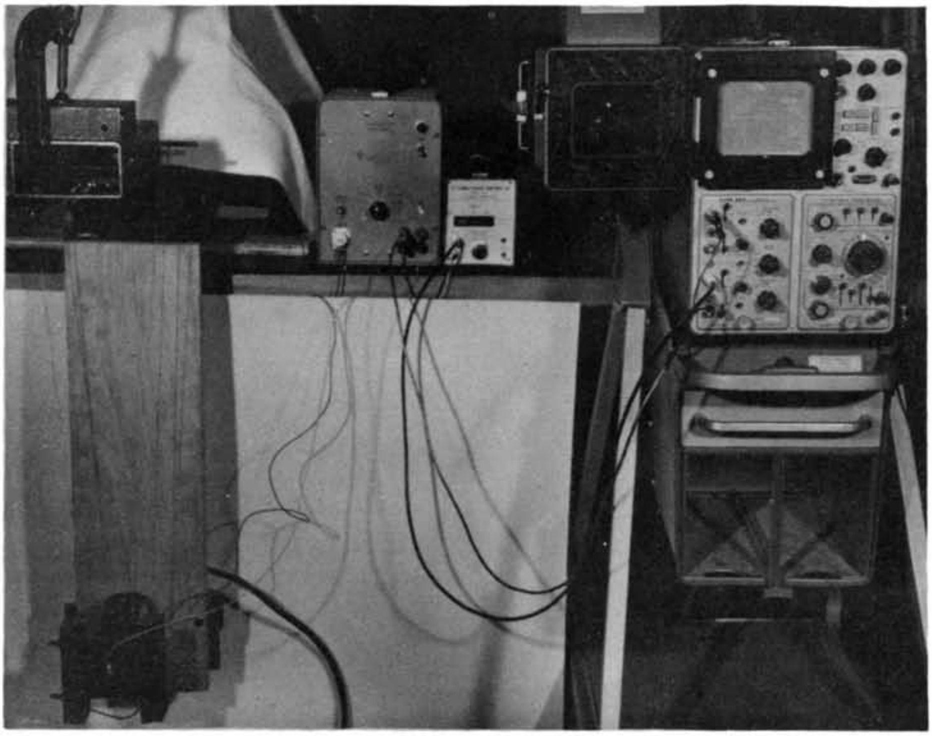

Figure 4-11. Apparatus Used to Measure Tire Radial Damping.

TABLE 4-5. Scale Model Tire Radial Damping Coefficients

	Damping ratio ζ	Damping coefficient C_d (lb-sec/in)
Rear tires		
Case A	0.07	0.54
Case B	0.10	0.49
Front tires		
Case A	0.05	0.21
Case B	0.07	0.09

4.4. Overturn Tests

The response of the model tractor as it traverses the model overturn test course may be observed from actual tests after all the model characteristics have been determined. Because the tractor model was an unpowered vehicle, a starting ramp (as shown in Figure 4-12) was used to provide the tractor a controlled speed as it encountered the test terrain. The ramp height was made adjustable so the tractor speed could be varied.

The tractor path of travel was controlled by setting the front wheels at given steer angles and by orienting the tractor relative to the test course as desired prior to release from the ramp.

Figure 4-13 shows the technique used to set the steer angle of the front tires in a repeatable manner. The tractor has two holes drilled in the bottom of its chassis centerline for use in alignment of the chassis. The tractor was set on two spring-loaded, pointed vertical rods so that they were inserted firmly into the two alignment holes as the tractor wheels contacted the platform shown. Then when a small rod was inserted into a horizontal hole in each spindle pointing forward parallel to the front wheel plane, this rod swept an arc as the wheel was turned. Marks on the platform provided reference points to assure that each front wheel was aimed in the proper direction relative to the tractor chassis. The steering knuckles were then tightened to hold the front wheels in the directions chosen for this test.

The tractor orientation on the starting ramp was also established by setting the tractor chassis on two pointed rods which were

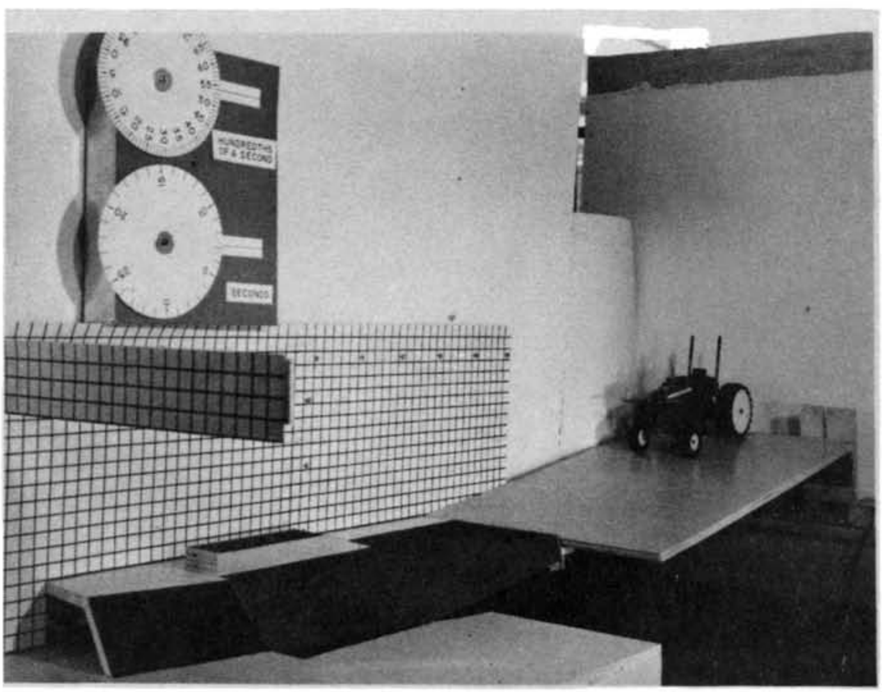

Figure 4-12. The Model Tractor in Position on the Starting Ramp.

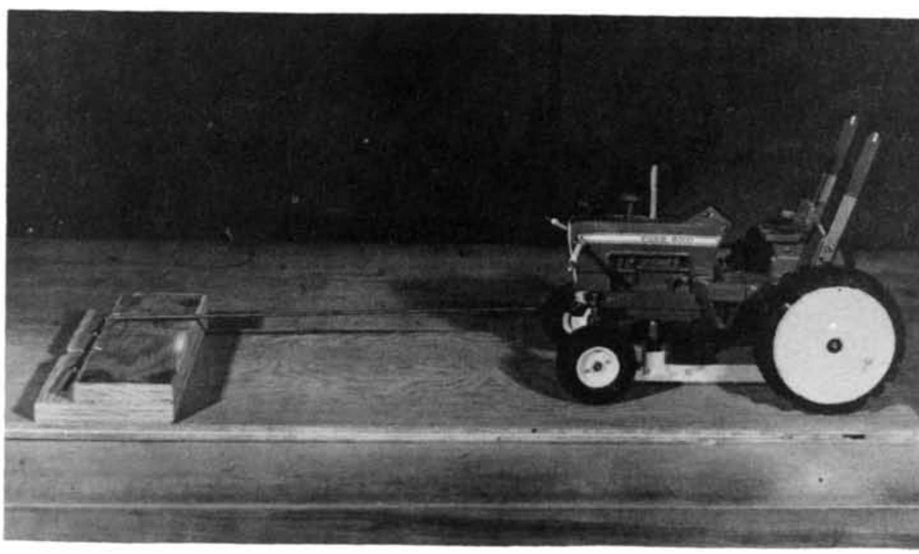

Figure 4-13. Aligning the Front Wheels of the Model Tractor.

previously aligned with the desired tractor path. After alignment of the tractor in this manner, the tractor drawbar was hooked with a solenoid-actuated release and the alignment points were lowered from the holes in the chassis. Then, when release was desired, a push-button actuated the release mechanism and the tractor rolled freely down the ramp toward the test course. Figure 4-14 shows the tractor as it sits above the alignment points. The lever under the ramp was used to raise and lower the alignment points. The push-botton release is also shown.

The motion of the tractor as it traversed the test terrain was studied in three dimensions by using a mirror arrangement as shown in Figure 4-15 and recording the two views simultaneously in high-speed movies. The movie camera-terrain-mirror arrangement was set so that one view was along the $\underline{e}_{I_2}$ axis at the origin while the mirror view was along the $\underline{e}_{I_1}$ (in the - $\underline{e}_{I_1}$ direction) axis at the origin. This provided simultaneous views from two perpendicular directions from which three-dimensional coordinates could be derived for points of interest.

The time base for studying the tractor motion was provided by the clock shown in Figure 4-15. This clock, constructed of two synchronous motors, was started by the tractor-release switch and was photographed together with the two views of the tractor during the overturn test.

The camera used in photographing the tractor model overturns was a Paillard-Bolex, H16 (16 mm) reflex movie camera with zoom lens.

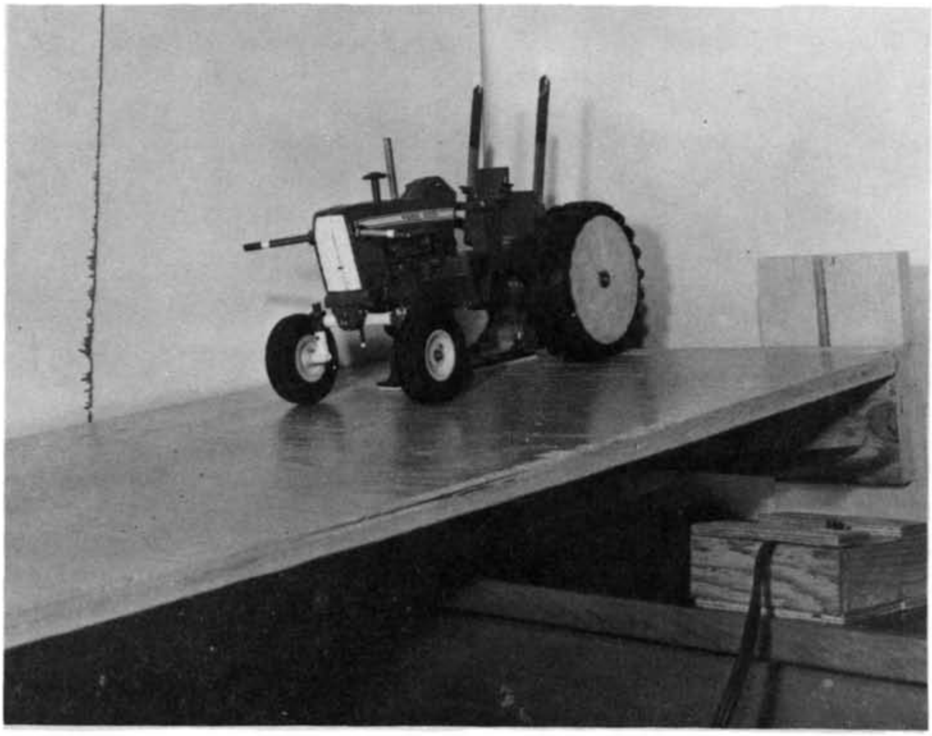

Figure 4-14. Model Tractor Over Alignment Points on the Starting Ramp.

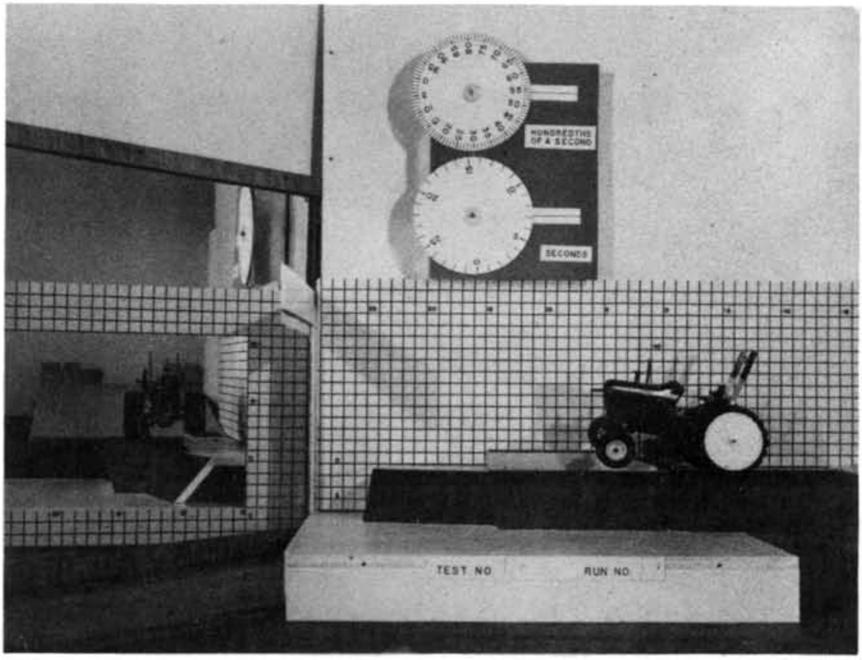

Figure 4-15. The 3-Dimensional View of the Scale-Model Tractor-Terrain System as Seen by the Movie Camera.

To obtain maximum depth-of-field (as required by the two views at different distances from the camera), the camera was located about thirteen feet from the test ramp and grid plane in the direct view. Filming at seventy-two frames per second (maximum rate for this camera), using color film to take advantage of the color contrast, and using a small aperture setting to increase depth-of-field greatly increased the lighting demands, thus requiring a large amount of auxiliary lighting. High-speed Ektachrome* EF 449 movie film with an aperture setting of f/11 provided a reasonable combination for the overturn movies.

Ten model tractor overturns were filmed to provide replication for five different tests. Tests 1 through 3 were overturns in which the tractor front wheel steer angles were set at 0.0 degrees, the maximum front-end rotation angle was set at 10.0 degrees, while three different starting heights were used. Test number 4 was similar to tests 1 through 3 except that the maximum front-end rotation angle was set at 2.0 degrees. Test number 5 was conducted with the maximum front-end rotation angle set at 2.0 degrees, and the right front steer angle set at -3.5 degrees, the left front steer angle set at -2.5 degrees, and the tractor oriented so as to miss the overturn ramp and run down the bank. Table 4-6 summarizes these five overturn test conditions.

4.5. Verification of the Mathematical Model

Verification of the mathematical model for the wide-front-end tractor was provided by comparing the filmed physical model overturns

TABLE 4-6. Steering and Front-End Rotation Conditions Set for the Model Overturn Tests.

Test no.	Front-end rotation limit (degrees)	Steering angles (degrees) left	right
1	10	0	0
2	10	0	0
3	10	0	0
4	2	0	0
5	2	-2.5	-3.5

to the mathematical model overturns generated by the digital computer program. Each physical model overturn (except test number 5) was replicated to provide an indication of the variation that could be expected from overturn tests in this manner.

The digital computer program used in the computer simulations is presented in Appendix C. The program is written in the Fortran IV programming language and contains in itself all the supportive subroutines needed for execution. Only standard functions which are available at most computing installations (e.g., absolute values, trigonometric functions, etc.) are omitted. Notation used in the program is usually suggestive of the variable names used in the description of the mathematical model given in Chapter III.

The position of the tractor during each of the overturns is defined by the positions of the four tractor-body reference points (described in Section 4.1) in the inertial reference frame. Comparisons of the tractor motion in the experimental and simulated cases are based upon the positions of these four points at instants in time common to both the experimental films and the simulation printouts. The positions of the reference points are provided by the computer program when these four points are defined as points to be monitored (input as data in data block 5; see Appendix C). For the experimental overturns the inertial coordinates of these points must be derived from geometric relationships for the test course, grid system, and movie camera locations.

Figure 4-16 shows a plan view of the arrangement used in filming the scale-model experimental overturns. (Figure 4-15 is a photograph, taken from a point near the movie camera position, showing the grid system and mirror arrangement.) The two grid planes - grid F which is vertical and parallel to the $\underline{e}_{I_1}$ axis, and grid S which is vertical and parallel to the $\underline{e}_{I_2}$ axis - provide three location readings for each point of interest. Grid F, behind the overturn course, provides a horizontal position reading (X_{R_1}) and a vertical position reading (X_{R_3}). Grid S, between the mirror and the test course, provides the second horizontal position reading (X_{R_2}). These three position readings and the camera-mirror-grid system geometry provide the information needed to determine the inertial coordinates for the points of interest.

The three position readings are converted into the inertial coordinates - X_{I_1}, X_{I_2}, X_{I_3} - respectively in the directions -

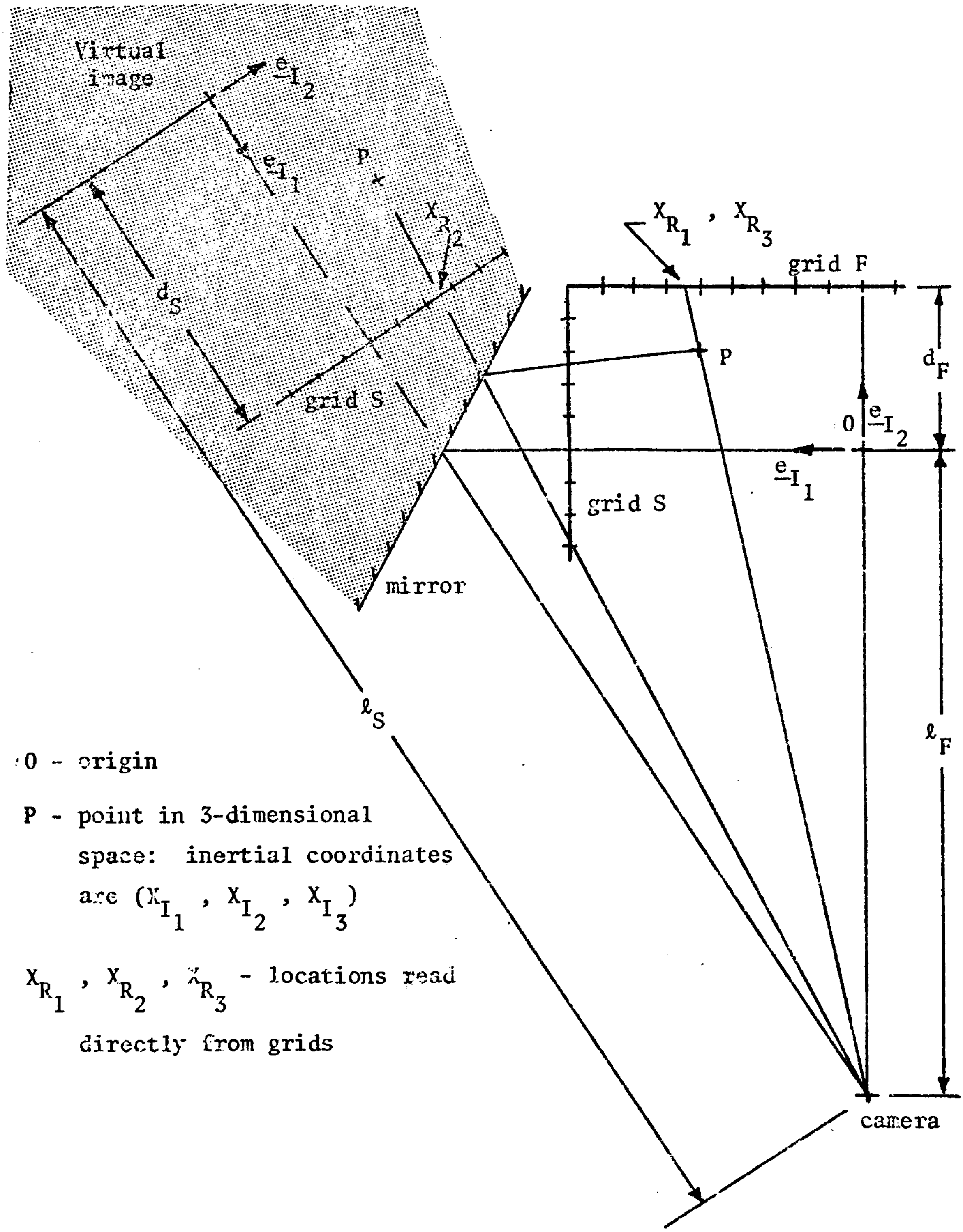

Figure 4-16. Geometric Relationships Determining Inertial Coordinates for Points in the Movies.

$\underline{e}_{I_1}$, $\underline{e}_{I_2}$, $\underline{e}_{I_3}$ - by the following geometrically-derived relationships

$$X_{I_1} = [(X_{R_1}\ell_F)(\ell_S - d_S) - (X_{R_2})(X_{R_1}\ell_F)] \\ /[(\ell_F + d_F)(\ell_S - d_S) + X_{R_1}X_{R_2}] \quad (4\text{-}6)$$

$$X_{I_2} = [(\ell_F + d_F)(X_{R_2}\ell_S) - (X_{R_2})(X_{R_1}\ell_F)] \\ /[(\ell_F + d_F)(\ell_S - d_S) + X_{R_1}X_{R_2}] \quad (4\text{-}7)$$

$$X_{I_3} = [(X_{R_3}\ell_F)(\ell_S - d_S) + (X_{R_3})(X_{R_2}\ell_S)] \\ /[(\ell_F + d_F)(\ell_S - d_S) + X_{R_3}X_{R_2}] \quad (4\text{-}8)$$

Frame-by-frame analysis of the overturn movies and the use of equations 4-6 through 4-8 provide the inertial coordinates of the four tractor-body reference points throughout the filmed overturns. These point locations are used not only to study the experimental overturns, but also to define the initial position and velocity of the tractor at the start of each test for use in defining the initial conditions for the computer-simulated overturns. Because the position and velocity of the tractor-body center of mass and the orientation of the tractor-axes coordinates are required as program initial conditions, this information must be obtained from the coordinates of the four tractor-body reference points.

Analysis of the tractor motion is interesting only after the tractor leaves the level, smooth surface and encounters the ramp and bank of the overturn test course. Thus the experimental analysis and the simulations commence when the tractor is near these irregular surfaces. Initiating the simulations just prior to the tractor's encountering the irregular surface simplifies the definition of initial conditions by allowing the computer program to define the vertical considerations appropriate for the tractor on a zero-elevation level surface. This requires definition of only horizontal position, velocity, and orientation initial conditions from the movie data.

Figure 4-17 shows the plan view of a tractor in the inertial reference frame. The four reference points - LR , RR , LF , and RF - and the tractor center of mass are shown, as are the horizontal unit vectors - $\underline{e}_{I_2}$, $\underline{e}_{I_1}$, and $\underline{e}_{I_2}$. The tractor plane of symmetry, denoted by the "centerline," passes through points R and F . The tractor initial conditions in the horizontal directions are derived from the geometric relationships of this figure.

The inertial coordinates of points R and F are defined, respectively, as the average values for the coordinates of the LR and RR and the LF and RF reference points,

$$\underline{X}_{RI} = \frac{1}{2}(\underline{X}_{LRI} + \underline{X}_{RRI}) \tag{4-9}$$

and

$$\underline{X}_{FI} = \frac{1}{2}(\underline{X}_{LFI} + \underline{X}_{RFI}) \; . \tag{4-10}$$

Then the location of the tractor-body center of mass is defined along the horizontal "centerline" by the geometry of the tractor

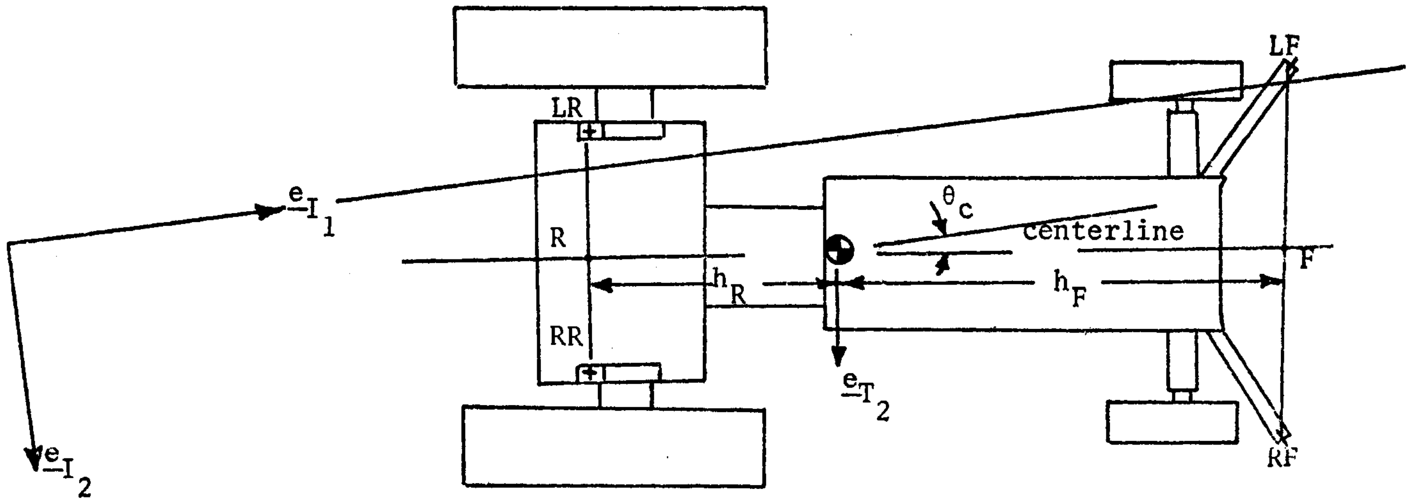

Figure 4-17. Notation for the Definition of Tractor Initial Conditions from Inertial Coordinates of the Tractor-Body Reference Points.

$$X_{BI_i} = X_{RI_i} + \frac{h_R}{(h_R+h_F)} (X_{FI_i} - X_{RI_i}) \ ; \quad i = 1,2 \ , \quad (4\text{-}11)$$

where

X_{BI_i} are the horizontal coordinates for the tractor-body center-of-mass location, in,

h_R is the horizontal distance along the tractor centerline from the tractor-body center of mass to the straight line connecting the two rear reference points, in, and

h_F is the horizontal distance along the tractor centerline from the tractor-body center of mass to the straight line connecting the two front reference points, in.

The orientation of the tractor in the horizontal plane is defined by the angle between the tractor centerline and the $\underline{e}_{I_1}$ axis. This angle is calculated from the coordinates of the reference points by

$$\theta_c = \arctan \left[\frac{X_{FI_2} - X_{RI_2}}{X_{FI_1} - X_{RI_1}} \right] , \qquad (4\text{-}12)$$

where

θ_c is the angle of the tractor centerline from the $\underline{e}_{I_1}$ axis (positive clockwise), rad.

The tractor velocity is determined from the locations of the tractor-body center of mass at the times associated with each of the movie frames. For each filmed overturn the times read from the clock were recorded and expressed as a linear function of the frame number

$$t = t_0 + bf \tag{4-13}$$

where

- t is the time for any frame number f, sec,
- t_0 is the time predicted for frame number zero, sec,
- f is the frame number, and
- b is the slope of the curve, i.e., the time elapsed per frame, sec/frame.

This linear relationship provides a more accurate definition of the film speed and the time for each frame than was obtained from individual time readings for the frames.

The tractor-body center-of-mass position was also expressed as a linear function of the frame number,

$$X_{BI_i} = X_{0_i} + c_i f \; ; \quad i = 1,2 \;, \tag{4-12}$$

where

- X_{BI_i} is the i^{th} inertial coordinate for the tractor-body center of mass in frame f, in,
- X_{0_i} is the i^{th} inertial coordinate for the tractor-body center of mass predicted for frame zero, in, and
- c_i is the slope of the position-frame relationship for the i^{th} coordinate, in/frame.

The use of the slopes of equations 4-13 and 4-14 then provides a measure

measure of the tractor center-of-mass velocity,

$$V_{BI_i} = \frac{c_i}{b} ; \quad i = 1,2 , \tag{4-15}$$

where

V_{BI_i} is the i^{th} horizontal component of the velocity for the tractor-body center of mass, in/sec.

The frame-by-frame analysis for the definition of initial conditions was limited to those frames prior to the tractor's reaching the ramp or bank; thus, from five to seven frames were used to establish the initial conditions for each overturn. The time-per-frame calibration, however, was determined by using all fifty-five frames of the first overturn to calculate the least squares regression equation. The initial conditions were defined for frame number 2 of each overturn so least squares linear equations were used to define the time, position, or orientation corresponding to that frame. Table 4-7 summarizes the initial conditions for each filmed overturn.

Analysis of the tractor motions recorded on film is accomplished by studying the three inertial coordinates of the four tractor-body reference points throughout the overturns. This analysis is presented together with the corresponding analysis of the simulated tractor overturns in Chapter V.

TABLE 4-7. Tractor Initial Conditions Obtained From Film Analysis.

Test no.	Run no.	Time* (sec)	Position (in) X_{BI_1}	X_{BI_2}	Velocity (in/sec) V_{BI_1}	V_{BI_2}	Orientation θ_c (rad)
1	1	1.50	-8.8	0.1	38.0	0.0	0.00
	2	1.49	-9.1	0.5	37.8	0.0	0.00
	3	1.46	-10.4	0.2	40.0	0.0	-0.02
2	1	1.24	-9.3	0.3	44.9	0.0	0.00
	2	1.27	-9.2	0.2	46.8	0.0	0.00
3	1	2.27	-9.8	0.2	21.9	0.0	0.00
	2	2.29	-9.4	0.3	20.7	0.0	0.00
4	1	1.64	-10.0	0.2	34.2	0.0	-0.02
	2	1.75	-7.63	0.0	32.9	0.0	-0.02
5	1	1.67	-7.41	-1.5	23.8	-6.2	-0.21

*Time calculations were based upon the coefficient obtained from the linear regression of time vs. frame - 0.0141 sec/frame.

CHAPTER V

RESULTS AND DISCUSSION

This study of tractor overturns includes the analysis of scale-model tractor overturns, verification of the mathematical model developed to simulate tractor overturns, and analysis of overturns simulated from the mathematical model. Section 5.1 presents the results of the experimental overturns and discusses the repeatability of tractor motions under laboratory conditions. Comparisons of simulated and experimental overturns to validate the mathematical model for tractor overturns are discussed in Section 5.2. Section 5.3 presents an analysis of the information generated in two overturn simulations.

5.1. Scale-Model Tractor Overturns

Ten side overturns of a scale-model tractor were filmed for five different overturn conditions. Frame-by-frame analysis of each filmed overturn yielded three grid readings* for each of the four tractor-body reference points from which the three inertial coordinates of these reference points were defined for each frame. Every frame of tests 1 through 3 was analyzed while only alternate frames of tests 4 and 5 were analyzed in this manner. The times and inertial coordinates of the reference points are tabulated in Appendix D for each of the ten filmed overturns.

---

*Grid readings from the films were estimated to the nearest 0.1 inch.

Tests 1 and 4 were selected for detailed analysis and for use in verifying the mathematical model. The tractor paths of travel while approaching the overturn ramp and bank were to be the same, but the tractor approach velocities and the front-end rotation limit were to differ for these two tests. These initial conditions as measured prior to the runs or prior to the tractor's contact with the overturn ramp are tabulated in Tables 4-6 and 4-7.

Three replications for test 1 and two for test 4 were filmed to obtain an indication of the test repeatability. Test repeatability was determined visually by plotting the tractor-body reference-point inertial coordinates as a function of time for each replication. Plotting all the replications of one coordinate path on a single set of plot axes provided a simple comparison of the reference-point paths throughout the overturns.

Observation of the overturn films and the final resting points of the scale-model tractor in replicated overturns indicated a high degree of repeatability between replications. This observation suggested that plotting all the reference points was not required to show the degree of repeatability. Thus the coordinate paths of only the left front reference point were plotted for this comparison. This point was selected because its motion showed the effects of the front-end motion and because this point always was a point of impact between the tractor and the ground.

Figure 5-1 shows the paths of the left front reference point in the $\underline{e}_{I_1}$ direction during the three replications of test 1.

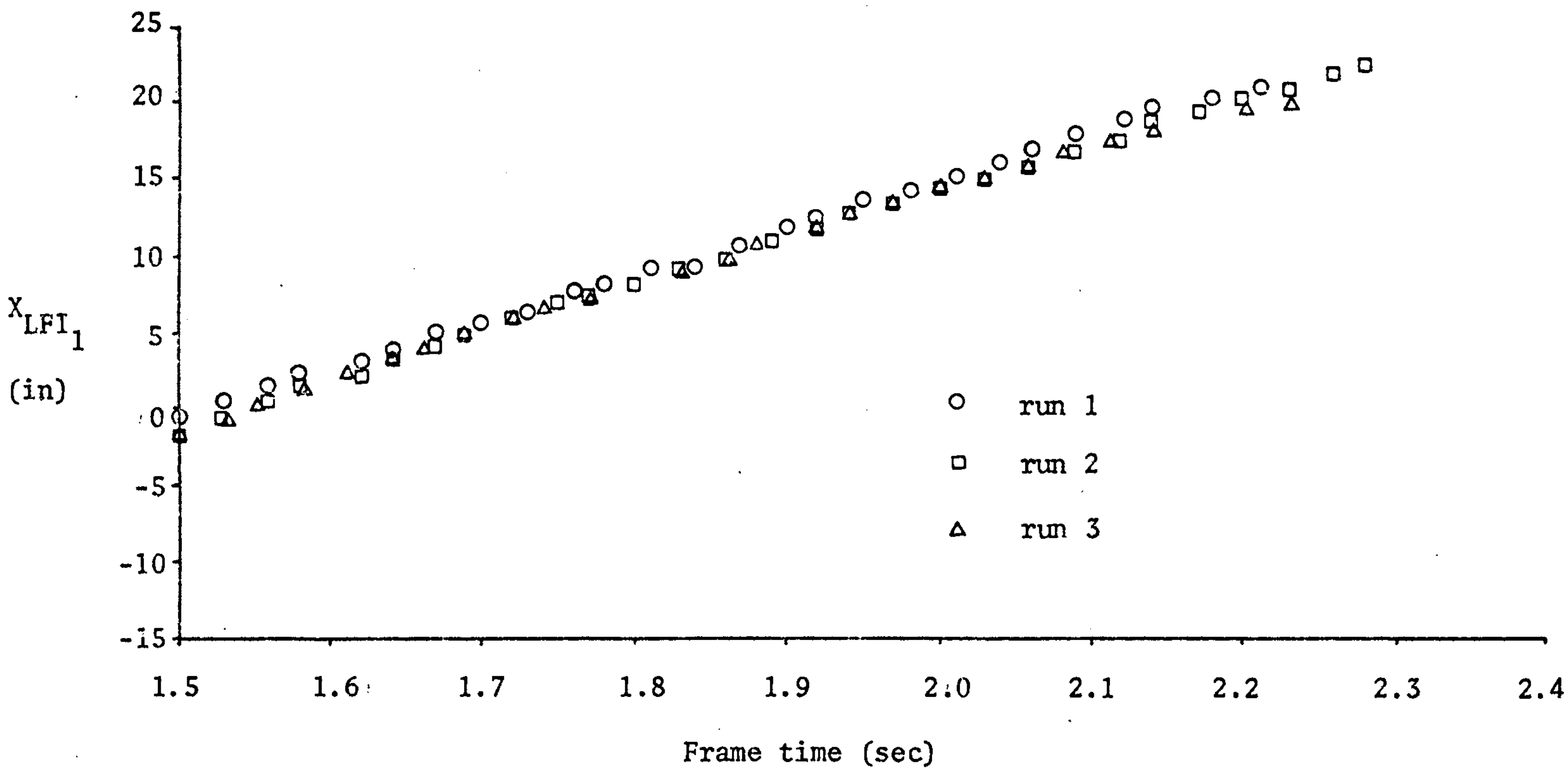

Figure 5-1. Component $\underline{e}_{I_1}$ of the Left Front Tractor-Body Reference-Point Paths for Test 1.

The parallel paths for runs 1 through 3 show that the tractor forward velocity was controlled well in each start. Because the path of run 3 usually is ahead of that for run 1 and the path for run 2 usually is behind that for run 1 (at the same frame time), the path discrepancies may be caused by slightly different clock settings when the tractor was released from its starting position. An adjustment of 0.01 to 0.02 seconds would shift the paths into nearly perfect agreement. An error of nearly 0.02 seconds is easily imagined in any one zeroing of the clock prior to its start when the tractor was released.

Figure 5-2 shows the $\underline{e}_{I_2}$ component of the left front reference-point paths during test 1. Again the shapes of the paths for the three runs are very similar, but now the path of run 2 is distinctly offset from runs 1 and 3. The tractor in run 2 travelled along a path which was to the right of (in the + $\underline{e}_{I_2}$ direction from) the other two paths. This difference may be traced to the tractor-body center-of-mass initial conditions (given in Table 4-7) in which the tractor lateral position (X_{BI_2}) shows the tractor of run 2 approaching the terrain irregularities from a position 0.3 to 0.4 inch to the right of that in runs 1 and 3.

Figure 5-3 shows the $\underline{e}_{I_3}$ component of the left front reference-point paths during test 1. These vertical components of the reference-point paths differ more than did the other components, but this is to be expected when the left wheels travel on the steep bank. Because the path of the tractor in run 2 was distinctly to the right

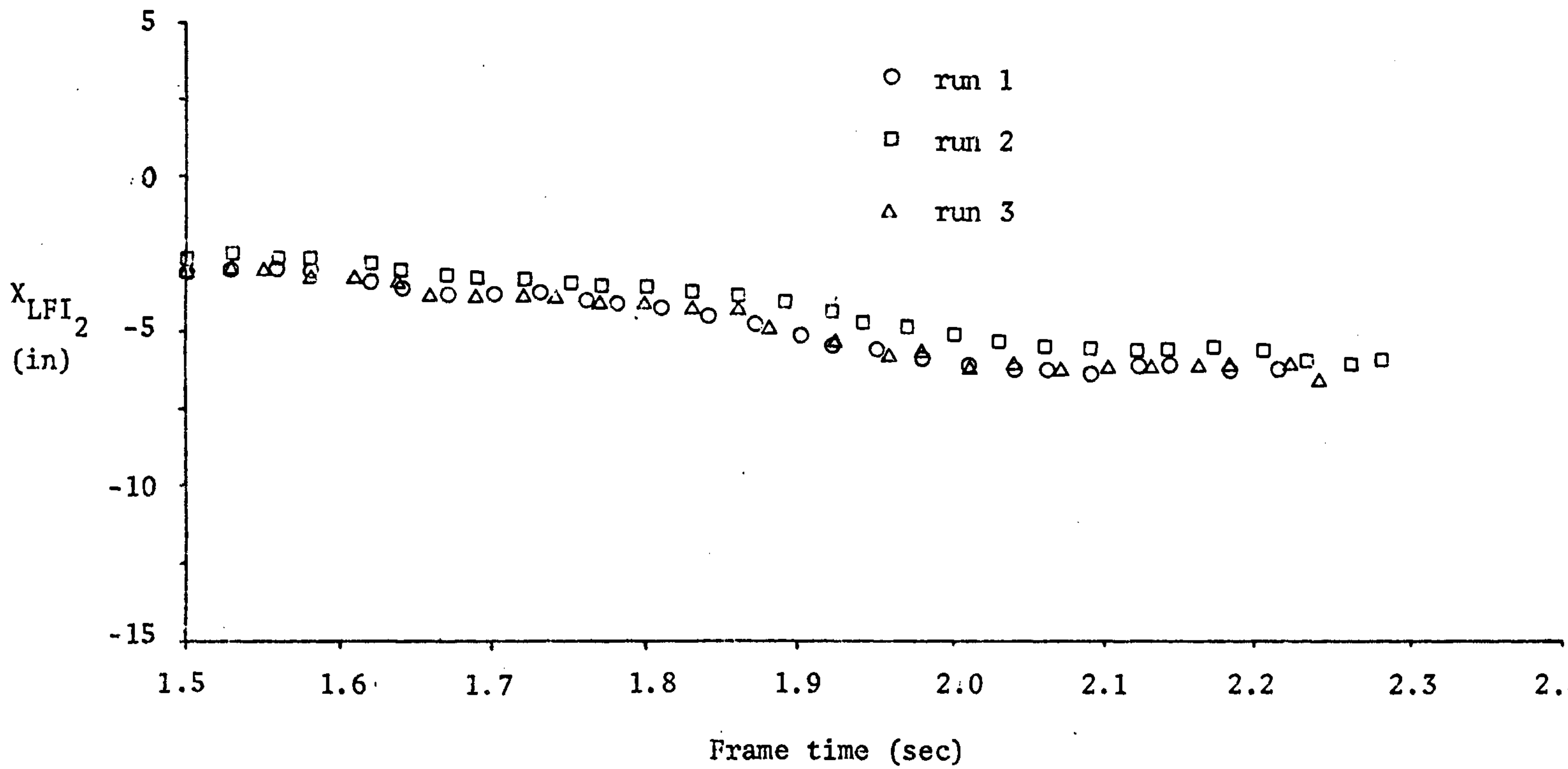

Figure 5-2. Component $\underline{e}_{I_2}$ of the Left Front Tractor-Body Reference-Point Paths for Test 1.

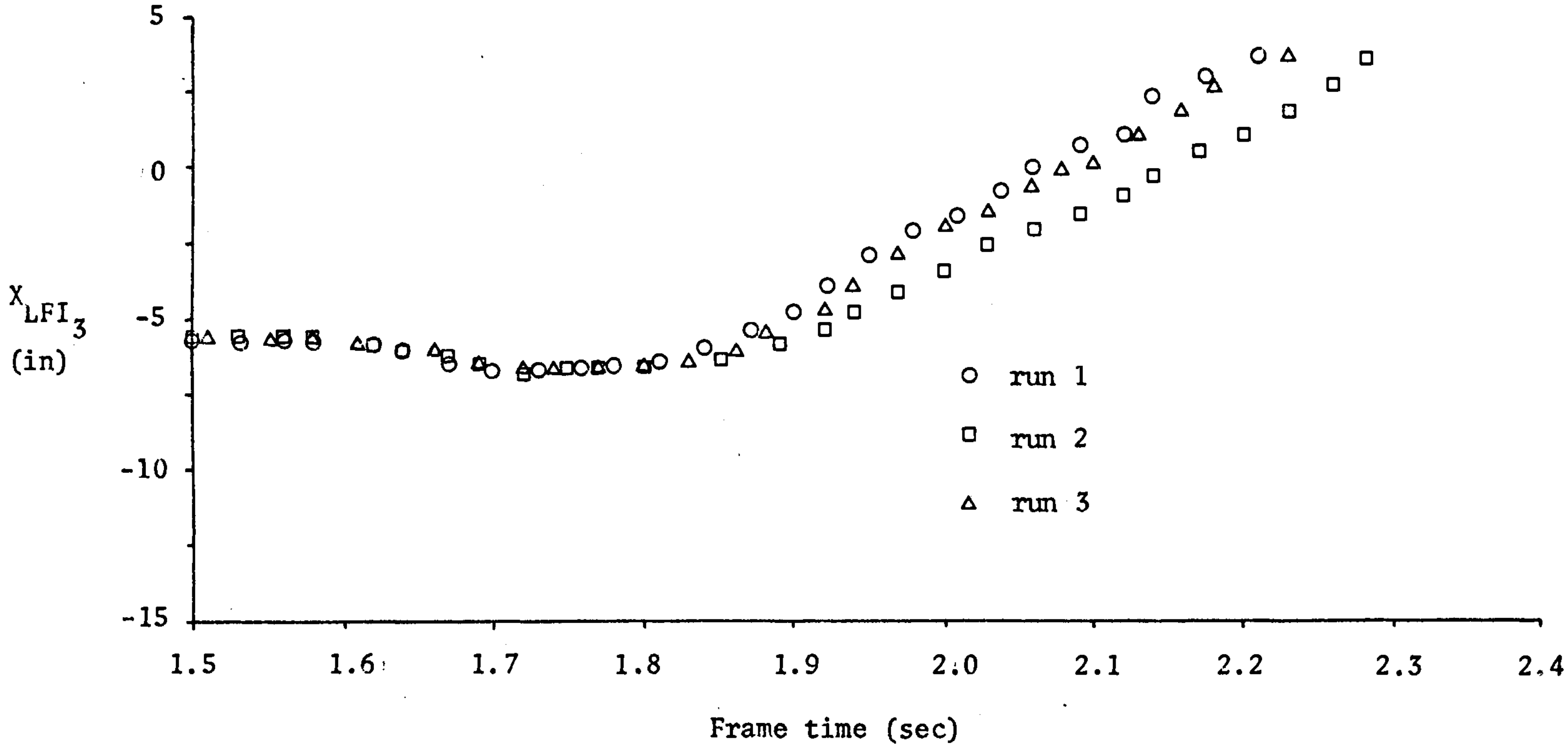

Figure 5-3. Component $\underline{e}_{I_3}$ of the Left Front Tractor-Body Reference-Point Paths for Test 1.

of those in runs 1 and 3, the tractor remained at the greater elevation (more negative values of X_{LFI_3}) for corresponding times in the overturns. This resulted in a greater time period for completing the overturn and, therefore a decreased velocity of ground impact for the left front reference point in run 2.

Whereas the overturns of test 1 differed primarily because their paths of approach were somewhat different, the discrepancies between the two runs of test 4 may be attributed to the clock initialization prior to these overturns. Figures 5-4, 5-5, and 5-6, respectively, show the $\underline{e}_{I_1}$, $\underline{e}_{I_2}$, and $\underline{e}_{I_3}$ components of the left front reference-point paths for test 4. If the frame times for run 2 were decreased by 0.04 second, then each of the plotted components of the reference-point paths would show extermely good agreement between the two runs. Thus the actual paths are in agreement for these two runs but the film frame times are in slight disagreement.

The repeatability of scale-model tractor overturns as demonstrated by the replications of tests 1 and 4 was very good. The lateral paths of the tractor in test 4 and again in runs 1 and 3 of test 1 usually remained within 0.25 inch of one another throughout the analyzed forward travel of the tractor which exceeded 20 inches. The lateral path of the tractor during run 2 of test 1 usually remained within 1.0 inch of the corresponding paths for runs 1 and 3 of the same test. Much of this latter discrepancy can be attributed to path deviations experienced during the travel down the starting ramp and through the approach to the overturn ramp and bank, a distance of

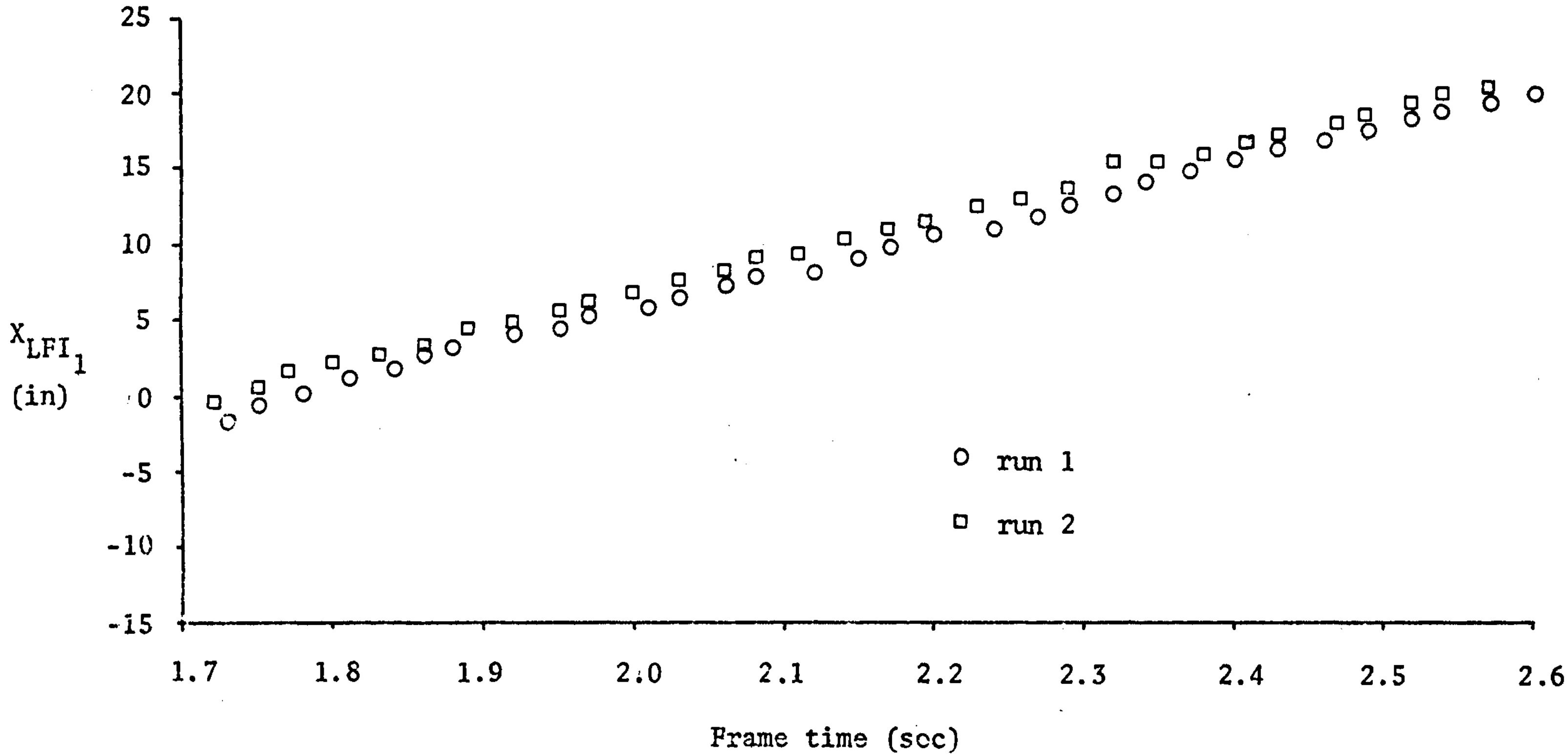

Figure 5-4. Component $\underline{e}_{I_1}$ of the Left Front Tractor-Body Reference-Point Paths for Test 4.

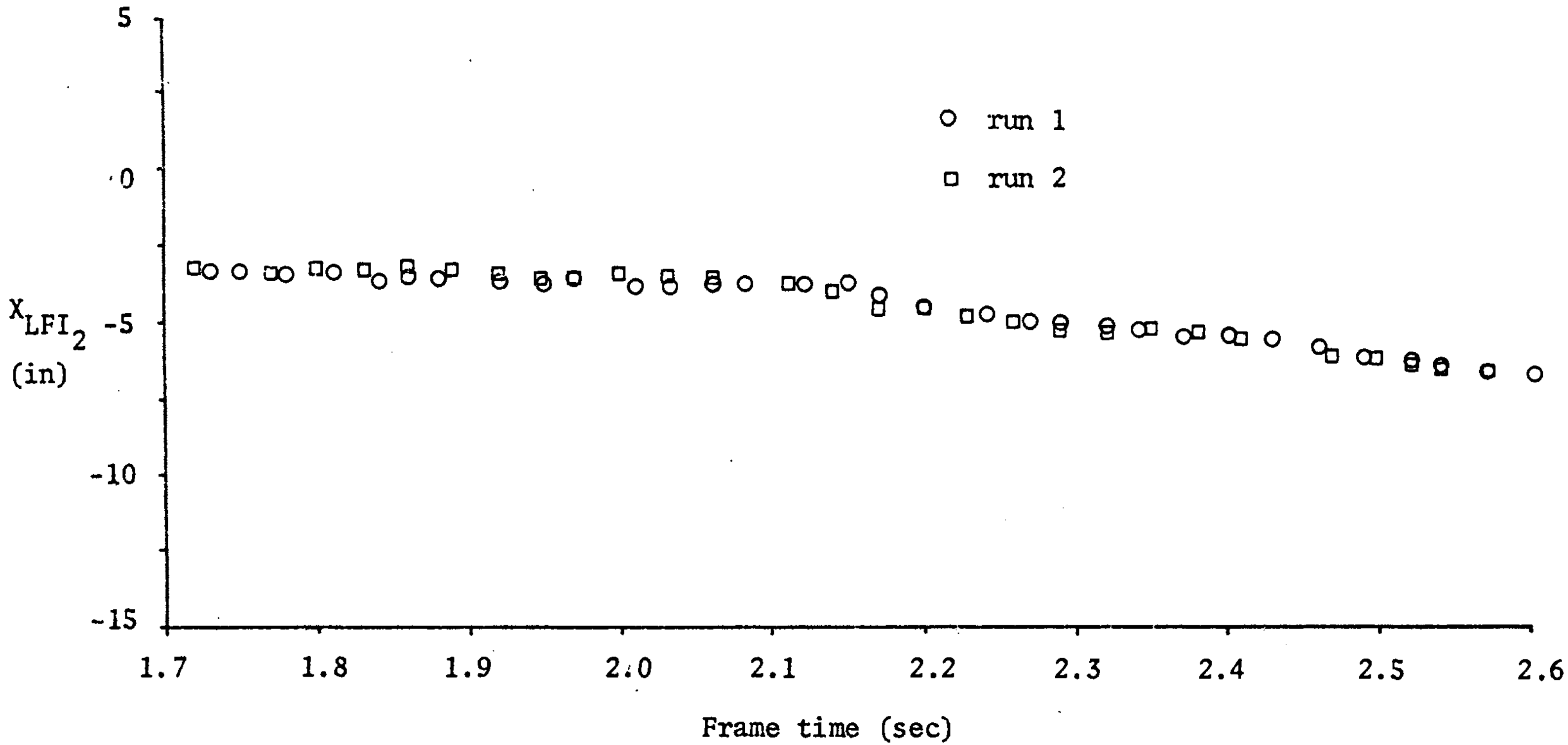

Figure 5-5. Component $\underline{e}_{I_2}$ of the Left Front Tractor-Body Reference-Point Paths for Test 4.

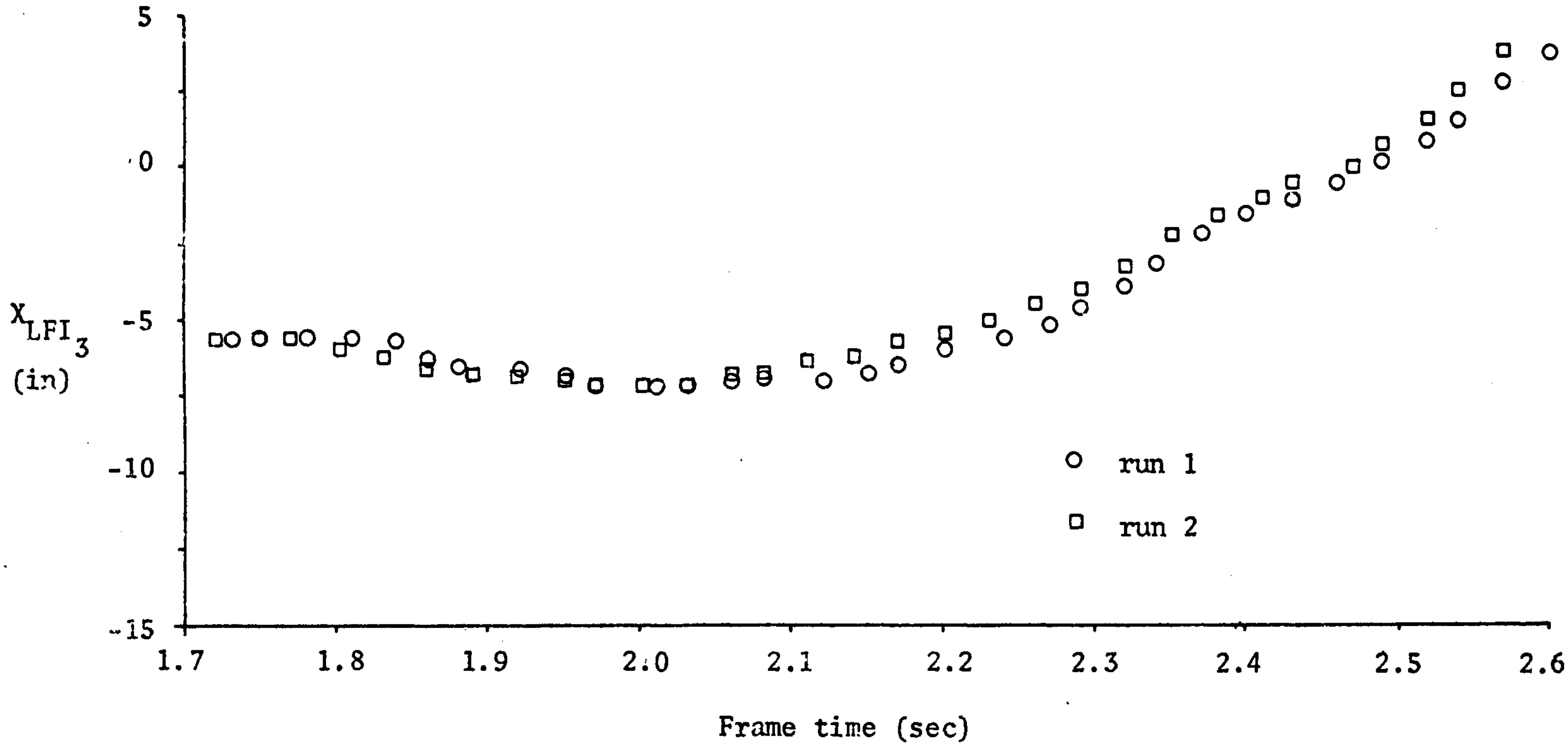

Figure 5-6. Component $\underline{e}_{I_3}$ of the Left Front Tractor-Body Reference-Point Paths for Test 4.

36 inches.

The vertical component of the left front reference-point paths showed very good agreement between runs 1 and 3 of test 1 and again between runs 1 and 2 of test 4. The discrepancies in vertical position were directly related to the lateral component of the tractor paths, i.e., those runs in which the tractor travelled to the right resulted in the wheel contact higher on the bank and thus greater elevations for the left front reference point. The elevations of this reference point seldom differed by more than 0.75 inch between runs 1 and 3 of test 1 and seldom by more than 2.0 inches between any two of the runs for test 1. Test 4, however, showed superb repeatability with elevation differences usually less than 0.25 inch after the frame-time adjustments had been considered.

The high repeatability of the scale-model tractor overturns on the ASAE side-overturn terrain provided evidence that the experimental overturn data was reliable. Thus it was reasonable to use any of the filmed overturns to validate the mathematical model for tractor overturns. Run 1 of test 1 and run 1 of test 4 were selected for use in the model verification. Section 5.2 presents the verification procedure.

5.2. Verification of the Mathematical Model

The mathematical model for wide-front-end wheel-tractor overturns was verified by using the mathematical model for simulation of specific tractor overturns and then comparing the simulated overturn motions to the corresponding scale-model overturn motions. The filmed run 1 of test 1 and run 1 of test 4 were selected as those experimental overturns used to verify the mathematical model. Thus two overturn simulations were generated using the tractor initial conditions of these two experimental overturns. (See Tables 4-6 and 4-7 for the initial conditions.)

As was done in checking the repeatability of experimental scale-model overturns, the comparison of experimental and simulated overturns was made by plotting the corresponding reference-point paths as functions of time. Because the initial times as well as initial positions and velocities of the tractors were specified in each simulation to match those of the corresponding filmed overturns, the paths of the tractor-body reference points for both the experimental and simulated overturns were poltted as functions of the same time scale. Comparisons were made by visual observation of these plotted reference-point paths.

As the tractor traversed the test terrain, three transition points which could significantly affect the tractor-terrain relationship were identified. These are:

1. The right front wheel contacts the ramp incline while the left front wheel reaches the terrain break at the top of the bank.

2. The right front wheel reaches the top of the ramp incline while the center of the left rear wheel tread reaches the terrain break at the top of the bank.

3. The right rear wheel contacts the ramp incline while the inner edge of the left rear wheel tread reaches the terrain break at the top of the bank.

These three events were observed when the front reference points reaches coordinate values in the $\underline{e}_{I_1}$ direction 0.5, 6.0, and 9.0 inches, respectively. These events were important in studying the experimental and simulation tractor motions and in explaining discrepancies.

Figures 5-7 and 5-8 show the $\underline{e}_{I_1}$ component for each of the four tractor-body reference-point paths obtained from both the experimental test 1 and the corresponding simulation. The slopes of these plotted curves, remaining relatively uniform throughout the overturn, show that the tractor forward velocity remained relatively constant throughout the overturn. All curves show a small decrease in forward velocity as the right front wheel climbs the ramp (time = 1.55 to 1.73); then as the left rear wheel reaches the break at the top of the bank, the tractor speed either increases or remains at a constant value.

The simulation tractor motion differs noticeably from the experimentally-observed motion only after the time exceeds 1.88 seconds. After this time the simulation tractor speed increases beyond that of the scale-model tractor resulting in a greater distance travelled and a greater $\underline{e}_{I_1}$ velocity at impact.

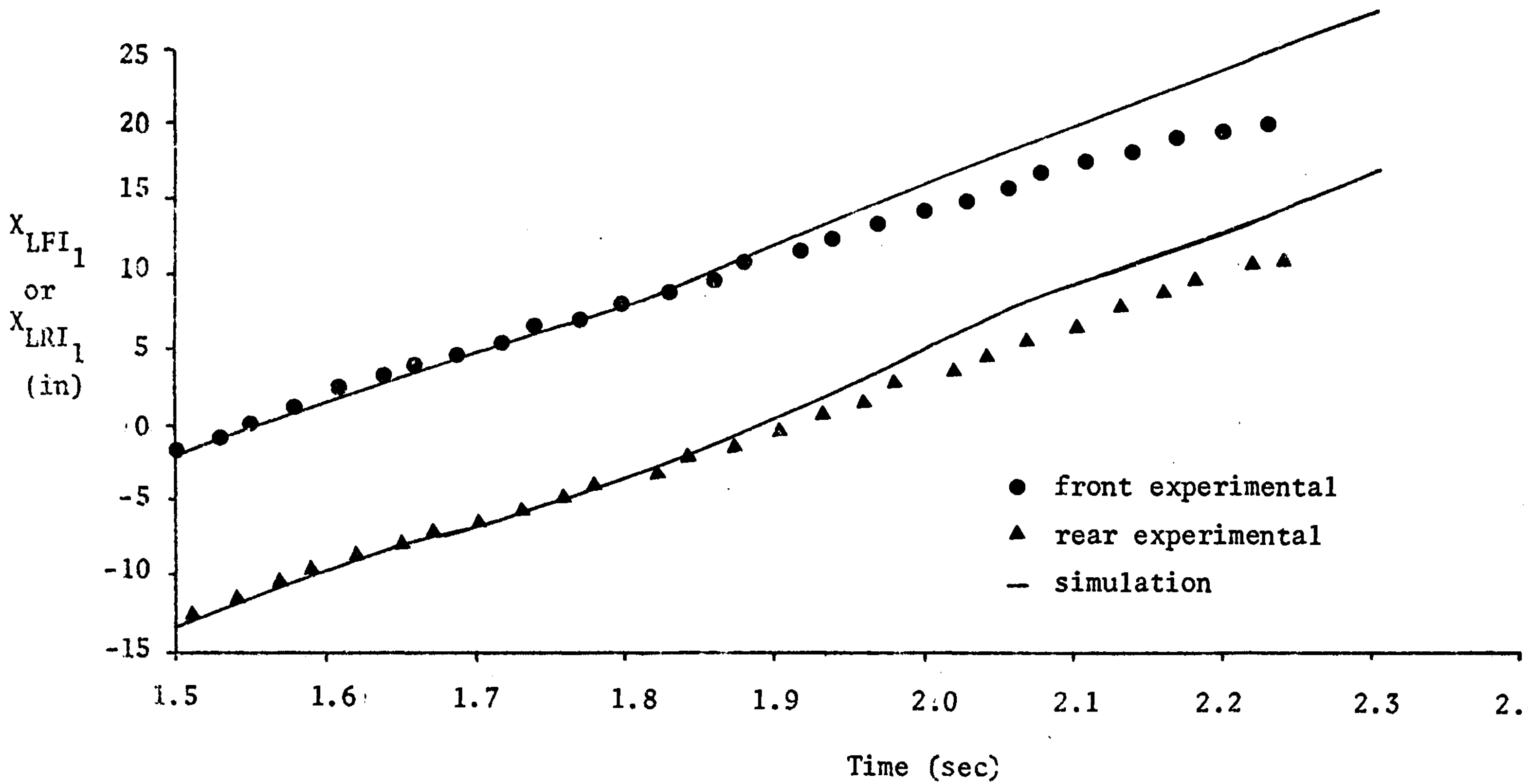

Figure 5-7. Component $\underline{e}_{I_1}$ of Simulation and Experimental Paths for the Left Front and Left Rear Tractor-Body Reference Points During Test 1.

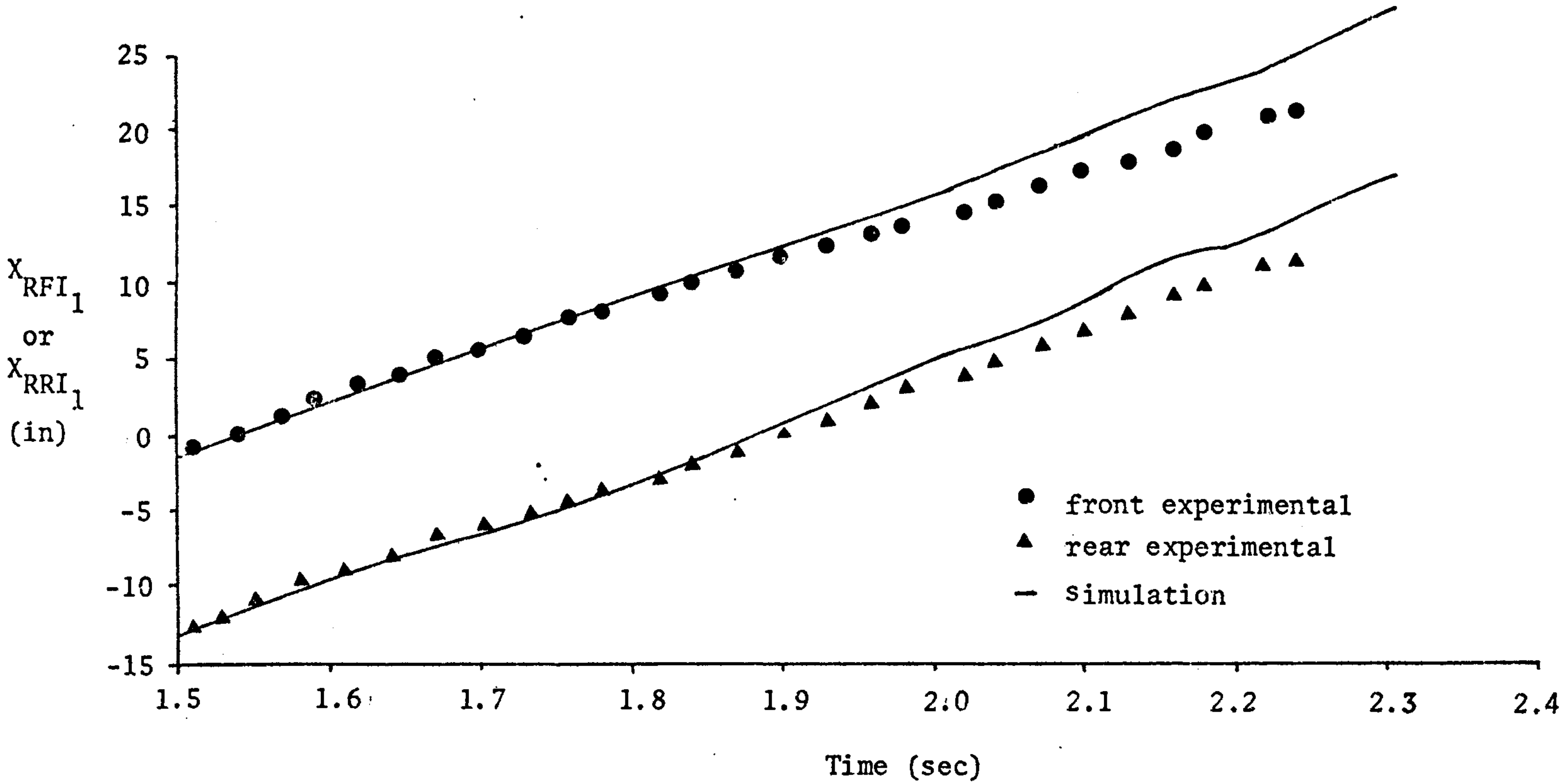

Figure 5-8. Component $\underline{e}_{I_1}$ of Simulation and Experimental Paths for the Right Front and Right Rear Tractor-Body Reference Points During Test 1.

The greatest discrepancy between simulation and experimental distances-of-travel in the $\underline{e}_{I_1}$ direction occurs with the left front reference points being 5 inches apart while the least discrepancy occurs with the right rear reference points 1.5 inches apart after 25 inches of travel. The simulation predicts greater travel distance and greater time elapse than those observed for the experimental overturn.

Figures 5-9 and 5-10 present the $\underline{e}_{I_2}$ component of the four tractor-body reference point paths for the experimental and simulation overturns of test 1. The four reference-point paths move to the left during the overturn, but the two rear reference points, being a greater distance from the tipping axis of the tractor, move left a greater distance than do the front points. The simulation paths of the rear reference points begin their lateral-left motion prior to their experimental counterparts, but the experimental paths then move more quickly and surpass the simulation paths in total lateral motion during the overturn. The simulation paths begin their lateral motion at the transition time (2) when the left rear wheel center is at the top of the bank, but the experimental paths move left only slowly until after the transition time (3) when the entire tire contact patch is over the bank.

The front reference points show little difference between simulation and experimental results prior to a time of 1.95 seconds. After this time the simulation paths for the front reference points diverge to the left of the experimental paths and remain generally to the left until the overturn is completed. The lateral discrepancies

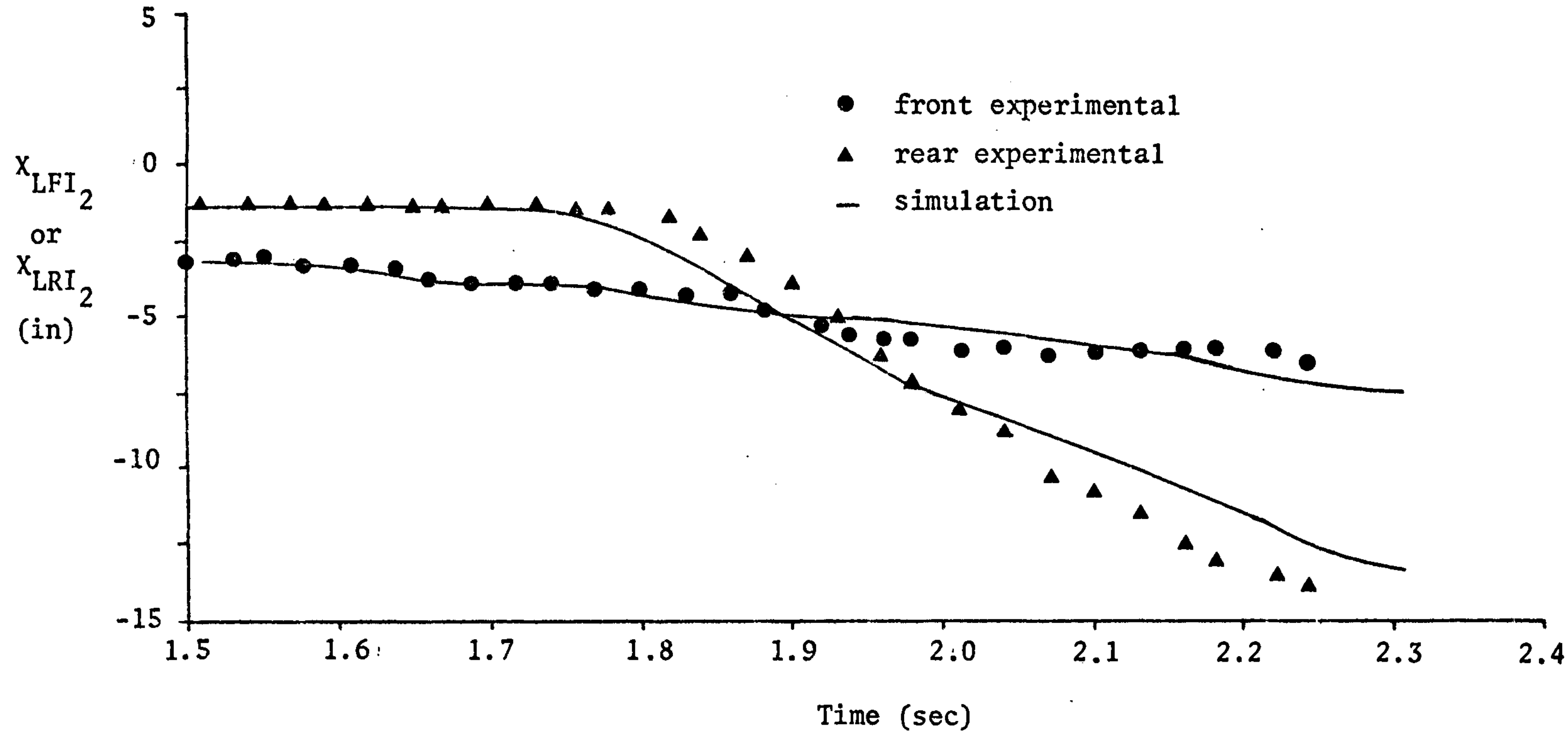

Figure 5-9. Component $\underline{e}_{I_2}$ of Simulation and Experimental Paths for the Left Front and Left Rear Tractor-Body Reference Points During Test 1.

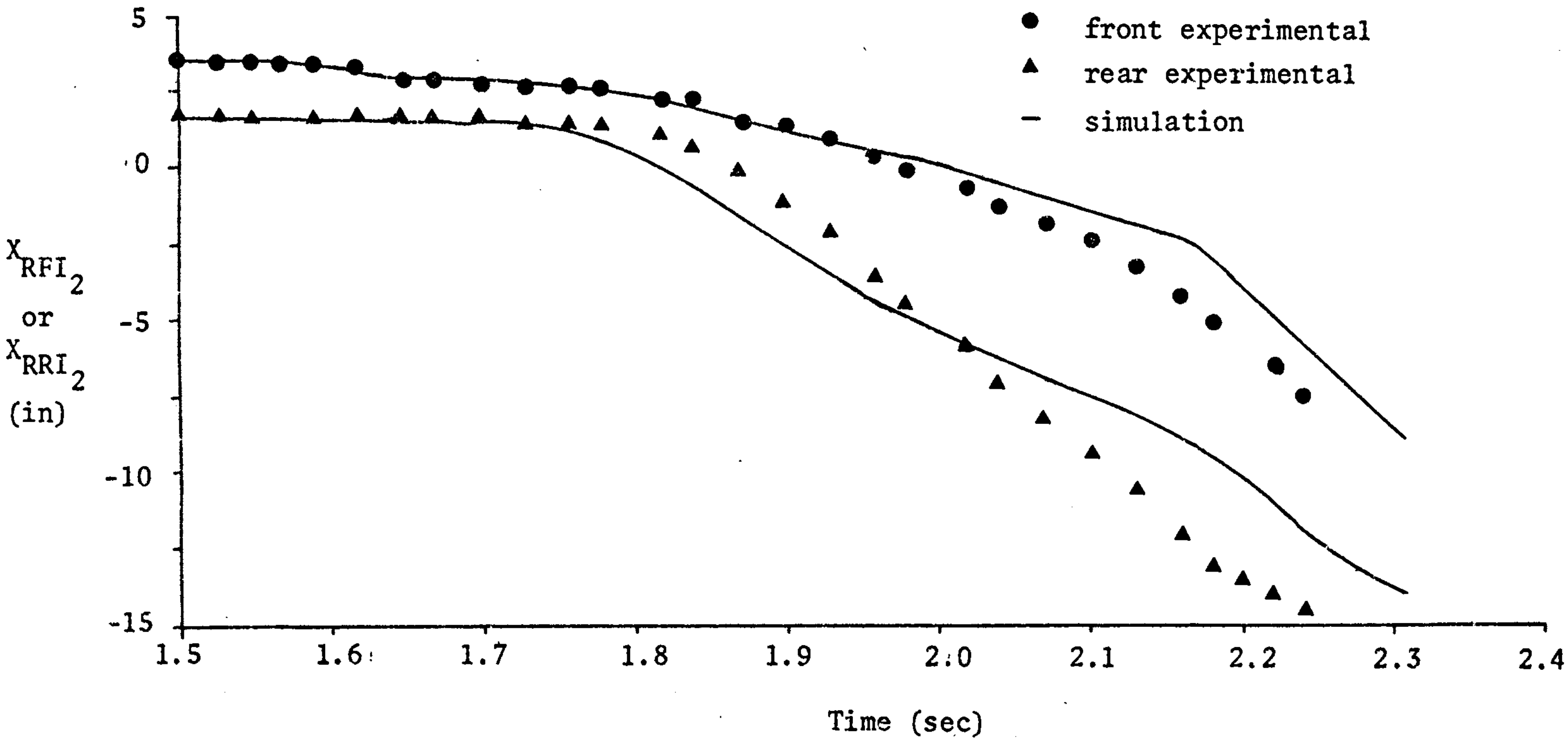

Figure 5-10. Component $\underline{e}_{I_2}$ of Simulation and Experimental Paths for the Right Front and Right Rear Tractor-Body Reference Points During Test 1.

between the reference-point paths of the experimental and simulation overturns seldom reached 2.0 inches while the total lateral distance of travel was nearly 15 inches. The lateral motion of the right rear reference point is an exception which showed 3.0 inch discrepancies during the final stage of the overturn.

Figures 5-11 and 5-12 show the $\underline{e}_{I_3}$ component of the experimental and simulation paths for the four tractor-body reference points during test 1. Remarkable similarity between experimental and simulation paths is seen for all four reference points prior to the transition time (2) when the center of the left rear wheel reaches the break at the top of the bank. At this time the thin simulation wheel begins dropping in elevation, but the thick scale-model wheel continues to support the rear axle at its original elevation. At the transition time (3) when the inner edge of the tire tread passes the break at the top of the bank, the experimental paths also show the effects of a decreasing elevation for the left rear wheel.

A general similarity in the vertical component of the experimental and simulation paths for the reference points is evident. The simulation curves exhibit some abrupt changes which do not occur in the experimental curves, but these variations are not major deviations from the scale-model paths. The abrupt irregularities in the simulation paths appear to be caused by impacts of the tractor tires against the ground surfaces especially as the left tires reach the bottom of the bank and strike the level ground surface. The thin-tire model being more sensitive to terrain changes perpendicular to the tire plane resulted in more abrupt tractor responses in the simulation

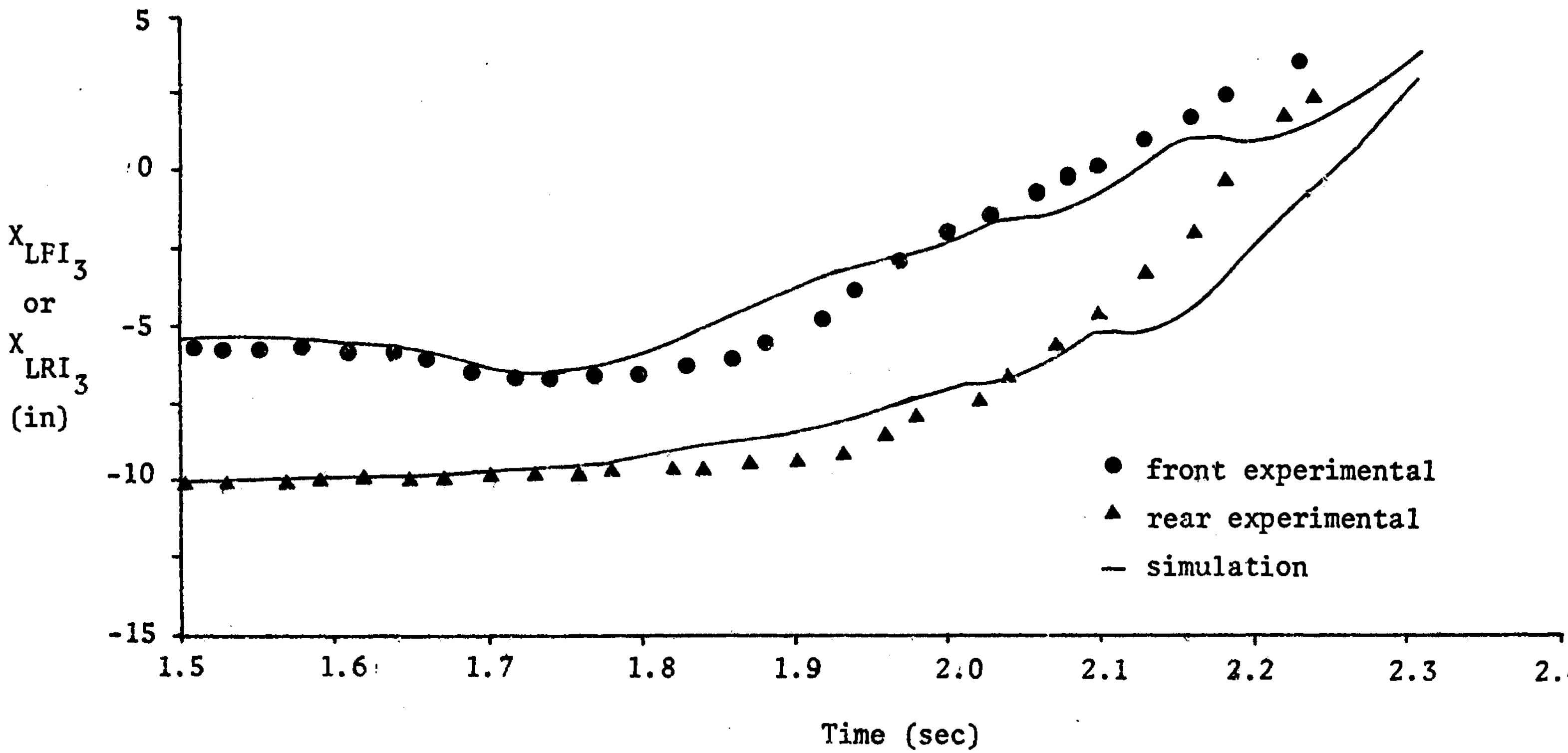

Figure 5-11. Component $\underline{e}_{I_3}$ of Simulation and Experimental Paths for the Left Front and Left Rear Tractor-Body Reference Points During Test 1.

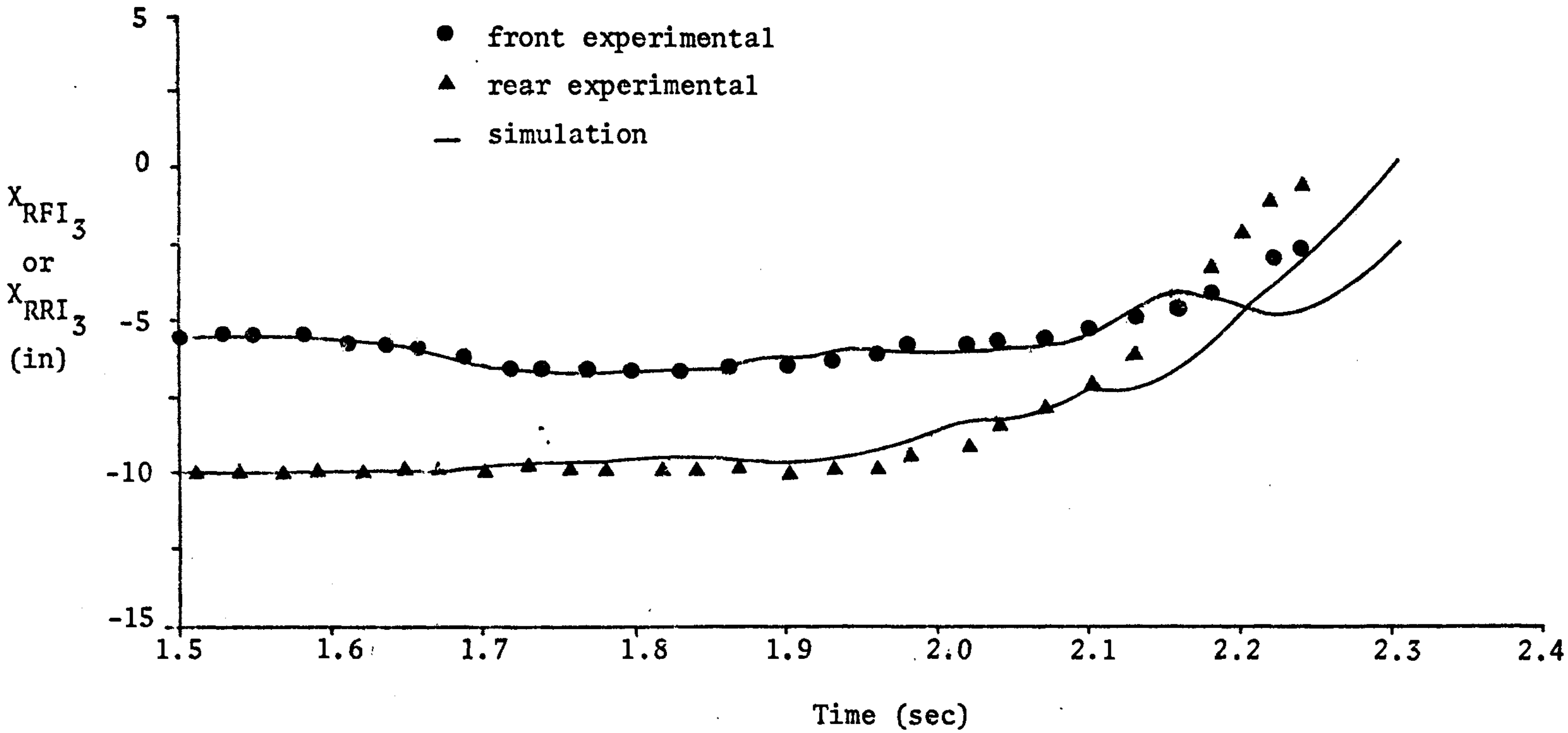

Figure 5-12. Component $\underline{e}_{I_3}$ of Simulation and Experimental Paths for the Right Front and Right Rear Tractor-Body Reference Points During Test 1.

overturn than in the experimental overturn.

The second overturn simulation differed from the first in the tractor initial velocities and positions as well as the rotation limit for the tractor front end. The simulation parameters were defined according to the values of test 4, run 1 of the experimental overturns. (Initial conditions are defined in Tables 4-6 and 4-7.) This overturn resulted from a tractor travelling 90% as fast as the previous case while the front-end rotation was limited to 20% of that for the first simulation overturn.

The experimental and simulation paths for the four tractor-body reference points during test 4 are presented in Figures 5-13 through 5-18. The simulation paths again show the tractor travelling beyond the distance measured experimentally, the discrepancy exceeding that observed for test 1. Again the divergence of simulation and experimental paths begins as the left rear wheel reaches the terrain break at the top of the bank.

The smaller front-end rotation limit in test 4 causes the tractor body to rotate laterally earlier in its travel across the overturn course and increases the weight transfer to the left rear wheel beyond that for test 1. The increased left wheel reactions provide greater accelerating forces in the forward direction causing the thin-wheel model of the simulation for test 4 to predict forward motion exceeding that measured experimentally, the discrepancy being larger than that in test 1.

The lateral component ($\underline{e}_{I_2}$ direction) of the reference-point paths for test 4 are very similar to those for test 1. The

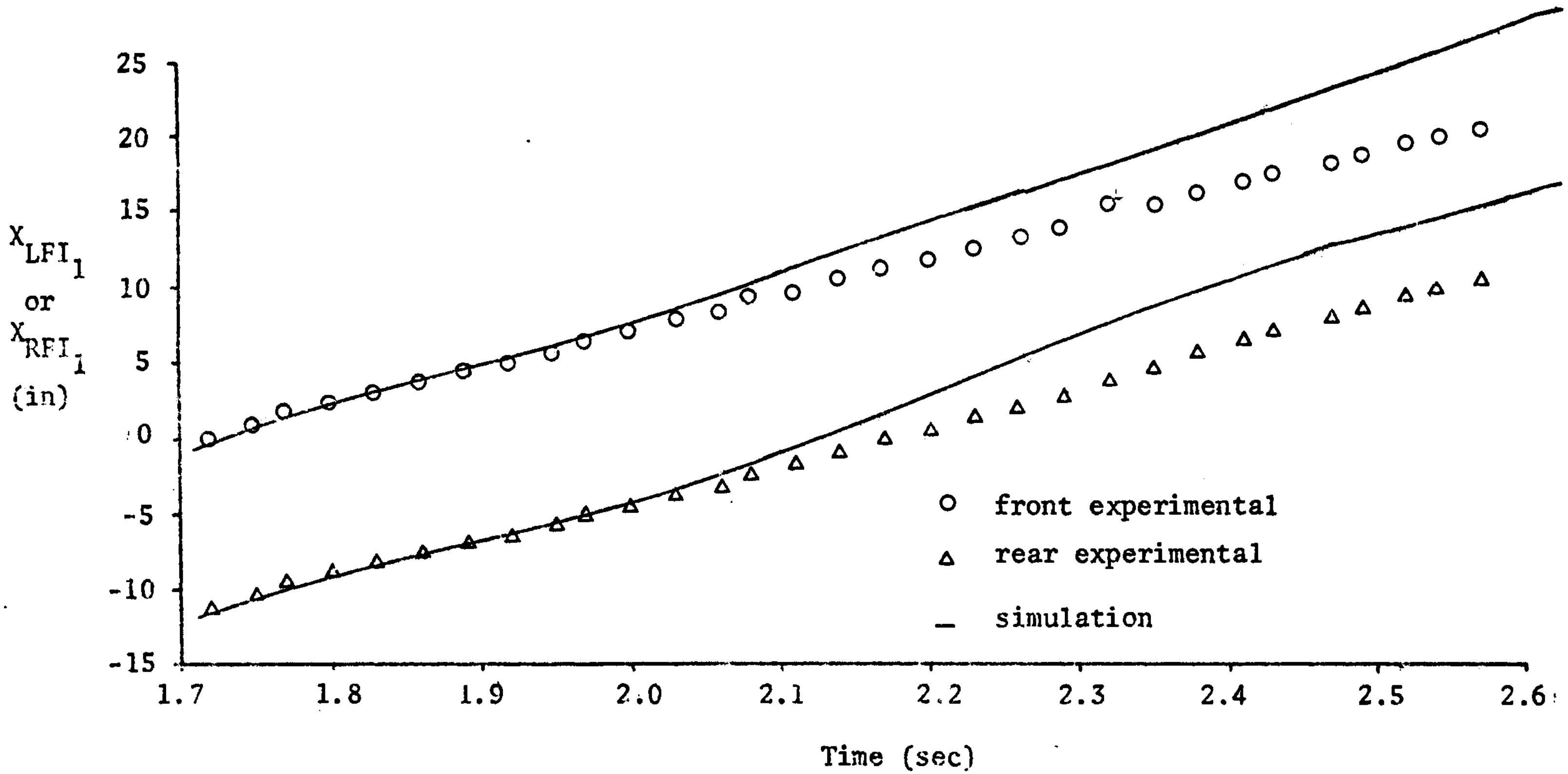

Figure 5-13. Component $\underline{e}_{I_1}$ of Simulation and Experimental Paths for the Left Front and Left Rear Tractor-Body Reference Points During Test 4.

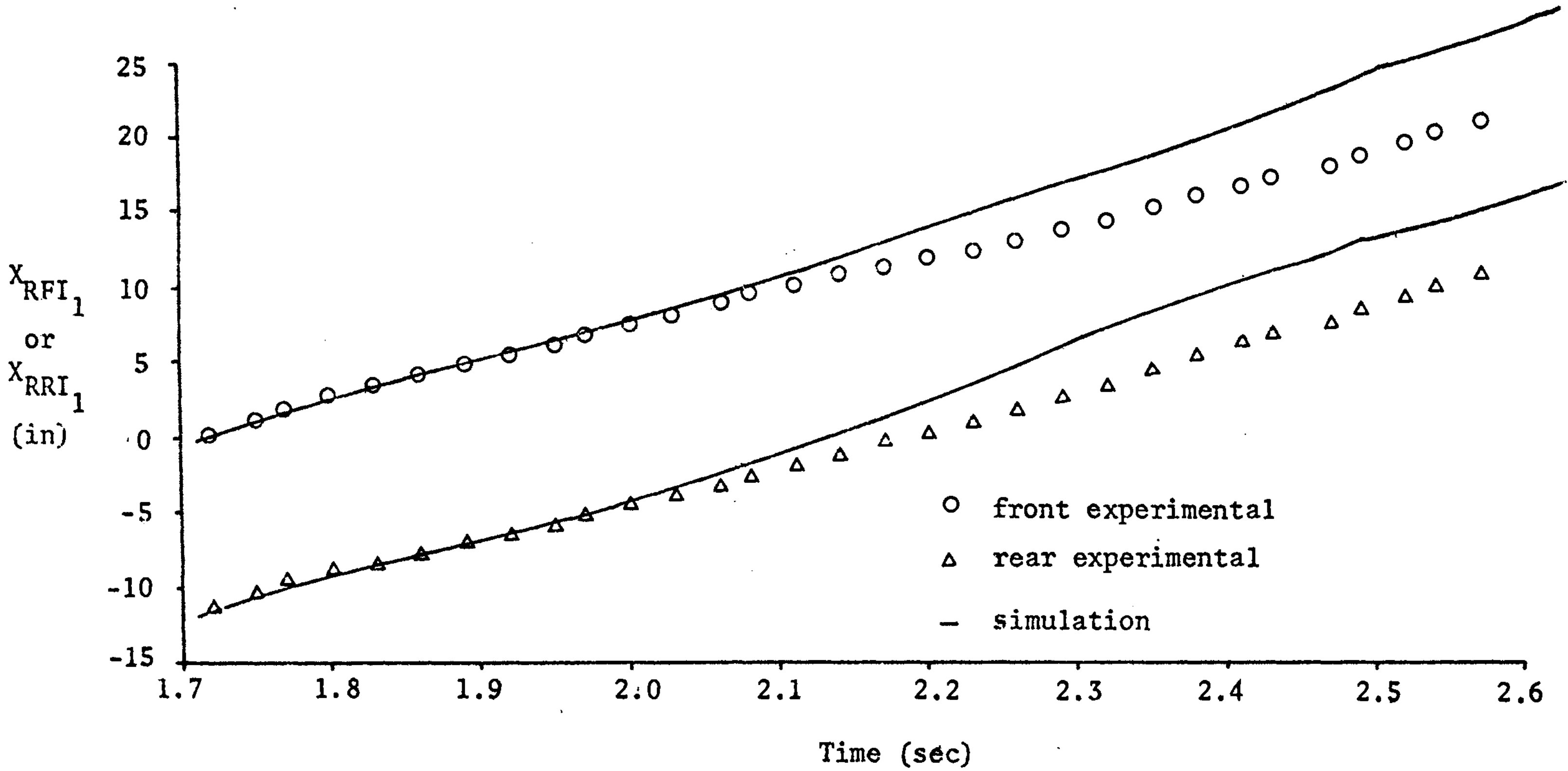

Figure 5-14. Component $\underline{e}_{I_1}$ of Simulation and Experimental Paths for the Right Front and Right Rear Tractor-Body Reference Points During Test 4.

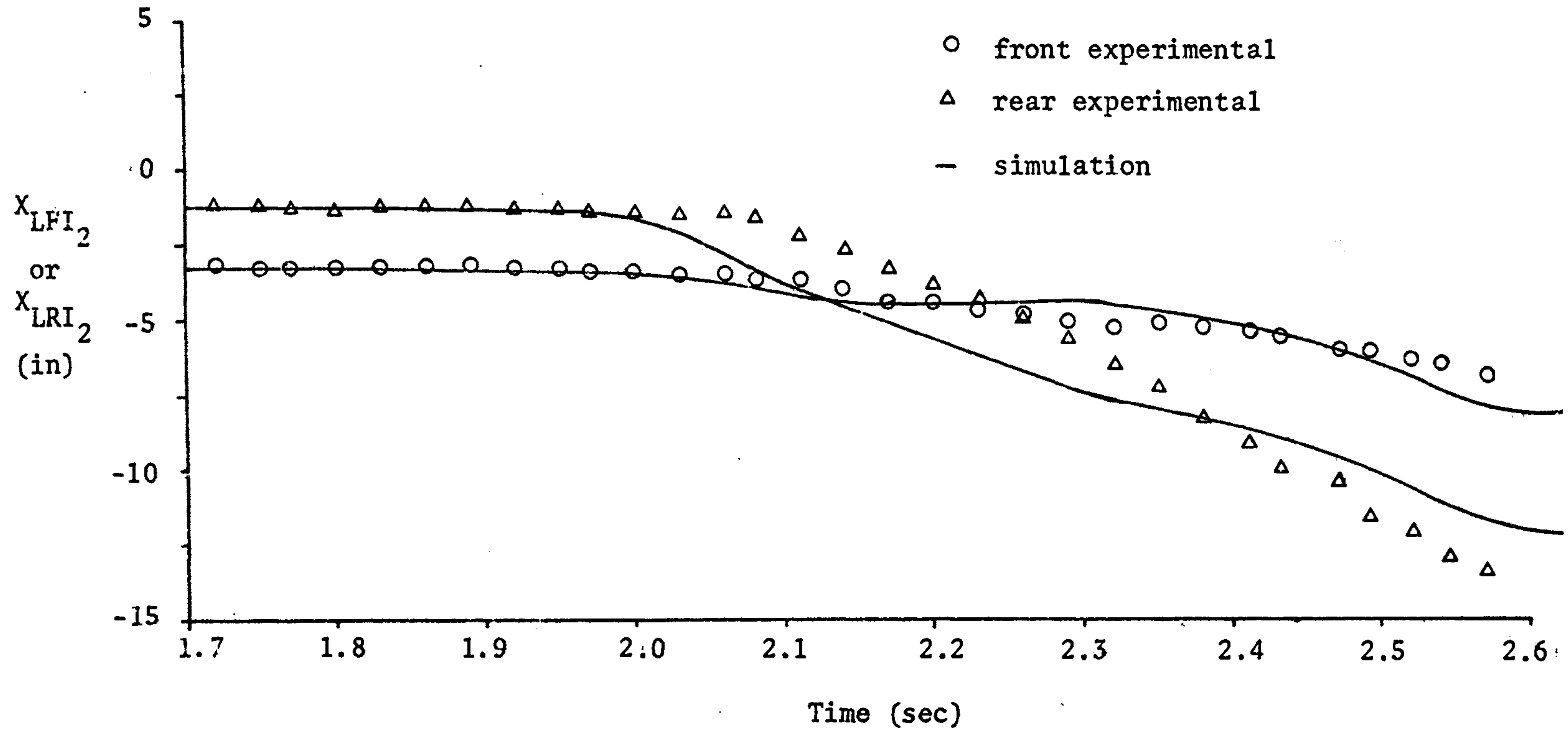

Figure 5-15. Component $\underline{e}_{I_2}$ of Simulation and Experimental Paths for the Left Front and Left Rear Tractor-Body Reference Points During Test 4.

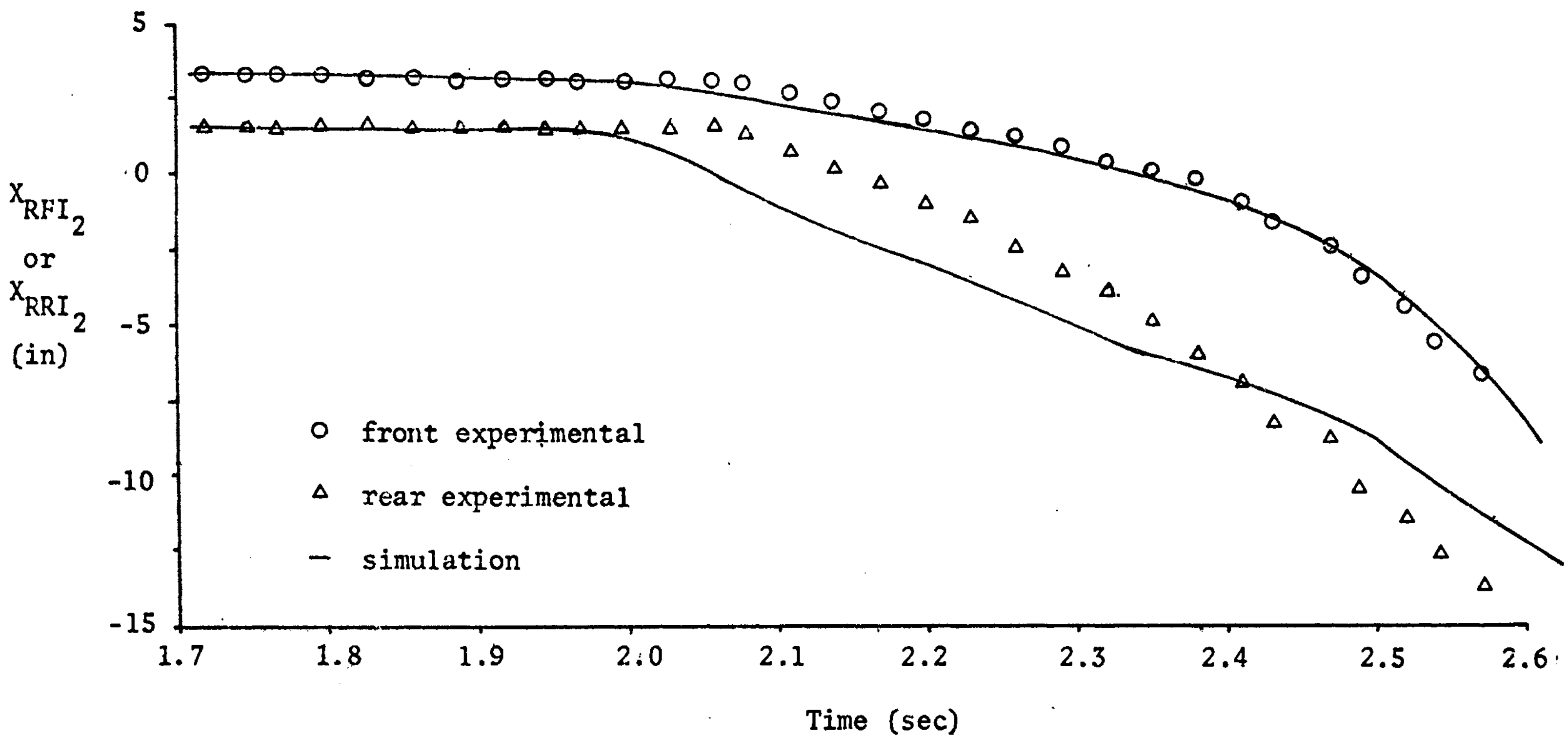

Figure 5-16. Component $\underline{e}_{I_2}$ of Simulation and Experimental Paths for the Right Front and Right Rear Tractor-Body Reference Points During Test 4.

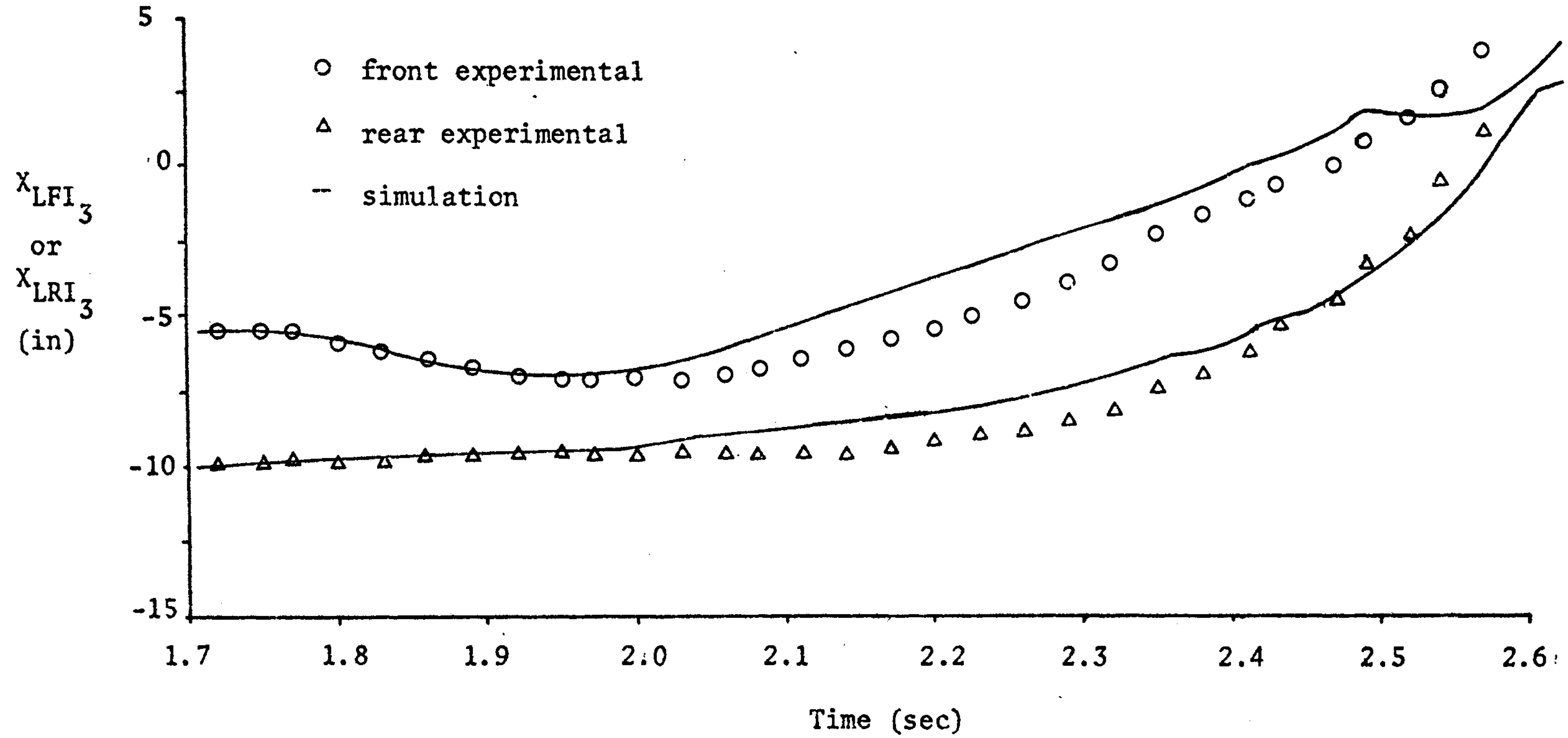

Figure 5-17. Component $\underline{e}_{I_3}$ of Simulation and Experimental Paths for the Left Front and Left Rear Tractor-Body Reference Points During Test 4.

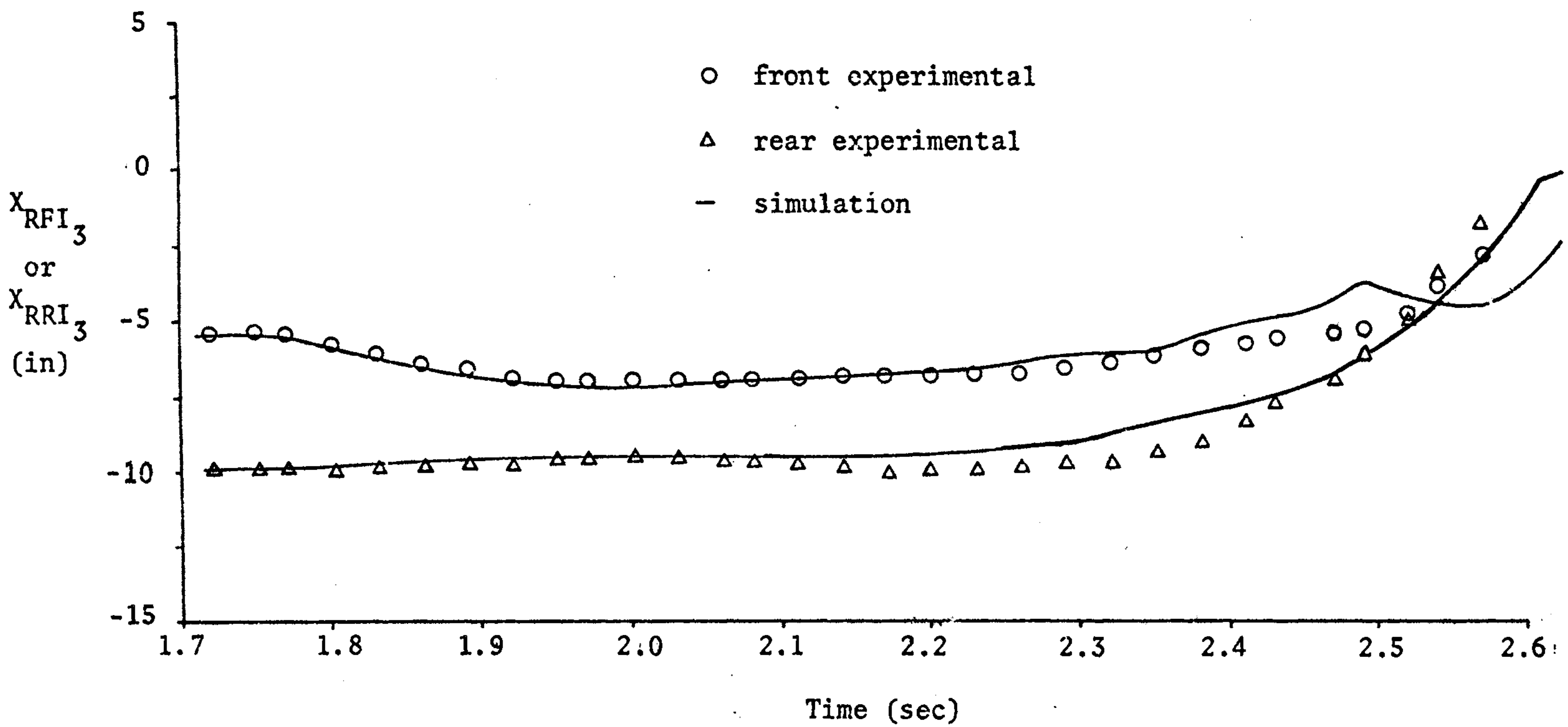

Figure 5-18. Component $\underline{e}_{I_3}$ of Simulation and Experimental Paths for the Right Front and Right Rear Tractor-Body Reference Points During Test 4.

rear reference-point paths for test 4 again show simulation paths to the left (- $\underline{e}_{I_2}$ direction) of the experimental paths as the left rear wheel begins down the bank, the discrepancy being greater in test 4 due to the increased weight transfer in that test. The simulation and experimental paths for the front reference points, however, differed less in test 4 than they did in test 1.

The vertical components ($\underline{e}_{I_3}$ direction) of the reference-point paths for test 4 again show the simulation curves diverging from the experimental curves after the left rear wheel has reached the terrain break at the top of the bank. As would be expected, the left reference points show the greatest differences between simulation and experimental paths, but nowhere do the differences reach 2.0 inches. The difference for the right reference-point paths rarely exceeds 0.5 inch and only once approaches 1.0 inch. The abrupt change in the point elevations at time 2.49 second identifies the time at which the left tires reach the bottom of the bank.

Verification of the mathematical model for tractor overturns rests upon the similarities between the tractor motions predicted by the mathematical model and those observed experimentally for the same tractor and terrain conditions. The tractor and terrain conditions of experimental overturn tests 1 and 4 were used with the mathematical model to simulate two overturns. Comparisons of the simulation and experimental overturns, based upon the paths of reference points fixed to the tractor body, showed generally similar tractor motions in every case.

Discrepancies between simulation and experimental paths of the reference points were shown to develop from the thin-wheel assumption used in the mathematical model, especially as the left rear wheel encountered the terrain break at the top of the bank and again as it reached the bottom of the bank. The thin wheel of the simulation model began descent prior to and sensed the bottom of the bank subsequent to, that of the thick scale-model wheel. The rigid-terrain test course emphasized the limitations of the thin-wheel model and introduced bouncing which was not observed experimentally. Simulation of tractor motions on a deformable terrain would reduce the inaccuracies caused by the thin-wheel assumption of the mathematical model. Despite numerical differences between simulation and experimental motions, both simulations predicted ground impact at the left front reference point as was observed experimentally.

The comparisons of simulation and experimental paths for the tractor-body reference points during two overturns show that the mathematical model does predict tractor motions throughout overturning situations. While the tractor travelled over 20 inches in the $\underline{e}_{I_1}$ direction, simulation discrepancies for the reference-point paths in this direction were less than 3.0 inches in test 1 and up to 6.0 inches in test 4. The lateral ($\underline{e}_{I_2}$ direction) motion of the reference points seldom showed discrepancies beyond 1.5 inches while total lateral motion exceeded 10 inches. Vertical path discrepancies usually were less than 1.0 inch while the total vertical displacement of the reference points approached 15 inches.

The over-all similarities between the simulation and experimental overturn results, obtained without any parameter variation to improve the agreement of the results, demonstrate that the mathematical model for tractor overturns does accurately describe the dynamics of the tractor. Adjustment of the parameter values for the mathematical model probably would result in improved agreement between simulation and experimental results, but the validity of the model has been demonstrated already.

The tractor overturn simulations provide much information about details of the overturn besides the paths of the four tractor-body reference points. Having shown that the mathematical model is valid for overturning motions, the details of the tractor dynamics throughout the overturn may be assumed valid as well and may be used to study interesting aspects of the two overturn simulations for tests 1 and 4.

5.3. Analysis of Overturn Simulations

Simulation of wide-front-end wheel-tractor overturns provides much detailed information about the response of the entire tractor to the specified terrain and tractor operating conditions. In contrast to the experimental overturns in which only position-time data are available for specific points on the tractor, overturn simulations provide position, velocity, and force data for any of the tractor parts specifically included in the mathematical model. The availability of state variable information for the tractor also provides the means for determining energy and momentum information pertinent to the study of tractor overturns.

The digital computer program used for overturn simulations together with examples of the input data required, printed output generated, and punched output generated are presented in Appendix C. Because the punched output was specifically defined to be used in graphic analysis of the tractor motions, a sample drawing of the tractor and terrain obtained from the example punched output is shown in Figure 5-19. The program used to direct a plotter to generate the desired line drawings is not presented because plotter instructions are often unique to a particular computing installation. The simulation program documentation in Appendix C provides the information needed to use the punched output for generating drawings if this is desired.

Figure 5-20 presents the tractor-body center-of-mass path for the simulation of overturn test 1 expressed in its three inertial-coordinate components. The plot of X_{BI_1}, nearly a straight-line function of time, shows that the tractor velocity component in the $\underline{e}_{I_1}$ direction remained very constant throughout the entire overturn. The smooth curves for the X_{BI_2} and X_{BI_3} components of the center-of-mass path show that the tractor body motion in the lateral and vertical directions did not change as abruptly as may have been suggested by the reference-point paths which were discussed previously.

The tractor-body center-of-mass velocities for overturn simulation 1 are presented in Figure 5-21. The plot of V_{BI_1} shows

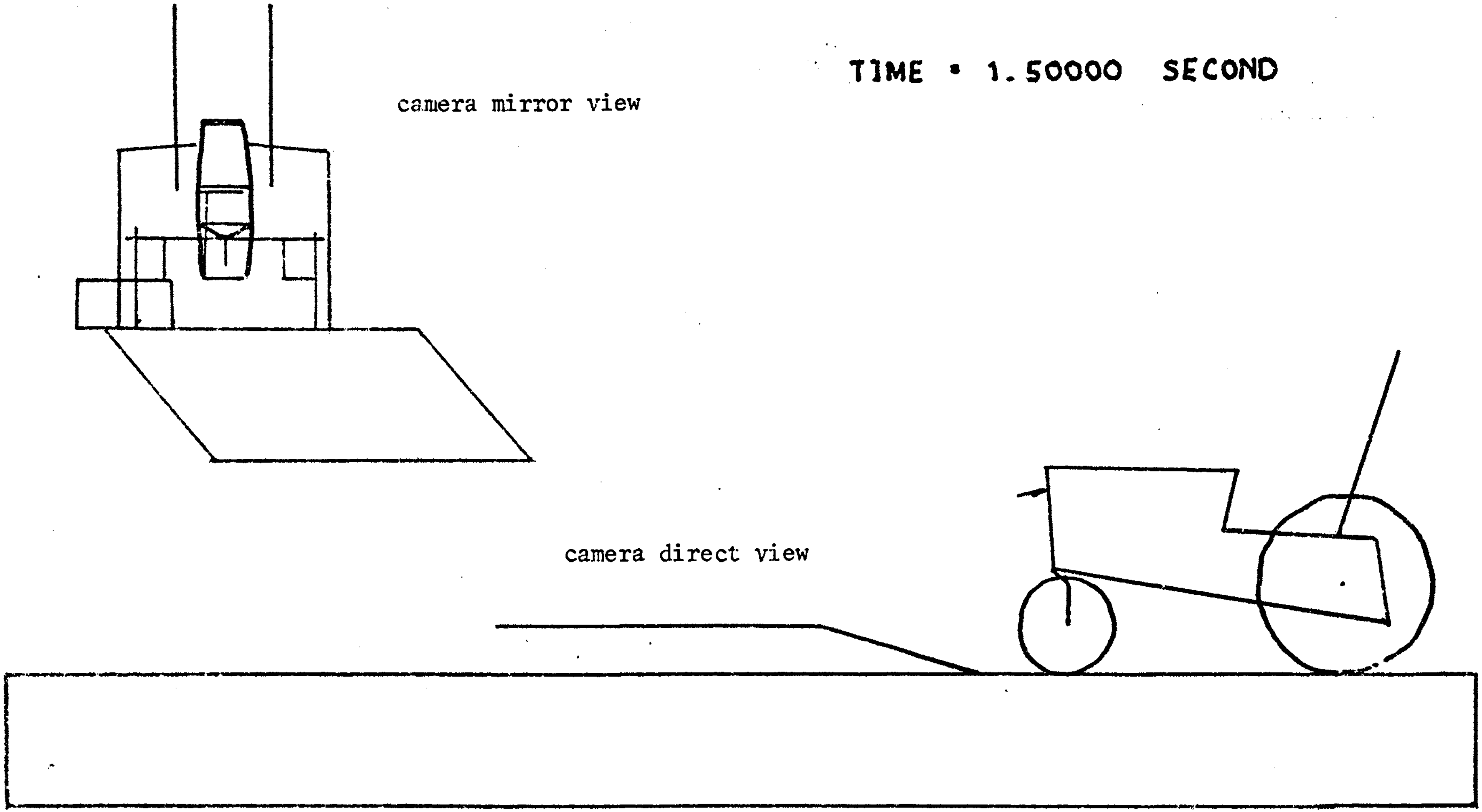

Figure 5-19. Example Graphic Representation of Tractor and Terrain Plotted From Punched Output.

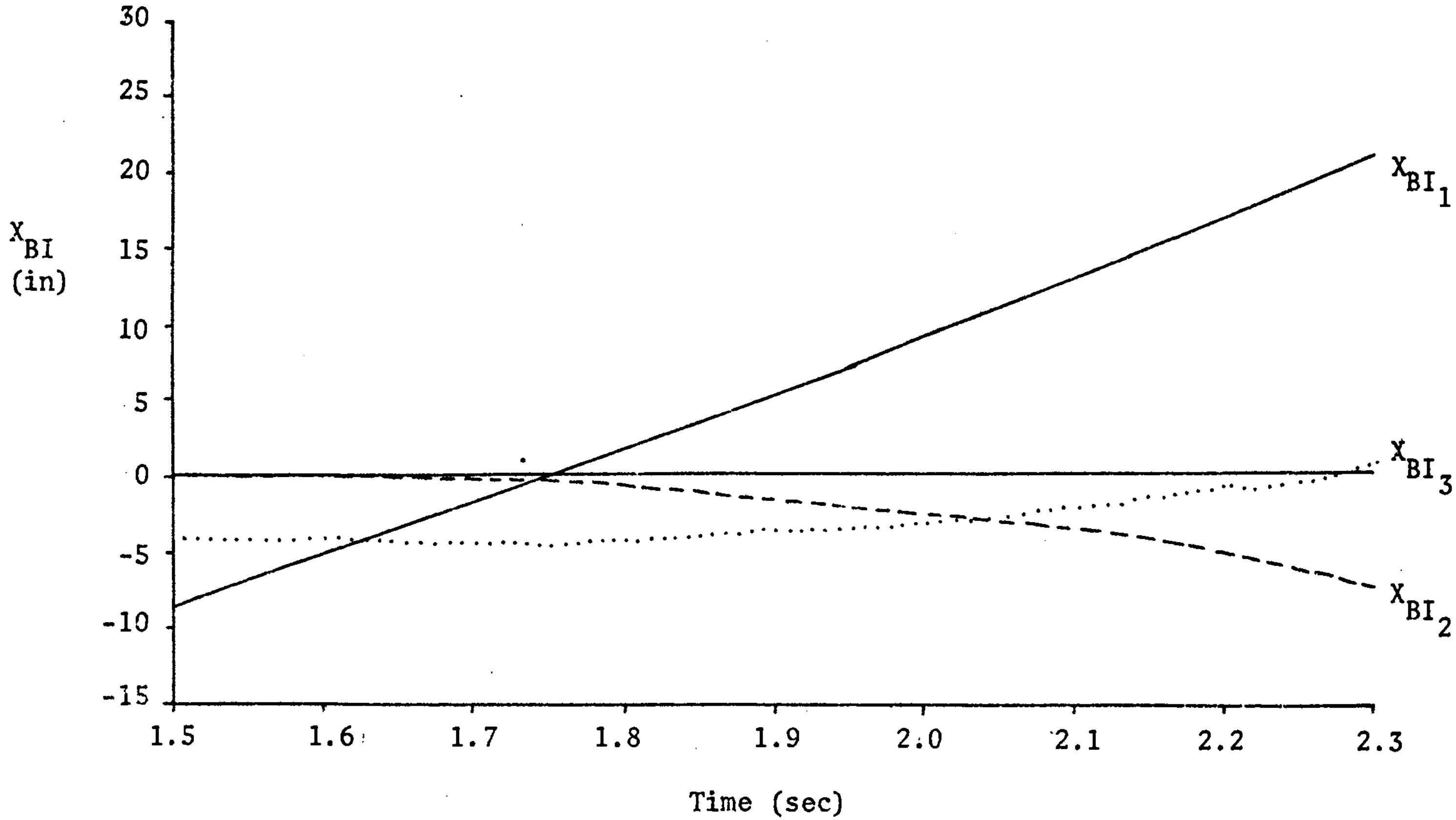

Figure 5-20. Tractor-Body Center-of-Mass Paths Defined by the Simulation of Test 1.

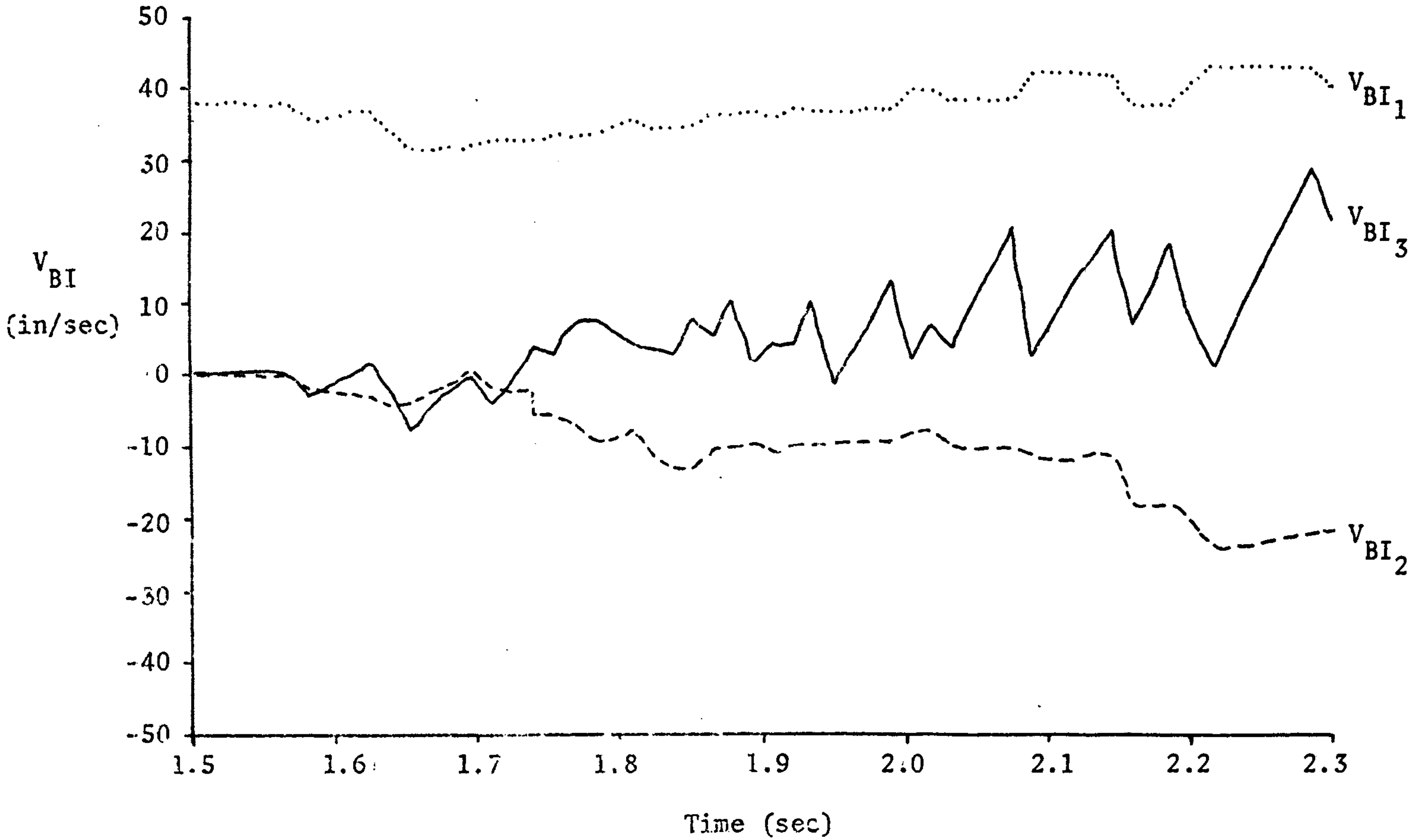

Figure 5-21. Tractor-Body Center-of-Mass Velocities Defined by the Simulation of Test 1.

that the velocity of the tractor body in the $\underline{e}_{I_1}$ direction, appearing constant from the plot of X_{BI_1}, actually is not constant throughout the simulation. The other components of the tractor-body velocity, likewise, are much more abruptly changing than was suggested by the plots of the tractor-body center-of-mass position. Vertical bounce is especially noticeable as the tractor-body center-of-mass moves down the bank. These plots suggest sizable tractor-body accelerations which, although not apparent from observations of the scale-model tractor overturn, may affect significantly the detection of an impending overturn and the tractor operator's response.

Figure 5-22 shows the angular velocities of the tractor body throughout the duration of the overturn simulation for test 1. The abrupt changes in the tractor-body-axes components of the angular velocities throughout the overturn, and especially after time 2.1 seconds, show the effects of the rigid ground surface, sharp terrain features, and the thin-wheel assumption used in the mathematical model for the tractor-terrain system.

The tractor-body pitch velocity, given by the ω_{BT_2} curve, shows the two positive pitch rotations due to the ramp displacement at the right front wheel (at time = 1.57) and the impact of the front end against the right-hand "stop" (at time = 1.63). The pitch rotation then becomes negative as the tractor nose begins descent down the bank. The tractor roll velocity, given by ω_{BT_1}, shows significant roll excitations due to the impact at the right-hand "stop" followed by

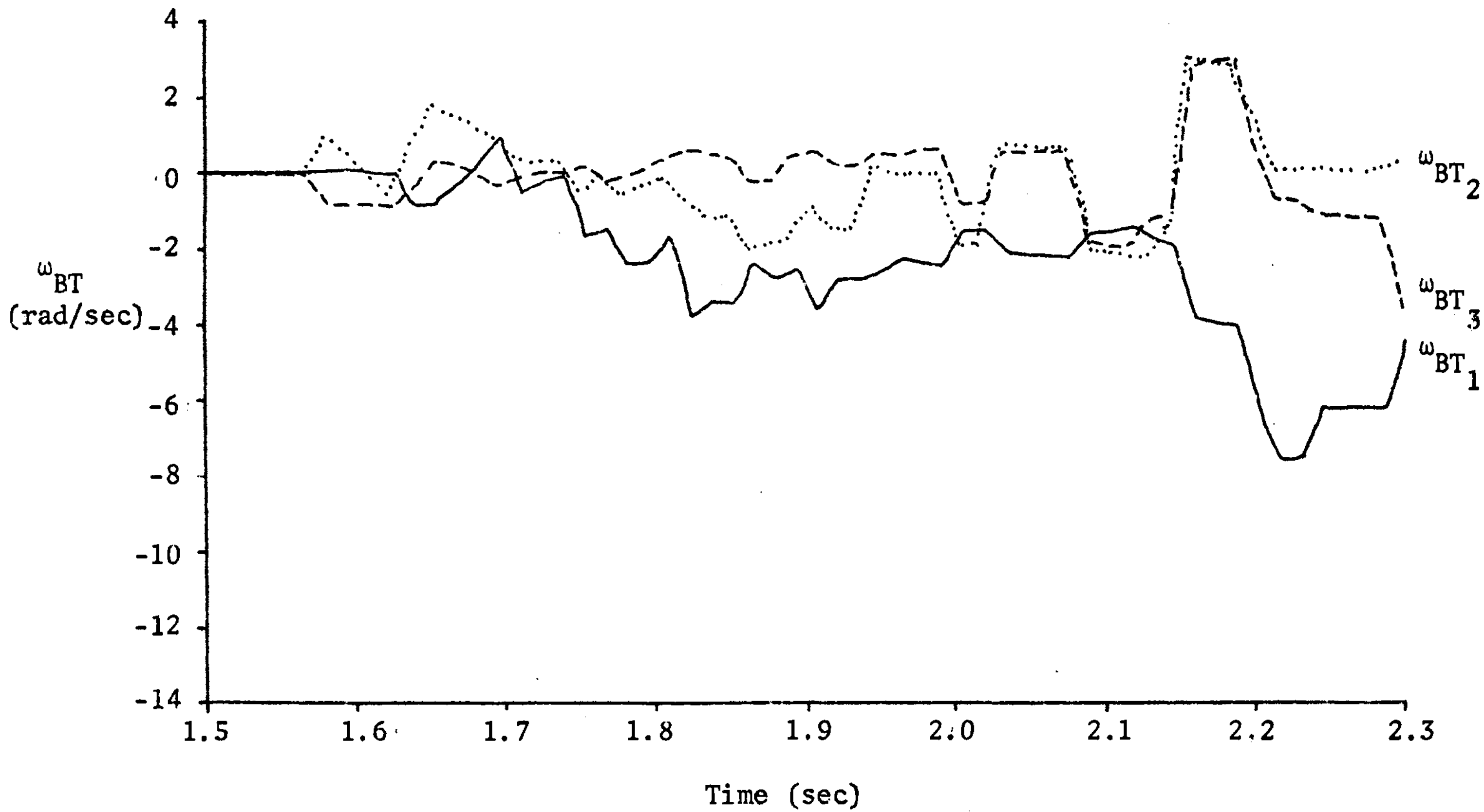

Figure 5-22. Tractor-Body Angular Velocities Defined by the Simulation of Test 1.

the expected left roll as the tractor travels down the bank.

The yaw velocities of the tractor, given by ω_{BT_3}, show an initial negative (left) rotation due to the right front wheel climbing the ramp followed by slightly positive oscillations. This positive yaw indicates that the rear wheel slip down the bank exceeds the side slip of the front wheels.

The rotational velocities of the tractor body prior to time 2.10 show a generally negative roll, negative pitch, and slightly positive yaw. From these rotational trends the tractor is seen travelling generally straight ahead with only minor skidding down the bank. At time 2.10 the right front wheel impacts the level surface at the bottom of the bank and initiates positive pitch and yaw but negative roll motions. These motions are quite reasonable because an upward and to the right impulse at the left front wheel would cause sudden increases in the pitch and yaw but negative roll when the tractor is already leaning to the left at the time of the impulse. Subsequently the pitch motion stops as the two left wheels become pivot points for the final stage of the tractor overturn.

Figure 5-23 presents the front-end rotation relative to the tractor body plotted as a function of time for overturn test 1. The front-end rotation remained negligible until the right front tire encountered the ramp at time 1.57, then rotation gradually increased until impact against the right-hand "stop" occurred at time 1.63. Variations in the ground reactions and the "stop" reactions allowed intermittent separation from the right-hand "stop" prior to time 1.90 when the negative roll of the tractor body caused full separation.

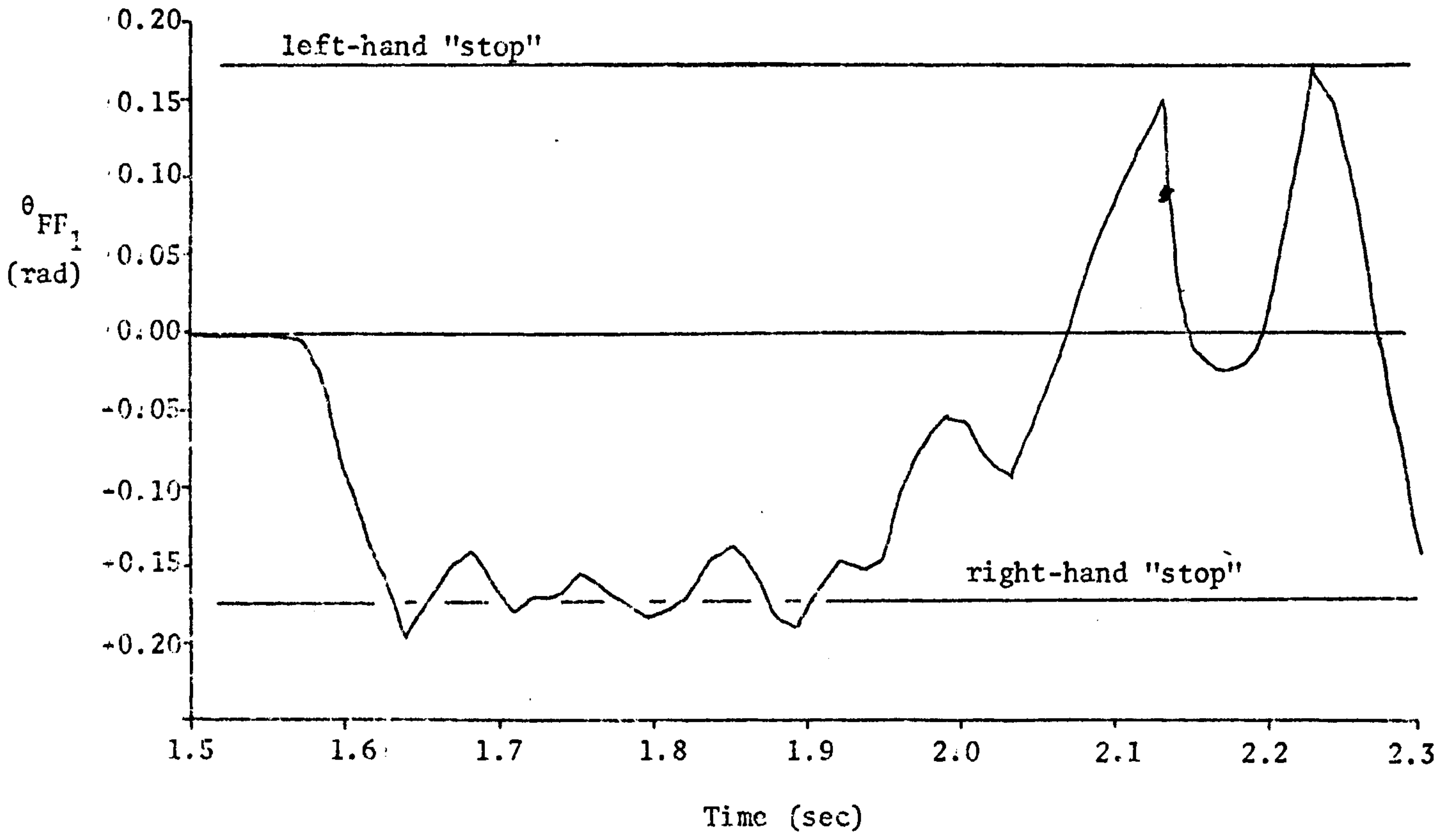

Figure 5-23. Tractor Front-End Rotation Defined by the Simulation of Test 1.

Continued negative roll of the tractor body caused the front end to approach the left-hand "stop" immediately prior to the left front wheel's impact on the level surface at the bottom of the bank. The ground impulse at that time caused the front end to momentarily move toward the right-hand "stop" before the roll of the tractor body led to contact at the left-hand "stop". When the tractor had nearly completed its overturn to the left, the ground force (acting upon the left side of the left front tire) moved the front end rapidly toward the right-hand "stop".

Velocities as well as positions of the tractor-body reference points are provided by the overturn simulations. Because the position of the left rear reference point on the tractor body closely matches the upper left corner of a two-post roll-over protection structure, this point is a highly probable point of impact with the ground during overturns. Because the velocities of ground impact may be important in determining the loads on roll-over protection structures, the velocities of the left rear reference point are presented as a function of time in Figure 5-24. Both the forward $(\underline{e}_{I_1})$ and vertical $(\underline{e}_{I_3})$ components of this reference-point velocity have magnitudes at the time of overturn completion comparable to the initial forward velocity of the tractor, the vertical component being 50 per cent greater yet just prior to that time. Thus the simulation indicates that a two-post frame may strike a ground obstacle at velocities greater than the tractor initial velocity.

The positions and velocities of the tractor parts, being defined by the mathematical model throughout an overturn simulation,

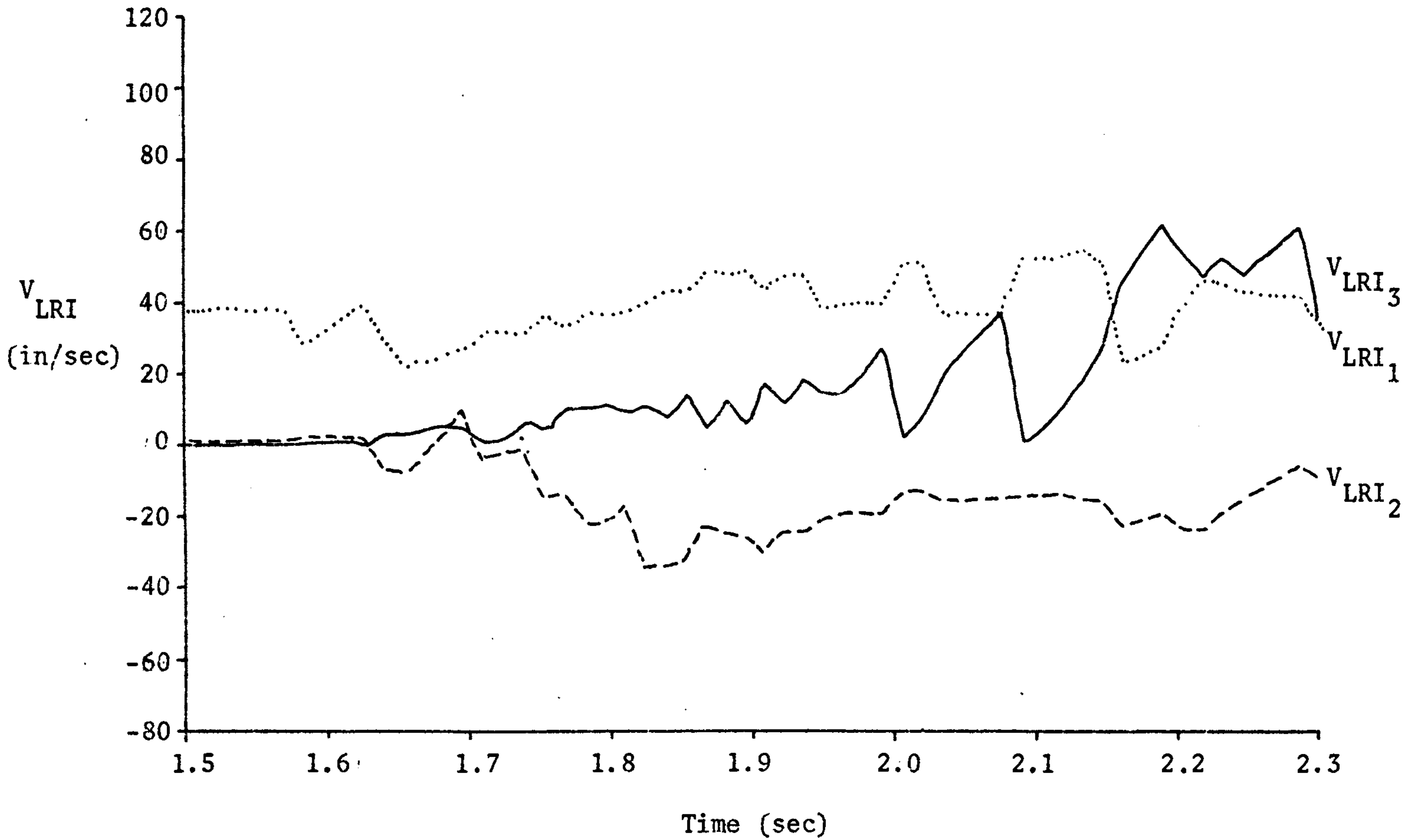

Figure 5-24. Velocities of the Left Rear Tractor-Body Reference Point Defined by the Simulation of Test 1.

are available for calculation of the energies of each tractor part. Figure 5-25 shows the translational, and rotational kinetic energies and gravitational potential energy for the entire tractor and the sum of these three energies throughout the simulation for overturn test 1. The energies throughout the simulation show a slow decrease in the total energy as would be expected due to tire losses and front-end "stop" losses. The increase in potential energy as the tractor climbs the ramp is reflected by a nearly equal decrease in translational kinetic energy. (Zero gravitational porential energy was defined at the ground level above the bank.) The rotational kinetic energy, principally from wheel rotations, remains relatively contant and only marginally significant throughout the simulation.

The abrupt variations in the energy curves, especially the translational and total energy curves, indicate points in time when the tractor tires experienced abrupt force changes and the tractor responded with sudden changes in its motion. Significant amounts of energy were dissipated during tire impacts and tractor rebound motions. The sharp decrease in translational and total energies at the completion of the overturn probably was due to energy losses at the left rear tire as the tractor rolled onto the side of the wheel, and thus suddenly shifted the axis of rotation for the overturn motion.

At the time of the left front point with the ground, less than 10 per cent of the total tractor kinetic energy was rotational kinetic energy. The translational kinetic energy increased to a level 200 per cent of its original energy level during the tractor overturn while the tractor velocity in the $\underline{e}_{I_1}$ direction remained relatively

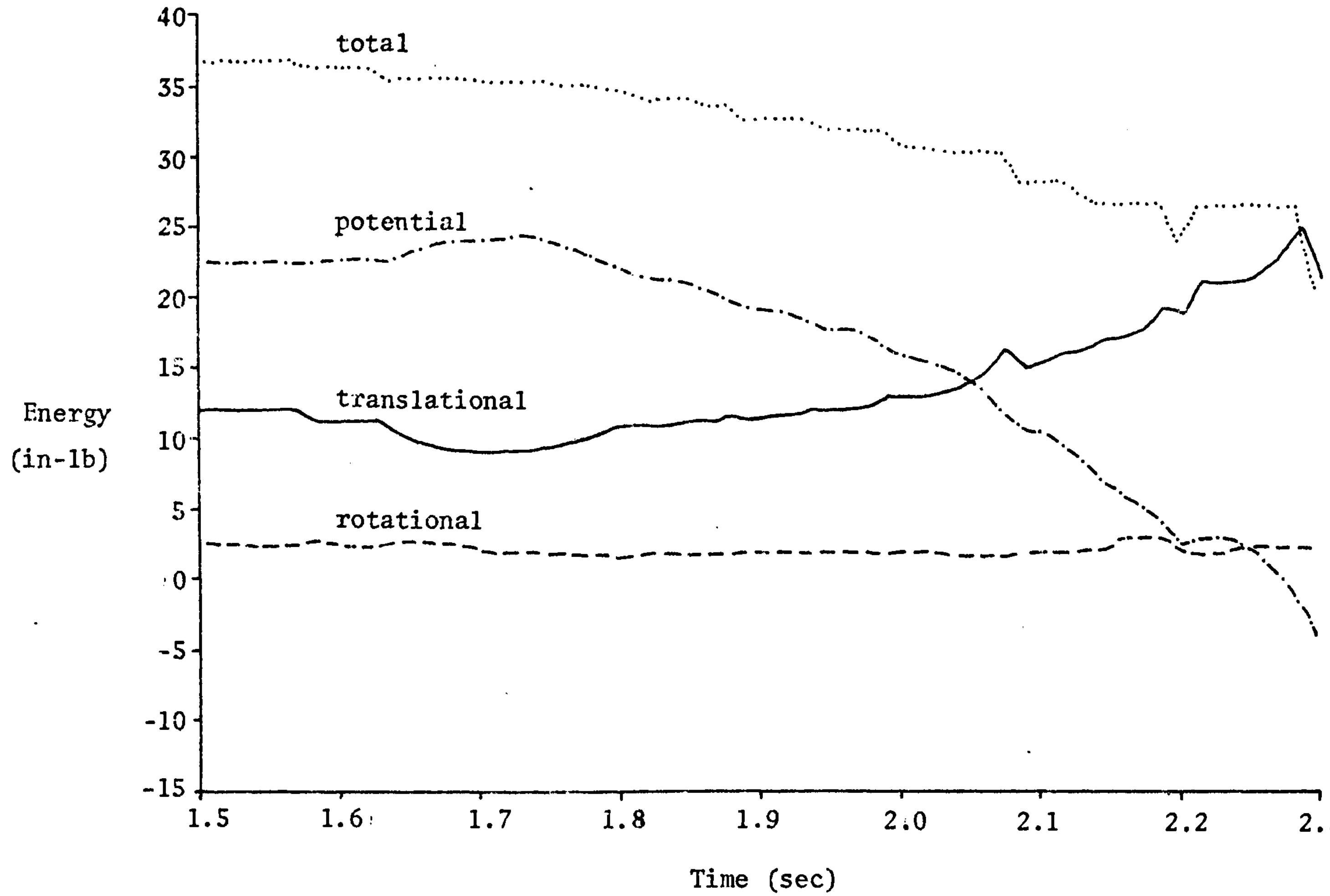

Figure 5-25. Translational, Rotational, and Potential Energies for the Tractor Defined by the Simulation of Test 1.

constant. The major kinetic energy increase resulted from greater tractor velocities in the $\underline{e}_{I_2}$ and $\underline{e}_{I_3}$ directions.

Simulation of overturn test 4 also provided the positions, velocities, and energies for the tractor throughout the entire overturn. Because test 4 was selected to provide a different overturn situation from test 1 in both tractor speed and limit to front-end rotation, the individual effects of each change were not always identifiable. The major effect of the reduced front-end rotation limit, however, was the more rapid elevation of the tractor nose as the right front wheel climbed the ramp while the decreased tractor velocity produced a slower and less violent overturn.

The simulation of overturn test 4 showed a total overturn time after first contacting the ramp equal to 0.90 second while the corresponding time for test 1 was 0.75 second. This nearly 17 per cent reduction in time resulted from an 11 per cent increase in initial tractor speed. The same left front reference point impacted the ground in both overturns, but the vertical component of that reference-point velocity at the time of ground impact in test 4 increased by about 20 per cent while the forward $(\underline{e}_I)$ component of that velocity decreased by 83 per cent from that in test 1.

Figure 5-26 shows the translational and rotational kinetic energies and the gravitational potential energy for the tractor during the simulation of overturn test 4. Both the potential and translational energy curves show an indication of the reduced limit to front-end rotation when the tractor reaches the ramp. What was previously two distinct steps - front-end rotation, then common front-end and

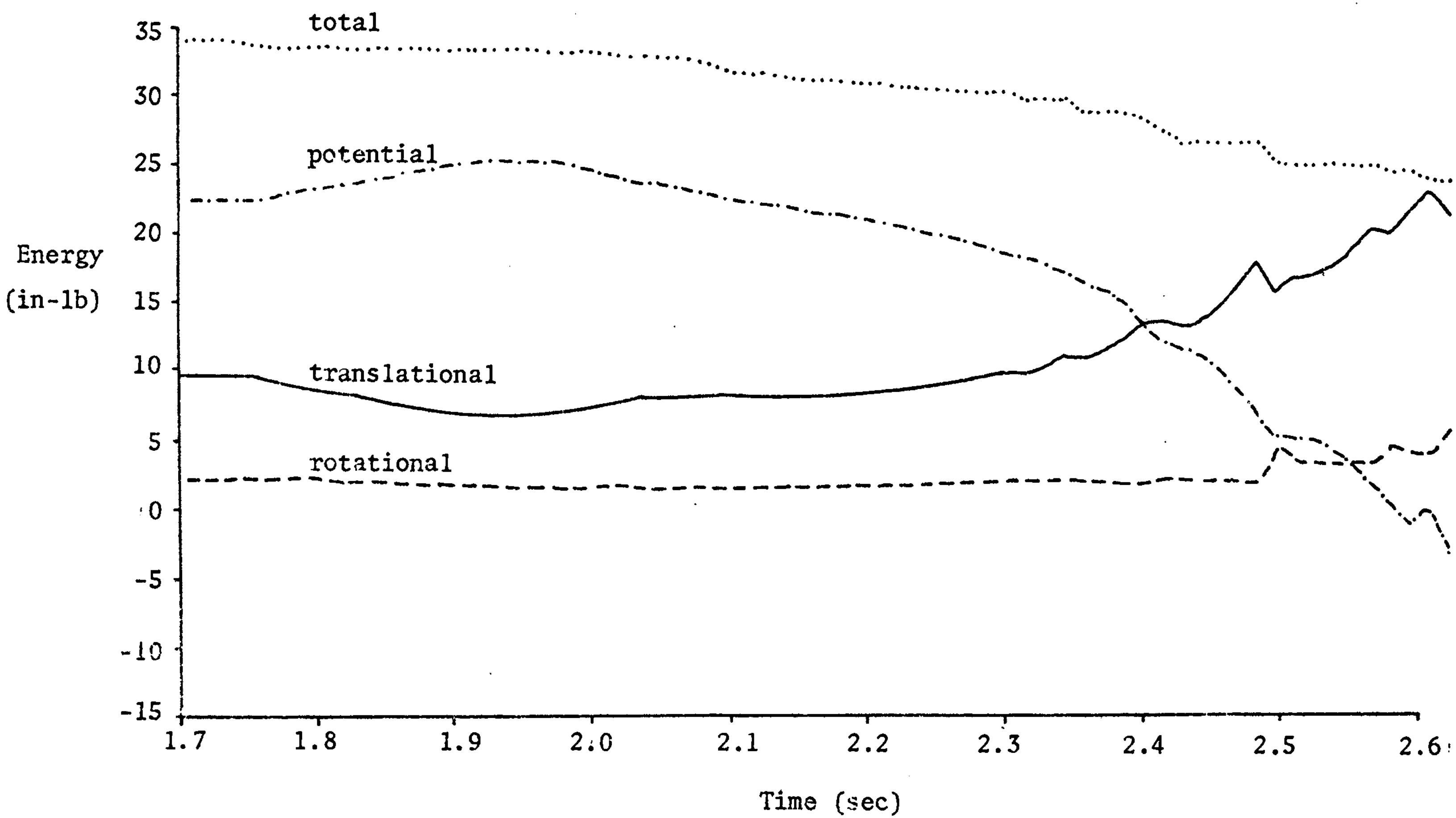

Figure 5-26. Translational, Rotational, and Potential Energies for the Tractor Defined by the Simulation of Test 4.

tractor-body motion - is now almost indistinguishable as two separate motions in raising the tractor center of mass.

The translational kinetic energy again became the predominent energy component by the time of tractor-ground impact. At this time the rotational kinetic energy displayed a sudden increase to become 20 per cent of the total kinetic energy, whereas in test 1 the rotational kinetic energy was only 10 per cent at the time of impact. In both simulation overturns the translational kinetic energy increased to a value near 200 per cent of its initial value by the time of impact. These observations simply indicate differences between these two simulations and should not be generalized without additional test results. The similar shapes of the energy curves for the two test tests does indicate, however, that the terrain has a major role in determining the tractor overturn energies.

5.4. Conclusions

The repeatability of scale-model tractor overturns on a rigid terrain has been demonstrated in Section 5.1. A wide-front-end tractor underwent ten side overturns on a test course which was a scale model of the ASAE side-overturn test course, but only five of the overturns were analyzed in detail. The analysis of three overturns replicating one overturn test and two overturns replicating a second overturn condition showed remarkable repeatability when the initial conditions for the tractor were carefully controlled.

Comparisons of the paths of four tractor-body reference points throughout two replications for each of the two overturn tests showed deviations between corresponding points for the replicate paths seldom greater than 1.0 inch while the tractor travelled a total distance exceeding 25 inches. The time periods measured for the durations of the experimental overturns differed between replications by about 0.02 second while between 0.65 and 0.85 second elapsed from the time of initial tractor contact with a terrain irregularity to the time at the completion of the overturn.

The high repeatability of the experimental overturns provided evidence that the position data for the tractor, derived from films of the overturns, were sufficiently accurate for use in verifying the mathematical model for tractor overturns.

Two tractor overturn simulations, generated using the mathematical model for tractor overturns and the tractor-terrain conditions corresponding to the experimental overturns, were used to check the validity of the mathematical model. Comparing the tractor-body reference-point paths in the experimental overturns to those in the simulation overturns showed good agreement for both overturn tests. Similarities in the tractor motions during simulation and experimental overturns demonstrated that the dynamics of the mathematical model were correct.

Although no parametric adjustments were made to make the simulation overturns match the experimental overturns, good agreement was obtained. Comparisons of the simulation and experimental results indicated that the thin-wheel model for the tractor tires caused simulation inaccuracies whenever abrupt terrain changes encountered by the tractor tires were nearly parallel to the wheel plane. The simulation overturns, with few exceptions, predicted paths for the tractor-body reference points within 2.0 inches of the experimental paths throughout the range of tractor motion. These discrepancies were usually less than 1.0 inch.

Comparisons between the tractor-body reference-point paths and the experimental paths for the two overturn tests showed that the mathematical model was valid for predicting tractor motions during overturns. Because the reference points were relatively distant from the tractor tipping axis, the accuracy in predicting center-of-mass paths could be expected to be greater than that shown by these results. Additional improvements in accuracy may be obtained by varying model parameter values to make them more correctly represent the conditions of the overturn test. The objective, to develop and verify a mathematical model for predicting tractor overturning motions, has been accomplished without any of these peripheral investigations into the sensitivity of the model to tractor and terrain parameters.

The simulation of tractor overturns made detailed information about the tractor response to terrain conditions more readily available than it was in experimental overturn studies. The two different overturn simulations used to verify the mathematical model provided an indication of the fruitfulness of future parametric studies of tractor overturns using this mathematical model. The positions, velocities, and energies of the tractor were studied throughout the full tractor overturn to relate the tractor responses to the tractor and terrain conditions. The momentum and tire-force values were also provided by the simulations, but these values were not discussed except as they aided in understanding the tractor response.

Although no parametric studies were designed and conducted using the mathematical model, the two simulations did indicate trends which require further study before they are confirmed. A reduced limit to the front-end rotation caused the front of the tractor body to respond to displacements of the front wheels more quickly than did the larger rotation limit, but its effect upon the overturning motion was not obvious. A reduction in the tractor speed prior to encountering terrain irregularities was shown to decrease the severity of the overturn and extend the time required for the complete overturn.

The merit of graphic analysis was realized during the analysis of the simulation overturns. A graphic representation of the tractor relative to the terrain is a valuable tool for clearly visualizing the numerical values printed for the simulation. Although each simulation may differ, similarities in the tractor motions between different simulations may make the graphic representation of one overturn useful in interpreting many other simulation overturns.

CHAPTER VI

SUMMARY AND RECOMMENDATIONS

6.1. Summary

The tractor overturn phenomenon is not fully understood even though roll-over protection structures are being designed to protect tractor operators from the consequences of tractor overturns. The objectives of this study were to develop a mathematical model which would quantify tractor overturns, to develop an experimental procedure for quantifying scale-model tractor overturns, and to verify the mathematical model so it could be used to study overturns in detail.

A mathematical model has been developed for the dynamics of a wide-front-end wheel tractor throughout overturning motions. The tractor was modelled as five different parts having ten total degrees of freedom. The tractor model included unrestricted rotational freedom for the tractor body, differential coupling of the rear wheels, an engine and drive train, thin terrain-enveloping tires, and variable limits to the front-end rotation. Planar symmetry assumptions were used for the tractor body, the rear wheels, and the tractor front end.

A 1/12 scale of the ASAE S306.2 side-overturn test course was used to study overturns of a 1/12 scale, unpowered wide-front-end tractor. Ten separate side overturns of the model tractor were filmed using a mirror arrangement to obtain three-dimensional data, but only five overturns replicating two different tests were analyzed in detail. Comparisons of the plotted paths for four tractor-body reference points showed that the experimental overturns provided highly repeatable position-time data throughout the overturns.

A digital computer program developed from the mathematical model was used to simulate two different overturns, each corresponding to one of the experimental tests that was analyzed in detail. Comparisons of the four tractor-body reference-point paths obtained from the simulations to those paths obtained from the experimental overturns showed good agreement throughout the overturns. Those discrepancies which did occur between corresponding experimental and simulation overturns were traced to the thin-wheel assumption used in the mathematical model. The favorable agreement between experimental and simulation overturns verified the mathematical model for simulating general overturns of wide-front-end wheel tractors.

The digital computer simulations of tractor overturns provided detailed position, velocity, and energy information for the tractor throughout the overturn, but because parametric studies were not conducted, no definite statements could be made to define the effects of various tractor and terrain parameter values on the severity of tractor overturns. The simulation outputs did, however, indicate the value of simulated overturns in conducting parametric studies.

The digital computer program optionally produced punched output defining the locations of specific points on the tractor throughout the overturn simulation. These point locations were used to generate graphic output showing the tractor position relative to the terrain. The aid which this graphic output provided in interpreting the simulations indicated that graphic display was a valuable tool in simulation studies.

6.2. Recommendations

The strengths and limitations of the tractor overturn simulations suggest recommendations for future work in the study of tractor overturns. The versatility of digital computer simulations, especially with graphical output, makes simulation a valuable tool for determining the effects of various tractor and terrain parameters on the severity of tractor overturns. Information about the effects of tractor speed, inertia and geometry of the tractor, tire-ground forces, and terrain geometry on the tractor motions could provide valuable data for the design of roll-over protection structures (ROPS) or for the establishment of standard tests for ROPS.

The thin-wheel assumption used in the mathematical model introduced inaccuracies in the simulation when abrupt terrain changes at the wheels occurred nearly parallel to the wheel plane. Improved accuracy of the simulations could be obtained if a thick-wheel model were developed. One possible approach would be to represent the thick wheel by two thin wheels spaced at the inner and outer planes of the thick wheel. A generalization of this idea could allow the specification of many thin wheels of varying diameters, stiffnesses, and inertias to model tires with curved tread, dual tires on an axle, or solid ballast attached to a wheel.

The simulation of tractor motions could be used to study the effects of operator responses upon tractor overturns. Operator response studies would be especially valuable if braking and smooth clutching features were added to the model and if a cathode-ray display were used to monitor the tractor response while inputs were introduced interactively.

CITED REFERENCES

Albert, C.J. 1961. A method of simulating tire enveloping power in calculations of vehicle ride performance. Technical Report YM-1424-V-300, Cornell Aeronautical Lab, Buffalo, N.Y., Nov. 1961.

ASAE. 1972. Protective frame - test procedures and performance requirements, ASAE Standard: ASAE S306.2. Agricultural Engineers Yearbook, p. 258-262.

Arndt, J.F. 1971. Roll-over protective structures for farm and construction tractors - a 50-year review. SAE Paper No. 710508, SAE, Two Pennsylvania Plaza, N.Y., N.Y. 10001.

Baillie, W.F. 1971. The current program of the Werribee tractor testing station. Paper presented at the National Agricultural Machinery Conference, Melbourne, Australia.

Baker, L.D., and Steinbruegge, G.W. 1972. A tractor overturn study. ASAE Paper No. 72-615, ASAE, St. Joseph, Mich. 49085.

Barger, E.L., Liljedahl, J.B., Carleton, W.M., and McKibben, E.G. 1963. Tractors and their power units, 2nd ed. John Wiley and Sons, Inc., N.Y., N.Y.

Bartz, J.A. 1972. CAL develops three-dimensional computer simulation of crash victim. Research Trends 21 (Summer-Autumn): 28-32.

Bickford, J.H. 1968. How to make the most - or the least - out of impact. Machine Design 40 (11):165-171.

Bucher, D.H. 1967. The design and evaluation of a protective canopy for agricultural tractors. Agricultural Engineering 48 (9): 496-499, 506.

Conte, S.D. 1965. Elementary numerical analysis. McGraw-Hill Book Company, N.Y., pp. 65-69, 72-73, 187-189.

Deprit, A. 1970. The theory of special perturbations: A tutorial survey. Lecture notes from 1970 Summer Institute of Astronomy, University of Texas, Austin, Texas 78712.

Floyd, C.S. 1971. Cab makers confer on DOT manifesto. Implement and Tractor 86(14):12-19.

Ford, J.E., and Thompson, J.E. 1969. Vehicle rollover dynamics prediction by mathematical model. SAE Paper No. 690804, SAE, Two Pennsylvania Plaza, N.Y., N.Y. 10001.

Gilfillan, G. 1970. Tractor behavior during motion uphill. J. Agr. Engg. Res. 15(3):221-235, 236-243.

Goering, C.E., and Buchele, W.F. 1967. Computer simulation of an unsprung vehicle. Trans. ASAE 10(2):272-280.

Greenwood, D.T. 1965. Principles of dynamics. Prentice-Hall, inc., Englewood Cliffs, New Jersey.

Grevis-James, I.W., and Vaxey, G.H. 1971. Longitudinal stability of tractors. Paper presented at the National Agricultural Machinery Conference, Melbourne, Australia.

Hahn, R.H. 1973. Revised standards on ROPS for ag tractors. Agricultural Engineering 54 (2):29.

Hansen, M. 1966. Reducing tractor fatalities. Agricultural Engineering 47(9):472-474.

Hansen, M. 1971. Personal communication. Letter of October 27, 1971.

Huang, B.K., Liljedahl, J.B., and Quinn, B.E. 1964. Model study of dynamic behavior of farm tractors with elastic rims and wheel suspension. Trans. ASAE 7(3):321-325, 328.

Jensen, J.K. 1970. Report to FIEI industrial safety committee. John Deere Waterloo Tractor Works, Waterloo, Iowa 70704.

Jensen, J.K. 1973. Comments on ASAE paper 72-615, "A tractor overturn study." Agricultural Engineering 54(3):28.

Klose, G.L. 1969. Engineering basics of roll over protection structures. SAE Paper No. 690569, SAE Two Pennsylvania Plaza, N.Y., N.Y. 10001.

Koch, J.A., Buchele, W.F., and Marley, S.J. 1970. Verification of a mathematical model to predict tractor tipping behavior. Trans. ASAE 13(1):67-72, 76.

Krick, G. 1970. Kräfte und Momente an augetriebenen, schräglaufenden Reifen und die Auswirkung auf das Fahrzeug. Unpublished research paper, Technische Hochschule, Munich, W. Germany.

Larson, D.L., and Liljedahl, J.B. 1971. Simulation of sideways overturning of wheel tractors on side slopes. SAE Paper No. 710709, SAE, Two Pennsylvania Plaza, N.Y., N.Y. 10001.

Macarus, W.P. 1971. Design and testing of roll over protective structures in accordance with SAE J395. SAE Paper No. 710509, SAE, Two Pennsylvania Plaza, N.Y., N.Y. 10001.

McCormick, E. 1941. Some engineering implications of high speed farming. Agricultural Engineering 22(5):165-167.

McHenry, R.R. 1969. An analysis of the dynamics of automobiles during simultaneous cornering and ride motions. Proc. of the Institution of Mech. Engrs., Vol. 183, Part 3H, Handling of vehicles under emergency conditions.

McHenry, R.R., and Deleys, N.J. 1968. Vehicle dynamics in single vehicle accidents - validation and extension of a computer simulation. Technical Report VJ-2251-V-3, Cornell Aeronautical Lab., Buffalo, N.Y., Dec. 1968.

McKibben, E.G. 1927. The kinematics and dynamics of the wheel type farm tractor. Agricultural Engineering 8(1):15-16, 8(2):39-40, 43, 8(3):58-60, 8(4):90-93, 8(5):119-122, 8(6):155-160, 8(7): 187-189.

McWilliams, P.H., and Maxwell, M.E. 1960. Ride improvement - analogue simulation of vehicle suspension systems as a means of obtaining optimum performance. Automobile Engineer 50(2):51-53.

Mitchell, B.W., Zachariah, G.L., and Liljedahl, J.B. 1972. Prediction and control of tractor stability to prevent rearward overturning. Trans. ASAE 15(5):838-844, 848.

Möberg, H.A. 1964. Tractor safety cabs, test methods, and experiences gained during ordinary farm work in Sweden. Report by National Swedish Testing Institute for Agricultural Machinery, Uppsala 7, Sweden.

Nordström, O. 1970. Safety and comfort test program - Swedish approach. ASAE Paper No. 70-105, ASAE, St. Joseph, Mich. 49085.

Pershing, R.L. 1971. Simulating tractive performance. SAE Paper No. 710525, SAE, Two Pennsylvania Plaza, N.Y., N.Y. 10001.

Pershing, R.L., and Yoerger, R.R. 1964. Steady-state behavior of tractors on roadside slopes. SAE Paper No. 903B, SAE, Two Pennsylvania Plaza, N.Y., N.Y. 10001.

Pershing, R.L., and Yoerger, R.R. 1969. Simulation of tractors for transient response. Trans ASAE 12(5):715-719.

Persson, S.P.E. 1967. Parameters for tractor wheel performance, Part I: Definitions, Part II: Description and use. Trans. ASAE 10(3):420-426, 428.

Phelan, R.M. 1967. Dynamics of machinery. McGraw-Hill Book Company, N.Y.

Raney, J.P., Liljedahl, J.B., and Cohen, R. 1961. The dynamic behavior of farm tractors. Trans. ASAE 4(2):215-218,221.

Sack, H.W. 1956. Longitudinal stability of tractors. Agricultural Engineering 37(5):328-333.

Schuring, D., and Belsdorf, M.R. 1969. Analysis and simulation of dynamical vehicle-terrain interaction. Technical Report VJ-2330-G-56, Cornell Aeronautical Lab, Buffalo, N.Y., May 1969.

Schwanghart, H. 1968. Lateral forces on steered tyres in loose soil. J. of Terramechanics 5(1):9-27.

Sharp, R.S., and Gordall, J.R. 1969. A mathematical model for the simulation of vehicle motions. J. of Engineering Math. 3(3): 219-237.

Smith, D. 1972. The handling behavior of farm tractors. Term project report, Mech. Engg. 336, University of Illinois, Urbana, Ill. 61801.

Smith, D.W., and Liljedahl, J.B. 1972. Simulation of rearward overturning of farm tractors. Trans. ASAE 15(5):818-821.

Smith, D.W., Perumpral, J.V., and Liljedahl, J.B. 1971. A mathematical model to predict the sideways overturning behavior of farm tractors. ASAE Paper No. 71-604, ASAE, St. Joseph, Mich. 49085.

Smith, R.E. 1965. Optimum vehicle suspension designs by computer simulations. J. of Terramechanics 2(4):17-29.

Smith, R.E. 1967. Computer applications for suspension and frame design of agricultural equipment. SAE Paper No. 670723, SAE, Two Pennsylvania Plaza, N.Y., N.Y. 10001.

Steinbruegge, G.W. 1971. Critique of ASAE tractor overturn standard S306.2. Unpublished paper prepared at Agr. Eng. Dept., Univ. of Nebraska, Lincoln, Nebr. 68503.

Stevenson, D.L. 1970. Discussion prepared for Department of Transportation meeting. October 23, 1970, International Harvester Company, Research and Engineering Center, Hinsdale, Ill. 60521.

Thompson, L.J., Liljedahl, J.B., and Quinn, B.E. 1972. Dynamic motion responses of agricultural tires. Trans. ASAE 15(2): 206-210.

Thomson, W.T. 1965. Vibration theory and applications. Prentice-Hall, Inc., Englewood Cliffs, N.J.

United States Steel. 1971. Design analysis - ROPS. Application bulletin - USS/1, Dynamic testing and computer analysis activity, Structural Dynamics Res. Corp., Cincinnati, Ohio.

Unruh, D. 1969. Mathematical model to predict tip-over stability of articulated off-road vehicle. ASME Paper No. 69-WA/Aut 21. 345 East 47th St., N.Y., N.Y.

Volpe, J.W. 1971. Agricultural tractor safety on public roads and farms. A Report to Congress, Supt. of Documents, U.S. Govt. Printing Office, Washington, D.C. 20402

Watson, E.M. 1967. The structural testing of tractor safety frames. Research Publication R/1, New Zealand Agricultural Engineering Institute, Lincoln College, Canterbury, New Zealand.

Wilson, R.A., and Gannon, R.R. 1972. Rollover testing. SAE Paper No. 720495, SAE, Two Pennsylvania Plaza, N.Y., N.Y. 10001.

Wolken, L.P., and Yoerger, R.R. 1972. Dynamic response of a prime mover to random inputs. ASAE Paper No. 72-613, ASAE, St. Joseph, Mich. 49085.

Worthington, W.H. 1949. Evaluation of factors affecting the operating stability of wheel tractors. Agricultural Engineering 30(3):119-123, 30(4):179-183.

GENERAL REFERENCES

ASAE. 1972. Uniform terminology for traction of agricultural tractors, self-propelled implements, and other traction and transport devices. ASAE Recommendation R296.1. Agricultural Engineers Yearbook, pp. 288-289.

Bekker, M.G. 1969. Introduction to terrain-vehicle systems, Part I: The terrain. Part II: The vehicle. The University of Michigan Press, Ann Arbor, Mich.

Buchele, W.F. 1962. The utility-roll bar. ASAE Paper No. 62-632, ASAE, St. Joseph, Mich. 49085.

Burke, J., ed. 1972. Tractor overturn protection. Farm Safety Review 30(1):13-15.

Chang, C.S., and Cooper, A.E. 1969. A study of the mechanics of tractor wheels. Trans. ASAE 12(3):384-388.

Chenchanna, P. 1969. Ride-comfort and road holding - An investigation with the aid of an analogue computer. Automobile Engineer 59(7):296-300.

de St. Paer, C. 1971. National Safety Council activities. ASAE Paper No. 71-563, ASAE, St. Joseph, Mich. 49085.

Domier, K.W., Friesen, O.H., and Townsend, J.S. 1971. Traction characteristics of two-wheel drive, four wheel drive and crawler tractors. Trans. ASAE 14(3):520-522.

Egging, J. 1973. Prevention of injury and death to extra riders. Agricultural Engineering 54(3):24.

Egging, J.A. 1966. Cabs for farm tractors. ASAE Paper No. 66-626, ASAE, St. Joseph, Mich. 49085.

Fletcher, W.J. 1972. ASAE safety plan on the move. Agricultural Engineering 54(2):25.

Floyd, C.S. 1972. Testing the cab - why and how. Implement and Tractor 87(19):12-14.

Floyd, C.S. 1972. Tractor cab roundup. Implement and Tractor 87(19):4-6.

Goering, C.E., Marley, S.J., Koch, J.A., and Parish, R.L. 1968. Determining the mass moment of inertia of a tractor using floor suspension. Trans. ASAE 11(3):416-418.

Hahn, R.H. 1970. Voluntary standardization and ASAE. Agricultural Engineering 51(4):231-232.

Hansen, M. 1966. The design and evaluation of a protective canopy for agricultural tractors. ASAE Paper No. 66-625, ASAE, St. Joseph, Mich. 49085.

Hansen, M. 1966. Roll guards for tractors. SAE Paper No. 660583, SAE, Two Pennsylvania Plaza, N.Y., N.Y. 10001.

Hanson, W., and Olien, C. 1971. Rural accidents in Minnesota. Special Report 39, Agricultural Extension Service, U. of Minnesota, St. Paul, Minn. 55101.

Hodges, L.H. 1971. The FIEI Safety plan. ASAE Paper No. 71-565, ASAE, St. Joseph, Mich. 49085.

Hoff, P.R. 1970. Accidents in agriculture: A survey of their causes and prevention. Information Bulletin 1, An Extension Publication of N.Y. State College of Agr., Cornell U., Ithaca, N.Y. 14850.

Knapp, L.W. 1970. Small tractor operator position and safety behavior. Agricultural Engineering 51(8):456-459.

Lamouria, L.H., Lorenzen, C., and Parks, R.R. 1962. Design criteria for a driver safety frame. ASAE Paper No. 62-633, ASAE, St. Joseph, Mich. 49085.

McClure, W.R., and Benson, J.L. 1961. An analysis of 212 fatal Ohio farm tractor accidents. ASAE Paper No. 61-129, ASAE, St. Joseph, Mich. 49085.

McDonald, G.L. 1968. An investigation of Australian tractor accidents. Paper presented at Symposium on Farm Mechanisation at the 40th ANZAAS Congress, Christchurch, New Zealand.

National Safety Council. 1967. A study of 789 farm tractor fatalities. Farm Safety Review 25(2):3-6.

Persson, S.P.E. 1967. European experiences with operator protection frames and cabs. Agricultural Engineering 48(10):554-557.

Pfister, R.G. 1972. A projection of new problems and opportunities for tractor safety. ASAE Paper No. 72-605, ASAE, St. Joseph, Mich. 49085.

Pfundstein, K.L. 1971. Corporate product safety for farm and industrial machinery. Agricultural Engineering 52(6):309-311.

Redt, H.S., and Milliken, W.F. 1960. Motions of skidding automobiles. SAE Paper No. 205A, SAE Two Pennsylvania Plaza, N.Y., N.Y. 10001.

Schnieder, R.D., and Hull, D.O. 1971. The occupational safety and health act: How it affects Ag Engineers. Agricultural Engineering 52(10):509.

Schnieder, R.D., and Baker, L.D. 1972. Prevention of injury or death from tractor overturns. ASAE Paper No. 72-604, ASAE, St. Joseph, Mich. 49085.

Steinbruegge, G.W. 1969. Improved methods of locating centers of gravity. Trans. ASAE 12(5):681-684, 689.

Stephens, L.E., Zachariah, G.L., and Liljedahl, J.B. 1972. Vibration effects on tractor overturn recognition. ASAE Paper No. 72-614, ASAE, St. Joseph, Mich. 49085.

Stevenson, D.L., and Gustin, W.E. 1968. Development of a protective frame and cab recommended practice for agricultural and light industrial tractors in the United States. ASAE Paper No. 68-110, ASAE, St. Joseph, Mich. 49085.

Swanson, R.C. 1972. Product safety and liability trends. Agricultural Engineering 53(2):21-22.

Tanquary, E.W. 1969. Implications of safety legislation on equipment design, SAE Paper No. 690440, SAE, Two Pennsylvania Plaza, N.Y., N.Y. 10001.

Taylor, P.A., and Birtwistle, R. 1966-67. Experimental studies of force systems on steered agricultural tires. Proc. of Inst'n. of Mech. Engrs., Auto Division, Part 2A, 181(4):133-148.

Townsend, J.S., Domier, K.W., and Garg, N.C. 1971. Traction characteristics of an agricultural tractor. ASAE Paper No. 71-134, ASAE, St. Joseph, Mich. 49085.

Watson, E.M., and Garden, G.M. 1970. New Zealand Comments on ISO/TC 22T/WG7. Unpublished comments based on testing at New Zealand Agricultural Engineering Institute, Lincoln College, Canterbury, New Zealand.

Willsey, F.R. 1971. The national institute for farm safety plan for safety. ASAE Paper No. 71-564, ASAE, St. Joseph, Mich. 49085.

Willsey, F.R., and Liljedahl, J.B. 1969. A study of tractor overturning accidents. ASAE Paper No. 69-639, ASAE, St. Joseph, Mich. 49085.

Zink, C.L. 1963. Anti-roll bars: Can they reduce tractor fatalities? Agricultural Engineering 44(6):308.

Ziskal, J.F. 1970. Safety concerns of PM division. ASAE Paper No. 70-562, ASAE, St. Joseph, Mich. 49085.

APPENDICES

APPENDIX A

DERIVATION OF THE EQUATIONS OF MOTION

The seven coupled differential equations defining the accelerations of the component parts of the tractor are

$$\dot{\underline{V}}_{BI} = \frac{1}{m_B} (\underline{W}_{BI} - \underline{F}_{FPI} - \underline{F}_{LAI} - \underline{F}_{RAI} + \underline{F}_{BEI}) \quad \text{(A-1)}$$

$$\dot{\omega}_{BP_i} = \frac{-1}{I_{BP_{ii}}} [M_{FPP_i} + (\underline{R}_{PBP} \times \underline{F}_{FPP})_i + M_{LAP_i} + M_{RAP_i}$$

$$+ (\underline{R}_{LBP} \times \underline{F}_{LAP})_i + (\underline{R}_{RBP} \times \underline{F}_{RAP})_i - M_{BEP_i}$$

$$+ (I_{BP_{jj}} - I_{BP_{kk}}) \omega_{BP_j} \omega_{BP_k}] \quad \text{(A-2)}$$

where

$j = 3$, $k = 2$ when $i = 1$

$j = 1$, $k = 3$ when $i = 2$, and

$j = 2$, $k = 1$ when $i = 3$

and

$$\dot{\omega}_{FF_1} = \frac{1}{I_{FF_{11}}} [- I_{FF_{13}} (\dot{\omega}_{FF_3} + \omega_{FF_1} \omega_{FF_2})$$

$$- (I_{FF_{33}} - I_{FF_{22}}) \omega_{FF_2} \omega_{FF_3} + M_{FF_1}] . \quad \text{(A-3)}$$

The notation used in defining variables in this appendix is that defined in Chapter III.

Because the constraint forces and moments are functions of accelerations, substitutions of the appropriate constraint equations into equations A-1 through A-3 must be accomplished before these equations can be expressed as the following set of simultaneous equations:

$$\begin{bmatrix} B_{11} & B_{12} & B_{13} & B_{14} & B_{15} & B_{16} & B_{17} \\ B_{21} & B_{22} & B_{23} & B_{24} & B_{25} & B_{26} & B_{27} \\ B_{31} & B_{32} & B_{33} & B_{34} & B_{35} & B_{36} & B_{37} \\ B_{41} & B_{42} & B_{43} & B_{44} & B_{45} & B_{46} & B_{47} \\ B_{51} & B_{52} & B_{53} & B_{54} & B_{55} & B_{56} & B_{57} \\ B_{61} & B_{62} & B_{63} & B_{64} & B_{65} & B_{66} & B_{67} \\ B_{71} & B_{72} & B_{73} & B_{74} & B_{75} & B_{76} & B_{77} \end{bmatrix} \begin{Bmatrix} X_1 \\ X_2 \\ X_3 \\ X_4 \\ X_5 \\ X_6 \\ X_7 \end{Bmatrix} = \begin{Bmatrix} C_1 \\ C_2 \\ C_3 \\ C_4 \\ C_5 \\ C_6 \\ C_7 \end{Bmatrix} \tag{A-4}$$

where

X_i are the derivatives as defined in Table A-1,

B_{ij} are the coupling coefficients to be derived, and

C_i are the constants to be derived.

Derivation of the coupling coefficients and constants for derivatives X_1 , X_2 , and X_3 is accomplished by substituting the following supporting equations into the equations A-1.

$$\underline{F}_{FPI} = m_F\dot{\underline{V}}_{FI} - \underline{F}_{FGI} - \underline{W}_{FI} \tag{A-5}$$

$$\underline{F}_{LAI} = m_R\dot{\underline{V}}_{LI} - \underline{F}_{LGI} - \underline{W}_{RI} \tag{A-6}$$

$$\underline{F}_{RAI} = m_R\dot{\underline{V}}_{RI} - \underline{F}_{RGI} - \underline{W}_{RI} \tag{A-7}$$

$$\begin{aligned} \dot{\underline{V}}_{FI} = \dot{\underline{V}}_{BI} &+ (\dot{\underline{\omega}}_{BI} \times \underline{R}_{PBI}) + \underline{\omega}_{BI} \times (\underline{\omega}_{BI} \times \underline{R}_{PBI}) \\ &+ (\dot{\underline{\omega}}_{FI} \times \underline{R}_{FPI}) + \underline{\omega}_{FI} \times (\underline{\omega}_{FI} \times \underline{R}_{FPI}) \end{aligned} \tag{A-8}$$

$$\dot{\underline{V}}_{LI} = \dot{\underline{V}}_{BI} + (\dot{\underline{\omega}}_{BI} \times \underline{R}_{LBI}) + \underline{\omega}_{BI} \times (\underline{\omega}_{BI} \times \underline{R}_{LBI}) \tag{A-9}$$

$$\dot{\underline{V}}_{RI} = \dot{\underline{V}}_{BI} + (\dot{\underline{\omega}}_{BI} \times \underline{R}_{RBI}) + \underline{\omega}_{BI} \times (\underline{\omega}_{BI} \times \underline{R}_{RBI}) \tag{A-10}$$

TABLE A-1. Definition of Derivative Variables for the System of Linear Equations

X_i	Variable	Definition
		acceleration of tractor body -
X_1	$\dot{V}_{BI_1}$	$\underline{e}_{I_1}$ direction
X_2	$\dot{V}_{BI_2}$	$\underline{e}_{I_2}$ direction
X_3	$\dot{V}_{BI_3}$	$\underline{e}_{I_3}$ direction
		angular acceleration of tractor body -
X_4	$\dot{\omega}_{BP_1}$	$\underline{e}_{P_1}$ direction
X_5	$\dot{\omega}_{BP_2}$	$\underline{e}_{P_2}$ direction
X_6	$\dot{\omega}_{BP_3}$	$\underline{e}_{P_3}$ direction
		angular acceleration of tractor front end about front pin -
X_7	$\dot{\omega}_{FF_1}$	$\underline{e}_{F_1}$ direction

Note that because the left rear and right rear wheels are considered identical m_L was replaced by m_R and $\underline{W}_{LI}$ was replaced by $\underline{W}_{RI}$.

Recall that the transformation of coordinates is defined by a premultiplication of one vector by a matrix of direction cosines to obtain a new vector representation of the same quantity, only expressed in different coordinate directions. The following is one such operation which is typical of any that may be desired.

The vector $\dot{\underline{\omega}}_{BP}$ is the angular acceleration of the tractor body as expressed in the tractor principal-axes directions. This angular velocity is needed as expressed in the inertial directions (i.e., $\dot{\underline{\omega}}_{BI}$ is desired). For a known orientation of the tractor body (attitude is defined by $\underline{A}_{PI}$), the relationship of the two angular accelerations is

$$\dot{\underline{\omega}}_{BP} = A_{PI}\dot{\underline{\omega}}_{BI} \tag{A-11}$$

so inversely,

$$\dot{\underline{\omega}}_{BI} = A_{PI}^{-1}\dot{\underline{\omega}}_{BP} \tag{A-12}$$

where A_{PI}^{-1} is the inverse of matrix A_{PI} .

But the inverse of a direction cosine matrix (an orthonormal matrix) is simply the transpose of that matrix. Thus,

$$\dot{\underline{\omega}}_{BI} = A_{PI}^{T}\dot{\underline{\omega}}_{BP} \tag{A-13}$$

where the superscript T denotes the transpose.

Performing the required substitutions, coordinate transformations, vector cross products, and defining the following new variables,

$$m_T = m_B + m_F + 2m_R \ , \tag{A-14}$$

$$\underline{F}_{TI} = \underline{W}_{BI} + \underline{W}_{FI} + 2\underline{W}_{RI} + \underline{F}_{BEI} + \underline{F}_{FGI} + \underline{F}_{LGI} + \underline{F}_{RGI} \ , \tag{A-15}$$

and

$$\underline{R}_{MI} = m_F\underline{R}_{PBI} + m_R(\underline{R}_{LBI} + \underline{R}_{RBI}) \tag{A-16}$$

results in definition of the first three rows of coupling coefficients B_{ij} and constants C_i for equation A-4:

$$B_{11} = B_{22} = B_{33} = m_T \tag{A-17}$$

$$B_{12} = B_{13} = B_{21} = B_{23} = B_{31} = B_{32} = 0 \tag{A-18}$$

$$\begin{aligned} B_{i,\ell+3} = {} & A_{PI_{\ell k}} R_{MI_j} - A_{PI_{\ell j}} R_{MI_k} \\ & + m_F[A_{PF_{\ell 2}}(A_{FI_{2k}} R_{FPI_j} - A_{FI_{2j}} R_{FPI_k}) \\ & + A_{PF_{\ell 3}}(A_{FI_{3k}} R_{FPI_j} - A_{FI_{3j}} R_{FPI_k})] \end{aligned} \tag{A-19}$$

$$B_{i7} = m_F(A_{FI_{1k}} R_{FPI_j} - A_{FI_{1j}} R_{FPI_k}) \tag{A-20}$$

$$\begin{aligned} C_i = {} & F_{TI_i} - [\underline{\omega}_{BI} \times (\underline{\omega}_{BI} \times \underline{R}_{MI})]_i \\ & - [\underline{\omega}_{FI} \times (\underline{\omega}_{FI} \times m_F\underline{R}_{FPI})]_i \end{aligned} \tag{A-21}$$

where

$i = 1 \ , 2 \ , 3$

while $j = 3 \ , k = 2$ when $i = 1$

$j = 1$, $k = 3$ when $i = 2$

$j = 2$, $k = 1$ when $i = 3$

and $\ell = 1,2,3$ for each value of i .

Derivation of the coupling coefficients and constants for derivatives X_4 , X_5 , and X_6 is accomplished by substituting the following supporting equations:

$$M_{FPF_1} = 0 \tag{A-22}$$

$$\begin{aligned} M_{FPF_2} = {} & I_{FF_{22}} \dot{\omega}_{FF_2} + (I_{FF_{11}} - I_{FF_{33}}) \omega_{FF_1} \omega_{FF_3} \\ & + I_{FF_{13}} (\omega^2_{FF_3} - \omega^2_{FF_1}) - M_{FGF_2} \\ & + (\underline{R}_{FPF} \times \underline{F}_{FPF})_2 \end{aligned} \tag{A-23}$$

$$\begin{aligned} M_{FPF_3} = {} & I_{FF_{33}} \dot{\omega}_{FF_3} + I_{FF_{13}} (\dot{\omega}_{FF_1} - \omega_{FF_2} \omega_{FF_3}) \\ & + (I_{FF_{22}} - I_{FF_{11}}) \omega_{FF_1} \omega_{FF_2} - M_{FGF_3} \\ & + (\underline{R}_{FPF} \times \underline{F}_{FPF})_3 \quad . \end{aligned} \tag{A-24}$$

$$M_{LAP_1} = I_{LP_{11}} \dot{\omega}_{LP_1} + (I_{LP_{33}} - I_{LP_{22}}) \omega_{LP_2} \omega_{LP_3} - M_{LGP_1} \tag{A-25}$$

$$M_{LAP_2} = - \frac{1}{2} R_2 T_d \tag{A-26}$$

$$M_{LAP_3} = I_{LP_{33}} \dot{\omega}_{LP_3} + (I_{LP_{22}} - I_{LP_{11}}) \omega_{LP_1} \omega_{LP_2} - M_{LGP_3} \tag{A-27}$$

$$M_{RAP_1} = I_{RP_{11}} \dot{\omega}_{RP_1} + (I_{RP_{33}} - I_{RP_{22}}) \omega_{RP_2} \omega_{RP_3} - M_{RGP_1} \tag{A-28}$$

$$M_{RAP_2} = - \frac{1}{2} R_2 T_d \tag{A-29}$$

$$M_{RAP_3} = I_{RP_{33}}\dot{\omega}_{RP_3} + (I_{RP_{22}} - I_{RP_{11}})\omega_{RP_1}\omega_{RP_2} - M_{RGP_3} \quad \text{(A-30)}$$

and equations A-5 through A-10 into the three rotational equations A-2 (after appropriate coordinate transformations have been performed to convert the front-end-axes vectors and inertial-axes vectors into principal-axes vectors).

After transforming equations A-22 through A-24 into principal-axes vectors, substituting them into equations A-2, expanding the vector cross products, and substituting for the forces included in the cross products, the equations may be regrouped into the following form:

$$I_{BP_{ii}}\dot{\omega}_{BP_i} + I_{FF_{13}}A_{PF_{i3}}\dot{\omega}_{FF_1} + M_{LAP_i} + M_{RAP_i}$$

$$+ \sum_{n=1}^{3} (C_{B_{in}}\dot{\omega}_{BP_n} + C_{F_{in}}F_{FPI_n} + C_{L_{in}}F_{LAI_n} + C_{R_{in}}F_{RAI_n}) = C_{N_i} \quad \text{(A-31)}$$

where

$$C_{B_{in}} = A_{PF_{i2}}I_{FF_{22}}A_{PF_{n2}} + A_{PF_{i3}}I_{FF_{33}}A_{PF_{n3}} \quad \text{(A-32)}$$

$$C_{F_{in}} = A_{PF_{i2}}(R_{FPF_3}A_{FI_{1n}} - R_{FPF_1}A_{FI_{3n}}$$

$$+ A_{PF_{i3}}(R_{FPF_1}A_{FI_{2n}} - R_{FPF_2}A_{FI_{1n}})$$

$$+ R_{PBP_k}A_{PI_{jn}} - R_{PBP_j}A_{PI_{kn}} \quad \text{(A-33)}$$

$$C_{L_{in}} = R_{LBP_k}A_{PI_{jn}} - R_{LBP_j}A_{PI_{kn}} \quad \text{(A-34)}$$

$$C_{R_{in}} = R_{RBP_k}A_{PI_{jn}} - R_{RBP_j}A_{PI_{kn}} \quad \text{(A-35)}$$

$$C_{N_i} = M_{BEP_i} - (I_{BP_{jj}} - I_{BP_{kk}})\omega_{BP_j}\omega_{BP_k}$$

$$- A_{PF_{i2}}[(I_{FF_{11}} - I_{FF_{33}})\omega_{FF_1}\omega_{FF_3}$$

$$+ I_{FF_{13}}(\omega^2_{FF_3} - \omega^2_{FF_1}) - M_{FGF_2}]$$

$$- A_{PF_{i3}}[(I_{FF_{22}} - I_{FF_{11}})\omega_{FF_1}\omega_{FF_2}$$

$$- I_{FF_{13}}\omega_{FF_2}\omega_{FF_3} - M_{FGF_3}] \quad \text{(A-36)}$$

while $i = 1, 2, 3$ and $n = 1, 2, 3$

$j = 3, k = 2$ when $i = 1$

$j = 1, k = 3$ when $i = 2$

$j = 2, k = 1$ when $i = 3$.

Substitution for the forces in equation A-31 and regrouping by the inertial components of the accelerations yields the following equation:

$$I_{BP_{ii}}\dot{\omega}_{BP_i} + I_{FF_{13}}A_{PF_{i3}}\dot{\omega}_{FF_1} + M_{LAP_i} + M_{RAP_i}$$

$$+ \sum_{\ell=1}^{3} [C_{B_{i\ell}}\dot{\omega}_{BP_\ell} + (m_F C_{F_{i\ell}} + m_R C_{L_{i\ell}} + m_R C_{R_{i\ell}})\dot{V}_{BI_\ell}$$

$$+ D_{F_{i\ell}}\dot{\omega}_{FI_\ell} + D_{B_{i\ell}}\dot{\omega}_{BI_\ell}] = D_{N_i} \quad \text{(A-37)}$$

where

$$D_{B_{i\ell}} = m_F(C_{F_{im}}R_{PBI_n} - C_{F_{in}}R_{PBI_m}) + m_R(C_{L_{im}}R_{LBI_n} - C_{L_{in}}R_{LBI_m})$$

$$+ m_R(C_{R_{im}}R_{RBI_n} - C_{R_{in}}R_{RBI_m}) \quad \text{(A-38)}$$

$$D_{F_{i\ell}} = m_F(C_{F_{im}}R_{FPI_n} - C_{F_{in}}R_{FPI_m}) \quad \text{(A-39)}$$

$$D_{N_i} = C_{N_i} - \sum_{\ell=1}^{3} C_{F_{i\ell}} \{ [\underline{\omega}_{BI} \times (\underline{\omega}_{BI} \times m_F \underline{R}_{PBI})]_\ell$$

$$+ [\underline{\omega}_{FI} \times (\underline{\omega}_{FI} \times m_F \underline{R}_{FPI})]_\ell - F_{FGI_\ell} - W_{FI_\ell} \}$$

$$- \sum_{\ell=1}^{3} C_{L_{i\ell}} \{ [\underline{\omega}_{BI} \times (\underline{\omega}_{BI} \times m_R \underline{R}_{LBI})]_\ell - F_{LGI_\ell} - W_{RI_\ell} \}$$

$$- \sum_{\ell=1}^{3} C_{R_{i\ell}} \{ [\underline{\omega}_{BI} \times (\underline{\omega}_{BI} \times m_R \underline{R}_{RBI})]_\ell - F_{RGI_\ell} - W_{RI_\ell} \} \tag{A-40}$$

for $i = 1, 2, 3$ and $\ell = 1, 2, 3$

$m = 3, n = 2$ when $\ell = 1$

$m = 1, n = 3$ when $\ell = 2$

$m = 2, n = 1$ when $\ell = 3$.

Converting the front-end accelerations and tractor-body accelerations to the appropriate coordinates and regrouping yields the desired coupling coefficients, B_{ij}, and constants, C_i, for the fourth, fifth and sixth rows of equation A-4.

$$B_{i+3,\ell} = m_F C_{F_{i\ell}} + m_R C_{L_{i\ell}} + m_R C_{R_{i\ell}} \tag{A-41}$$

$$B_{i+3,\ell+3} = C_{B_{i\ell}} + \sum_{n=1}^{3} [D_{F_{in}} (A_{FI_{2n}} A_{PF_{\ell 2}} + A_{FI_{3n}} A_{PF_{\ell 3}})$$

$$+ D_{B_{in}} A_{PI_{\ell n}}] + D_{E_i} \tag{A-42}$$

where

$$D_{E_i} = \text{sum of} \begin{cases} I_{BP_{ii}} & \text{if } i = \ell \text{, and} \\ 2I_{RP_{ii}} & \text{if } i \neq 2 \text{ (i.e., if } \underline{e}_{P_i} \text{ is not parallel to the rear axle)} \end{cases}$$

$$B_{i7} = m_F(A_{FI_{1k}} R_{FPI_j} - A_{FI_{1j}} R_{FPI_k}) \tag{A-43}$$

$$C_i = F_{TI_i} - [\underline{\omega}_{BI} \times (\underline{\omega}_{BI} \times \underline{R}_{MI})\ i$$

$$- [\underline{\omega}_{FI} \times (\underline{\omega}_{FI} \times m_F\underline{R}_{FPI})]_i \tag{A-44}$$

$$C_{i+3} = D_{N_i} \tag{A-45}$$

for $i = 1 , 2 , 3$ and $\ell = 1 , 2 , 3$

while $j = 3 , k = 2$ when $i = 1$ and $m = 3 , n = 2$ when $\ell = 1$

$j = 1 , k = 3$ when $i = 2$ and $m = 1 , n = 3$ when $\ell = 2$

$j = 2 , k = 1$ when $i = 3$ and $m = 2 , n = 1$ when $\ell = 3$.

The final row of coupling coefficients, B_{ij} , and the constant, C_7 , are derived from equation A-46,

$$I_{FF_{11}} \dot{\omega}_{FF_1} + I_{FF_{13}}(\dot{\omega}_{FF_3} + \omega_{FF_1}\omega_{FF_2})$$

$$+ (I_{FF_{33}} - I_{FF_{22}})\omega_{FF_2}\omega_{FF_3} = M_{FF_1} , \tag{A-46}$$

with the substitution of

$$\underline{M}_{FF} = \underline{M}_{FPF} + \underline{M}_{FGF} - (\underline{R}_{FPF} \times \underline{F}_{FPF}) \tag{A-47}$$

and

$$M_{FPF_1} = 0 . \tag{A-48}$$

Only the M_{FF_1} component of equation A-47 is required by equation A-46. Substituting equation A-47 into equation A-46, expanding the cross product, and substituting equations A-5 and A-8 for $\underline{F}_{FPI}$ yields the following intermediate relationship:

$$
\begin{aligned}
I_{FF_{11}}\dot{\omega}_{FF_1} + I_{FF_{13}} \sum_{\ell=1}^{3} (A_{PF_{\ell 3}}\dot{\omega}_{BP_\ell}) \\
+ m_F \sum_{\ell=1}^{3} E_{F_\ell}(\dot{V}_{BI_\ell} + \dot{\omega}_{BI_n} R_{PBI_m} - \dot{\omega}_{BI_m} R_{PBI_n} \\
+ \dot{\omega}_{FI_n} R_{FPI_m} - \dot{\omega}_{FI_m} R_{FPI_n}) = E_N \quad \text{(A-49)}
\end{aligned}
$$

while

$m = 3$, $n = 2$ when $\ell = 1$

$m = 1$, $n = 3$ when $\ell = 2$

$m = 2$, $n = 1$ when $\ell = 3$

where

$$E_{F_\ell} = R_{FPF_2} A_{FI_{3\ell}} - R_{FPF_3} A_{FI_{2\ell}} , \quad \text{(A-50)}$$

and

$$
\begin{aligned}
E_N = M_{FGF_1} - (I_{FF_{33}} - I_{FF_{22}})\omega_{FF_2}\omega_{FF_3} - I_{FF_{13}}\omega_{FF_1}\omega_{FF_2} \\
\sum_{\ell=1}^{3} (R_{FPF_2} A_{FI_{3\ell}} - R_{FPF_3} A_{FI_{2\ell}})\{m_F[\underline{\omega}_{BI} \times (\underline{\omega}_{BI} \times \underline{R}_{PBI})]_\ell \\
+ m_F[\underline{\omega}_{FI} \times (\underline{\omega}_{FI} \times \underline{R}_{FPI})]_\ell - F_{FGI_\ell} - W_{FI_\ell}\} . \quad \text{(A-51)}
\end{aligned}
$$

Transforming the angular accelerations to the desired coordinates and regrouping according to accelerations yields a second intermediate relationship,

$$\sum_{i=1}^{3} (m_F E_{F_i} \dot{V}_{BI_i} + G_{B_i} \dot{\omega}_{BP_i}) + G_{F_1} \dot{\omega}_{FF_1}$$

$$+ G_{F_2} \sum_{\ell=1}^{3} A_{PF_{\ell 2}} \dot{\omega}_{BP_\ell} + G_{F_3} \sum_{\ell=1}^{3} A_{PF_{\ell 3}} \dot{\omega}_{BP_\ell} = E_N \tag{A-52}$$

where

$$G_{B_i} = I_{FF_{13}} A_{PF_{i3}} + \sum_{\ell=1}^{3} m_F A_{PI_{i\ell}} (E_{F_m} R_{PBI_n} - E_{F_n} R_{PBI_m}) \tag{A-53}$$

$$G_{F_i} = G_{E_i} + \sum_{\ell=1}^{3} m_F A_{FI_{i\ell}} (E_{F_m} R_{FPI_n} - E_{F_n} R_{FPI_m}) \tag{A-54}$$

$$G_{E_i} = \begin{cases} I_{FF_{11}} & \text{for } i = 1 \\ 0 & \text{for } i = 2 , 3 \end{cases}$$

while

$m = 3 , n = 2$ when $\ell = 1$

$m = 1 , n = 3$ when $\ell = 2$

$m = 2 , n = 1$ when $\ell = 3$.

The coupling coefficients, B_{ij} , and the constant, C_7 , for row number seven of equation A-4 are defined by equation A-52 as

$$B_{7,j} = m_F E_{F_j} \tag{A-55}$$

$$B_{7,j+3} = G_{B_j} + G_{F_2} A_{PF_{j2}} + G_{F_3} A_{PF_{j3}} \tag{A-56}$$

$$B_{77} = G_{F_1} \tag{A-57}$$

$$C_7 = E_N \tag{A-58}$$

where $j = 1 , 2 , 3$.

APPENDIX B

MEASUREMENT OF TIRE FORCE CHARACTERISTICS

The measurement of tire-ground forces required the design of special equipment for this purpose. The lateral tire force, F_{ℓ}, and the circumferential tire force, F_c, defined to act in the ground plane, were to be described as functions of the load on the tire normal to the ground surface, F_n, and the tire slip angle, θ_s. The tire damping characteristics were to be described by a viscous damping coefficient C_d. The instrumentation used in measuring the tire forces was much different from that used to measure the tire damping.

B.1. Circumferential and Lateral Forces

The circumferential and lateral tire forces were derived from the forces F_s and F_a measured with the testing apparatus described in Section 4.3.2. The tire was held with a fixed slip angle relative to the moving surface beneath the tire while weights stacked above the tire changed the tire normal force. The axial tire force, F_a, was measured by the axial displacement of the tire and axle as they compressed a spring. The spring calibration provided the conversion from dial gage readings (axial displacement) to axial tire force. (See Figure B-1 for the physical arrangement.) Thus, the axial tire force, F_a, was given by

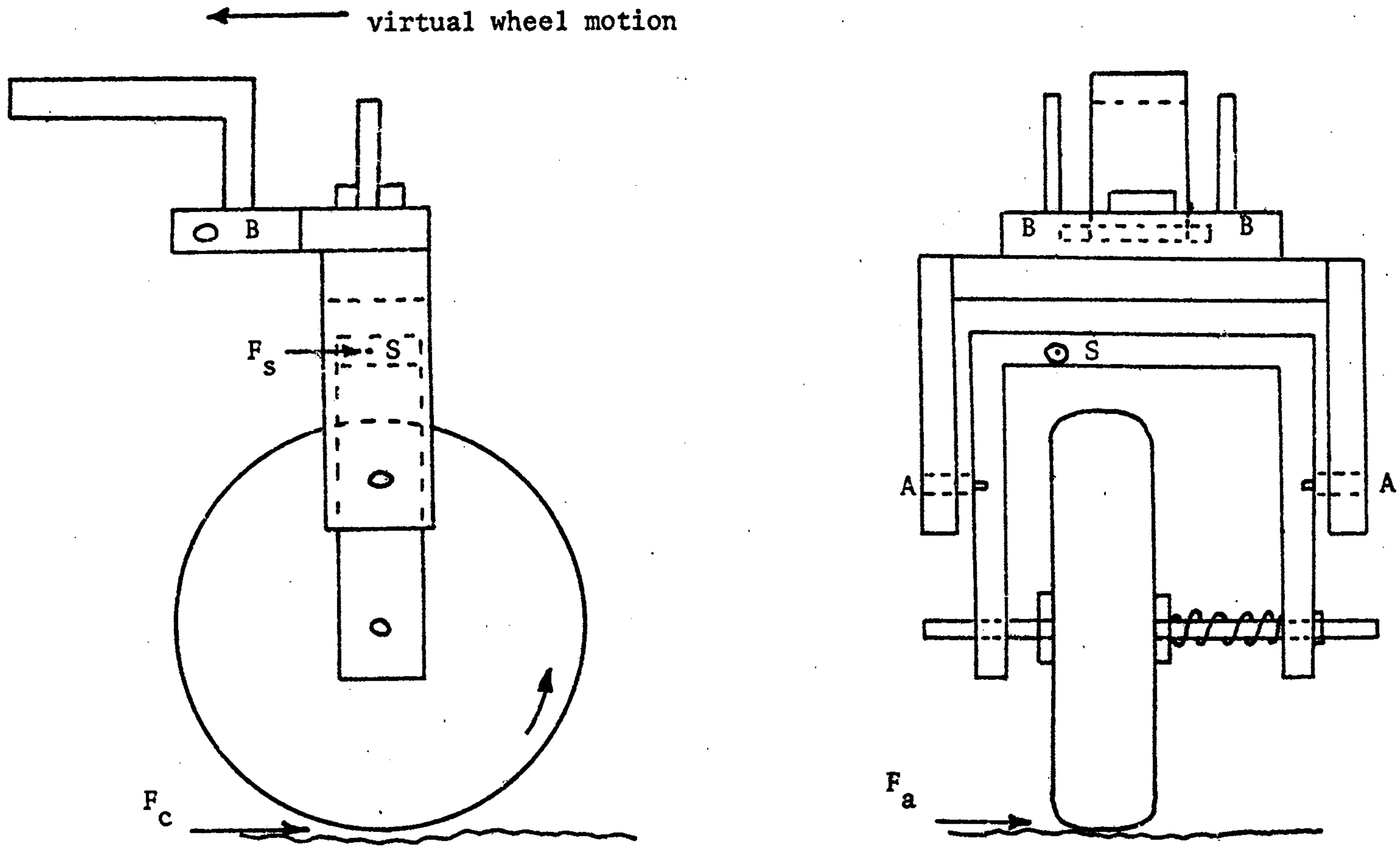

Figure B-1. Apparatus Used in Measuring Tire Lateral and Circumferential Forces.

$$F_a = K_a(DGR - DGR_0) \tag{B-1}$$

where

K_a is the spring calibration constant, lb/in,

DGR_0 is the dial gage reading with zero axial load, in,

DGR is the dial gage reading for the desired axial load, F_a , in.

A strain-gaged cantilever beam was used to measure the restraining force, F_s , necessary to prevent rotation of the inner yoke due to the circumferential force, F_c , on the tire. The inner yoke was supported at points A with ball bearings to minimize friction in rotation. A screw at point S transmitted the restraining force, F_s , between the inner yoke and the cantilever beam (fastened to the outer yoke) to hold the inner yoke in a vertical plane while the beam was deflected.

The strip chart used to record the strain bridge output was calibrated to provide a chart reading that could be read directly as that force magnitude applied in the circumferential forced direction at the axle to obtain the strain bridge output. Thus the circumferential force, F_c , was a constant multiple (based upon the yoke geometry) of the strip chart reading. By equating moments about pins A, this relationship becomes

$$F_c = \frac{d_2}{(d_2+r)} \text{SBR} \tag{B-2}$$

where

d_2 is the distance from points A to the axle, in,

r is the radius of the tire, in, and

SBR is the strain bridge reading as recorded on the strip chart recorder, providing directly the value of the force applied to F_c at the axle while this beam deflection exists.

Because the inner yoke was fixed in position while all data readings were taken, the derivations to relate the measured forces - F_c, F_a, and the load W_p - to the desired normal force F_n and the lateral force F_ℓ consider the two yokes as one. Figure B-2 shows the physical arrangement used in derivation of the force relationships.

The tire-yoke system is supported by the horizontal pin (designated pin B) which allows only rotation about that horizontal axis. Seven different forces act upon this system to maintain an equilibrium condition. These are:

1. The yoke weight - This force includes the weight of the yoke, axle, and gages, and acts vertically downward through the center of mass for this unit, point Y.
2. The wheel weight - This force acts downward through the wheel center of mass where the wheel remains while deflecting the axial spring, point W.
3. The load weight - This force is varied to change the normal load during the tests. The force acts downward through point P.

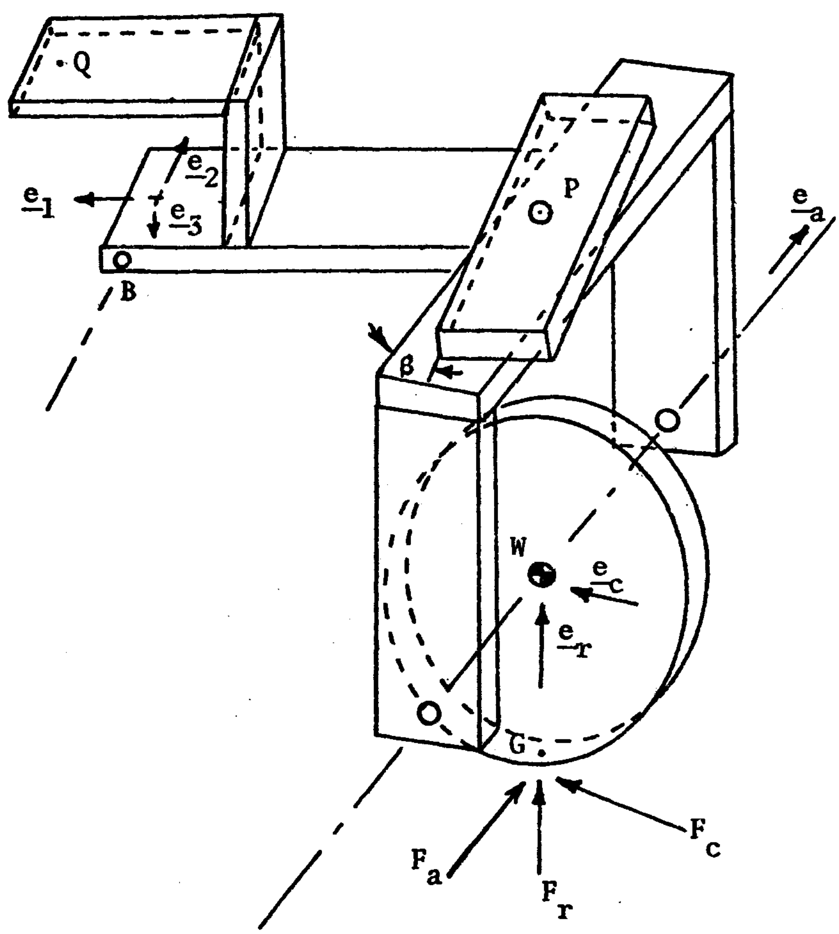

Figure B-2. Coordinate Systems Used in the Derivation of Tire Lateral and Circumferential Forces.

4. The counterweight - This force is applied at the point Q to enable low-magnitude normal loads to be applied to the tire. The force acts downward through the point Q.
5. The axial tire force - This force acts in the direction of the wheel axle. The force is applied to the system at the "ground-contact point" G.
6. The radial tire force - This force acts radially toward the wheel center. The force is applied to the tire at its point of contact with the moving surface G.
7. The circumferential tire force - This force acts in the direction parallel to the line-of-intersection between the moving-surface plane and the wheel plane. The force is applied to the tire at point G.

The total force acting on the tire due to its interaction with the ground surface (the sandpaper) is given in terms of the three orthogonal wheel unit vectors whown in Figure B-2 as

$$\underline{F}_T = F_a \underline{e}_a + F_r \underline{e}_r + F_c \underline{e}_c \tag{B-3}$$

where

$\underline{F}_T$ is the resultant force vector acting at point G, lb.

Coordinate systems similar to those defined in Chapter III are defined for use in the derivation of force relationships for the test apparatus. The appartus is free to rotate about axis $\underline{e}_2$ while $\underline{e}_3$ points vertically down. The sandpaper surface moves in the $-\underline{e}_1$ direction creating virtual apparatus movement in the $+\underline{e}_1$

direction. Thus the $\underline{e}_1$, $\underline{e}_2$, $\underline{e}_3$ triad is similar to a tractor-axes system of vectors.

A second set of coordinates are defined in directions associated with the wheel orientation and tire forces. The $\underline{e}_a$ vector is parallel to the wheel axis, the $\underline{e}_r$ vector is radially up from the surface to the wheel center, while the $\underline{e}_c$ vector is parallel to the line-of-intersection for the wheel plane and the plane of the moving-sandpaper surface. Because the apparatus is maintained so that the yoke remains in a vertical plane, the $\underline{e}_r$ vector is actually parallel to the normal vector of the sandpaper surface.

If the steer angle of the wheel is defined (as in Chapter III) as the angle of rotation about the $\underline{e}_3$ axis relative to the direction of motion, then the angle β shown in Figure B-2 is the steer angle. The transformation between the fixed unit vectors and the wheel unit vectors is given as

$$\begin{Bmatrix} \underline{e}_r \\ \underline{e}_a \\ \underline{e}_c \end{Bmatrix} = \begin{bmatrix} 0 & 0 & 0 \\ -\sin\beta & \cos\beta & 0 \\ \cos\beta & \sin\beta & 0 \end{bmatrix} \begin{Bmatrix} \underline{e}_1 \\ \underline{e}_2 \\ \underline{e}_3 \end{Bmatrix} . \qquad \text{(B-4)}$$

The equilibrium condition existing for the test apparatus is that of zero net moment about pin B as defined in the vector equation

$$\sum_{i=1}^{7} (\underline{R}_i \times \underline{F}_i) \cdot \underline{e}_2 = 0 \qquad \text{(B-5)}$$

where

$\underline{R}_i$ are vectors from pin B to the point of application of force $\underline{F}_i$, in, and

$\underline{F}_i$ are the seven forces listed previously, lb.

Note: The center of mass for the piece of apparatus containing pin B and points P and Q was above the pin, thereby creating no moment about the pin.

Table B-1 summarizes these seven radius vectors, forces, and final dot products as given by equations B-5. Those radius vectors defining points in the wheel axes directions are defined as the sum of the radius vector to the point P and the vector from P to the point of interest.

Equating the sum of the dot products in Table B-1 to zero yields the equation of equilibrium about pin B,

$$\begin{aligned} &-(R_{P_1}-R_{Y_2}\sin\beta+R_{Y_3}\cos\beta)W_Y - [R_{P_1}-(R_{W_2}+\delta)\sin\beta+R_{W_3}\cos\beta]W_W \\ &- R_{P_1}W_P-R_{Q_1}W_Q-(R_{P_3}-R_{W_1}+r)\sin\beta\ F_a + [R_{P_1}-(R_{W_2}+\delta)\sin\beta \\ &\qquad\qquad\qquad\qquad +R_{W_3}\cos\beta]F_r \\ &+ (R_{P_3}-R_{W_1}+r)\cos\beta\ F_c = 0\ . \qquad\qquad (B\text{-}6) \end{aligned}$$

The weights of the yoke W_Y, the wheel W_W, the load W_P, and the counterweight W_Q are known quantities, while the axial force F_a and the circumferential force F_c are obtainable from calibrations and the data recorded. The radial force F_r is obtained by solving equation B-6 for F_r,

TABLE B-1. Moment Components Affecting the Equilibrium of the Tire Testing Apparatus.

Radius vectors and forces	$(\underline{R}_i \times \underline{F}_i) \cdot \underline{e}_2$
Yoke Weight	
$\underline{R}_1 = R_{P_1}\underline{e}_1 + R_{P_2}\underline{e}_2 + R_{P_3}\underline{e}_3 + R_{Y_1}\underline{e}_r + R_{Y_2}\underline{e}_a + R_{Y_3}\underline{e}_c$	$-(R_{P_1} - R_{Y_2}\sin\beta + R_{Y_3}\cos\beta)W_Y$
$\underline{F}_1 = W_Y\underline{e}_3$	
Wheel weight	
$^{*}\underline{R}_2 = R_{P_1}\underline{e}_1 + R_{P_2}\underline{e}_2 + R_{P_3}\underline{e}_3 + R_{W_1}\underline{e}_r + R_{W_2}\underline{e}_a + R_{W_3}\underline{e}_c + \delta\underline{e}_a$	
$\underline{F}_2 = W_W\underline{e}_3$	$-[R_{P_1} - (R_{W_2} + \delta)\sin\beta + R_{W_3}\cos\beta]W_W$
Load weight	
$\underline{R}_3 = R_{P_1}\underline{e}_1 + R_{P_2}\underline{e}_2 + R_{P_3}\underline{e}_3$	
$\underline{F}_3 = W_P\underline{e}_3$	$-R_{P_1}W_P$
Counterweight	
$\underline{R}_4 = R_{Q_1}\underline{e}_1 + R_{Q_2}\underline{e}_2 + R_{Q_3}\underline{e}_3$	
$\underline{F}_4 = W_Q\underline{e}_3$	$-R_{Q_1}W_Q$
Axial tire force	
$\underline{R}_5 = R_{P_1}\underline{e}_1 + R_{P_2}\underline{e}_2 + R_{P_3}\underline{e}_3 + R_{W_1}\underline{e}_r + R_{W_2}\underline{e}_a + R_{W_3}\underline{e}_c + \delta\underline{e}_a - r\underline{e}_r$	
$\underline{F}_5 = F_a\underline{e}_a$	$-(R_{P_3} - R_{W_1} + r)\sin\beta\ F_a$
Radial tire force	
$\underline{R}_6 = \underline{R}_5$	
$\underline{F}_6 = F_r\underline{e}_r$	$[R_{P_1} - (R_{W_2} + \delta)\sin\beta + R_{W_3}\cos\beta]F_r$
Circumferential tire force	
$\underline{R}_7 = \underline{R}_5$	
$\underline{F}_7 = F_c\underline{e}_c$	$(R_{P_3} - R_{W_1} + r)\cos\beta\ F_c$

* δ is the axial displacement of the wheel due to the applied forces.

$$F_r = W_W + [(R_{P_1} - R_{Y_2}\sin\beta + R_{Y_3}\cos\beta)W_Y + R_{P_1}W_P + R_{Q_1}W_Q$$
$$+(R_{P_3} - R_{W_1} + r)(F_a\sin\beta - F_c\cos\beta)]/[R_{P_1} - (R_{W_2} + \delta)\sin\beta$$
$$+R_{W_3}\cos\beta] \qquad \text{(B-7)}$$

The normal force F_n, the lateral force F_ℓ, and the circumferential force F_c were required for the mathematical model. Because the axis of pin B was horizontal for the tire force tests, the normal force and radial force were identical, i.e.,

$$F_n = F_r , \qquad \text{(B-8)}$$

while the axial force and lateral force were identical, i.e.,

$$F_\ell = F_a . \qquad \text{(B-9)}$$

Table B-2 defines the values or range of values for the tire testing parameters.

The tire test data was collected as values of SBR and DGR for each steer angle, β, setting and for each load W_P. Knowing the initial dial gage reading DGR_0, the axial force or lateral force is then determined from equation B-1. The circumferential force is then calculated from equation B-2 and the radial force or normal force from equation B-7. Table B-3 shows a sample set of data for the rear wheel while the steer angle is set at 5°. Note that the steer angle β is the same as the tire slip angle θ_s. Table B-4 provides a tabulation of the lateral and normal forces measured for both rear

TABLE B-2. Definition of Tire Testing Parameters.

Sandpaper speed, in/min	26.1	
Yoke weight (W_Y), lb	5.60	
Counterweight (W_Q), lb	2.46	
Load (W_P), lb	0.0 to 7.4	
Steer angle (β), degrees	0 to 30	
Radius vector components, in:		
R_{P_1}	-2.95	
R_{P_3}	0.00	
R_{Y_2}	-1.10	
R_{Y_3}	0.00	
R_{W_1}	-5.35	
R_{W_3}	0.00	
R_{Q_1}	6.92	
Calibration parameters:		
d_2 , in	1.90	
K_a , lb/in	-51.24	
Tire-dependent parameters:	Rear	Front
Tire radius (r), in	2.75	1.50
Wheel weight (W_W), lb	0.99	0.23
Radius vector component (R_{W_2}), in	-0.45	0.20

TABLE B-3. Sample Tire Test Data for Rear Tire While β is 5°.

W_p (lb)	SBR (lb)	DGR* (in)	F_ℓ (lb)	F_c (lb)	F_n (lb)
0.00	-0.125	0.295	0.87	-0.051	0.28
0.63	-0.150	0.282	1.54	-0.061	0.73
1.20	-0.200	0.275	1.90	-0.082	1.16
2.40	-0.225	0.254	2.97	-0.092	2.09
3.60	-0.225	0.235	3.95	-0.092	3.07
4.80	-0.250	0.219	4.77	-0.102	4.07
5.90	-0.200	0.209	5.28	-0.082	5.12
7.40	-0.225	0.195	6.00	-0.092	6.44

*The initial dial gage reading (DGR_0) was 0.312 in.

and front tires at various steer angles. Selected sets of these data are plotted in Figures 4-9 and 4-10 while the parameters for least squares linear equations for these data are tabulated in Table 4-4.

B-2. Radial Damping Force

The scale-model tractor tire radial damping was determined using the assumption that the tire was a lumped mass with a parallel combination of a linear spring and a linearly-viscous dashpot transmitting forces between it and other bodies. The tire rested against a surface having a sinusoidal oscillation, thus being excited by a sinusoidal base motion. Thomson (1965, pp. 61-62) shows that if the base motion is

$$y = Y \sin \omega t \tag{B-10}$$

TABLE B-4. Lateral and Normal Tire Forces Measured for Slip Angles From 5 to 30 Degrees.

Slip angle	Front tire F_ℓ	Front tire F_n	Rear tire F_ℓ	Rear tire F_n
5°	0.4100	0.3270	0.8711	0.2794
	0.8711	0.8011	1.5373	0.7282
	1.3323	1.8701	1.8960	1.1627
	1.7423	2.9178	2.9721	2.0912
	2.0497	4.0185	3.9458	3.0742
	2.2547	5.0404	4.7657	4.0669
	2.5622	6.4083	5.2781	5.1182
	-	-	5.9955	6.4425
10°	0.5124	0.0266	1.3836	0.2404
	0.7687	0.4566	1.8960	0.5468
	1.5886	1.2860	2.9721	1.2543
	2.2547	2.1781	4.0483	1.9066
	2.8606	3.0918	5.0219	2.6679
	3.3308	3.9368	5.9443	3.3527
	4.0483	5.1420	7.2766	4.1952
15°	0.1025	0.0282	1.0249	0.0045
	0.6149	0.2550	1.5373	0.1902
	1.4861	0.8597	2.4597	0.7583
	2.3060	1.5275	3.821	1.2715
	3.0234	2.2575	4.2532	1.8529
	3.6895	2.9207	5.1756	2.3214
	4.5607	3.8607	6.2517	3.0696
20°	0.3075	0.2101	2.0497	0.3880
	1.1274	0.6880	2.9209	0.7645
	1.8960	1.2375	3.6895	1.2450
	2.6134	1.8287	4.4070	1.6718
	3.3308	2.2933	5.3293	2.3506
	4.2532	2.9946	-	-

TABLE B-4 (continued)

Slip angle	Front tire F_ℓ	Front tire F_n	Rear tire F_ℓ	Rear tire F_n
25°	0.2050	0.0915	1.6398	0.2563
	0.7174	0.4355	2.8184	0.4935
	1.6910	0.9244	3.1259	0.9271
	2.3060	1.4804	3.6895	1.3815
	3.0234	1.8422	4.6632	1.7564
	3.9458	2.4019	-	-
30°	0.4100	0.1981	2.1522	0.2098
	0.7174	0.4355	2.8184	0.4935
	1.3836	0.8503	3.2796	0.9775
	2.0497	1.2123	4.0995	1.3887
	2.6134	1.6486	-	-
	3.4846	2.0756	-	-

then the excited body, i.e., the tire motion will be given by

$$x = X \sin (\omega t - \phi) \tag{B-11}$$

where

- y is the base displacement, in,
- Y is the magnitude of the base displacement, in,
- t is the time at which y is defined, sec,
- ω is the circular frequency of oscillation, rad/sec,
- x is the tire displacement with time, in,
- X is the magnitude of the tire displacement, in, and
- ϕ is the phase angle by which the base motion leads the tire motion, rad.

The phase angle, ϕ, also is given by Thomson as

$$\phi = \arctan\left[\frac{2\zeta(\omega/\omega_n)^3}{1-(\omega/\omega_n)^2+(2\zeta\omega/\omega_n)^2} \right] \tag{B-12}$$

and the magnitude ratio, X/Y, as

$$\left| \frac{X}{Y} \right| = \sqrt{\frac{1+(2\zeta\omega/\omega_n)^2}{1-(\omega/\omega_n)^2+(2\zeta\omega/\omega_n)^2}} \tag{B-13}$$

where

ζ is the damping factor defined by

$$\zeta = \frac{C_d}{2m_W\omega_n} \tag{B-14}$$

m_W is the mass of the wheel, tire, etc. being oscillated, lb-sec^2/in,

ω_n is the natural frequency of free vibration for the tire, rad/sec, and

C_d is the tire damping coefficient.

The accelerations of the oscillating surface and of the tire can be obtained by differentiating twice with respect to time equations B-10 and B-11, respectively, yielding

$$\ddot{y} = - \omega^2 Y \sin \omega t \tag{B-15}$$

and

$$\ddot{x} = - \omega^2 X \sin (\omega t - \phi) \tag{B-16}$$

where

$\ddot{y}$ is the acceleration of the base, in/sec^2, and

$\ddot{x}$ is the acceleration of the tire, in/sec^2.

Because the phase angle ϕ is the same for the accelerations as it is for the displacements, the relationship between the phase angle, ϕ, the damping factor, ζ, and the frequency ratio, ω/ω_n, given in equation B-12 may be used to determine the damping ratio from the accelerations. Thus the accelerations of the base and tire, when monitored by two accelerometers and displayed simultaneously on an oscilloscope screen, yield a phase angle between these two periodic functions which then can be used to determine the tire damping factor, ζ.

The physical arrangement used in measuring the tire radial damping is shown in Figure 4-12. A closer view of the weighted tire resting on the exciting surface is given in Figure B-3. The

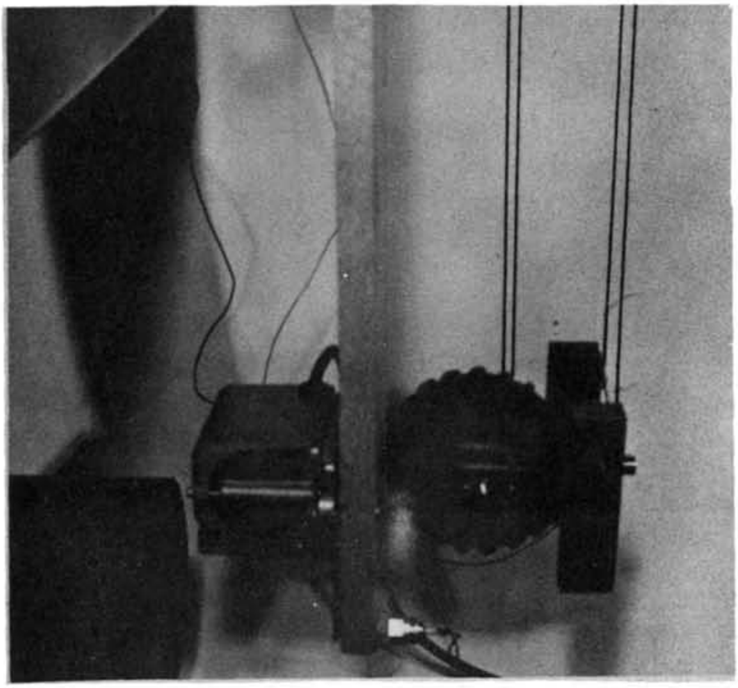

Figure B-3. Close-up View of the Tire Resting Against the Oscillation Platform.

base oscillation was generated by an electromagnetic shaker bolted to an oak board hinged at the top. The shaker vibration induced vibration of the same frequency (120 cycles/sec) to the board thus providing the periodic base oscillation. The accelerometer fastened to the board provided a signal proportional to the base acceleration.

The model tractor tire was clamped to a yoke, suspended by cords to provide free movement normal to the base, and sometimes weighted to change the natural frequency of the tire-on-board system. A second accelerometer, bolted to the yoke provided a signal proportional to the tire acceleration.

The acceleration signal from each accelerometer was amplified and provided as a channel input to a dual-trace storage oscilloscope. As the tire rested against the oscillating board, the two acceleration signals were displayed simultaneously on the oscilloscope and the traces were photographed with an oscilloscope camera. Figure B-4 shows an oscilloscope record from which the phase angle was measured. The equipment used in measuring the tire damping is listed in Table B-5.

Measurement of the front and rear tire damping was performed for two different cases - with the tire clamped in the yoke without additional weight, and with extra weight bolted to the yoke-tire system. In either case the natural frequency of the tire system against the board was required.

The natural frequency was determined by clamping the board in place by fastening it to a massive steel cylinder (shown in Figure B-3) and setting the tire system into transient free oscillation against the board. By releasing the tire while very near the board

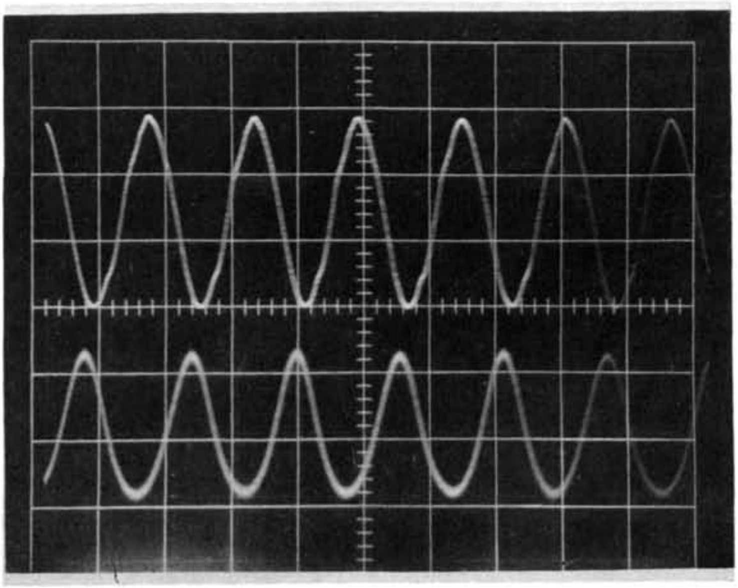

Figure B-4. Sample Oscilloscope Record for Measurement of Phase Angle for Determination of Tire Damping.

TABLE B-5. Equipment Used in Measuring Tire Radial Damping.

Shaker

- Syntron electric controller, model VC-4AC
- Syntron electric vibrator, model V4-AC
  - Syntron Company, Homer City, Pa.

Base accelerometer

- Columbia accelerometer
- Columbia amplifier, model 6000

Tire accelerometer

- Columbia accelerometer, Model 302-6
- Columbia charge amplified, model 4102
  - Columbia Research Laboratories, Inc., Woodlyn, Pa.

Oscilloscope

- Tektronix storage oscilloscope
  - Type 3A3 dual-trace differential amplifier
  - Type 3B3 time base
  - C-12 oscilloscope camera
    - Tektronix, Inc., Portland Oregon

and allowing it to swing into the board, the tire oscillation decayed until it provided an acceleration output such as shown in Figure B-5. The frequency of tire oscillation obtained from the acceleration decay curve provided the natural frequency of that system.

The natural frequencies and phase angles were measured for the weighted and un-weighted cases for both front and rear tires. The results of these tests are summarized in Table B-6.

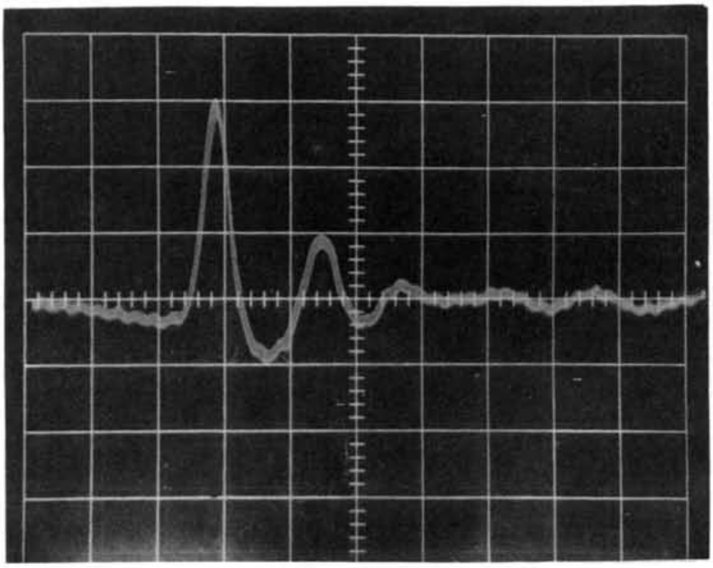

Figure B-5. Oscilloscope Record of Tire Free Vibration for Determination of Tire Natural Frequency of Vibration.

TABLE B-6. Summary of Data for Scale-Model Tire Radial Damping Tests.

	Total weight (lb)	Natural frequency ω_n (rad/sec)	Frequency* ratio ω/ω_n	Phase angle ϕ (degrees)	Damping ratio ζ
Rear tires					
Case A	7.11	209	3.66	154	0.07
Case B	2.09	449	1.71	154	0.10
Front tires					
Case A	6.34	126	6.10	149	0.05
Case B	1.33	192	3.99	149	0.07

*The base excitation frequency, ω, was 766 rad/sec.

APPENDIX C

THE DIGITAL COMPUTER PROGRAM

Appendix C presents the digital computer program used to simulate wheel tractor overturns. Section C.1 provides narrative and diagrammatic description, Section C.2 provides a complete listing of the program, Section C.3 provides a description of the use of the program and the necessary data, and Section C.4 provides some sample output obtained from an overturn simulation.

C.1. Program Description

Section C.1 presents a description of the digital computer program used to simulate tractor overturns by the theory developed in this dissertation. Each program, subroutine, and function is described in detail determined by its complexity. The most complex or lengthy program parts also are shown diagrammatically with flow charts to explain the relationships between the major steps of the program.

C.1.1. The MAIN program

The MAIN program acts as the interfacing element between the program user and the bulk of the simulation program. It contains all the data reading capabilities of the entire program so it provides the only control over the conditions of the simulation. The data is passed to the appropriate subroutines by block COMMON statements found in those routines between which the data is passed.

The MAIN program coordinates the establishment of initial conditions and the integration of the differential equations of motion by first calling subroutine SETUP to define the needed initial conditions, and then calling subroutine DHPCG to integrate between the desired time limits. Other necessary steps such as derivative evaluation and output generation are controlled by DHPCG within the ranges specified by the input data.

A flow chart showing the major steps of the MAIN program is given in Figure C-1.

C.1.2. Subroutine SETUP

A person can describe the state of a tractor most easily when the positions, velocities, and orientations are specified in tractor-axes directions. Because the differential equations are not written for the coordinate directions most easily interpreted by a person, subroutine SETUP is used to convert input specifications of the tractor-state to the form required for the initial conditions of the differential equations.

Subroutine SETUP calls subroutine EIGVAL to define the eigenvalues of the tractor-axes inertia matrix thus defining the principal moments of inertia for the tractor body. It then calls subroutine VECT33 to define the eigenvectors of the inertia matrix. The principal-axes unit vector directions are defined in terms of the tractor-axes directions by the transpose of the eigenvector matrix.

The initial conditions for the differential equations are calculated using a procedure specified by input parameter INIT. This parameter specifies whether the clutch is engaged or disengaged and whether the input data is to be used in calculating the initial

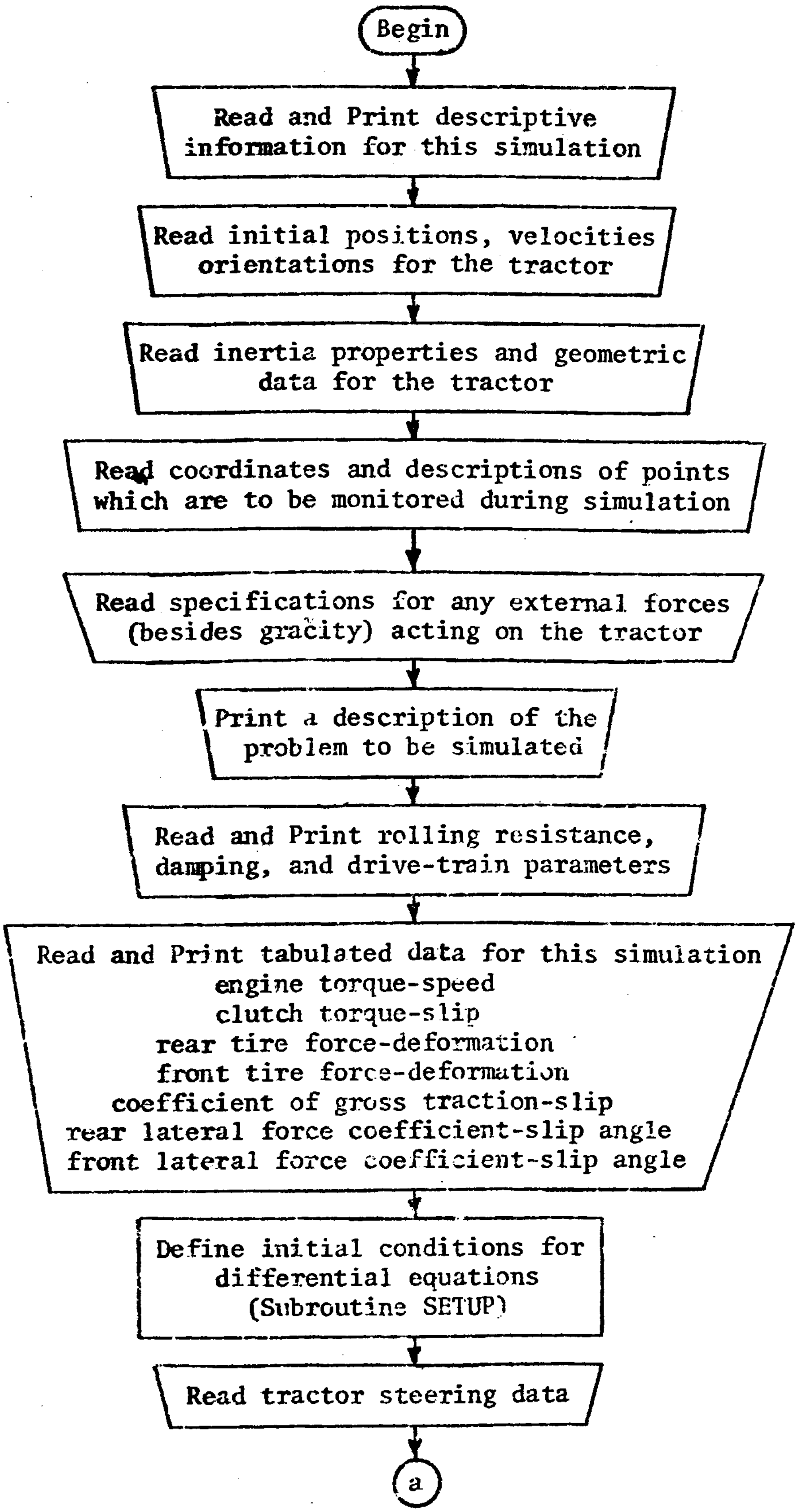

Figure C-1. Flow Chart for MAIN Program.

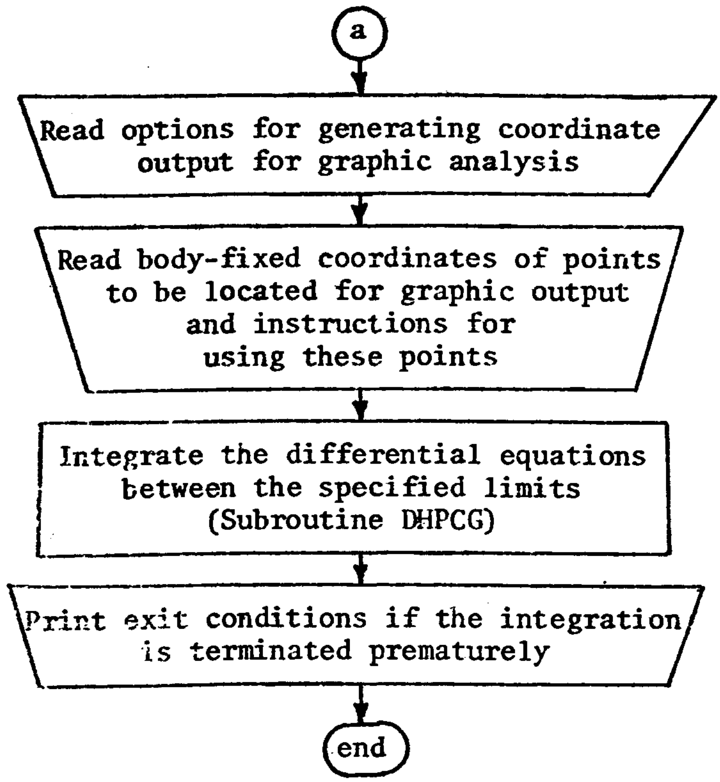

Figure C-1 (continued).

conditions or the initial conditions should be calculated for the tractor operating in a level surface of zero elevation. When the tractor is on the zero elevation surface (i.e., when INIT = 2 or INIT = 3), all the tractor positions and velocities are defined by the state of equilibrium between the tire and ground reaction (and the drive-train and engine reactions when INIT = 3).

The translational positions and velocities are converted to inertial-coordinate directions for the initial condition specification. The tractor-body angular velocities are transformed into principal-axes directions while the rear wheel and front-end angular velocities and positions are specified as scalar quantities. The engine speed is that specified by input data unless INIT = 3 when the speed is redefined as the equilibrium engine speed. The tractor body orientation is determined by calling subroutine EULPAR which defines the four Euler parameters from the principal-axes orientations in the inertial reference frame.

The major program steps and program logic of subroutine SETUP are shown in Figure C-2.

C.1.3. Subroutine DHPCG

Integration of the differential equations to generate a simulation of the tractor motion is performed by subroutine DHPCG. This subroutine, provided as part of the IBM System/360 Scientific Subroutine Package - Version 3, uses the Hamming predictor-corrector method of integration with a fourth-order Runge-Kutta method to generate starting values. The program provides error-checking features

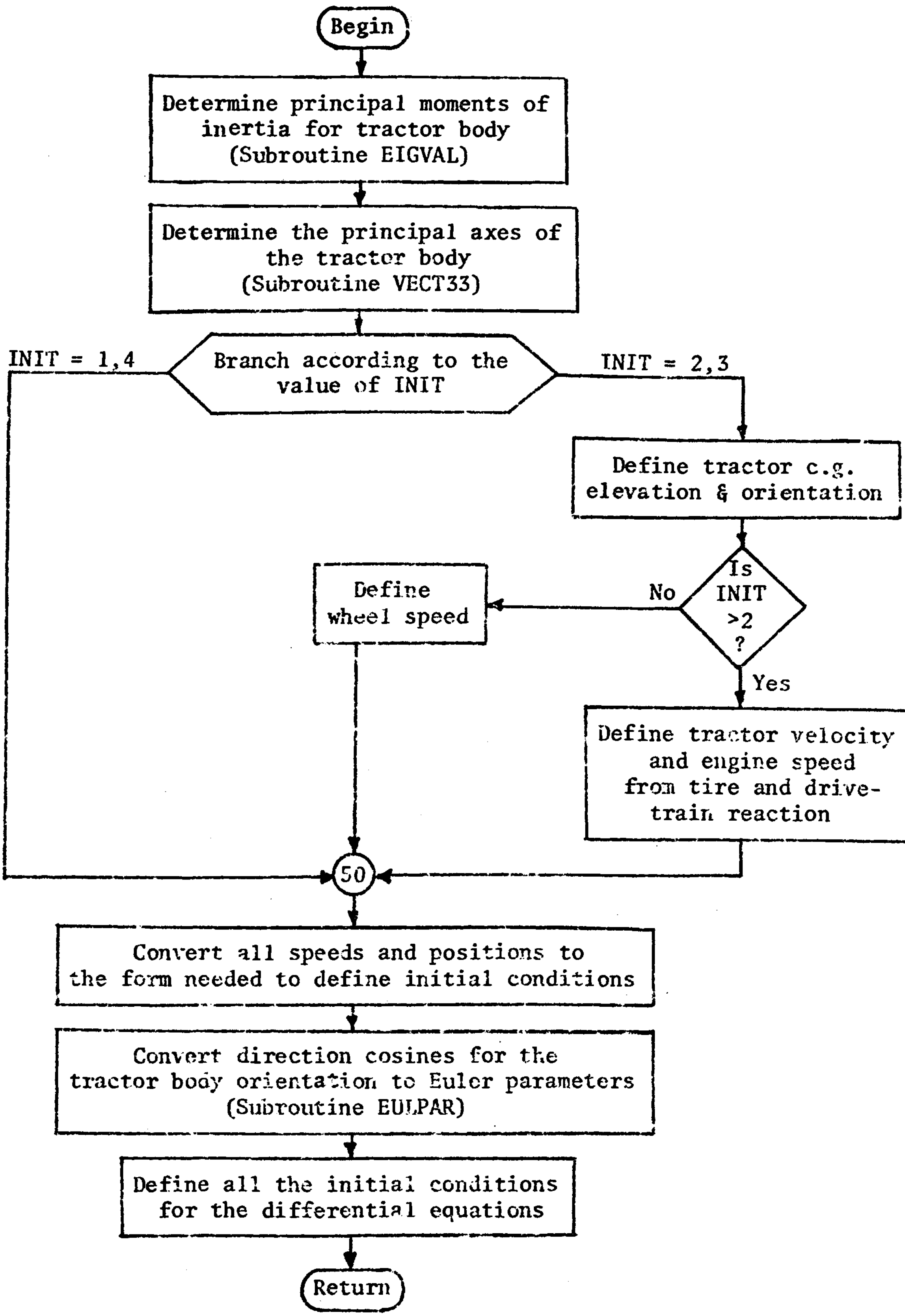

Figure C-2. Flow Chart for Subroutine SETUP.

which can halve or double the integration step size to maintain the specified integration accuracy.

This program has been modified by J.R. Cooke, Department of Agricultural Engineering, Cornell University, to assure that output cycles are provided at specified equally-spaced time intervals even when the time step size has been altered by the program.

Subroutine DHPCG obtains derivative evaluations at particular simulation times by calling subroutine FCT, which in this program is subroutine DERIV. As the simulation reaches one of the equally-spaced time intervals at which output may be desired, subroutine DHPCG calls subroutine OUTPUT to generate printed and/or, punched output. The simulation continues until the specified time interval has been completed or until n excessive number of interval bisections was required to obtain the desired integration accuracy.

The major steps and program logic of subroutine DHPCG are shown in the flow chart of Figure C-3.

C.1.4. Subroutine OUTPUT

Subroutine OUTPUT controls the output of information generated by the simulation proper. (Only peripheral output information is provided by the MAIN program.) Whenever this subroutine is called, the parameter ICOUNT is checked to identify the equally-spaced time intervals which are integer multiples of the specified maximum-allowable integration time step. Output may occur only at these points in time; between these times simulation continues without any output being generated.

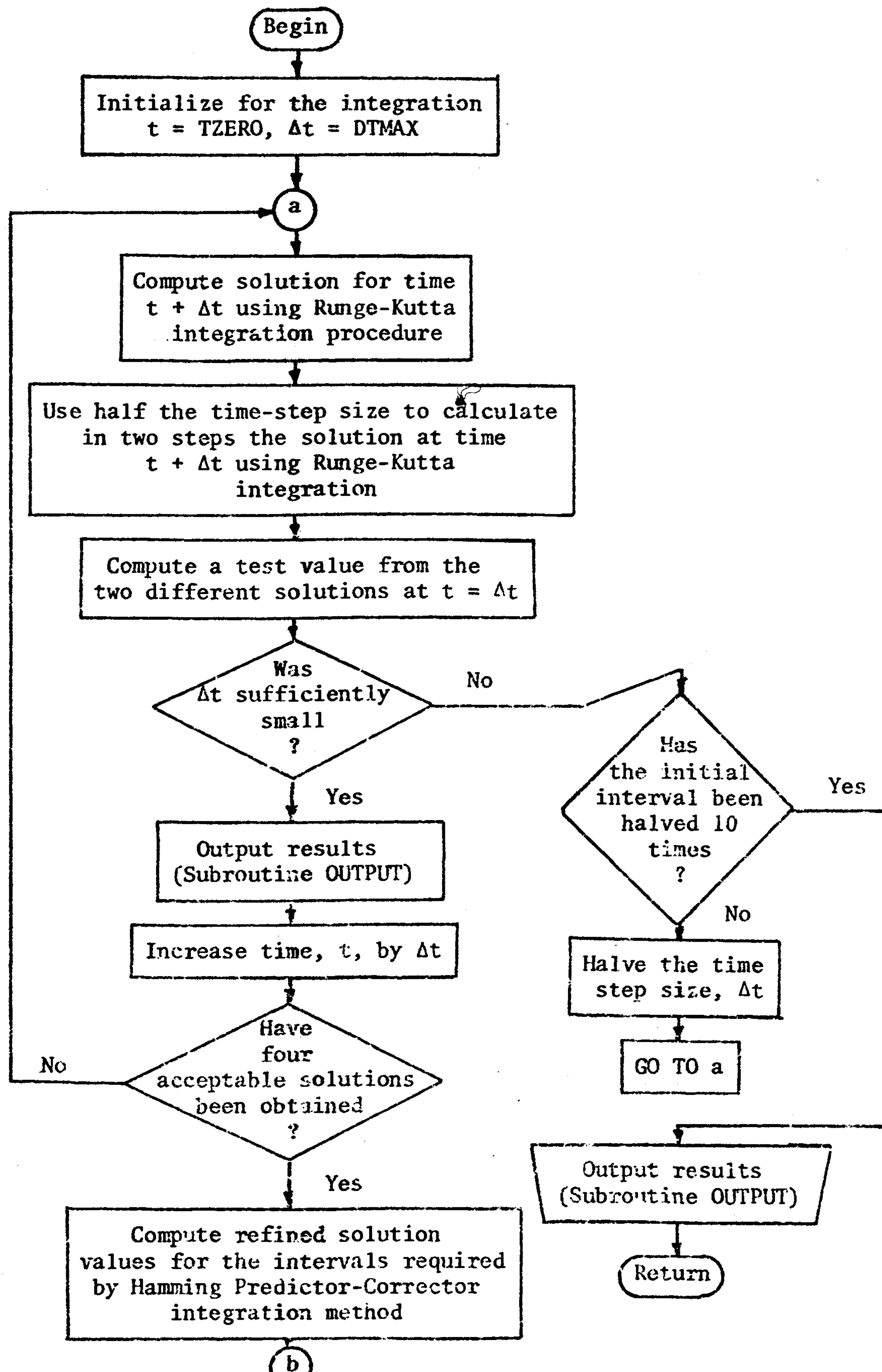

Figure C-3. Flow Chart for Subroutine DHPCG.

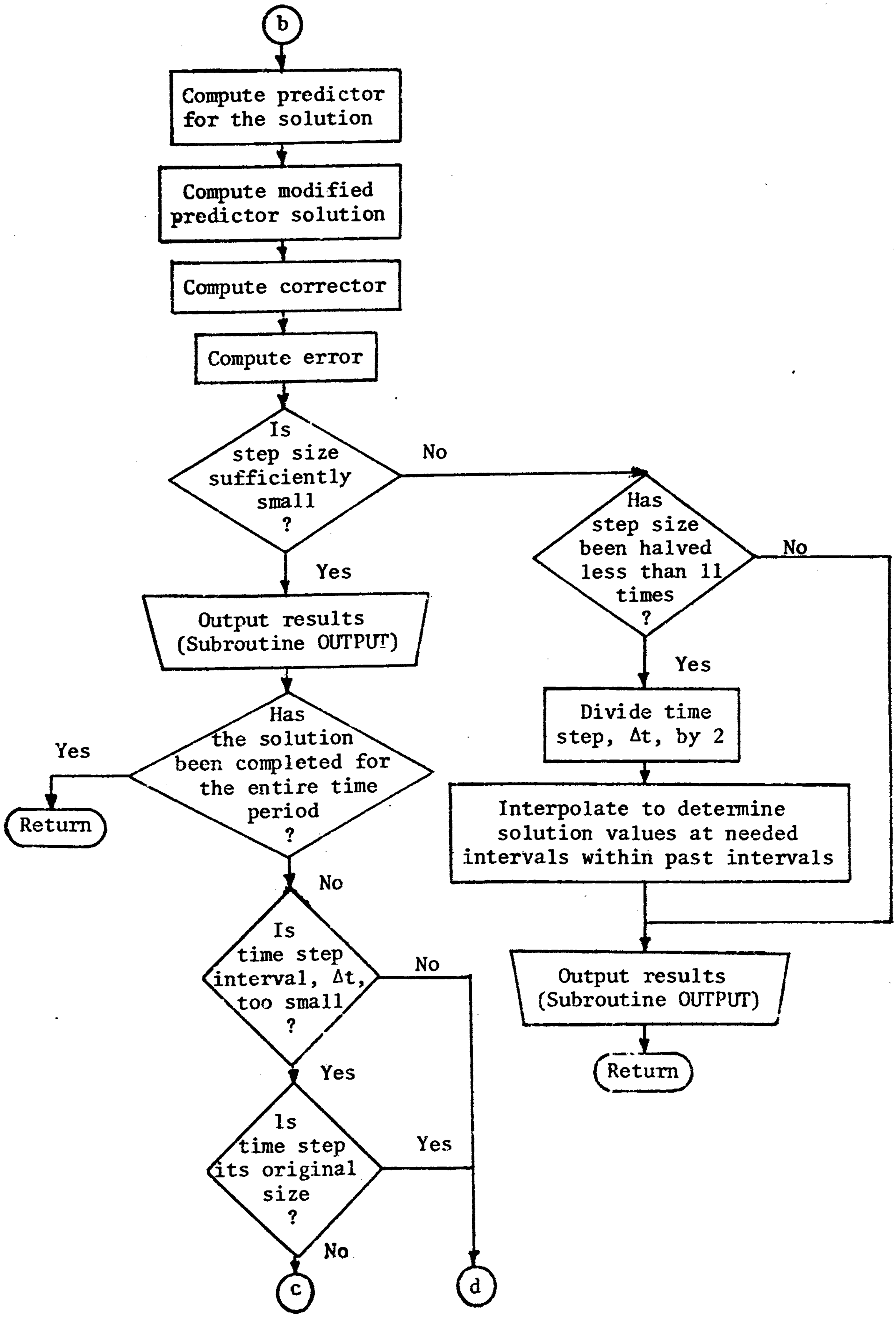

Figure C-3 (continued).

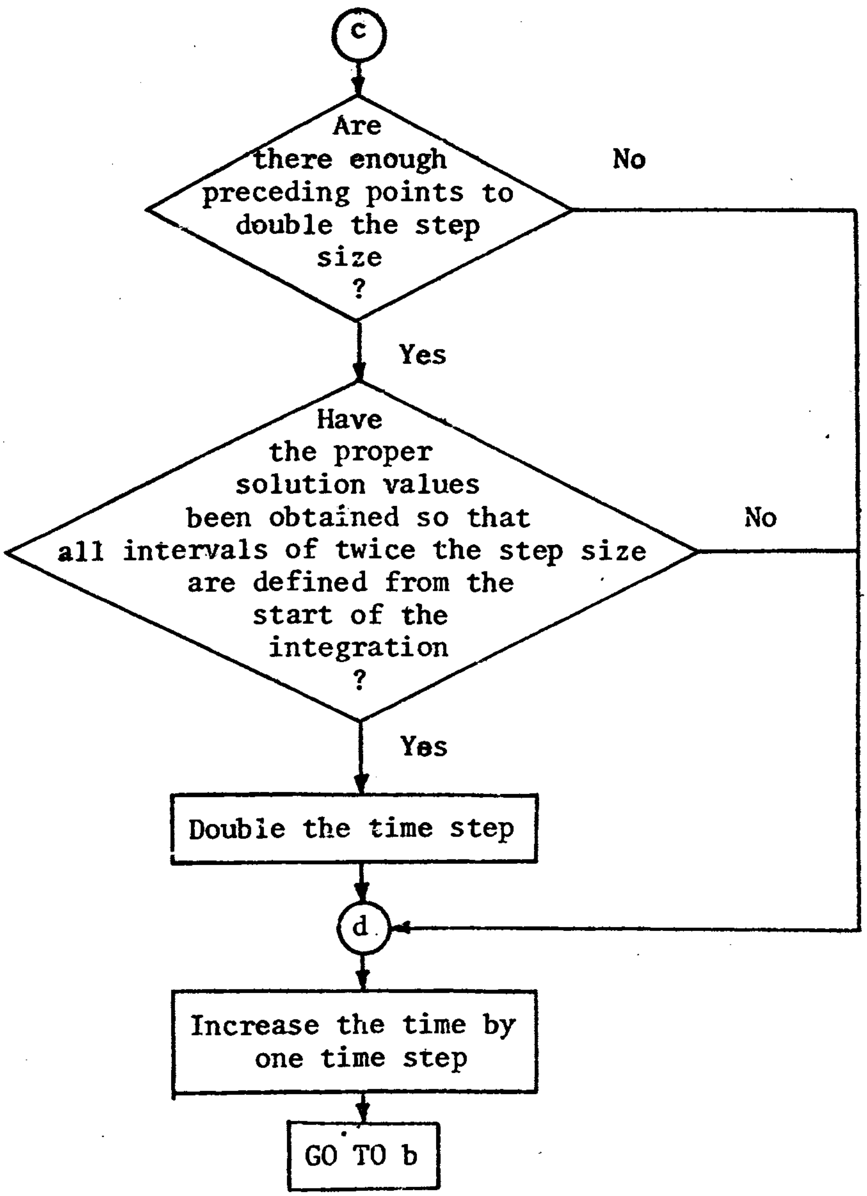

Figure C-3 (Continued).

Two parameters, NPRINT and NPUNCH, control the frequency of printed and punched output relative to the maximum-allowable time step interval. Punched data is generated to provide coordinates of tractor points at various times whenever graphical analysis of the tractor motion is desired.

The parameter IPLOT requests or suppresses printed and punched output for graphical analysis. Whenever graphical punchout is requested the four wheel peripheries are defined by coordinates of the points at 20-degree intervals as are points defining the terrain features. All other points to be located are specified by input data.

Subroutine OUTPUT also has capabilities for monitoring the simulation at each of the evenly-spaced times when printout could occur and terminating the simulation prior to the preplanned completion time if desired. Termination occurs when a nonzero value of PRMT(5) is returned to the integration subroutine DHPCG. This features is used in the tractor overturn simulations to terminate the program whenever any of certain points on the tractor (defined by input data) strikes the ground.

At each printout cycle all position and velocity information describing the state of the tractor is printed in a form similar to that originally supplied as input data. The translational velocities and positions of the tractor body center of mass are given in the inertial-coordinates directions. The body angular orientation is given as direction cosines of the tractor axes while the tractor body angular velocities are given in tractor-axes directions. The states of the rear wheels, front end, and engine are specified as scalar quantities. The positions and velocities of the points being monitored for program termination are printed together with a 20-character description of each point.

At each printout cycle the integration step size is indicated by printing the number of interval halvings for this step. The tire forces are printed, as is the steering angle at each print time. Whenever the front end has rotated to its limit, a message is printed to indicate this condition. Also, to provide information about the tractor overturn energies, the momenta vectors, the potential energy, the kinetic energy, and the total energy of the tractor body, front end, and rear wheels are printed during each print cycle.

A flow chart to show the major functions of subroutine OUTPUT is presented in Figure C-4.

C.1.5. Subroutine DERIV

The derivatives of the twenty state variables describing the tractor motion are defined in subroutine DERIV. Thus, this subroutine incorporates the many dynamic relationships defined in sections of Chapter III into twenty simultaneous first-order differential equations. These derivatives are evaluated at appropriate points in time (as specified by subroutine DHPCG) so they may be integrated to obtain the velocities and positions of the tractor as it encounters the prescribed terrain.

Both ground forces at the wheels and external forces or moments on the tractor body, the rear wheels, or the front end may provide variable input reactions to the tractor. The ground forces are determined by subroutine WHEEL as it evaluates the individual tire-ground interactions due to the position and velocity of each tire

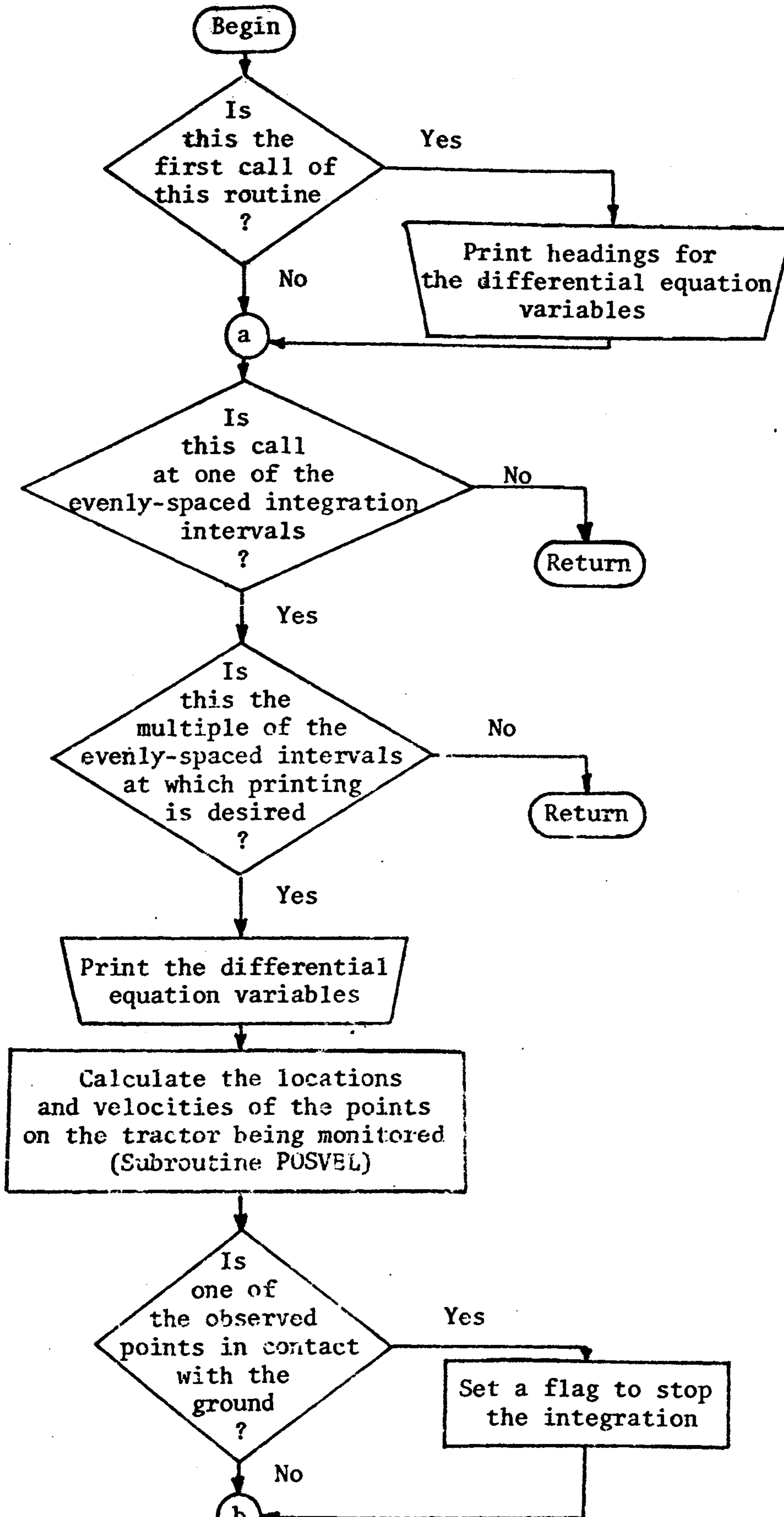

Figure C-4. Flow Chart for Subroutine OUTPUT.

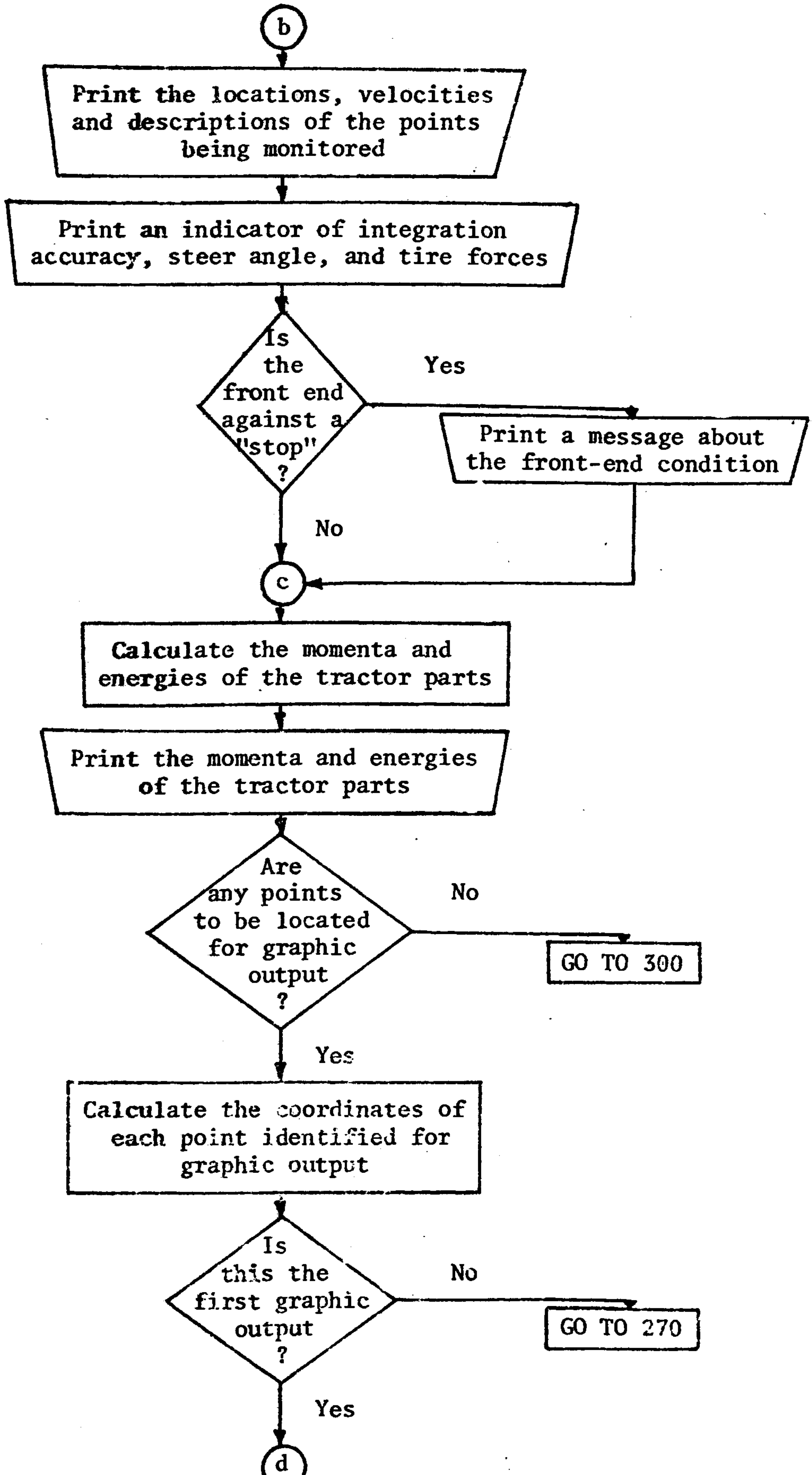

Figure C-4 (continued).

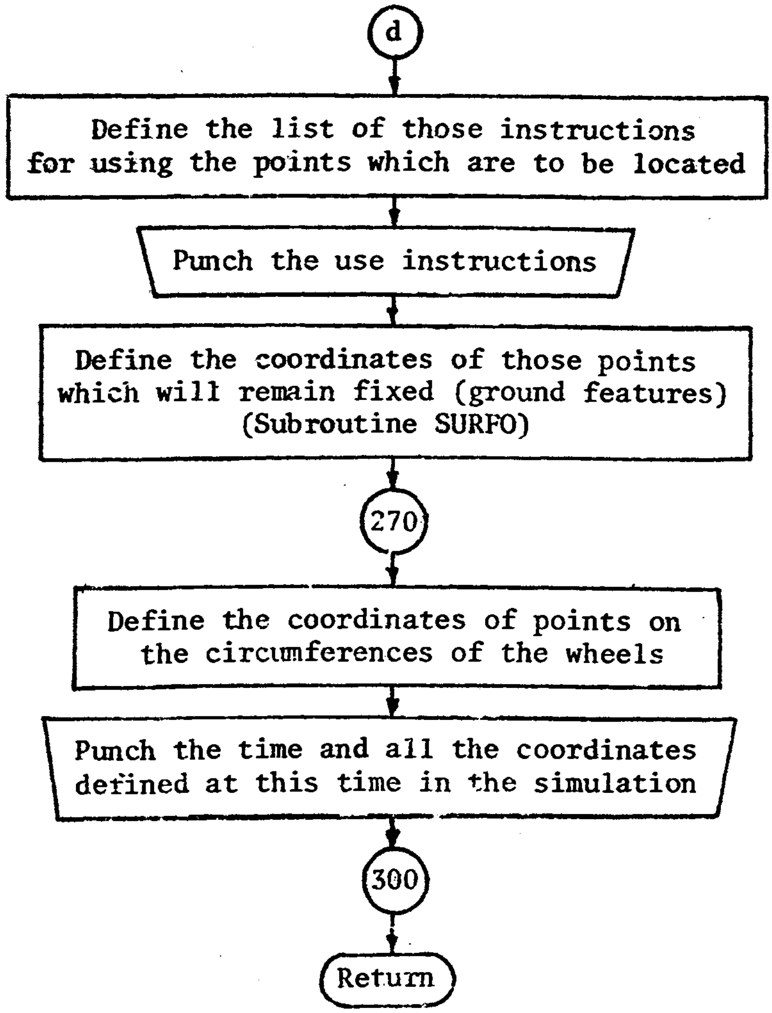

Figure C-4 (continued).

relative to the ground surface. External forces and moments are specified as input data and evaluated at any time by subroutine FORTQ. Gravitational forces are automatically defined by the weights of the tractor parts, so are not considered to be external forces. When the front end is against a "stop", reactions at the stop are considered in a manner similar to external reactions.

The highest-order derivatives (the accelerations) are evaluated first while the lower-order derivatives (velocities) are assumed to remain constant during the time interval. This enables the velocity-dependent forces to be considered as constants so the accelerations may be obtained from the equations in Chapter III. The seven simultaneous equations relating the coupled accelerations are solved to yield these accelerations by the use of subroutine SOLVE.

Figure C-5 shows a flow chart for the major steps of subroutine DERIV.

C.1.6. Subroutine WHEEL

The forces acting on the tractor wheels and the moments resulting at the wheel centers are determined by subroutine WHEEL. When the location, orientation, and velocity of a wheel are provided to this subroutine, the tire-ground interaction is converted into a resultant force composed of radial, lateral, and circumferential force components. Each of the force components is defined by a separate empirical relationship obtained from measurements of the tire performance on the specific ground conditions desired for this simulation.

The tire-ground interaction is assumed to be a thin radially-deformable circular wheel on a locally-planar, rigid ground surface.

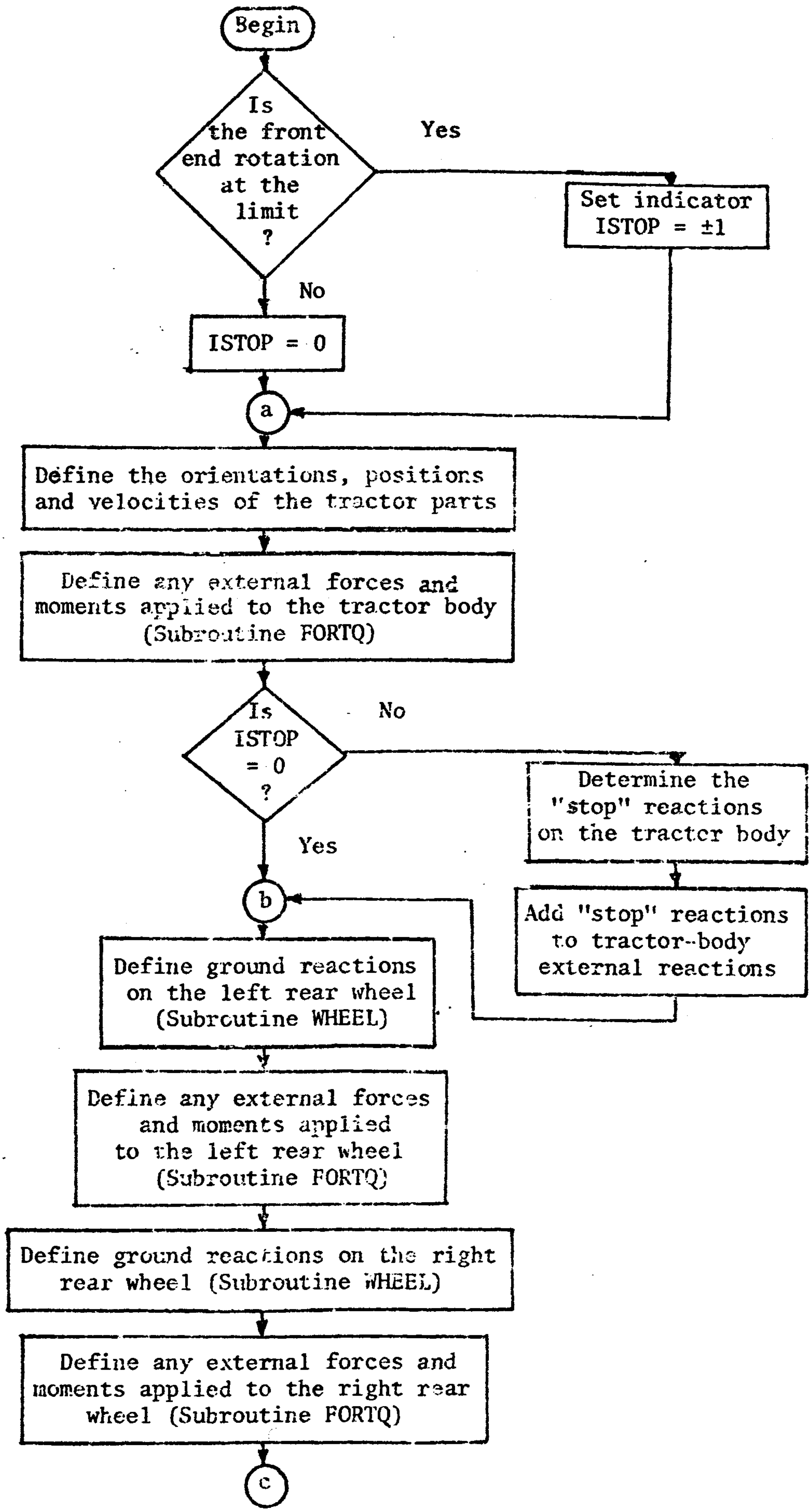

Figure C-5. Flow Chart for Subroutine DERIV.

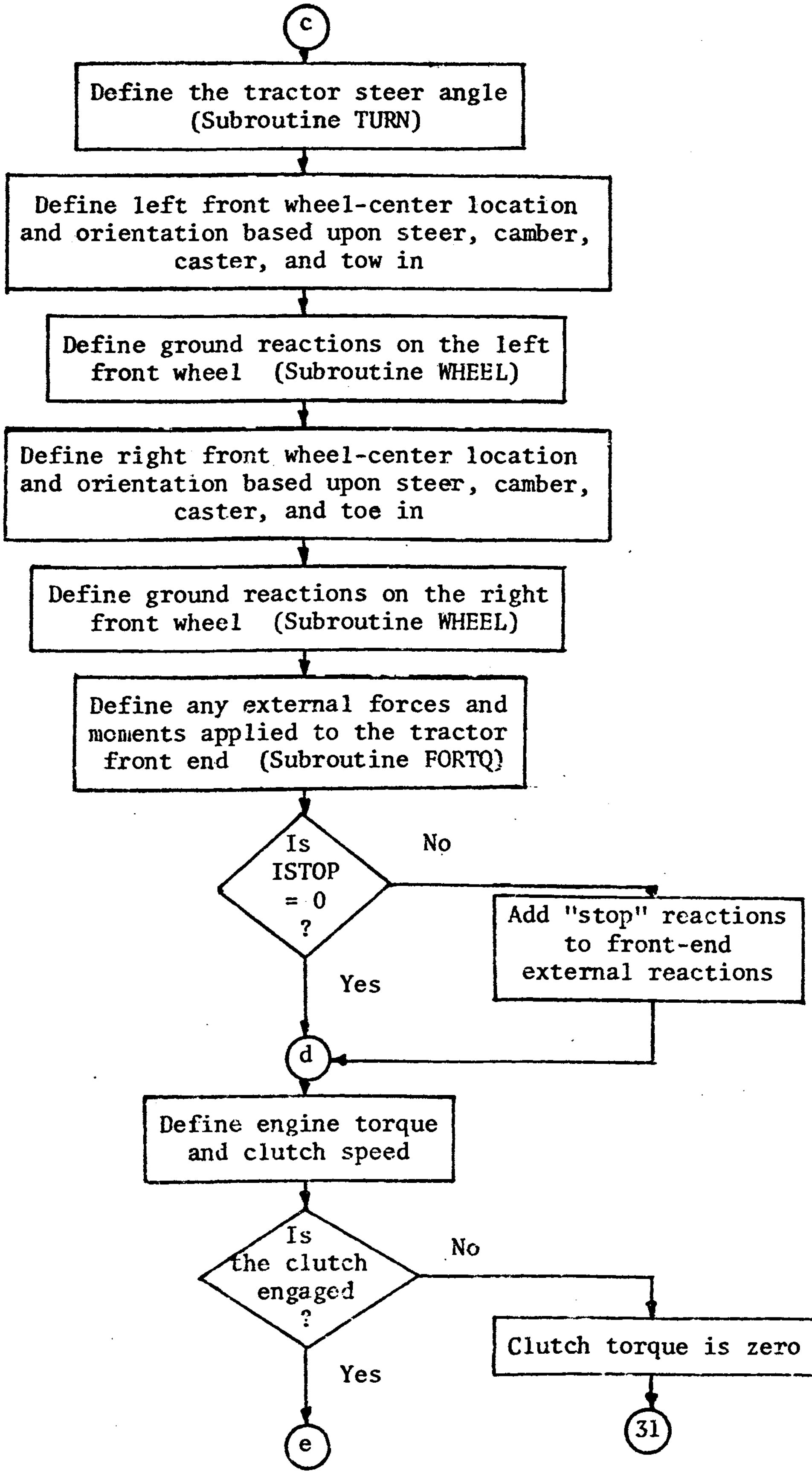

Figure C-5 (continued).

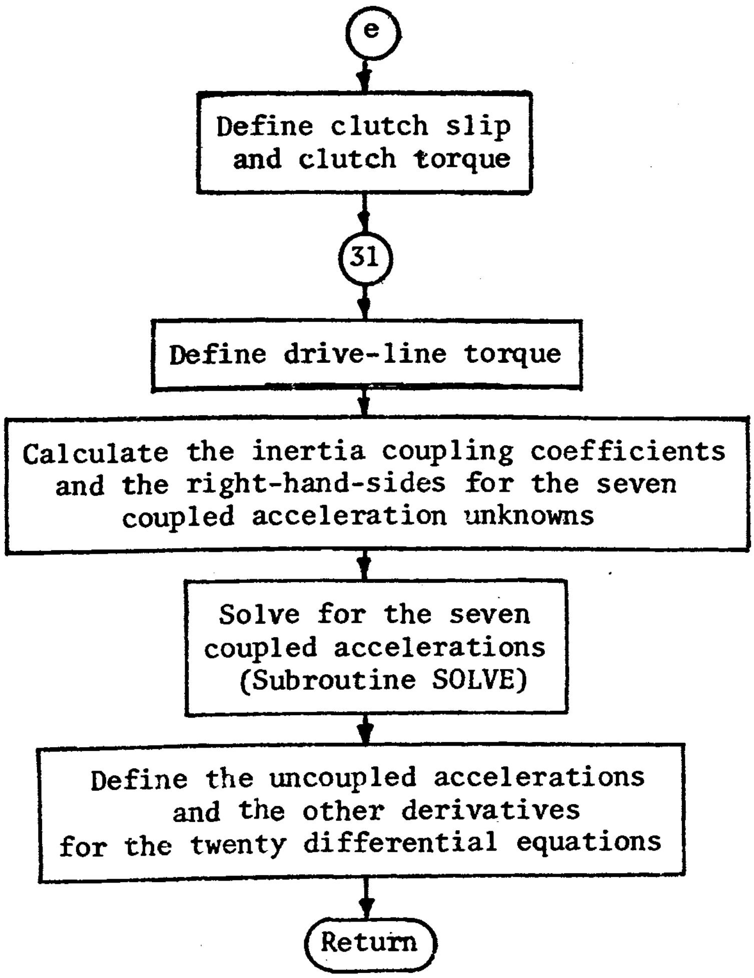

Figure C-5 (continued).

The forces on the tire are assumed to act through a "ground-contact point", thus making the tire model a point-contact model. The "ground-contact point" and the ground plane are defined in alternative ways depending upon the regularity of the ground surface. If the ground surface is "regular" or "smooth" beneath the tire, the plane tangent to the ground surface beneath the tire is used to determine the tire forces, otherwise an "equivalent" plane is defined to provide a smooth surface.

Subroutine WHEEL scans the ground surface beneath the tire by checking three points beneath the tire - one below, one 45 degrees ahead, and one 45 degrees behind the wheel center - to see if the ground surface may be represented by the same plane in these three regions. The same plane is suggested at the three points only when the ground normal vectors at these three points are parallel and the vectors connecting the three points are perpendicular to the ground normal vectors. The ground is "irregular" if these two conditions are not met. (The ground elevation and the ground normal vector are defined for any horizontal location by calling subroutine SURFAC.)

The "ground-contact point" for a smooth ground surface is defined as the point-of-intersection for three planes - the wheel plane, the ground plane, and the plane containing both the axle and the ground normal vector. This point is determined by solving the equations of the three planes for the common point. The radial tire deflection is defined as the distance between the wheel center and the "ground-contact point".

The "equivalent" ground plane for an irregular surface is defined to provide the proper radial force direction, radial force magnitude, lateral force direction, and circumferential force direction. The radial force direction is assigned by the direction of the resultant force vector obtained by summing incremental radial forces due to the deflections of 5-degree circumferential segments of the tire. The radial force magnitude is that force obtained from the tire-on-flat-surface force-deformation curve at the point where the displaced area of the thin tire on the flat surface equals the displaced area of the 5-degree segmented tire on the irregular surface. This then defines the radial deformation for the tire on the "equivalent" plane and the "ground-contact point". The plane orientation is defined by determining the ground normal vector for the original surface at the "ground-contact point" and rotating it about the axis of the axle until it is in the plane that is common to the axle and the radial force vector.

Once the "ground-contact point" and the ground normal vector have been defined, subroutine WHEEL is unaffected by the actual ground surface beneath the tire. The next differentiation occurs between traction (driven) wheels and towed wheels denoted, respectively, as rear and front wheels. For each type wheel, the radial force, a lateral force coefficient, the normal force, and the rolling resistance are evaluated from empirical relationships for the appropriate tire. The traction force and a friction ellipse modification of the lateral force coefficient are added to rear wheel forces. Then the resultant force vector is defined and the moment of this force about the axle is defined prior to returning these reactions to the DERIV subroutine.

The major program steps of subroutine WHEEL are shown diagrammatically in the flow chart of Figure C-6.

C.1.7. Subroutine FORTQ

Externally applied forces and moments on the tractor body, the rear wheels, or the front end are evaluated by subroutine FORTQ. The number and type of external reactions on each body are defined by data cards initially read into the MAIN program and transferred to this subroutine. Subroutine DERIV then calls subroutine FORTQ whenever these reactions need to be evaluated. Each external reaction is defined by a type specification (ITYPE), a body-fixed vector location of the point of application, and numerical values specifying the magnitudes of parameters used in calculating the magnitudes.

Seven different types of external reactions may be specified to be evaluated in subroutine FORTQ. They are:

1. A constant moment specified in body-axes directions (ITYPE = -2),
2. A constant moment specified in inertial directions (ITYPE = -1),
3. A constant force specified in inertial directions (ITYPE = 1),
4. A constant force specified in body-axes directions (ITYPE = 2),
5. A force which is a linear function of the position and velocity of the body-fixed point relative to a point fixed in space (ITYPE = 3),

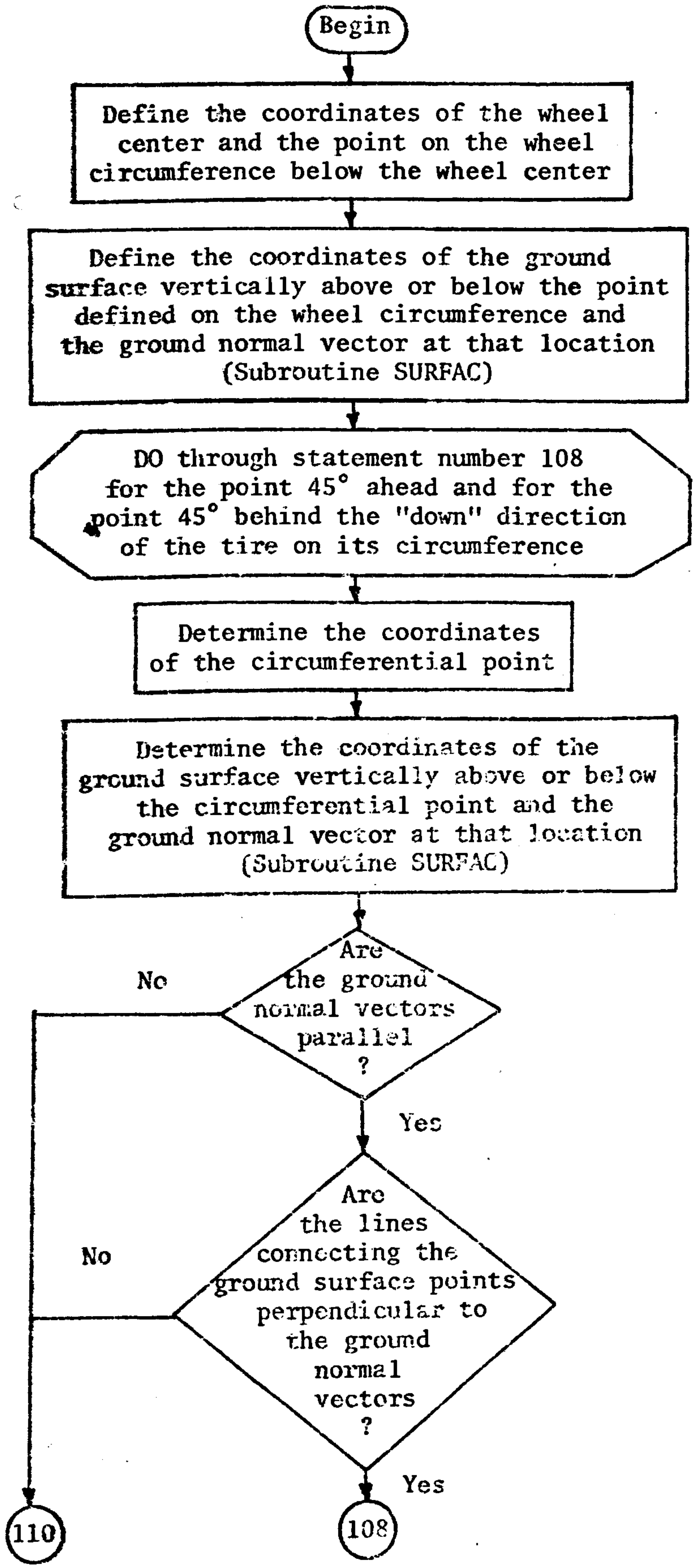

Figure C-6. Flow Chart for Subroutine WHEEL.

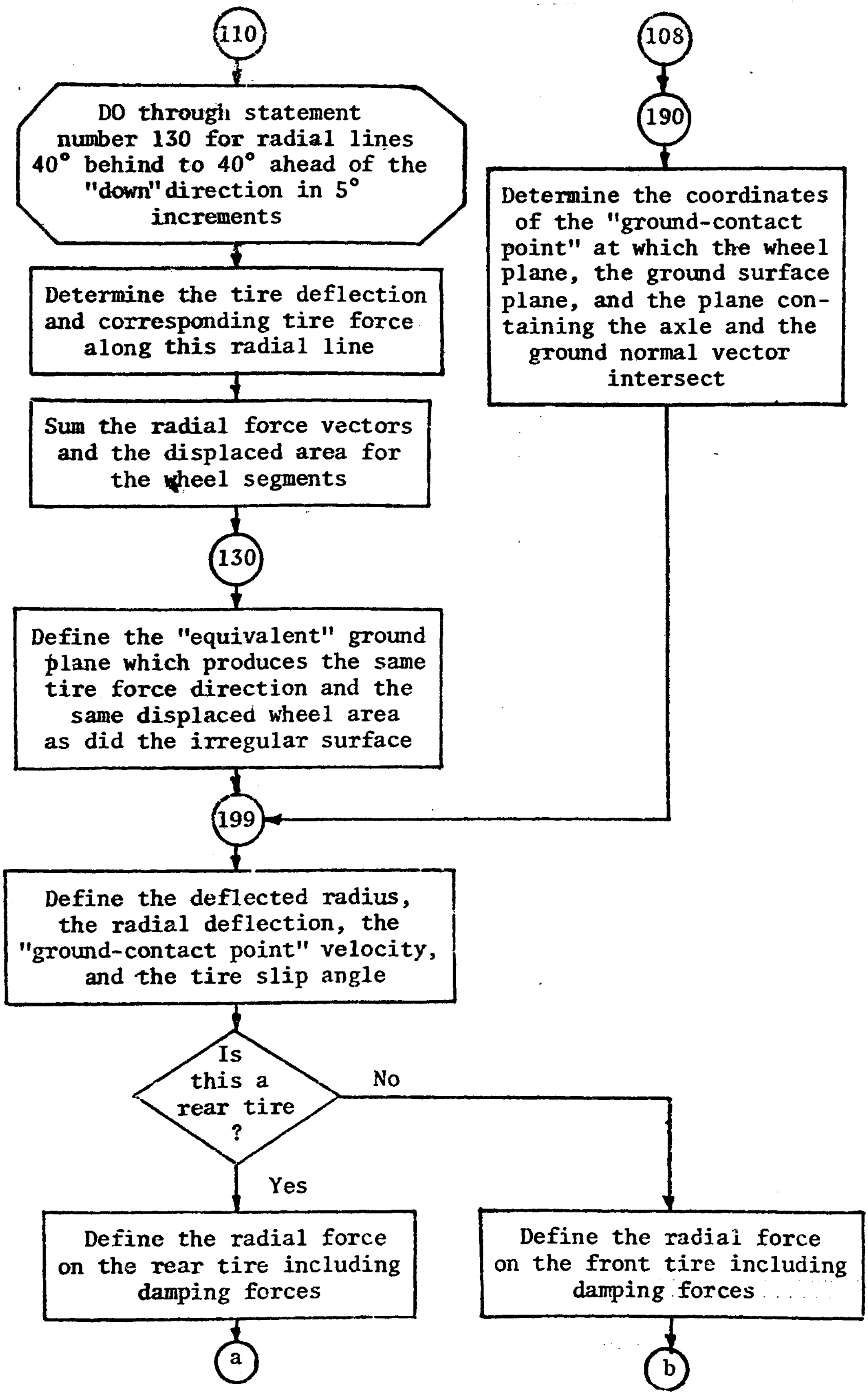

Figure C-6 (continued).

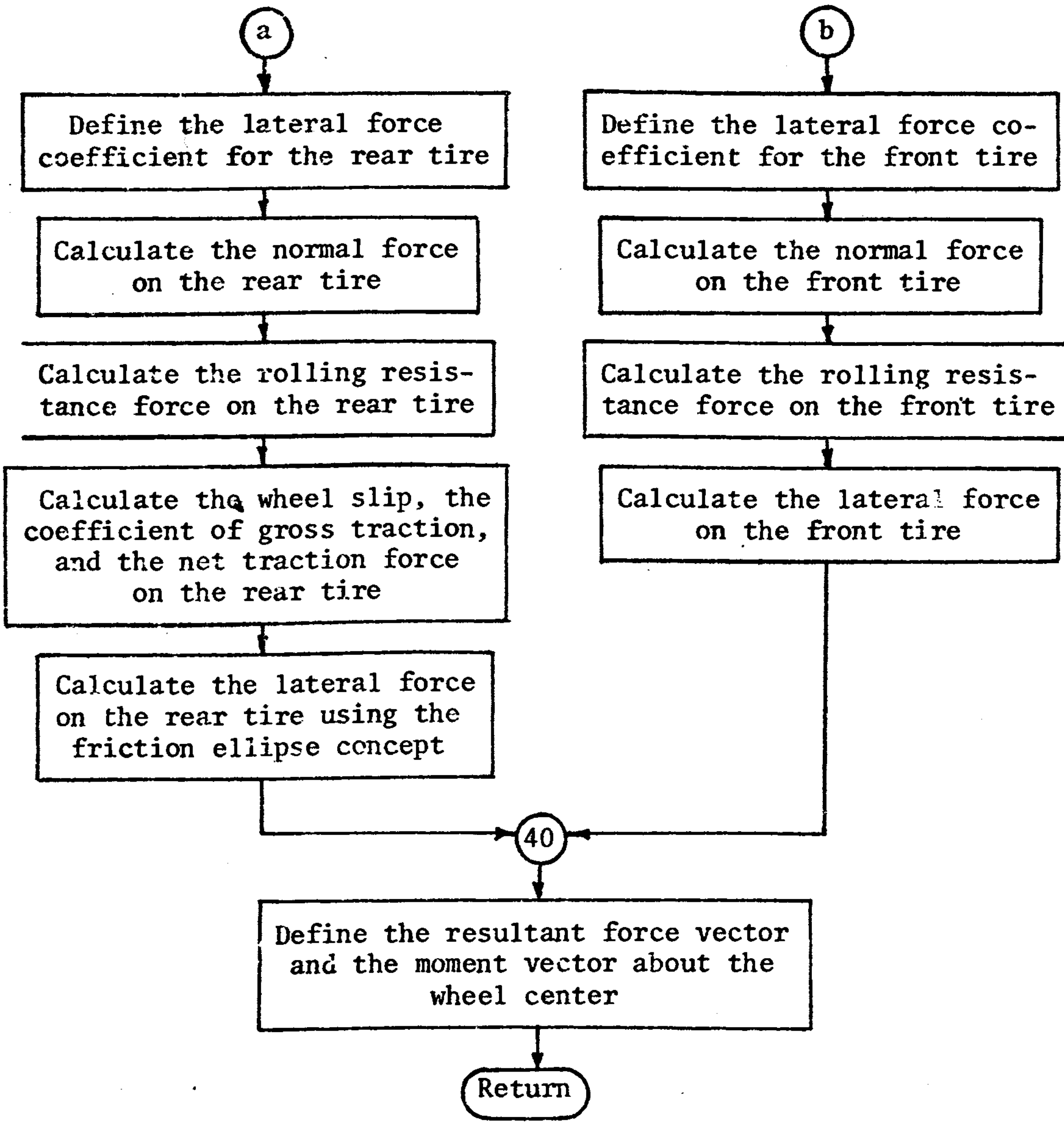
a
b
Define the lateral force coefficient for the rear tire
Define the lateral force coefficient for the front tire
Calculate the normal force on the rear tire
Calculate the normal force on the front tire
Calculate the rolling resistance force on the rear tire
Calculate the rolling resistance force on the front tire
Calculate the wheel slip, the coefficient of gross traction, and the net traction force on the rear tire
Calculate the lateral force on the front tire
Calculate the lateral force on the rear tire using the friction ellipse concept
40
Define the resultant force vector and the moment vector about the wheel center
Return

6. A force as in (5) except that the force is applied only when the two points are closer together than a prescribed distance (ITYPE = 4),

7. A force as in (5) except that the force is applied only when the two points are farther apart than a prescribed distance (ITYPE = 5).

The last three reaction types represent parallel spring and dash-pot connections between the body-fixed point and the inertial point, but case 6 functions only in compression and case 7 only in tension. The vector sums of all moments and forces acting on a body are returned to the calling program in inertial coordinates.

A flow chart showing the logical sequence of steps in subroutine FORTQ is given in Figure C-7.

C.1.8. <u>Subroutines EIGVAL, EIGP3, and VECT33</u>

Subroutines EIGVAL, EIGP3, and VECT33 are used to determine the eigenvalues and eigenvectors of the tractor-body inertia matrix, thus defining the principal moments of inertia and principal-axes directions for that body. Subroutine EIGVAL uses Muller's method of quadratic interpolation to find zeros of the characteristic polynomial for the inertia matrix. Subroutine EIGP3 evaluates the characteristic polynomial at the trial values used in the search for zeros of the polynomial. After one eigenvalue is determined, the deflated polynomial function is used in the search for other eigenvalues. (See Conte, 1965, pp. 65-69, 187-189, for a detailed description of Muller's method and a flow chart of the program steps.)

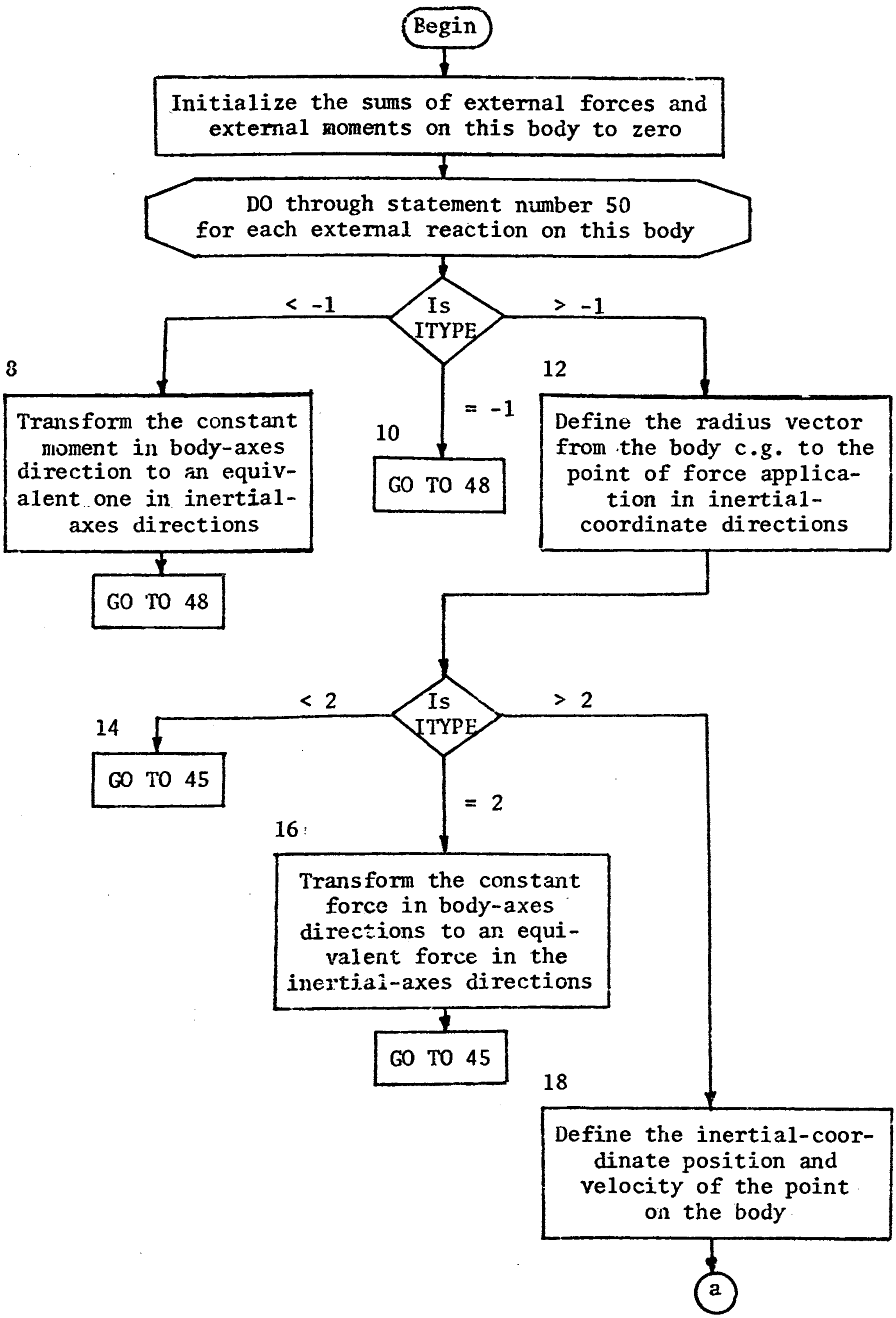

Figure C-7. Flow Chart for Subroutine FORTQ.

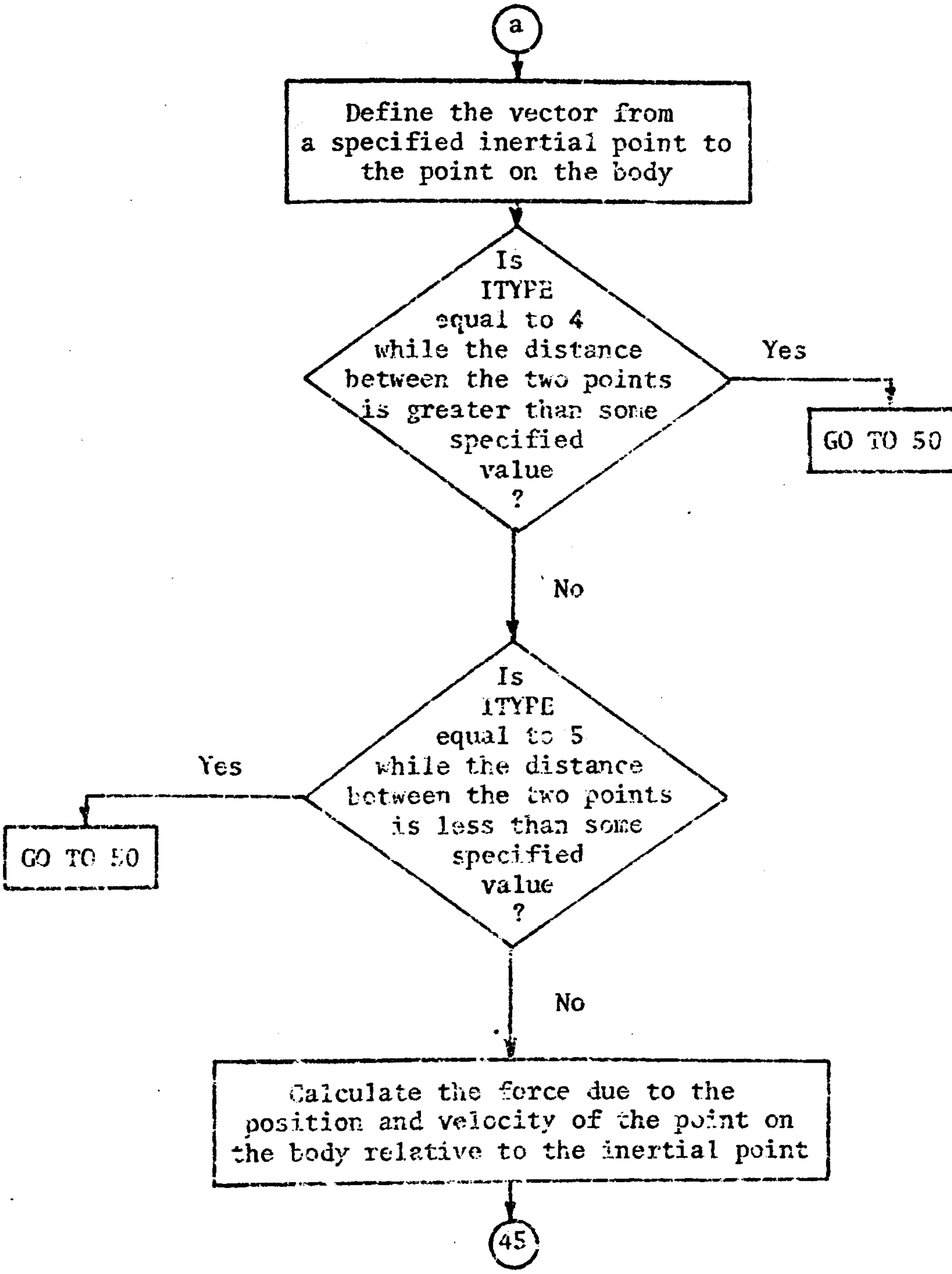

Figure C-7 (continued).

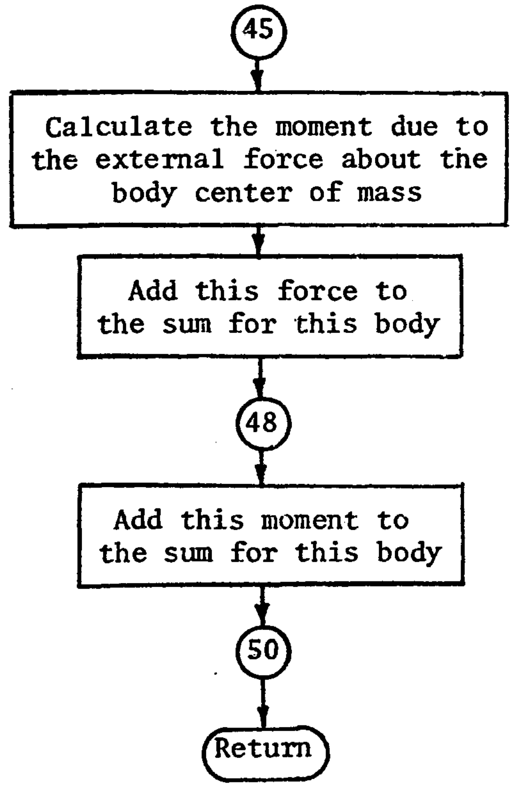

Figure C-7 (continued).

After the three eigenvalues have been obtained, subroutine VECT33 is called to determine the eigenvectors for the inertia matrix. This subroutine successively uses each eigenvalue in a reduced matrix equation to determine the relative magnitudes of each eigenvector component for that eigenvalue. (See Greenwood, 1965, pp. 304-305.) The magnitude of each eigenvector is then adjusted to unity so the resulting 3-by-3 matrix of eigenvectors may be used as a direction cosine matrix. Note that subroutine SETUP does check to see that this direction cosine matrix defines a right-hand unit vector triad.

C.1.9. Subroutines SURFAC and SURFO.

Subroutines SURFAC and SURFO are used to define special features of the terrain in the vicinity of the tractor. Both subroutines evaluate features of the 1/12th scale model side-overturn test course described in Section 4.2. Subroutine SURFAC defines the ground elevation and the ground normal vector at the vertical line passing through a point specified in inertial coordinates. This subroutine is used to locate the ground surface when subroutine WHEEL is evaluating the relative positions of points on the tires and the ground surface.

Subroutine SURFO defines three-dimensional inertial coordinates of critical points on the test course and paired instructions for connecting these points to give a graphic representation of the overturn test course. The points defined are the ground break points at the top and bottom of the bank plus an outline of the ramp which the tractor's right wheels encounter. This subroutine is called once if the graphical output has been requested; otherwise, it is not used.

C.1.10. Subroutine TURN.

Subroutine TURN is used to define the steer angle of the tractor. The subroutine defines the rotation of the steering axis (in radians) relative to the tractor body, with a positive rotation being clockwise when viewed from above.

Two steering options are provided but others could be added without changing any other parts of the program. The steering option (IST) and five constants (ST1, ST2, ST3, ST4, and ST5) are read by the main program and transferred to subroutine TURN. If IST = 0 , the steer angle is defined as the constant value, ST1, throughout all time. If IST = -1 , the steering angle begins with the value ST1, changes to value ST3 at time ST2, and maintains the value ST5 after time ST4.

C.1.11. Subroutine POSVEL.

Subroutine POSVEL determines the absolute position and velocity of a point in a rotating and translating coordinate system. The absolute position and velocity of the coordinate system origin, the orientation of the moving axes, the rotational velocity of the axes, and the location of the point (expressed in moving coordinate directions) relative to the moving origin are used to calculate the absolute position and velocity of the point expressed in inertial coordinates. If IVEL = 0 , only the position is determined.

C.1.12. Subroutine SOLVE.

Subroutine SOLVE is a program written by J.F. Booker, Mechanical and Aerospace Engineering, Cornell University, to solve linear systems of equations. The method employed is Gaussian elimination with pivotal condensation. Conte describes this method and provides a flow chart for a computer program utilizing the method (Conte, 1965, pp. 156-161, 175-176).

Subroutine SOLVE is called by subroutine DERIV to solve the seven simultaneous linear equations relating the coupled accelerations. Solution of the matrix equation yields seven of the accelerations which are required as definitions of derivatives.

C.1.13. <u>Subroutines EULPAR and DIRCOS.</u>

Subroutines EULPAR and DIRCOS are inverse relationships for converting a matrix of direction cosines to Euler parameters and converting Euler parameters to direction cosines. Subroutine EULPAR evaluates the Euler parameters from the four equations 3-12 through 3-15 while subroutine DIRCOS uses equations 3-20 through 3-28 to define the direction cosines. Each subroutine is used only once - EULPAR in defining the initial conditions in subroutine SETUP, and DIRCOS in defining the attitude of the tractor body each time that subroutine DERIV is called.

C.1.14. <u>Subroutines MULT31, MULT33, and ROTATE.</u>

Subroutines MULT31, MULT33, and ROTATE provide basic matrix multiplication operations. The premultiplication of a 3-dimensional vector by a 3 by-3 square matrix is performed by subroutine MULT31. The parameter ITYPE allows the option of premultiplying by the 3-by-3 matrix as it exists (ITYPE = 1) or premultiplying by the transpose of the 3-by-3 matrix (ITYPE = -1). Whenever the 3-by-3 matrix is a direction cosine matrix, the premultiplication of a vector by that matrix or its transpose constitutes a transformation of coordinates for the vector.

Subroutine MULT33 provides the same multiplication options as does MULT31 except that now both inputs are 3-by-3 matrices resulting in a 3-by-3 product. If both input matrices are direction cosine matrices, the product is a third direction cosine matrix.

Subroutine ROTATE provides the operation of rotating a matrix by premultipling it by a direction cosine matrix which defines the relative orientation of the before and after directions of the vectors being rotated. Again, if the first matrix is a direction cosine matrix, rotation of that matrix surely yields a second direction cosine matrix. The subroutine is used by specifying the matrix to be rotated (ATTOLD), the angle through which the rotation will occur (THETAR, in radians), and the axis about which the rotation should occur (IAXIS). The direction cosine matrix for the rotation is constructed from THETAT and IAXIS, subroutine MULT33 is used to perform the direction cosine matrix multiplication, and the rotated vector directions are defined as the matrix ATTNEW. This subroutine is used to rotate the wheel-coordinate axes (direction cosines) to obtain their orientation after camber, caster, toe-in, and steering adjustments.

C.1.15. Subroutines CROSS and DBLCRS.

Subroutines CROSS and DBLCRS provide vector cross product operations. Subroutine CROSS simply evaluates the cross product of the two 3-dimensional input vectors yielding a third 3-dimensional vector perpendicular to the other two. This operation is used frequently to calculate torques, calculate rotational velocities, and define a unit vector direction perpendicular to two others.

Subroutine DBLCRS evaluates a double cross product in which the first vector of the first cross product is again crossed onto the result of the first operation. This operation is used in determining the radial component of accelerations due to a body moving on a curved path. In this case the cross product of the angular velocity and the radius vector yields the tangential velocity. Then the cross product of the angular velocity and the tangential velocity results in the radial or normal acceleration.

C.1.16. Function Subroutine DOT.

The dot product operation is provided by function subroutine DOT. This function calculates the dot or scalar product of the two 3-dimensional vector arguments. Dot products are used extensively in determining desired components of vectors, in checking for parallel vectors, and in the first step of determining the magnitude of a vector (followed by the square root of the dot product).

C.1.17. Function Subroutine TABLE.

Function subroutine TABLE provides interpolation between two columns of tabulated data. The method used is the Lagrangian form of the interpolating polynomial as described by Conte (1965, pp. 72-73).

When corresponding values of two arrays X and Y have been assigned to the same numbered elements of the two arrays, interpolation between the two arrays may be performed in either direction.

If XARG is the value of X for which the corresponding value of Y is desired, then X is the first argument, Y is the second, and XARG is the third. IDEG specifies the degree of interpolation desired (1 = linear, 2 = quadratic, etc.) and NDIM specifies the number of stored elements in the X and Y arrays. JMIN specifies the element number of the first X value at which to begin searching for the interval containing XARG.

Because much of the tire force data and other empirical data is defined in tabular form, function subroutine TABLE is used to define specific data values from the tables of data. The specific radial tire force corresponding to some nonzero radial tire deformation is defined by using function TABLE with parameters for the tire deformations, the tire forces, the given tire deformation, and others. The value of the function TABLE is the desired radial force interpolated from the tabulated data.

C.2. Program Listing.

The digital computer program for simulating wheel tractor overturns is written in the Fortran IV computer language. All floating point calculations are performed as double precision operations (16 significant digits) to overcome the round off problems inherent in the short word length of IBM 360 single precision constants (7 significant digits). Nearly all input and output operations, however, handle the floating point variables as F-formatted numbers. This enables punched data to be used as single precision constants which frequently is the form required by plotting programs.

The digital computer simulations are generated by numerical integration of the differential equations defining the conditions of dynamic equilibrium for the tractor. Twenty variables are used to define the state of the tractor at any given time, thus twenty first-order differential equations describe the dynamic equilibrium. The twenty variables whose derivatives make up the differential equations are called state variables. Table C-1 provides a definition of the state variables and the notation used for these variables in Chapter III of this dissertation and in the digital computer program. Table C-2 presents the notations used for the derivatives of the state variables in the dissertation and in the program.

The subroutine descriptions of Section C.1, the comment cards used throughout the program, and a general description of the notation similarities between the variables of Chapter III and the variable names of the computer program should enable the interested person to follow the program steps from the program listing. The variable names used in the computer program are frequently very similar to the variables of Chapter III. The first letter or two represent the variable type while succeeding letters represent the pertinent bodies and/or coordinate systems involved. Table C-3 provides a comparative definition of many variables which are used in Chapter III of this dissertation and/or in the computer program.

The digital computer program is presented in its entirety in Figure C-8.

TABLE C-1. Comparative Notation for the Twenty State Variables.

	Dissertation notation (Chapter III)	Subroutine DHPCG notation	General program notation
Velocities of the tractor-body centers of mass, expressed in inertial coordinate directions (in/sec)	V_{BI_1} V_{BI_2} V_{BI_3}	Y(1) Y(2) Y(3)	VBI(1) VBI(2) VBI(3)
Positions of the tractor-body centers of mass, expressed in inertial coordinate directions (in)	X_{BI_1} X_{BI_2} X_{BI_3}	Y(4) Y(5) Y(6)	XBI(1) XBI(2) XBI(3)
Angular velocities of the tractor-body expressed in the tractor's principal-axes directions (rad/sec)	ω_{BP_1} ω_{BP_2} ω_{BP_3}	Y(7) Y(8) Y(9)	OMBP(1) OMBP(2) OMBP(3)
Euler parameters of the vector of finite rotation for the tractor's principal axes	λ_0 λ_1 λ_2 λ_3	Y(10) Y(11) Y(12) Y(13)	E0 E1 E2 E3
Angular velocity of the left rear wheel about the axle (rad/sec)	ω_{LP_2}	Y(14)	OMLP(IAXLE)*,-SPEEDL
Angular rotation of the left rear wheel about the axle (rad)	θ_{LP_2}	Y(15)	

TABLE C-1 (continued).

	Dissertation notation (Chapter III)	Subroutine DHPCG notation	General program notation
Angular velocity of the right rear wheel about the axle (rad/sec)	ω_{RP_2}	Y(16)	OMRP(IAXLE)*, -SPEEDR
Angular rotation of the right rear wheel about the axle (rad)	θ_{RP_2}	Y(17)	
Angular velocity of the front end about the front pin (rad/sec)	ω_{FF_1}	Y(18)	OMFF(1), OMFF1
Angular rotation of the front end relative to the tractor body and about the front pin (rad)	θ_{FF_1}	Y(19)	THETF
Engine speed (rad/sec)	ω_e	Y(20)	SPEEDE

*IAXLE is the subscript of the principal axis which is parallel to the rear axle.

TABLE C-2. Comparative Notation for the Derivatives of the Twenty State Variables.*

Dissertation notation (Chapter III)	Subroutine DHPCG notation	Subroutine DERIV notations
$\dot{V}_{BI_1}$	DERY(1)	DYDT(1), X(1)
$\dot{V}_{BI_2}$	DERY(2)	DYDT(2), X(2)
$\dot{V}_{BI_3}$	DERY(3)	DYDT(3), X(3)
$\dot{X}_{BI_1}$	DERY(4)	DYDT(4)
$\dot{X}_{BI_2}$	DERY(5)	DYDT(5)
$\dot{X}_{BI_3}$	DERY(6)	DYDT(6)
$\dot{\omega}_{BP_1}$	DERY(7)	DYDT(7), X(4)
$\dot{\omega}_{BP_2}$	DERY(8)	DYDT(8), X(5)
$\dot{\omega}_{BP_3}$	DERY(9)	DYDT(9), X(6)
$\dot{\lambda}_0$	DERY(10)	DYDT(10)
$\dot{\lambda}_1$	DERY(11)	DYDT(11)
$\dot{\lambda}_2$	DERY(12)	DYDT(12)
$\dot{\lambda}_3$	DERY(13)	DYDT(13)
$\dot{\omega}_{LP_2}$	DERY(14)	DYDT(14)
$\dot{\theta}_{LP_2}$	DERY(15)	DYDT(15)
$\dot{\omega}_{RP_2}$	DERY(16)	DYDT(16)
$\dot{\theta}_{RP_2}$	DERY(17)	DYDT(17)
$\dot{\omega}_{FF_1}$	DERY(18)	DYDT(18), X(7)
$\dot{\theta}_{FF_1}$	DERY(19)	DYDT(19)
$\dot{\omega}_e$	DERY(20)	DYDT(20)

*The variables are defined in Table C-1.

TABLE C-3. Comparative Notation for Other Important Variables.

	Dissertation notation (Chapter III)	Computer program notation
Direction cosines		
principal axes in terms of tractor axes	A_{PT}	APT
tractor axes in terms of inertial axes	A_{TI}	ATI
principal axes in terms of inertial axes	A_{PI}	API
front-end axes in terms of inertial axes	A_{FI}	AFI
wheel axes in terms of inertial axes	A_{WI}	AWI
left rear wheel		ALRI
right rear wheel		ARRI
left front wheel		ALFI
right front wheel		ARFI
Velocities, inertial coordinates (in/sec)		
left rear wheel center	V_{LI}	VLI
right rear wheel center	V_{RI}	VRI
front pin	V_{PI}	VPI
front-end center of mass	V_{FI}	VFI
a wheel center	V_{CI}	VCI
wheel-ground contact point	V_{WGI}	VWGI

TABLE C-3 (continued).

			Dissertation notation (Chapter III)	Computer program notation
Positions, inertial coordinates (in)				
left rear wheel center			X_{LI}	XLI
right rear wheel center			X_{RI}	XRI
front pin			X_{PI}	XPI
front-end center of mass			X_{FI}	XFI
left front wheel center				XLFI
right front wheel center				XRFI
a wheel center			X_{CI}	XCI
Forces (lb)				
acting on	acting from	coordinates		
left rear wheel	axle	inertial	F_{LAI}	
right rear wheel	axle	inertial	F_{RAI}	
front end	pin	inertial	F_{FPI}	
tractor body	external	inertial	F_{BEI}	FBEI
left rear wheel	axle	principal	F_{LAP}	
right rear wheel	axle	principal	F_{RAP}	
front end	pin	principal	F_{FPP}	
front end	pin	front end	F_{FPF}	
left rear wheel	ground	inertial	F_{LGI}	FLGI
right rear wheel	ground	inertial	F_{RGI}	FRGI

TABLE C-3 continued).

			Dissertation notation (Chapter III)	Computer program notation
Forces (lb)				
acting on	acting from	coordinates		
front end	ground	inertial	F_{FGI}	FFGI
left front wheel	ground	inertial		FLFGI
right front wheel	ground	inertial		FRFGI
tractor body	total	inertial	F_{BI}	
left rear wheel	total	inertial	F_{LI}	
right rear wheel	total	inertial	F_{RI}	
front end	total	inertial	F_{FI}	
a general body	external	inertial		FI
Unit vectors, in inertial coordinates				
perpendicular to wheel plane			U_{WI}	UWI
perpendicular to ground plane			U_{GI}	UGI
radially from wheel center to ground-contact point			U_{RI}	URI
parallel to line-of-intersection of the wheel and ground planes			U_{WGI}	UWGI
perpendicular to the line-of-intersection of the wheel and ground planes, but in the ground plane			U_{LI}	ULI

TABLE C-3 (continued).

			Dissertation notation (Chapter III)	Computer program notation
Relative position (in)				
position of	relative to	in coordinates of		
L.R. wheel ctr	tractor body c.m.	principal	R_{LBP}	RLBP
R.R. wheel ctr	tractor body c.m.	principal	R_{RBP}	RRBP
front pin	tractor body c.m.	principal	R_{PBP}	RPBP
front-end c.m.	front pin	inertial	R_{FPI}	RFPI
front-end c.m.	front pin	front end	F_{FPF}	RFPF
Mass moments of inertia (lb-in-sec^2)				
body	coordinate directions			
tractor body	tractor axes		I_{BT}	IBT
tractor body	principal axes		I_{BP}	IBP
front end	front-end axes		I_{FF}	IFF
rear wheel	tractor axes		I_{RT}	IRT
rear wheel	principal axes		I_{RP}	IRP
drive train			I_d	ID
engine			I_e	IE
Mass (lb-sec^2/in)				
tractor body			m_B	MB
rear wheel			m_R	MR
front end			m_F	MF

TABLE C-3 (continued).

			Dissertation notation (Chapter III)	Computer program notation
Tire forces (lb)				
total ground force in inertial directions			F_{WGI}	FWGI
normal to ground surface			F_n	FNORM
circumferential in ground plane			F_c	FCIR
lateral to tire in ground plane			F_ℓ	FLAT
radial to tire			F_r	FRAD
component due to spring deflection			F_s	
component due to dashpot motion			F_d	
Moment reactions (in-lb)				
acting on	acting from	coordinates		
left rear wheel	axle	principal	M_{LAP}	
right rear wheel	axle	principal	M_{RAP}	
front end	front pin	principal	M_{FPP}	
front end	front pin	front end	M_{FPF}	
tractor body	external sources	principal	M_{BEP}	MOBEP
left rear wheel	ground	principal	M_{LGP}	MOLGP
right rear wheel	ground	principal	M_{RGP}	MORGP
front end	ground	front end	M_{FGF}	MOFGF
tractor body	total	principal	M_{BP}	
left rear wheel	total	principal	M_{LP}	

TABLE C-3 (continued).

			Dissertation notation (Chapter III)	Computer program notation
Moment reactions (in-lb)				
acting on	acting from	coordinates		
right rear wheel	total	principal	M_{RP}	
front end	total	front end	M_{FF}	
a general body	external	inertial		TQI
a wheel	ground-contact point	inertial		MOWGCI

```
      IMPLICIT REAL*8(A-H,O-Z)
      COMMON /MSD/ TENG,SENG,TCLUT,SCLUT,RRBT,RPBT,RFPF,RRFF,TEFF,
     %RATIOT,RATIOD,WB,WF,WR,INIT
      COMMON /MSOD/ APT,RADR,RADF
      COMMON /MSW/ COTR,SWHEEL,FREAR,DREAR,FFRONT,DFRONT,
     %AF,BF,DMPF,AR,BR,DMPR
      COMMON /MO/ RHOLT,WHERE,RHODB,IDB,ICON,JRHO,NODB,NODL,NODR,NODF,
     %NODLF,NODRF,NTOTAL,IPLOT,NOS,NPRINT,NPUNCH
      COMMON /MD/ RHOFBT,RHOFLT,RHOFRT,RHOFFF,PB,PL,PR,PF,
     %FB1,FL1,FR1,FF1,FB2,FL2,FR2,FF2,FB3,FL3,FR3,FF3,
     $RLBT,RLFF,THMAX,ALENG,CASTER,CAMBER,TOEIN,SLENG,SK,SC,
     %ITYPEB,ITYPEL,ITYPER,ITYPEF,NFBOD,NFLR,NFRR,NFFE
      COMMON /MOD/ IFF,IRP,ID,IE,MB,MR,MF
      COMMON /MTURN/ ST1,ST2,ST3,ST4,ST5,IST
      COMMON /MW/ SLOPER,SLANR,SLOPEF,SLANF
      COMMON /MS/ IBT,SPEEDE,SPEEDL,SPEEDR,THETF,OMFF1
      DIMENSION ATI(3,3),APT(3,3),RHOLT(3,8),Y(20),YZERO(20)
      DIMENSION XBI(3),VBI(3),OMBT(3),XX(3)
      DIMENSION AUX(16,20),DERY(20),PRMT(5),RHODB(3,50)
      DIMENSION RHOFBT(5,3),RHOFLT(5,3),RHOFRT(5,3),RHOFFF(5,3)
      DIMENSION PB(5,3),PL(5,3),PR(5,3),PF(5,3),FB1(5),FL1(5),FR1(5),
     %FF1(5),FB2(5),FL2(5),FR2(5),FF2(5),FB3(5),FL3(5),FR3(5),FF3(5)
      DIMENSION RLBT(3),RRBT(3),RPBT(3),RFPF(3),RLFF(3),RRFF(3)
      DIMENSION TCLUT(5),SCLUT(5),TENG(5),SENG(5)
      DIMENSION COTR(5),SWHEEL(5),FREAR(5),DREAR(5),FFRONT(5),DFRONT(5)
      DIMENSION SLOPER(5),SLANR(5),SLOPEF(5),SLANF(5)
      DIMENSION ITYPEB(5),ITYPEL(5),ITYPER(5),ITYPEF(5),IDB(50),
     %ICON(100)
      REAL*4 WHERE(5,8),DESCR(20),TABDAT(10),STOP
      REAL*8 IBT(3,3),IFF(3,3),IRT(3),IRP(3)
      REAL*8 ID,IE,MB,MR,MF
      EXTERNAL DERIV,OUTPUT,DOT,TABLE
      DATA STOP/'STOP'/,G/386.D0/
C  READ CARDS CONTAINING 80 COLUMNS OF DESCRIPTIVE INFORMATION WHICH
C         IS TO BE PRINTED UPON EXECUTION OF THE PROGRAM.
C         WHEN A CARD HAVING THE WORD "STOP" IN THE FIRST FOUR COLUMNS
C         IS ENCOUNTERED, THIS CARD IS NOT PRINTED; THE REMAINDER OF
C         THE PROGRAM IS EXECUTED.
  109 READ 11, (DESCR(I),I=1,20)
   11 FORMAT (20A4)
      IF(DESCR(1).EQ.STOP) GO TO 12
      PRINT 11, (DESCR(I),I=1,20)
      GO TO 109
   12 CONTINUE
C  READ THE INITIAL CONDITIONS FOR THE PROBLEM: UNITS - LB, IN, SEC.
C         CENTER OF MASS POSITION: X1,X2,X3 DIRECTIONS, RESPECTIVELY
C         WHERE: X1=FORWARD, X2=DRIVER'S RIGHT, X3=DOWN.
C                                          K1=0  -  FIXED COORDINATE SYSTEM
C                                          K1=1  -  TRACTOR-AXIS COORDINATES
      READ 1, K1,(XBI(I),I=1,3)
    1 FORMAT (I5,3F10.0)
C         CENTER OF MASS VELOCITY: X1,X2,X3 DIRECTIONS, RESPECTIVELY
C                                          K2=0  -  FIXED COORDINATE SYSTEM
C                                          K2=1  -  TRACTOR-AXIS COORDINATES
      READ 2, K2,(VBI(I),I=1,3)
```

Figure C-8. Digital Computer Program.

```
      2 FORMAT (I5,3F10.0)
C          ANGULAR ORIENTATION: DIRECTION COSINES DEFINING THE TRACTOR-
C                                         AXIS DIRECTIONS, XT, IN TERMS OF
C                                         THE FIXED (INERTIAL) DIRECTIONS, XI,
C                                         I.E.,    XT = ATI * XI.
        READ 3, ((ATI(I,J),J=1,3),I=1,3)
      3 FORMAT (9F8.5)
C          ANGULAR VELOCITY: X1,X2,X3 DIRECTIONS, RESPECTIVELY
C                                         K3=0  -  FIXED COORDINATE SYSTEM
C                                         K3=1  -  TRACTOR-AXIS COORDINATES
        READ 4, K3, (OMBT(I),I=1,3)
      4 FORMAT (I5,3F10.0)
C     READ INITIAL VALUES FOR FRONT-END ORIENTATION & ANGULAR
C          VELOCITY (RADIANS)
        READ 400, THETF,OMFF1
    400 FORMAT (2F10.5)
C    SPEEDE IS ENGINE SPEED; SPEEDL & SPEEDR ARE REAR WHEEL SPEEDS(RAD/S).
C    INIT DESIGNATES THE TYPE OF INITIAL CONDITIONS DESIRED:
C         INIT = 1 - CLUTCH DISENGAGED; ALL I.C. SPECIFIED BY DATA.
C              = 2 - CLUTCH DISENGAGED; I.C. ARE CALCULATED FOR TRACTOR
C                     ON ZERO ELEVATION, LEVEL SURFACE.
C              = 3 - CLUTCH ENGAGED; I.C. ARE EVALUATED FOR TRACTOR ON
C                     ZERO ELEVATION, LEVEL SURFACE.
C              = 4 - CLUTCH ENGAGED; ALL I.C. SPECIFIED BY DATA.
        READ 401, INIT,SPEEDE,SPEEDL,SPEEDR
    401 FORMAT (I5,3F10.2)
C    TRANSFORM THE C.G. POSITION INTO FIXED COORDINATES, IF NECESSARY.
        IF(K1.EQ.0) GO TO 21
        CALL MULT31(ATI,XBI,-1,XX)
        DO 20 I=1,3
     20 XBI(I)=XX(I)
     21 CONTINUE
C    TRANSFORM THE C.G. VELOCITY INTO FIXED COORDINATES, IF NECESSARY.
        IF(K2.EQ.0) GO TO 23
        CALL MULT31(ATI,VBI,-1,XX)
        DO 22 I=1,3
     22 VBI(I)=XX(I)
     23 CONTINUE
C    TRANSFORM ANGULAR VELOCITY INTO TRACTOR-AXIS COORDS, IF NECESSARY.
        IF(K3.NE.0) GO TO 25
        CALL MULT31(ATI,OMBT,1,XX)
        DO 24 I=1,3
     24 OMBT(I)=XX(I)
     25 CONTINUE
C    READ THE INERTIA MATRIX FOR THE TRACTOR, USING THE CENTER OF MASS
C          AND TRACTOR-AXIS DIRECTIONS, XT, FOR THESE DEFINITIONS.
        READ 5, ((IBT(I,J),J=1,3),I=1,3)
      5 FORMAT (9F8.0)
C    READ THE INERTIA MATRIX FOR THE TRACTOR FRONT-END, DEFINED ABOUT THE
C          FRONT-END C.G. AND IN THE TRACTOR-AXIS DIRECTIONS (WHILE THE
C          FRONT AXLES ARE PARALLEL TO THE REAR AXLES).
        READ 5, ((IFF(I,J),J=1,3),I=1,3)
C    READ OTHER INERTIA VALUES AND PERTINENT WEIGHTS.
        READ 6, (IRT(I),I=1,3),ID,IE,WB,WR,WF
      6 FORMAT (6F10.2)
```

Figure C-8 (continued).

```
      MB=WB/G
      MR=WR/G
      MF=WF/G
C READ THE LOCATIONS OF THE REAR WHEEL CENTERS, FRONT-END PIN,
C        FRONT-END C.G. (FROM THE PIN), FRONT WHEEL TURNING POINTS
C        (FROM C.G.), REAR WHEEL RADIUS, FRONT WHEEL RADIUS, LENGTH
C        OF FRONT AXLE, FRONT WHEEL TOE-IN (RADIANS), FRONT WHEEL
C        CAMBER (RADIANS), MAX FRONT-END ROTATION (RADIANS).
      READ 6, (RLBT(I),I=1,3),(RRBT(I),I=1,3),(RPBT(I),I=1,3),(RFPF(I),
     %I=1,3),(RLFF(I),I=1,3),(RRFF(I),I=1,3),RADR,RADF,ALENG,TOEIN,
     $CAMBER,CASTER,THMAX,SLENG,SK,SC
C READ VECTOR VALUES DEFINING THE LOCATION OF PERTINENT POINTS RELATIVE
C        TO THE TRACTOR C.G. AND IN TERMS OF THE TRACTOR-AXIS COORDS.
C        THE LOCATION AND VELOCITY OF EACH POINT WILL BE CALCULATED.
      JRHO=0
   69 JRHO=JRHO+1
      READ 7, (RHOLT(I,JRHO),I=1,3),(WHERE(I,JRHO),I=1,5),MORE
    7 FORMAT (3F10.0,5A4,I5)
omit
      IF(MORE.NE.0) GO TO 69
C READ DESCRIPTIONS OF EXTERNAL FORCES AND MOMENTS.
C   CARD 1 ...
C     COL. 1-5 - NO. OF EXTERNAL FORCES AND MOMENTS.
C   CARD 2 ... (REPEAT THIS CARD FOR EACH FORCE OR MOMENT)
C     COL. 1-5 - TYPE OF REACTION
C                    -2 = CONSTANT MOMENT IN BODY-AXIS DIRECTIONS
C                    -1 = CONSTANT MOMENT IN INERTIAL COORD DIRECTIONS
C                     1 = CONSTANT FORCE IN INERTIAL COORD DIRECTIONS
C                     2 = CONSTANT FORCE IN BODY-AXIS DIRECTIONS
C                     3 = FORCE AS FUNCTION OF POSITION AND/OR VELOCITY OF
C                           A POINT ON THE BODY RELATIVE TO A FIXED POINT
C                     4 = SAME AS 3 EXCEPT FORCE LIMITED TO COMPRESSION
C                     5 = SAME AS 3 EXCEPT FORCE LIMITED TO TENSION
C          6-29 - BODY-AXIS COORDS OF POINT OF FORCE OR MOMENT APPLIC'N
C         30-53 - WHEN TYPE.LT.2,
C                     VALUE OF FORCE(LB) OR MOMENT(IN.LB) COMPONENTS
C               WHEN TYPE.GE.3,
C                     LOCATION OF REFERENCE POINT(IN.) IN INERTIAL COORDS
C         54-61 - SPRING RATE(LB/IN)
C         62-69 - DAMPING RATE(LB.SEC/IN)
C         70-77 - RELATIVE DISTANCE(IN.) WHEN ZERO SPRING FORCE
C     ... FORCES AND MOMENTS ON THE TRACTOR BODY.
      READ 30, NFBOD
   30 FORMAT (I5)
      IF(NFBOD.EQ.0) GO TO 33
      DO 31 I=1,NFBOD
   31 READ 32, ITYPEB(I),(RHOFBT(I,J),J=1,3),(PB(I,J),J=1,3),FB1(I),
     %FB2(I),FB3(I)
   32 FORMAT (I5,9F8.2)
C     ... FORCES AND MOMENTS ON LEFT REAR WHEEL.
   33 READ 30, NFLR
      IF(NFLR.EQ.0) GO TO 35
      DO 34 I=1,NFLR
   34 READ 32, ITYPEL(I),(RHOFLT(I,J),J=1,3),(PL(I,J),J=1,3),FL1(I),
     %FL2(I),FL3(I)
C     ... FORCES AND MOMENTS ON RIGHT REAR WHEEL.
```

Figure C-8 (continued).

```
      35 READ 30, NFRR
         IF(NFRR.EQ.0) GO TO 37
         DO 36 I=1,NFRR
      36 READ 32, ITYPER(I),(RHOFRT(I,J),J=1,3),(PR(I,J),J=1,3),FR1(I),
        %FR2(I),FR3(I)
C        ... FORCES AND MOMENTS ON FRONT-END.
      37 READ 30, NFFE
         IF(NFFE.EQ.0) GO TO 39
         DO 38 I=1,NFFE
      38 READ 32, ITYPEF(I),(RHOFFF(I,J),J=1,3),(PF(I,J),J=1,3),FF1(I),
        %FF2(I),FF3(I)
      39 CONTINUE
C     PRINT A QUANTITATIVE DESCRIPTION OF THE PROBLEM.
      49 PRINT 50, ((IBT(I,J),J=1,3),(IFF(I,J),J=1,3),I=1,3),(IRT(I),I=1,3)
      50 FORMAT (//1H0,9X,'MOMENTS OF INERTIA (LB.SEC**2.IN.) IN TRACTOR-AX
        %IS DIRECTIONS:'/1H0,19X,'TRACTOR BODY',30X,'FRONT-END'/1H ,1X,
        $2(8X,'--',29X,'--')/3(1H ,1X,2(8X,'|',3G10.3,' |')/),1H ,1X,
        %2(8X,'--',29X,'--')/1H0,13X,'REAR WHEEL'/1H ,4X,
        $(8X,'--',8X,'--')/3(1H ,4X, (8X,'|',G10.3,'|')/),1H ,4X,
        %(8X,'--',8X,'--'))
         PRINT 51, IE,ID
      51 FORMAT (1H0,13X,'ENGINE',6X,'DRIVE TRAIN'/(1H ,7X,2(4X,G10.3)))
         PRINT 52, WB,WF,WR
      52 FORMAT (//1H ,9X,'WEIGHTS (LB.):'/1H0,11X,'TRACTOR BODY',5X,
        %'FRONT-END',5X,'REAR WHEEL'/1H ,12X,G10.3,5X,G10.3,5X,G10.3)
         PRINT 54
      54 FORMAT (//1H ,9X,'LOCATIONS OF POINTS (IN.) AS TRACTOR-AXIS VECTOR
        %S:'/1H0,12X,'L.R. WHEEL',8X,'R.R. WHEEL',6X,'FRONT-END PIN')
         PRINT 56, (RLBT(I),RRBT(I),RPBT(I),I=1,3)
      56 FORMAT (1H ,3X,3( 9X,'--',5X,'--')/3(1H ,3X,3( 9X,'|',F7.2,'|')/),
        %1H ,3X,3( 9X,'--',5X,'--'))
         PRINT 58
      58 FORMAT (1H0,10X,'FRONT-END C.G.',7X,'L.F. --WHEEL PIVOTS-- R.F.')
         PRINT 56, (RFPF(I),RLFF(I),RRFF(I),I=1,3)
         PRINT 59, ALENG,THMAX,SLENG,SK,SC,CASTER,CAMBER,TOEIN
      59 FORMAT (1H0,12X,'FRONT AXLE LENGTHS(IN.):',F7.2/1H0,12X,'FRONT-END
        % ROTATION LIMIT(RADIANS):',F8.4/1H0,12X,'DISTANCE FROM FRONT PIN T
        $O "STOP"(IN):',F7.2/1H0,12X,'"STOP" STIFFNESS(LB/IN):',F9.1/1H0,12
        %X,'"STOP" DAMPING(LB-SEC/IN):',F9.3/1H0,12X,'CASTER(RAD):',F8.4/
        $1H0,12X,'CAMBER(RADIANS):',F8.4/1H0,12X,'TOEIN(RADIANS):',F8.4)
         PRINT 60, RADR,RADF
      60 FORMAT (//1H ,9X,'WHEEL RADII (IN.):'/1H0,15X,'REAR',14X,'FRONT'/
        %1H ,14X,F5.2,13X,F5.2)
C     READ ROLLING RESISTANCE & DAMPING PARAMETERS, DIFFERENTIAL RATIO,
C             TRANSMISSION RATIO & EFFICIENCY.
         READ 61, AR,BR,DMPR,AF,BF,DMPF,RATIOD,RATIOT,TEFF
      61 FORMAT (6F10.4)
         PRINT 64, AF,BF,DMPF,AR,BR,DMPR,RATIOD,RATIOT,TEFF
      64 FORMAT (/1H0,9X,'TIRE ROLLING RESISTANCE COEF. AND RADIAL DAMPING
        %COEF.:'/1H ,12X,'( ROLLING RESISTANCE COEF.= A + B * SLIP ANGLE(DE
        $G) )'/1H ,12X,'( DAMPING COEF. UNITS ARE LB.SEC/IN )'/1H ,27X,
        %'A',9X,'B',7X,'DAMP'/1H ,15X,'FRONT',4X,F7.4,F10.5,F9.4/1H ,15X,'R
        $EAR',5X,F7.4,F10.5,F9.4/1H0,9X,'DIFFERENTIAL RATIO =',F8.3/1H0,9X,
        %'TRANSMISSION RATIO =',F8.3/1H0,9X,'TRANSMISSION EFFICIENCY =',
        $F7.3)
```

Figure C-8 (continued).

```
C  READ TABULATED DATA FOR THE ENGINE TORQUE(IN.LB)-SPEED(RAD/S) CURVE.
       READ 10, (TENG(I),SENG(I),I=1,5),(TABDAT(I),I=1,10)
    10 FORMAT (6F10.2/4F10.2,10A4)
       PRINT 110, (TABDAT(I),I=1,10),(TENG(I),SENG(I),I=1,5)
   110 FORMAT (1H0,5X,'TABULATED INPUT DATA:',5X,10A4/(15X,2F15.4))
C  READ TABULATED DATA FOR CLUTCH TORQUE(IN.LB)-SLIP CURVE.
       READ 10, (TCLUT(I),SCLUT(I),I=1,5),(TABDAT(I),I=1,10)
       PRINT 110, (TABDAT(I),I=1,10),(TCLUT(I),SCLUT(I),I=1,5)
C  READ TABULATED DATA FOR REAR TIRE  FORCE(LB)-DEFLECTION(IN) CURVE.
       READ 10, (FREAR(I),DREAR(I),I=1,5),(TABDAT(I),I=1,10)
       PRINT 110, (TABDAT(I),I=1,10),(FREAR(I),DREAR(I),I=1,5)
C  READ TABULATED DATA FOR FRONT TIRE  FORCE(LB)-DEFLECTION(IN) CURVE.
       READ 10, (FFRONT(I),DFRONT(I),I=1,5),(TABDAT(I),I=1,10)
       PRINT 110, (TABDAT(I),I=1,10),(FFRONT(I),DFRONT(I),I=1,5)
C  READ TABULATED DATA FOR WHEEL  COEF.TRACTION-SLIP  CURVE.
       READ 10, (COTR(I),SWHEEL(I),I=1,5),(TABDAT(I),I=1,10)
       PRINT 110, (TABDAT(I),I=1,10),(COTR(I),SWHEEL(I),I=1,5)
C  READ TABULATED DATA FOR REAR WHEEL LAT.F.COEF.-SLIP ANGLE(DEG.) DATA.
       READ 10, (SLOPER(I),SLANR(I),I=1,5),(TABDAT(I),I=1,10)
       PRINT 110, (TABDAT(I),I=1,10),(SLOPER(I),SLANR(I),I=1,5)
C  READ TABULATED DATA FOR FRONT WHEEL LAT.F.COEF.-SLIP ANGLE(DEG.) DATA.
       READ 10, (SLOPEF(I),SLANF(I),I=1,5),(TABDAT(I),I=1,10)
       PRINT 110, (TABDAT(I),I=1,10),(SLOPEF(I),SLANF(I),I=1,5)
       CALL SETUP(ATI,XBI,VBI,OMBT,YZERO,NEQNS)
       CALL MULT31(APT,IRT,1,IRP)
C  READ INSTRUCTIONS FOR STEERING THE TRACTOR.
       READ 89,IST,ST1,ST2,ST3,ST4,ST5
    89 FORMAT (I5,5F10.3)
C  READ INSTRUCTIONS FOR GRAPHIC DISPLAY OF THE OUTPUT.
C          IPLOT DEFINES THE TYPE OF OUTPUT.
C                 IPLOT = -1 - LOCATIONS ARE CALCULATED AND PRINTED ONLY.
C                       =  0 - NO OUTPUT OF THIS TYPE GENERATED.
C                       =  1 - POINT LOCATIONS ARE PRINTED AND PLOTTED.
C                       =  2 - POINT LOCATIONS ARE PLOTTED ONLY.
C          OTHER VARIABLES DEFINE NO. OF POINTS FOR EACH BODY.
       READ 91, IPLOT,NODB,NODL,NODR,NODF,NODLF,NODRF
    91 FORMAT (7I5)
       NTOTAL=NODB+NODL+NODR+NODF+NODLF+NODRF
       IF(NTOTAL.EQ.0) GO TO 96
C  READ AN IDENTIFIER, IDB, TO DEFINE THE APPROPRIATE BODY,
C                 WHERE: 1=TRACTOR,2=L.R.,3=R.R.,4=F.E.,5=L.F.,6=R.F.,
C          AND A RADIUS VECTOR, RHODB, LOCATING THE POINT WITH RESPECT
C          TO THE BODY C.G. AND IN THAT BODY'S COORDINATE DIRECTIONS.
       READ 92, (IDB(JD),(RHODB(J,JD),J=1,3),JD=1,NTOTAL)
    92 FORMAT (I5,3F10.3)
C  NOW DEFINE THE DESIRED CONNECTION OF THE DESIGNATED POINTS
C      ... HOW MANY CONTINUOUS LINES?  (A LINE MAY BE ONLY ONE POINT.)
       READ 93, NLINES
    93 FORMAT (I5)
C      ... USE NUMBER PAIRS, N(I) & N(I+1), TO DEFINE THE EXTENT OF EACH
C                LINE:
C                       IF N(I+1)=N(I)  - PLOT ONLY POINT NO. N(I);
C                       IF N(I+1)<N(I)  - DRAW A LINE FROM POINT NO. N(I+1)
C                                              TO POINT NO. N(I);
C                       IF N(I+1)>N(I)  - CONNECT CONSECUTIVELY THE POINTS
```

Figure C-8 (continued).

```
C                                                NUMBERED N(I) TO N(I+1).
C                  NOTE: THE POINT NUMBERS ARE THE ORDER IN WHICH THEY ARE
C                        READ AS DATA, EXCEPT -     0 = ORIGIN,
C                             -6 = CHASSIS C.G., -5 = L.R. WHEEL C.G.,
C                             -4 = R.R. WHEEL C.G., -3 = FRONT-END C.G.,
C                             -2 = L.F. WHEEL C.G., -1 = R.F. WHEEL C.G.
      NOS=2*NLINES
      READ 94, (ICON(I),I=1,NOS)
   94 FORMAT (12I5)
   96 CONTINUE
C  READ AND PRINT THE INTEGRATION PARAMETERS.
C        NPRINT DEFINES THE NO. OF DTMAX TIME STEPS PER PRINT CYCLE.
C        NPUNCH DEFINES THE NO. OF PRINT CYCLES PER PUNCH CYCLE.
C        BOTH NPRINT & NPUNCH MUST BE INTEGERS GREATER THAN ZERO.
C        IERWT SPECIFIES TYPE OF ERROR WEIGHTING
      READ 97, TZERO,DTMAX,TFINAL,ERROR,NPRINT,NPUNCH,IERWT
   97 FORMAT (4F10.5,3I5)
      PRINT 98, TZERO,DTMAX,TFINAL,ERROR,NPRINT,NPUNCH
   98 FORMAT (1H0,12X,'INTEGRATION PARAMETERS:  TZERO, DTMAX, TFINAL, ER
     %ROR'/15X,4F15.5/15X,'PRINT EVERY',I4,' DTMAX TIME STEPS'/15X,
     $'PUNCH EVERY',I4,' PRINT CYCLES')
C         ... IF IERWT =1, ALL 20 VARIABLES ARE WEIGHTED EQUALLY;
C         ... OTHERWISE, READ ALL 20 RELATIVE WEIGHTINGS.
      IF(IERWT.NE.1) READ 99, (DERY(I),I=1,20)
   99 FORMAT (10F6.1)
C         ... DIVIDE EACH BY 20 TO PROVIDE "AVERAGING".
      DO 100 I=1,20
      IF(IERWT.EQ.1) DERY(I)=1.0D0
  100 DERY(I)=0.5D-1*DERY(I)
C     ... PRINT THE ADJUSTED ERROR WEIGHTS.
      IF(IERWT.EQ.1) PRINT 101, DERY(1)
  101 FORMAT (1H0,15X,'ALL VARIABLES HAVE ERROR WEIGHT:',F7.4)
      IF(IERWT.NE.1) PRINT 102, (DERY(I),I=1,20)
  102 FORMAT (1H0,15X,'THE EQUATION VARIABLES HAVE THE FOLLOWING ERROR W
     %EIGHTS:'/(15X,10F8.4))
      PRMT(1)=TZERO
      PRMT(2)=TFINAL
      PRMT(3)=DTMAX
      PRMT(4)=ERROR
      CALL DHPCG(PRMT,YZERO,DERY,NEQNS,IHLF,DERIV,OUTPUT,AUX)
      IF(PRMT(5).NE.0.0D0) PRINT 104, ((AUX(I,J),J=1,NEQNS),I=1,16)
  104 FORMAT (1H1,'ABORT'/(10F12.6))
      IF(IHLF.GE.10) PRINT 105, IHLF
  105 FORMAT (1H0,'***** PROGRAM HALT DUE TO SMALL STEP SIZE;'
     %,I5, 'HALVINGS')
      IF(IHLF.GE.10) PRINT 104,((AUX(I,J),J=1,NEQNS),I=1,16)
      STOP
      END
      FUNCTION DOT(A,B)
C  THIS FUNCTION DEFINES THE DOT PRODUCT OF THE VECTORS A AND B.
      IMPLICIT REAL*8(A-H,O-Z)
      DIMENSION A(3),B(3)
      DOT=A(1)*B(1)+A(2)*B(2)+A(3)*B(3)
      RETURN
      END
```

Figure C-8 (continued).

```
      FUNCTION TABLE(X,Y,XARG,IDEG,NDIM,JMIN)
C
C  THIS FUNCTION USES LAGRANGIAN INTERPOLATION OF DEGREE  IDEG  TO
C        DETERMINE A VALUE OF  Y  CORRESPONDING TO  XARG, BASED UPON
C        THE NDIM  PAIRED VALUES OF  X  AND  Y.
C        INTERPOLATION USES VALUES SUBSCRIPTED.GE. JMIN.
C  EXAMPLE USE:
C        TWO ARRAYS, TEMP(I) AND HUMID(I), IN SOME PROGRAM CONTAIN
C            CONSECUTIVE VALUES OF TWO VARIABLES.  THERE ARE  NDIM
C            OF EACH VARIABLE, WITH THOSE HAVING EQUAL SUBSCRIPTS
C            CORRESPONDING TO ONE ANOTHER.  TO OBTAIN THE INTERPOLATED
C            VALUE, HVALUE, CORRESPONDING TO A SPECIFIC VALUE WITHIN
C            THE TEMP(I) RANGE, SAY  TVALUE, THE FOLLOWING ASSIGNMENT
C            STATEMENT WOULD BE USED IN THE PROGRAM WHICH HAS THE TWO
C            ARRAYS STORED:
C                HVALUE = TABLE(TEMP,HUMID,TVALUE,IDEG,NDIM,JMIN)
C
C  *** CAUTION ***   X AND Y MUST BE DIMENSIONED  NDIM  IN MAIN PROG.
C
      IMPLICIT REAL*8(A-H,O-Z)
      DIMENSION X(NDIM),Y(NDIM)
C  SEARCH FOR THE INTERVAL CONTAINING XARG.
      IF(IDEG.LE.NDIM-JMIN) GO TO 9
      PRINT 1
    1 FORMAT (1H0,'***  INSUFFICIENT NUMBER OF TABULATED POINTS FOR DESI
     *RED DEGREE OF INTERPOLATION')
    9 J=JMIN-1
   10 IF(J.EQ.NDIM) GO TO 300
      J=J+1
      IF(X(J).EQ.XARG) GO TO 20
      IF(J.GE.NDIM-1) GO TO 300
      IF(X(J).LT.XARG.AND.X(J+1).GE.XARG) GO TO 30
      IF(X(J).GT.XARG.AND.X(J+1).LE.XARG) GO TO 30
      GO TO 10
   20 TABLE=Y(J)
      RETURN
   30 JHALF=(IDEG+1)/2
      IF(JHALF.GE.J) GO TO 31
      J1=J-JHALF
      IF(J1+IDEG.LE.NDIM) GO TO 32
  300 J1=NDIM-IDEG
      GO TO 32
   31 J1=JMIN
   32 JMAX=J1+IDEG
C  START THE LAGRANGIAN INTERPOLATION.
      FACTOR=1.0D0
      DO 33 J=J1,JMAX
      IF(X(J).EQ.XARG) GO TO 20
   33 FACTOR=FACTOR*(XARG-X(J))
      YEST=0.0D0
      DO 35 I=J1,JMAX
      TERM=Y(I)*FACTOR/(XARG-X(I))
      DO 34 J=J1.JMAX
   34 IF(I.NE.J) TERM=TERM/(X(I)-X(J))
   35 YEST=YEST+TERM
```

Figure C-8 (continued).

```
      TABLE=YEST
      RETURN
      END
      SUBROUTINE SETUP(ATI,XBI,VBI,OMBT,YZERO,NEQNS)
C  THIS ROUTINE CONVERTS THE PHYSICAL STATE OF THE TRACTOR SYSTEM INTO
C          THE FORM REQUIRED FOR SOLVING THE DIFFERENTIAL EQUATIONS.
C          DETERMINE THE PRINCIPAL MOMENTS OF INERTIA AND THE PRINCIPAL
C                AXES AT THE TRACTOR CENTER OF GRAVITY (C.G.).
      IMPLICIT REAL*8(A-H,O-Z)
      COMMON /MSD/ TENG,SENG,TCLUT,SCLUT,RRBT,RPBT,RFPF,RRFF,TEFF,
     %RATIOT,RATIOD,WB,WF,WR,INIT
      COMMON /MSOD/ APT,RADR,RADF
      COMMON /MSW/ COTP,SWHEEL,FREAR,DREAR,FFRONT,DFRONT,
     %AF,BF,DMPF,AR,BR,DMPR
      COMMON /SOD/ IBP
      COMMON /MS/ IBT,SPEEDE,SPEEDL,SPEEDR,THETF,OMFF1
      DIMENSION ATI(3,3),ATP(3,3),APT(3,3),API(3,3)
      DIMENSION XBI(3),VBI(3),VBT(3),OMBT(3),OMBP(3),YZERO(20)
      DIMENSION U1(3),U2(3),U3(3),UCHK(3)
      DIMENSION COTR(5),SWHEEL(5),FREAR(5),DREAR(5),FFRONT(5),DFRONT(5)
      DIMENSION TCLUT(5),SCLUT(5),TENG(5),SENG(5)
      DIMENSION RRBT(3),RPBT(3),RFPF(3),RRFF(3)
      REAL*8 IBT(3,3),IBP(3)
      CALL EIGVAL(IBT,3,3,IBP)
C          THE EIGENVECTOR MATRIX IS THE TRANSPOSE OF THE MATRIX APT.
      CALL VECT33(IBT,IBP,ATP)
C                NOTE THAT A DIAGONAL MATRIX HAVING THE PRINCIPAL MOMENTS
C                      OF INERTIA, IBP, AS ITS DIAGONAL ELEMENTS WOULD
C                      SATISFY THE MATRIX EQUATION
C                                     DIAGM = APT * IBT * ATP.
C  CHECK TO SEE THAT THE DIRECTION COSINES, APT, DEFINE A RIGHT-HAND
C          COORDINATE SYSTEM.
      DO 508 I=1,3
      U1(I)=ATP(I,1)
      U2(I)=ATP(I,2)
  508 U3(I)=ATP(I,3)
      CALL CROSS(U1,U2,UCHK)
      REVERS=DOT(U3,UCHK)
      DO 509 J=1,3
      APT(3,J)=DSIGN(ATP(J,3),REVERS)
      DO 509 I=1,2
  509 APT(I,J)=ATP(J,I)
C  DETERMINE FORWARD COMPONENT OF TRACTOR VELOCITY.
C          U2 = TO TRACTOR RIGHT, U3 = VERT DOWN, U1 = TRACTOR FORWARD
      DO 9 I=1,3
      U2(I)=ATI(2,I)
    9 U3(I)=0.0D0
      U3(3)=1.0D0
      CALL CROSS(U2,U3,U1)
      VFWD=DOT(VBI,U1)
C  BRANCH ACCORDING TO THE TYPE OF INITIAL CONDITIONS.
      GO TO(50,30,30,50), INIT
   30 CONTINUE
C  TRACTOR STARTS ON LEVEL GROUND.
C          DEFINE THE WHEEL REACTIONS, REAR WHEEL SPEED, AND TRACTOR
```

Figure C-8 (continued).

```
C             ORIENTATION FOR ZERO ACCELERATION CONDITIONS.
      RF=.5D0*(-WB*RRBT(1)+WF*(RPBT(1)+RFPF(1)+RRFF(1)))/(RRBT(1)
     $-RPBT(1)-RFPF(1)-RRFF(1))
      RR=(WB+WF+2.0D0*WR-2.0D0*RF)/2.0D0
      DF=TABLE(FFRONT,DFRONT,RF,2,5,1)
      DR=TABLE(FREAR,DREAR,RR,2,5,1)
C         ITERATE TO DETERMINE THE TRACTOR ORIENTATION.
      THETAR=(RADR-RADF+DF-DR+RRBT(3)-RPBT(3)-RFPF(3)-RRFF(3))/
     $(RRBT(1)-RPBT(1)-RFPF(1)-RRFF(1))
      SINTH=(RADR-RADF+DF-DR-(-RRBT(3)+RPBT(3)+RFPF(3)+RRFF(3))*DCOS(THE
     $TAR))/(RRBT(1)-RPBT(1)-RFPF(1)-RRFF(1))
      COSTH=DCOS(DARSIN(SINTH))
      XBI(3)=-RADR+DR+RRBT(1)*SINTH-RRBT(3)*COSTH
      ATI(1,1)=COSTH
      ATI(1,3)=-SINTH
      ATI(3,1)=SINTH
      ATI(3,3)=COSTH
      IF(INIT.GT.2) GO TO 35
      SPEEDL=VFWD/(RADR-DR)
      SPEEDR=SPEEDL
      GO TO 50
   35 CONTINUE
C         ROLLING RESISTANCE FOR EACH FRONT TIRE.
      ROLLR=-AF*RF-AR*RR
C         TRACTIVE FORCES ARE EQUAL AND OPPOSITE TO ROLLING RESISTANCE.
      TRACT=-ROLLR
C         DRIVE WHEEL TORQUES
      TQ= TRACT*(RADR-DR)
C         DRIVE LINE TORQUE
      TD=TQ/RATIOD
C         CLUTCH TORQUE
      TC=TD/(RATIOT*TEFF)
C         CLUTCH SLIPPAGE
      SLIPC=TABLE(TCLUT,SCLUT,TC,2,5,1)
C         ENGINE TORQUE = CLUTCH TORQUE.
C         ENGINE SPEED IS DETERMINED BY ENGINE TORQUE (GOVERNED RANGE).
      SPEEDE=TABLE(TENG,SENG,TC,2,5,3)
C         CLUTCH SPEED
      SPEEDC=SPEEDE*(1.0D0-SLIPC)
C         REAR WHEEL SPEEDS
      SPEEDL=SPEEDC/(RATIOD*RATIOT)
      SPEEDR=SPEEDL
C         COEFFICIENT OF TRACTION
      COT=TRACT/RR
C         REAR WHEEL SLIP
      SLIPW=TABLE(COTR,SWHEEL,COT,2,5,1)
C         FORWARD TRAVEL VELOCITY
      VFWD=RADR*SPEEDR*(1.0D0-SLIPW)
      DO 39 I=1,3
   39 VBI(I)=VFWD*UI(I)
   50 CALL MULT31(APT,OMBT,1,OMBP)
      CALL MULT33(APT,ATI,1,API)
C         DEFINE THE TRACTOR BODY POSITION & VELOCITY VARIABLES.
      CALL EULPAR(API,YZERO(10),YZERO(11),YZERO(12),YZERO(13))
      DO 51 I=1,3
```

Figure C-8 (continued).

```
      YZERO(I)=VBI(I)
      YZERO(I+3)=XBI(I)
   51 YZERO(I+6)=OMBP(I)
      YZERO(14)=-SPEEDL
      YZERO(15)=0.0D0
      YZERO(16)=-SPEEDR
      YZERO(17)=0.0D0
      YZERO(18)=0.0D0
      IF(OMFF1.NE.0.0D0) YZEFO(18)=OMFF1
      YZERO(19)=0.0D0
      IF(THETF.NE.0.0D0) YZERO(19)=THETF
      YZERO(20)=SPEEDE
      NEQNS=20
   60 CONTINUE
      RETURN
      END
      SUBROUTINE OUTPUT(TIME,Y,DERY,IHLF,NEQNS,PRMT)
C  THIS ROUTINE CONVERTS THE OUTPUT GENERATED FROM INTEGRATION OF
C        THE DIFFERENTIAL EQUATIONS INTO A FORM WHICH IS MORE EASILY
C        INTERPRETED.
C        THE RESULTS ARE EXPRESSED AS VECTOR QUANTITIES AND MATRICES
C        OF DIRECTION COSINES.
C  ICOUNT DEFINES THE TIMES WHEN PRINTING SHOULD OCCUR.
C        ICOUNT = 0 - HEADING PRINTED WITH ALL OTHER OUTPUT.
C        ICOUNT = INTEGER MULTIPLE OF 1024 - PRINTS THE DESIRED OUTPUT.
C        ICOUNT = ALL OTHER - RETURN WITHOUT PRINTING.
      IMPLICIT REAL*8(A-H,O-Z)
      COMMON /IO/ ICOUNT
      COMMON /MO/ RHOLT,WHERE,RHODB,IDB,ICON,JRHO,NODB,NODL,NODR,NODF,
     %NODLF,NODRF,NTOTAL,IPLOT,NOS,NPRINT,NPUNCH
      COMMON /MSOD/ APT,RADR,RADF
      COMMON /DOW/ ATI
      COMMON /MOD/ IFF,IRP,ID,IE,MB,MR,MF
      COMMON /SOD/ IBP
      COMMON /CD/ API,AFI,ALRI,ARRI,ALFI,ARFI,XBI,XLI,XRI,XFI,XLFI,
     %VBI,VLI,VRI,VFI,OMBI,OMLI,OMRI,OMFI,OMBP,OMLP,OMRP,OMFF,XRFI
      COMMON /OD/ FLGI,FRGI,FLFGI,FRFGI,STEER,ISTOP
      DIMENSION API(3,3),APT(3,3),ATI(3,3),AFI(3,3),ALRI(3,3),ARRI(3,3)
      DIMENSION ALFI(3,3),ARFI(3,3),RHOLT(3,8),RHODB(3,50)
      DIMENSION Y(20),DERY(20),PRMT(5),XBI(3),XLI(3),XRI(3),XFI(3)
      DIMENSION VBI(3),VLI(3),VRI(3),VFI(3),OMBI(3),OMLI(3),OMRI(3),
     %OMFI(3),OMBT(3),OMBP(3),OMLP(3),OMRP(3),OMFF(3)
      DIMENSION RDB(3),XDI(3),VDI(3),XLFI(3),XRFI(3),FLGI(3),FRGI(3),
     %FLFGI(3),FRFGI(3),X1(200),X2(200),X3(200),XG1(12),XG2(12),XG3(12),
     $XWI(3),UGI(3),S(36),C(36)
      DIMENSION PBI(3),FLI(3),PRI(3),PFI(3),HBP(3),HLP(3),HRP(3),HFF(3),
     %HBI(3),HLI(3),HRI(3),HFI(3),PTOTAL(3),HTOTAL(3)
      DIMENSION IDB(50),ICON(100),ISCON(10)
      REAL*4 WHERE(5,6),SIDE(2)
      REAL*5 IFF(3,3),IBP(3),IRP(3),ID,IE,MB,MR,MF
      DATA G/386.D0/,SIDE(1),SIDE(2)/' LEF','RIGH'/
      DATA S(1),C(10),S(19),C(28)/4*0.D0/,S(2),S(18),C(9),C(29)/4*.174D0
     %/,S(3),S(17),C(8),C(30)/4*.342D0/,S(4),S(16),C(7),C(31)/4*.5D0/,
     $S(5),S(15),C(6),C(32)/4*.643D0/,S(6),S(14),C(5),C(33)/4*.766D0/
      DATA S(7),S(13),C(4),C(34)/4*.866D0/,S(8),S(12),C(3),C(35)/4*.94D0
```

Figure C-8 (continued).

```
      $/,S(9),S(11),C(2),C(36)/4*.985D0/,S(10),C(1)/2*1.D0/,S(20),S(36),
     %C(11),C(27)/4*-.174D0/,S(21),S(35),C(12),C(26)/4*-.342D0/,S(22),
     $S(34),C(13),C(25)/4*-.5D0/
      DATA S(23),S(33),C(14),C(24)/4*-.643D0/,S(24),S(32),C(15),C(23)/
     %4*-.766D0/,S(25),S(31),C(16),C(22)/4*-.866D0/,S(26),S(30),C(17),
     $C(21)/4*-.94D0/,S(27),S(29),C(18),C(20)/4*-.985D0/,S(28),C(19)/
     %2*-1.D0/,NSEGS,NPR,NPU/18,-1,-1/
      IF(ICOUNT.EQ.0) PRINT 1
    1 FORMAT (1H1,10X,'|<--------------- TRACTOR BODY (LESS REAR WHEELS
     %AND FRONTEND) --------------->|<--REAR WHEELS & FRONTEND -->|'/
     $1H0,4X,'TIME   C.G. POSITION    C.G. VELOCITY       TRACTOR ORIENTA
     %TION        ANGULAR VELOCITY   ANGULAR SPEEDS   ANGULAR POS.'
     $/1H ,4X,'(SEC)  (IN--FIXED CS)  (IN/SEC--FIXED)  (DIRECTION COSINE
     %S--FIXED)  (1/SEC--TR AXES)     (RADIAN/SEC)      (RADIANS)')
    2 FORMAT (1H ,13X,'--',6X,'--',6X,'--',7X,'--',4X,'--',21X,'--',6X,
     %'--',6X,'--')
    3 FORMAT (1H ,13X,'|',F8.3,'|',6X,'|',F9.3,'|',4X,'|',F7.4,2F8.4,
     %'|',6X,'|',F8.4,'|',7X,F8.3,3X,'LEFT',3X,F7.2)
    4 FORMAT (1H ,F9.4,3X,'<|',F8.3,'|>',4X,'<|',F9.3,'|>',3X,'|',F7.4,
     %2F8.4,'|',5X,'<|',F8.4,'|>',6X,F8.3,3X,'FR.END',2X,F6.3)
    5 FORMAT (1H ,13X,'|',F8.3,'|',6X,'|',F9.3,'|',4X,'|',F7.4,2F8.4,
     %'|',6X,'|',F8.4,'|',7X,F8.3,3X,'RIGHT',2X,F7.2)
    6 FORMAT (1H0)
C  CHECK ICOUNT FOR BEING AN INTEGER MULTIPLE OF 1024.
      IF((ICOUNT/1024)*1024.NE.ICOUNT) RETURN
C  CHECK TO SEE IF IT IS THE PROPER CYCLE FOR PRINTING.
      NPR=NPR+1
      IF((NPR/NPRINT)*NPRINT.NE.NPR) RETURN
C          CONVERT ANGULAR VELOCITY TO TRACTOR-AXIS DIRECTIONS.
      CALL MULT31(APT,OMBP,-1,OMBT)
      PRINT 6
      PRINT 2
      PRINT 3, XBI(1),VBI(1),(ATI(1,J),J=1,3),OMBT(1),Y(14),Y(15)
      PRINT 4, TIME,XBI(2),VBI(2),(ATI(2,J),J=1,3),OMBT(2),Y(18),Y(19)
      PRINT 5, XBI(3),VBI(3),(ATI(3,J),J=1,3),OMBT(3),Y(16),Y(17)
      PRINT 2
C  CALCULATE THE POSITIONS OF POINTS ON THE TRACTOR, IF DESIRED.
      IF(JRHO.EQ.0) GO TO 100
      DO 99 J=1,JRHO
      DO 91 I=1,3
   91 RDB(I)=RHOLT(I,J)
      CALL POSVEL(ATI,XBI,VBI,RDB,OMBT,1,XDI,VDI)
C************************SET FLAG*****************************************
C  SET FLAG IF ONE OF THE LOCATED POINTS HAS STRUCK THE GROUND.
      IF(XDI(3).GE.4.0D0) PRMT(5)=2.0D0
C************************SET FLAG*****************************************
   99 PRINT 94, (WHERE(I,J),I=1,5),(XDI(I),VDI(I),I=1,3)
   94 FORMAT (1H ,16X,5A4/(1H ,12X,F10.3,7X,F10.3))
  100 CONTINUE
      OMERPM=Y(20)*30.D0/3.1415926D0
      PRINT 7, Y(20),OMERPM
    7 FORMAT (1H0,5X,'ENGINE SPEED:',F9.0,' RAD/SEC  OR',F9.0,' RPM')
C  PRINT INFORMATION ABOUT THE INTEGRATION ACCURACY.
      PRINT 104, IHLF
  104 FORMAT (1H0,5X,'THE INITIAL INTEGRATION TIME INTERVAL WAS HALVED',
```

Figure C-8 (continued).

```
        %I4,' TIMES FOR THIS TIME STEP')
C  PRINT OTHER GENERATED INFORMATION.
      PRINT 105, STEER,(FLGI(I),FRGI(I),FLFGI(I),FRFGI(I),I=1,3)
  105 FORMAT (1H0,5X,'THE TRACTOR STEER ANGLE IS',F9.4,' RADIANS.'/1H0,
     %5X,'THE RESULTANT FORCE ON THE L.R., R.R., L.F., & R.F. TIRE IS,
     $RESPECTIVELY (LBS, INERTIAL DIRECTIONS):'/(10X,4F15.3))
      IS=1+(ISTOP+1)/2
      IF(ISTOP.NE.0) PRINT 106, SIDE(IS)
  106 FORMAT (1H0,5X,'THE TRACTOR FRONTEND IS IN CONTACT WITH THE ',A4,
     %'T-HAND "STOP".'/1H0)
C                 ... TRANSLATIONAL MOMENTA
      DO 110 I=1,3
      PBI(I)=MB*VBI(I)
      PLI(I)=MR*VLI(I)
      PRI(I)=MR*VRI(I)
  110 PFI(I)=MF*VFI(I)
C                 ... ANGULAR MOMENTA
      DO 120 I=1,3
      HBP(I)=IBP(I)*OMBP(I)
      HLP(I)=IRP(I)*OMLP(I)
  120 HRP(I)=IRP(I)*OMRP(I)
      CALL MULT31(IFF,OMFF,1,HFF)
      CALL MULT31(API,HBP,-1,HBI)
      CALL MULT31(API,HLP,-1,HLI)
      CALL MULT31(API,HRP,-1,HRI)
      CALL MULT31(AFI,HFF,-1,HFI)
C                 ... TOTALS
      DO 130 I=1,3
      PTOTAL(I)=PBI(I)+PLI(I)+PRI(I)+PFI(I)
  130 HTOTAL(I)=HBI(I)+HLI(I)+HRI(I)+HFI(I)
C                EVALUATE THE ENERGIES ...
C                 ... POTENTIAL ENERGIES
      EPOTB=-MB*G*XBI(3)
      EPOTL=-MR*G*XLI(3)
      EPOTR=-MR*G*XRI(3)
      EPOTF=-MF*G*XFI(3)
C                 ... ROTATIONAL KINETIC ENERGIES
      EROTB=0.5D0*DOT(HBI,OMBI)
      EROTL=0.5D0*DOT(HLI,OMLI)
      EROTR=0.5D0*DOT(HRI,OMRI)
      EROTF=0.5D0*DOT(HFI,OMFI)
C                 ... TRANSLATIONAL KINETIC ENERGIES
      ETRANB=0.5D0*MB*DOT(VBI,VBI)
      ETRANL=0.5D0*MR*DOT(VLI,VLI)
      ETRANR=0.5D0*MR*DOT(VRI,VRI)
      ETRANF=0.5D0*MF*DOT(VFI,VFI)
C                 ... TOTALS
      EPOTT=EPOTB+EPOTL+EPOTR+EPOTF
      EROTT=EROTB+EROTL+EROTR+EROTF
      ETRANT=ETRANB+ETRANL+ETRANR+ETRANF
      ETOTAL=EPOTT+EROTT+ETRANT
C                PRINT THE ENERGIES AND MOMENTA ...
C                 ... TRANSLATIONAL MOMENTA
      PRINT 140, (PBI(I),PLI(I),PRI(I),PFI(I),PTOTAL(I),I=1,3)
  140 FORMAT (1H0,5X,'TRANSLATIONAL MOMENTA (LB.SEC) - INERTIAL DIRECTIO
```

Figure C-8 (continued).

```
      %NS'/1H ,12X,'TRACTOR',6X,'L.R. WHEEL',5X,'R.R. WHEEL',6X,'FRONTEND
      $',8X,'TOTAL'/(1H ,5X,5F15.3))
C              ... ROTATIONAL MOMENTA
      PRINT 141, (HBI(I),HLI(I),HRI(I),HFI(I),HTOTAL(I),I=1,3)
  141 FORMAT (1H ,5X,'ROTATIONAL MOMENTA (LB.IN.SEC) - INERTIAL DIRECTIO
     %NS'/(1H ,5X,5F15.3))
C              ... ENERGIES
      PRINT 142, EPOTB,EPOTL,EPOTR,EPOTF,EPOTT,ETRANB,ETRANL,ETRANR,
     %ETRANF,ETRANT,EROTB,EROTL,EROTR,EROTF,EROTT,ETOTAL
  142 FORMAT (1H0,5X,'POTENTIAL ENERGIES (IN.LB)'/1H ,5X,5F15.3/1H ,5X,
     %'TRANSLATIONAL KINETIC ENERGIES (IN.LB.)'/1H ,5X,5F15.3/1H ,5X,
     $'ROTATIONAL KINETIC ENERGIES (IN.LB)'/1H ,5X,5F15.3/1H ,68X,
     %'--------------'/1H ,65X,F15.3)
C  PERFORM CALCULATIONS FOR PLOTTING, IF DESIRED.
      IF(NTOTAL.EQ.0) GO TO 300
      DO 250 JD=1,NTOTAL
      DO 205 I=1,3
  205 RDB(I)=RHODB(I,JD)
      IDBJD=IDB(JD)
      GO TO(210,215,220,225,230,235), IDBJD
  210 CALL POSVEL(ATI,XBI,VBI,RDB,OMBT,0,XDI,VDI)
      GO TO 240
  215 CALL POSVEL(ALRI,XLI,VLI,RDB,OMLP,0,XDI,VDI)
      GO TO 240
  220 CALL POSVEL(ARRI,XRI,VRI,RDB,OMRP,0,XDI,VDI)
      GO TO 240
  225 CALL POSVEL(AFI,XFI,VFI,RDB,OMFF,0,XDI,VDI)
      GO TO 240
  230 CALL POSVEL(ALFI,XLFI,VLI,RDB,OMFF,0,XDI,VDI)
      GO TO 240
  235 CALL POSVEL(ARFI,XRFI,VRI,RDB,OMFF,0,XDI,VDI)
C  FORM 3 ARRAYS, EACH CONTAINING ONE COORDINATE OF THE LOCATIONS.
  240 X1(JD)=XDI(1)
      X2(JD)=XDI(2)
      X3(JD)=XDI(3)
  250 CONTINUE
      IF(IABS(IPLOT).EQ.1) PRINT 253, (XBI(I),I=1,3),(XLI(I),I=1,3),
     %(XRI(I),I=1,3),(XFI(I),I=1,3),(XLFI(I),I=1,3),(XRFI(I),I=1,3)
  253 FORMAT (1H0,10X,'C.G. LOCATIONS:'/(1H,25X,3F15.6))
      IF(IABS(IPLOT).EQ.1) PRINT 255, (JD,IDB(JD),X1(JD),X2(JD),X3(JD),
     %JD=1,NTOTAL)
  255 FORMAT (5X,2I6,3F15.6)
      IF(IPLOT.LT.1) GO TO 300
C  CHECK TO SEE IF IT IS THE PROPER PRINT CYCLE FOR PUNCHING.
      NPU=NPU+1
      IF((NPU/NPUNCH)*NPUNCH.NE.NPU) GO TO 300
C  GENERATE THE OUTPUT REQUIRED FOR PLOTTING ...
      IF(NPU.GT.0) GO TO 270
C          DEFINE THOSE ITEMS WHICH ARE CONSTANT WITH TIME.
C          THE POINT ORDER IS: C.G.'S & ORIGIN                7
C                                DATA DEFINED PTS         NTOTAL
C                                WHEEL CIRCUMFERENCES    4*NSEGS
C                                GROUND SURFACE            NSURF
C          DEFINE THE ARRAY OF CONNECTING INSTRUCTIONS
C            (PT SUBSCRIPTS INCREASED BY 7 TO MAKE ALL POSITIVE)
```

Figure C-8 (continued).

```
      DO 261 I=1,NOS
  261 ICON(I)=ICON(I)+7
      DO 262 I=1,13,4
      ICON(NOS+I)=NTOTAL+8+(I/4)*NSEGS
      ICON(NOS+I+1)=NTOTAL+7+NSEGS+(I/4)*NSEGS
      ICON(NOS+I+2)=ICON(NOS+I+1)
  262 ICON(NOS+I+3)=ICON(NOS+I)
C          ESTABLISH THE GROUND SURFACE FOR PLOTTING.
      CALL SURFO(XG1,XG2,XG3,ISCON,NSCON,NSURF)
      DO 264 I=1,NSCON
  264 ICON(NOS+16+I)=NTOTAL+7+4*NSEGS+ISCON(I)
      NINST=NOS+16+NSCON
      NPTS=NTOTAL+7+4*NSEGS+NSURF
C     ... PUNCH THE NUMBER OF POINT LOCATIONS WHICH LATER WILL BE
C                 PUNCHED, AND THE NUMBER OF CONNECTION INSTRUCTIONS.
      PUNCH 265, NPTS,NINST
  265 FORMAT (2I5,50X,'NPTS,NINST')
C     ... PUNCH THE INSTRUCTIONS FOR CONNECTING THE POINTS.
      PUNCH 266, (ICON(I),I=1,NINST)
  266 FORMAT (12I5,9X,'INSTR PAIRS')
C          DEFINE THE GROUND SURFACE POINTS FOR PLOTTING.
      N=NTOTAL+4*NSEGS
      DO 268 I=1,NSURF
      X1(N+I)=XG1(I)
      X2(N+I)=XG2(I)
  268 X3(N+I)=XG3(I)
C  BEGIN CONSIDERING THE TIME VARIANT OUTPUTS FOR PLOTTING.
C          DEFINE THE WHEEL CIRCUMFERENCES.(NSEG STRAIGHT LINES EACH)
  270 N10DEG=36/NSEGS
      DO 275 K=1,NSEGS
      I=N10DEG*(K-1)+1
      J=NTOTAL+K
      X1(J)=XLI(1)+RADR*(C(I)*ALRI(3,1)+S(I)*ALRI(1,1))
      X2(J)=XLI(2)+RADR*(C(I)*ALRI(3,2)+S(I)*ALRI(1,2))
      X3(J)=XLI(3)+RADR*(C(I)*ALRI(3,3)+S(I)*ALRI(1,3))
      J=NTOTAL+NSEGS+K
      X1(J)=XRI(1)+RADR*(C(I)*ARRI(3,1)+S(I)*ARRI(1,1))
      X2(J)=XRI(2)+RADR*(C(I)*ARRI(3,2)+S(I)*ARRI(1,2))
      X3(J)=XRI(3)+RADR*(C(I)*ARRI(3,3)+S(I)*ARRI(1,3))
      J=NTOTAL+2*NSEGS+K
      X1(J)=XLFI(1)+RADF*(C(I)*ALFI(3,1)+S(I)*ALFI(1,1))
      X2(J)=XLFI(2)+RADF*(C(I)*ALFI(3,2)+S(I)*ALFI(1,2))
      X3(J)=XLFI(3)+RADF*(C(I)*ALFI(3,3)+S(I)*ALFI(1,3))
      J=NTOTAL+3*NSEGS+K
      X1(J)=XRFI(1)+RADF*(C(I)*ARFI(3,1)+S(I)*ARFI(1,1))
      X2(J)=XRFI(2)+RADF*(C(I)*ARFI(3,2)+S(I)*ARFI(1,2))
  275 X3(J)=XRFI(3)+RADF*(C(I)*ARFI(3,3)+S(I)*ARFI(1,3))
C     ... PUNCH INFORMATION FOR THIS SPECIFIC TIME.
      PUNCH 272,  TIME
  272 FORMAT (F10.5,50X,'TIME')
C     ... PUNCH THE COORDINATE POINTS IN THE ORDER DESCRIBED ABOVE,
C                 ALSO IDENTIFY EACH WITH ITS NEW NUMBER.
      PUNCH 277, (XBI(I),I=1,3),(XLI(I),I=1,3),(XRI(I),I=1,3),
     $(XFI(I),I=1,3),(XLFI(I),I=1,3),(XRFI(I),I=1,3)
  277 FORMAT (4X,'1',3F10.3,4X,'2',3F10.3/4X,'3',3F10.3,4X,'4',3F10.3/
```

Figure C-8 (continued).

```
     %4X,'5',3F10.3,4X,'6',3F10.3)
      PUNCH 278, (I,X1(I-7),X2(I-7),X3(I-7),I=8,NPTS)
  278 FORMAT (4X,'7',5X,'0.000',5X,'0.000',5X,'0.000',I5,3F10.3/
     %(I5,3F10.3,I5,3F10.3))
  300 CONTINUE
      RETURN
      END
      SUBROUTINE DHPCG(PRMT,Y,DERY,NDIM,IHLF,FCT,OUTP,AUX)
C
C
      DIMENSION PRMT(5),Y(NDIM),DERY(NDIM),AUX(16,NDIM)
      DOUBLE PRECISION Y,DERY,AUX,PRMT,X,H,Z,DELT,DABS
      DIMENSION IHLFEQ(14)
      DATA IHLFEQ /1024,512,256,128,64,32,16,8,4,2,1,0,0,0/
      COMMON/IO/ICOUNT
C...     INITIALIZE INTEGER STEP COUNTER. COMPENSATE FOR THE OUTPUT
C        OF THE STARTING VALUES. OUTPUT STEPS OF SIZE PRMT(3) OCCUR
C        AT INTEGER MULTIPLES OF 1024 IN ICOUNT
      ICOUNT = -1024
      N=1
      IHLF=0
      X=PRMT(1)
      H=PRMT(3)
      PRMT(5)=0.D0
      DO 1 I=1,NDIM
      AUX(16,I)=0.D0
      AUX(15,I)=DERY(I)
    1 AUX(1,I)=Y(I)
      IF(H*(PRMT(2)-X))3,2,4
C
C     ERROR RETURNS
    2 IHLF=12
      GOTO 4
    3 IHLF=13
C
C     COMPUTATION OF DERY FOR STARTING VALUES
    4 CALL FCT(X,Y,DERY)
C
C     RECORDING OF STARTING VALUES
C...     UPDATE THE INTEGER MEASURE OF X
      ICOUNT = ICOUNT + IHLFEQ(IHLF+1)
      CALL OUTP(X,Y,DERY,IHLF,NDIM,PRMT)
      IF(PRMT(5))6,5,6
    5 IF(IHLF)7,7,6
    6 RETURN
    7 DO 8 I=1,NDIM
    8 AUX(8,I)=DERY(I)
C
C     COMPUTATION OF AUX(2,I)
      ISW=1
      GOTO 100
C
    9 X=X+H
      DO 10 I=1,NDIM
   10 AUX(2,I)=Y(I)
```

Figure C-8 (continued).

```
C
C       INCREMENT H IS TESTED BY MEANS OF BISECTION
    11 IHLF=IHLF+1
       X=X-H
       DO 12 I=1,NDIM
    12 AUX(4,I)=AUX(2,I)
       H=.5D0*H
       N=1
       ISW=2
       GOTO 100
C
    13 X=X+H
       CALL FCT(X,Y,DERY)
       N=2
       DO 14 I=1,NDIM
       AUX(2,I)=Y(I)
    14 AUX(9,I)=DERY(I)
       ISW=3
       GOTO 100
C
C       COMPUTATION OF TEST VALUE DELT
    15 DELT=0.D0
       DO 16 I=1,NDIM
    16 DELT=DELT+AUX(15,I)*DABS(Y(I)-AUX(4,I))
       DELT= .6666666666666667D-1*DELT
       IF(DELT-PRMT(4))19,19,17
    17 IF(IHLF-10)11,18,18
C
C       NO SATISFACTORY ACCURACY AFTER 10 BISECTIONS. ERROR MESSAGE.
    18 IHLF=11
       X=X+H
       GOTO 4
C
C       THERE IS SATISFACTORY ACCURACY AFTER LESS THAN 11 BISECTIONS.
    19 X=X+H
       CALL FCT(X,Y,DERY)
       DO 20 I=1,NDIM
       AUX(3,I)=Y(I)
    20 AUX(10,I)=DERY(I)
       N=3
       ISW=4
       GOTO 100
C
    21 N=1
       X=X+H
       CALL FCT(X,Y,DERY)
       X=PRMT(1)
       DO 22 I=1,NDIM
       AUX(11,I)=DERY(I)
   220Y(I)=AUX(1,I)+H*(.375D0*AUX(8,I)+.7916666666666667D0*AUX(9,I)
     1-.2083333333333333D0 *AUX(10,I)+ .4166666666666667D-1*DERY(I))
    23 X=X+H
       N=N+1
       CALL FCT(X,Y,DERY)
C...      UPDATE THE INTEGER MEASURE OF X
```

Figure C-8 (continued).

```
      ICOUNT = ICOUNT + IHLFEQ(IHLF+1)
      CALL OUTP(X,Y,DERY,IHLF,NDIM,PRMT)
      IF(PRMT(5))6,24,6
   24 IF(N-4)25,200,200
   25 DO 26 I=1,NDIM
      AUX(N,I)=Y(I)
   26 AUX(N+7,I)=DERY(I)
      IF(N-3)27,29,200
C
   27 DO 28 I=1,NDIM
      DELT=AUX(9,I)+AUX(9,I)
      DELT=DELT+DELT
   28 Y(I)=AUX(1,I)+.33333333333333333D0 *H*(AUX(8,I)+DELT+AUX(10,I))
      GOTO 23
C
   29 DO 30 I=1,NDIM
      DELT=AUX(9,I)+AUX(10,I)
      DELT=DELT+DELT+DELT
   30 Y(I)=AUX(1,I)+.375D0*H*(AUX(8,I)+DELT+AUX(11,I))
      GOTO 23
C
C
C     *****************************************************************
C     THE FOLLOWING PART OF SUBROUTINE DHPCG COMPUTES BY MEANS OF
C     RUNGE-KUTTA METHOD STARTING VALUES FOR THE NOT SELF-STARTING
C     PREDICTOR-CORRECTOR METHOD.
  100 DO 101 I=1,NDIM
      Z=H*AUX(N+7,I)
      AUX(5,I)=Z
  101 Y(I)=AUX(N,I)+.4D0*Z
C     Z IS AN AUXILIARY STORAGE LOCATION
C
      Z=X+.4D0*H
      CALL FCT(Z,Y,DERY)
      DO 102 I=1,NDIM
      Z=H*DERY(I)
      AUX(6,I)=Z
  102 Y(I)=AUX(N,I)+.29697760924775360D0 *AUX(5,I)+.15875964497103583D0 *Z
C
      Z=X+.45573725421878943D0 *H
      CALL FCT(Z,Y,DERY)
      DO 103 I=1,NDIM
      Z=H*DERY(I)
      AUX(7,I)=Z
  103 Y(I)=AUX(N,I)+.21810038822592047D0 *AUX(5,I)-3.0509651486929308D0 *
     1AUX(6,I)+3.8328647604670100D0 *Z
C
      Z=X+H
      CALL FCT(Z,Y,DERY)
      DO 104 I=1,NDIM
 104OY(I)=AUX(N,I)+.17476028226269037D0 *AUX(5,I)-.55148066287873294D0 *
     1AUX(6,I)+1.2055355993965235D0 *AUX(7,I)+.17118478121951903D0 *
     2H*DERY(I)
      GOTO(9,13,15,21),ISW
C     *****************************************************************
```

Figure C-8 (continued).

```
C
C
C     POSSIBLE BREAK-POINT FOR LINKAGE
C
C
C     STARTING VALUES ARE COMPUTED.
C     NOW START HAMMINGS MODIFIED PREDICTOR-CORRECTOR METHOD.
  200 ISTEP=3
  201 IF(N-8)204,202,204
C
C     N=8 CAUSES THE ROWS OF AUX TO CHANGE THEIR STORAGE LOCATIONS
  202 DO 203 N=2,7
      DO 203 I=1,NDIM
      AUX(N-1,I)=AUX(N,I)
  203 AUX(N+6,I)=AUX(N+7,I)
      N=7
C
C     N LESS THAN 8 CAUSES N+1 TO GET N
  204 N=N+1
C
C     COMPUTATION OF NEXT VECTOR Y
      DO 205 I=1,NDIM
      AUX(N-1,I)=Y(I)
  205 AUX(N+6,I)=DERY(I)
      X=X+H
  206 ISTEP=ISTEP+1
      DO 207 I=1,NDIM
     0DELT=AUX(N-4,I)+1.3333333333333333D0 *H*(AUX(N+6,I)+AUX(N+6,I)-
     1AUX(N+5,I)+AUX(N+4,I)+AUX(N+4,I))
      Y(I)=DELT-.9256198347107438D0*AUX(16,I)
  207 AUX(16,I)=DELT
C     PREDICTOR IS NOW GENERATED IN ROW 16 OF AUX, MODIFIED PREDICTOR
C     IS GENERATED IN Y. DELT MEANS AN AUXILIARY STORAGE.
C
      CALL FCT(X,Y,DERY)
C     DERIVATIVE OF MODIFIED PREDICTOR IS GENERATED IN DERY
C
      DO 208 I=1,NDIM
     0DELT=.125D0*(9.D0*AUX(N-1,I)-AUX(N-3,I)+3.D0*H*(DERY(I)+AUX(N+6,I)
     1+AUX(N+6,I)-AUX(N+5,I)))
      AUX(16,I)=AUX(16,I)-DELT
  208 Y(I)=DELT+.0743801652892562D0 *AUX(16,I)
C
C     TEST WHETHER H MUST BE HALVED OR DOUBLED
      DELT=0.D0
      DO 209 I=1,NDIM
  209 DELT=DELT+AUX(15,I)*DABS(AUX(16,I))
      IF(DELT-PRMT(4))210,222,222
C
C     H MUST NOT BE HALVED. THAT MEANS Y(I) ARE GOOD.
  210 CALL FCT(X,Y,DERY)
C...     UPDATE THE INTEGER MEASURE OF X
      ICOUNT = ICOUNT + IHLFEQ(IHLF+1)
      CALL OUTP(X,Y,DERY,IHLF,NDIM,PRMT)
      IF(PRMT(5))212,211,212
```

Figure C-8 (continued).

```
      211 IF(IHLF-11)213,212,212
      212 RETURN
      213 IF(H*(X-PRMT(2)))214,212,212
      214 IF(DABS(X-PRMT(2))-.1D0*DABS(H))212,215,215
      215 IF(DELT-.02D0*PRMT(4))216,216,201
C
C
C     H COULD BE DOUBLED IF ALL NECESSARY PRECEEDING VALUES ARE
C     AVAILABLE
      216 IF(IHLF)201,201,217
      217 IF(N-7)201,218,218
      218 IF(ISTEP-4)201,219,219
C...      DOUBLE THE STEP SIZE ONLY IF CURRENT X VALUE COULD HAVE BEEN
C         REACHED BY AN INTEGER NUMBER OF EQUIVALENT STEPS (OF THE
C         DOUBLED SIZE).
      219 IF(ICOUNT.NE.(ICOUNT/IHLFEQ(IHLF))*IHLFEQ(IHLF)) GO TO 201
      220 H=H+H
          IHLF=IHLF-1
          ISTEP=0
          DO 221 I=1,NDIM
          AUX(N-1,I)=AUX(N-2,I)
          AUX(N-2,I)=AUX(N-4,I)
          AUX(N-3,I)=AUX(N-6,I)
          AUX(N+6,I)=AUX(N+5,I)
          AUX(N+5,I)=AUX(N+3,I)
          AUX(N+4,I)=AUX(N+1,I)
          DELT=AUX(N+6,I)+AUX(N+5,I)
          DELT=DELT+DELT+DELT
      2210AUX(16,I)=8.962962962962963D0*(Y(I)-AUX(N-3,I))
         1-3.361111111111111D0 *H*(DERY(I)+DELT+AUX(N+4,I))
          GOTO 201
C
C
C     H MUST BE HALVED
      222 IHLF=IHLF+1
          IF(IHLF-10)223,223,210
      223 H=.5D0*H
          ISTEP=0
          DO 224 I=1,NDIM
         0Y(I)=.390625D-2*(8.D1*AUX(N-1,I)+135.D0*AUX(N-2,I)+4.D1*AUX(N-3,I)
         1+AUX(N-4,I))-.1171875D0*(AUX(N+6,I)-6.D0*AUX(N+5,I)-AUX(N+4,I))*H
         0AUX(N-4,I)=.390625D-2*(12.D0*AUX(N-1,I)+135.D0*AUX(N-2,I)+
         1108.D0*AUX(N-3,I)+AUX(N-4,I))-.0234375D0*(AUX(N+6,I)+
         218.D0*AUX(N+5,I)-9.D0*AUX(N+4,I))*H
          AUX(N-3,I)=AUX(N-2,I)
      224 AUX(N+4,I)=AUX(N+5,I)
          X=X-H
          DELT=X-(H+H)
          CALL FCT(DELT,Y,DERY)
          DO 225 I=1,NDIM
          AUX(N-2,I)=Y(I)
          AUX(N+5,I)=DERY(I)
      225 Y(I)=AUX(N-4,I)
          DELT=DELT-(H+H)
          CALL FCT(DELT,Y,DERY)
```

Figure C-8 (continued).

```
      DO 226 I=1,NDIM
      DELT=AUX(N+5,I)+AUX(N+4,I)
      DELT=DELT+DELT+DELT
     0AUX(16,I)=8.962962962962963D0*(AUX(N-1,I)-Y(I))
     1-3.361111111111111D0 *H*(AUX(N+6,I)+DELT+DERY(I))
  226 AUX(N+3,I)=DERY(I)
      GOTO 206
      END
      SUBROUTINE DERIV(T,Y,DYDT)
      IMPLICIT REAL*8(A-H,O-Z)
      COMMON /MSD/ TENG,SENG,TCLUT,SCLUT,RRBT,RPBT,RFPF,RRFF,TEFF,
     %RATIOT,RATIOD,WB,WF,WR,INIT
      COMMON /MSDD/ APT,RADR,RADF
      COMMON /MD/ RHOFBT,RHOFLT,RHOFRT,RHOFFF,PB,PL,PR,PF,
     %FB1,FL1,FR1,FF1,FB2,FL2,FR2,FF2,FB3,FL3,FR3,FF3,
     $RLBT,RLFF,THMAX,ALENG,CASTER,CAMBER,TOEIN,SLENG,SK,SC,
     %ITYPEB,ITYPEL,ITYPER,ITYPEF,NFBOD,NFLR,NFRR,NFFE
      COMMON /MOD/ IFF,IRP,ID,IE,MB,MR,MF
      COMMON /SOD/ IBP
      COMMON /DOW/ ATI
      COMMON /OD/ API,AFI,ALRI,ARRI,ALFI,ARFI,XBI,XLI,XRI,XFI,XLFI,
     %VBI,VLI,VRI,VFI,OMBI,OMLI,OMRI,OMFI,OMBP,OMLP,OMRP,OMFF,XRFI
      COMMON /OD/ FLGI,FRGI,FLFGI,FRFGI,STEER,ISTOP
      DIMENSION ALRI(3,3),ARRI(3,3),ALFI(3,3),ARFI(3,3)
      DIMENSION API(3,3),APT(3,3),ATI(3,3),AFI(3,3),AWI(3,3)
      DIMENSION AIF(3,3),APF(3,3),Y(20),DYDT(20)
      DIMENSION XBI(3),XLI(3),XRI(3),XPI(3),XFI(3),XLFI(3),XRFI(3)
      DIMENSION VBI(3),VLI(3),VRI(3),VPI(3),VFI(3)
      DIMENSION OMBI(3),OMLI(3),OMRI(3),OMFI(3)
      DIMENSION OMBP(3),OMLP(3),OMRP(3),OMFF(3),OMBF(3)
      DIMENSION RLBP(3),RRBP(3),RPBP(3),RSFI(3),RSBI(3)
      DIMENSION RLBI(3),RRBI(3),RPBI(3),RFPI(3),RLFI(3),RRFI(3),RLFPI(3)
      DIMENSION RLBT(3),RRBT(3),RPBT(3),RFPF(3),RLFF(3),RRFF(3),RRFPI(3)
      DIMENSION FBEI(3),FLGI(3),FRGI(3),FFGI(3),FLFGI(3),FRFGI(3)
      DIMENSION TQLFGI(3),TQRFGI(3)
      DIMENSION RHOFBT(5,3),RHOFLT(5,3),RHOFRT(5,3),RHOFFF(5,3)
      DIMENSION PB(5,3),PL(5,3),PR(5,3),PF(5,3),FB1(5),FL1(5),FR1(5),
     %FF1(5),FB2(5),FL2(5),FR2(5),FF2(5),FB3(5),FL3(5),FR3(5),FF3(5)
      DIMENSION FI(3),TQI(3)
      DIMENSION ITYPEB(5),ITYPEL(5),ITYPER(5),ITYPEF(5)
      DIMENSION ORPI(3),ORFI(3),ORLI(3),ORRI(3),WFI(3),WBI(3),WRI(3)
      DIMENSION DB(3),DF(3),B(7,7),CB(3),CF(3),CL(3),CR(3),GB(3),GF(3)
      DIMENSION RMI(3),FTI(3),EF(3)
      DIMENSION C(7),X(7),ORMI(3),FBSI(3)
      DIMENSION SENG(5),TENG(5),TCLUT(5),SCLUT(5)
      REAL*8 IFF(3,3),IBP(3),IRP(3)
      REAL*8 MOBEI(3),MOLGI(3),MORGI(3),MOFGI(3),MOLFGI(3),MORFGI(3)
      REAL*8 MOBEP(3),MOLGP(3),MORGP(3),MOFGF(3),MOBSI(3),MOFSI(3)
      REAL*8 ID,IE,IR1,IR2,IR3,MB,MR,MF
C  DEFINE THE PRINCIPAL AXIS WHICH CORRESPONDS TO THE REAR AXLE DIRECTION.
      IAXLE=1
      AMAX=DABS(APT(1,2))
      DO 10 I=2,3
      ATEST=DABS(APT(I,2))
      IF(ATEST.GT.AMAX) IAXLE=I
```

Figure C-8 (continued).

```
      10 CONTINUE
         IR1=0.25D0*ID*RATIOD**2
         IR2=IR1+IRP(IAXLE)
         IR3=IRP(IAXLE)**2+0.5D0*IRP(IAXLE)*ID*RATIOD**2
         CALL DIRCOS(Y(10),Y(11),Y(12),Y(13),API)
         CALL MULT33(APT,API,-1,ATI)
         CALL ROTATE(ATI,Y(19),1,AFI)
         DO 11 I=1,3
         DO 11 J=1,3
      11 AIF(I,J)=AFI(J,I)
C     IS THE FRONTEND AGAINST A STOP?
C             ISTOP: 0=FREE, 1=AGAINST RIGHT, -1=AGAINST LEFT "STOP".
         ISTOP=0
         IF(DABS(Y(19)).LT.THMAX) GO TO 12
         ISTOP=1
         IF(Y(19).GT.0.0D0) ISTOP=-1
      12 CALL MULT33(API,AIF,1,APF)
         CALL MULT31(APT,RLBT,1,RLBP)
         CALL MULT31(APT,RRBT,1,RRBP)
         CALL MULT31(APT,RPBT,1,RPBP)
         CALL MULT31(ATI,RLBT,-1,RLBI)
         CALL MULT31(ATI,RRBT,-1,RRBI)
         CALL MULT31(ATI,RPBT,-1,RPBI)
         CALL MULT31(AFI,RFPF,-1,RFPI)
         CALL MULT31(AFI,RLFF,-1,RLFI)
         CALL MULT31(AFI,RRFF,-1,RRFI)
C     DEFINE POSITIONS OF THE WHEEL CENTERS AND THE FRONT END PIN & C.G.
         DO 20 I=1,3
         XBI(I)=Y(I+3)
         XLI(I)=XBI(I)+RLBI(I)
         XRI(I)=XBI(I)+RRBI(I)
         XPI(I)=XBI(I)+RPBI(I)
         XFI(I)=XPI(I)+RFPI(I)
      20 VBI(I)=Y(I)
C     DEFINE THE ANGULAR VELOCITIES (RADIANS/SEC).
         DO 21 I=1,3
         OMBP(I)=Y(I+6)
         OMLP(I)=OMBP(I)
      21 OMRP(I)=OMBP(I)
         OMLP(IAXLE)=Y(14)
         OMRP(IAXLE)=Y(16)
         CALL MULT31(API,OMBP,-1,OMBI)
         CALL MULT31(AFI,OMBI,1,OMBF)
         OMFF(1)=Y(18)
         DO 22 I=2,3
      22 OMFF(I)=OMBF(I)
         CALL MULT31(AFI,OMFF,-1,OMFI)
         CALL CROSS(OMBI,RLBI,VLI)
         CALL CROSS(OMBI,RRBI,VRI)
         CALL CROSS(OMBI,RPBI,VPI)
         CALL CROSS(OMFI,RFPI,VFI)
         DO 25 I=1,3
         VLI(I)=VBI(I)+VLI(I)
         VRI(I)=VBI(I)+VRI(I)
         VPI(I)=VBI(I)+VPI(I)
```

Figure C-8 (continued).

```
   25 VFI(I)=VPI(I)+VFI(I)
C  BEGIN DEFINITION OF ACCELERATION-INDEPENDENT VARIABLES.
C  REACTIONS OCCUR AT THE WHEELS AND MAY BE SPECIFIED ELSEWHERE.
C          ... EXTERNAL REACTIONS ON THE TRACTOR BODY
      DO 251 I=1,3
      MOBEI(I)=0.0D0
  251 FBEI(I)=0.0D0
      IF(NFBOD.NE.0) CALL FORTQ(ATI,XBI,VBI,OMBI,RHOFBT,PB,FB1,FB2,FB3,
     %ITYPEB,NFBOD,FBEI,MOBEI)
      IF(ISTOP.EQ.0) GO TO 2519
C              THE TRACTOR FRONT END IS AGAINST A STOP.
C               ... LOCATE THE POINT OF CONTACT, S.
      DO 2510 I=1,3
      RSFI(I)=-RFPI(I)-AFI(2,I)*DSIGN(SLENG,Y(19))
 2510 RSBI(I)= RPBI(I)-AFI(2,I)*DSIGN(SLENG,Y(19))
      SDEF=SLENG*(DABS(Y(19))-THMAX)
      SVEL=(OMFF(1)-OMBF(1))*DSIGN(SLENG,Y(19))
C               ... DEFINE THE REACTION AS FOR A SPRING IN PARALLEL
C                       WITH A RELAXATION-ONLY DASHPOT.
      FS=SK*SDEF
      IF(SVEL.LT.0.0D0) FS=FS+SC*SVEL
      IF(FS.LT.0.0D0) FS=0.0D0
      DO 2512 I=1,3
 2512 FBSI(I)=-FS*AFI(3,I)
      CALL CROSS(RSBI,FBSI,MOBSI)
      DO 2513 I=1,3
      FBEI(I)=FBEI(I)+FBSI(I)
 2513 MOBEI(I)=MOBEI(I)+MOBSI(I)
 2519 CALL MULT31(API,MOBEI,1,MOBEP)
C          ... REACTIONS ON THE LEFT REAR WHEEL
C               ... GROUND FORCES
      CALL WHEEL(ATI,XBI,VBI,RLBI,OMBI,OMLP(IAXLE),RADR,1,FLGI,MOLGI)
      CALL ROTATE(ATI,Y(15),2,ALRI)
      CALL MULT31(API,OMLP,-1,OMLI)
C               ... EXTERNAL REACTIONS
      IF(NFLR.EQ.0) GO TO 253
      CALL FORTQ(ALRI,XLI,VLI,OMLI,RHOFLT,PL,FL1.FL2,FL3,ITYPEL,NFLR,
     %FI,TQI)
      DO 252 I=1,3
      FLGI(I)=FLGI(I)+FI(I)
  252 MOLGI(I)=MOLGI(I)+TQI(I)
  253 CALL MULT31(API,MOLGI,1,MOLGP)
C         ... REACTIONS ON THE RIGHT REAR WHEEL
C               ... GROUND FORCES
      CALL WHEEL(ATI,XBI,VBI,RRBI,OMBI,OMRP(IAXLE),RADR,1,FRGI,MORGI)
      CALL ROTATE(ATI,Y(17),2,ARRI)
      CALL MULT31(API,OMRP,-1,OMRI)
C               ... EXTERNAL REACTIONS
      IF(NFRR.EQ.0) GO TO 255
      CALL FORTQ(ARRI,XRI,VRI,OMRI,RHOFRT,PR,FR1,FR2,FR3,ITYPER,NFRR,
     %FI,TQI)
      DO 254 I=1,3
      FRGI(I)=FRGI(I)+FI(I)
  254 MORGI(I)=MORGI(I)+TQI(I)
  255 CALL MULT31(API,MORGI,1,MORGP)
```

Figure C-8 (continued).

```
C           ... REACTIONS ON THE TRACTOR FRONTEND
C                   DETERMINE PERTINENT FRONTEND AND WHEEL LOCATIONS.
C                   THE FRONT WHEEL STEER ANGLE IS IN RADIANS.
      CALL TURN(T,Y,STEER)
C                         LEFT FRONT WHEEL
      CALL ROTATE(AFI,CASTER,2,ALFI)
      THETAR=-CAMBER
      IF(CAMBER.NE.0.0D0) CALL ROTATE(ALFI,THETAR,1,ALFI)
      THETAR=STEER+TOEIN
      IF(THETAR.NE.0.0D0) CALL ROTATE(ALFI,THETAR,3,ALFI)
      DO 259 I=1,3
      RLFPI(I)=RFPI(I)+RLFI(I)-ALENG*ALFI(2,I)
  259 XLFI(I)=XPI(I)+RLFPI(I)
      CALL WHEEL(ALFI,XPI,VPI,RLFPI,OMFI,OMLP(IAXLE),RADF,0,FLFGI,MOLFGI
     %)
C                         RIGHT FRONT WHEEL
      CALL ROTATE(AFI,CASTER,2,ARFI)
      IF(CAMBER.NE.0.0D0) CALL ROTATE(ARFI,CAMBER,1,ARFI)
      THETAR=STEER-TOEIN
      IF(THETAR.NE.0.0D0) CALL ROTATE(ARFI,THETAR,3,ARFI)
      DO 260 I=1,3
      RRFPI(I)=RFPI(I)+RRFI(I)+ALENG*ARFI(2,I)
  260 XRFI(I)=XPI(I)+RRFPI(I)
      CALL WHEEL(ARFI,XPI,VPI,RRFPI,OMFI,OMRP(IAXLE),RADF,0,FRFGI,MORFGI
     %)
      CALL CROSS(RLFI,FLFGI,TQLFGI)
      CALL CROSS(RRFI,FRFGI,TQRFGI)
      DO 262 I=1,3
      FI(I)=0.0D0
  262 TQI(I)=0.0D0
C                 EXTERNAL FORCES
      IF(NFFE.EQ.0) GO TO 263
      CALL FORTQ(AFI,XFI,VFI,OMFI,RHOFFF,PF,FF1,FF2,FF3,ITYPEF,NFFE,
     %FI,TQI)
  263 IF(ISTOP.EQ.0) GO TO 265
C                ADD THE REACTION OF THE BODY AT THE "STOP".
      CALL CROSS(RSFI,FBSI,MOFSI)
      DO 264 I=1,3
      FI(I)=FI(I)-FBSI(I)
  264 TQI(I)=TQI(I)-MOFSI(I)
  265 DO 27 I=1,3
      MOFGI(I)=MOLFGI(I)+MORFGI(I)+TQLFGI(I)+TQRFGI(I)+TQI(I)
   27 FFGI(I)=FLFGI(I)+FRFGI(I)+FI(I)
      CALL MULT31(AFI,MOFGI,1,MOFGF)
C  DEFINE THE DERIVATIVES FOR WHEEL AND ENGINE ANGULAR SPEEDS.
      TE=TABLE(SENG,TENG,Y(20),2,5,1)
      SPEEDC=0.5D0*RATIOT*RATIOD*(OMLP(IAXLE)+OMRP(IAXLE)-2.0D0*       3-38
     $OMSP(IAXLE))
      IF(INIT.LE.2) GO TO 30
C  CLUTCH IS DISENGAGED WHEN  INIT.LE.2
      SLIPC=1.0D0-DABS(SPEEDC)/Y(20)
      TC=TABLE(SCLUT,TCLUT,SLIPC,2,5,1)
      GO TO 31
   30 TC=0.0D0
   31 TD=TEFF*RATIOT*TC
```

Figure C-8 (continued).

```
      CALL DBLCRS(OMBI,RPBI,ORPI)
      CALL DBLCRS(OMFI,RFPI,ORFI)
      CALL DBLCRS(OMBI,RLBI,ORLI)
      CALL DBLCRS(OMBI,RRBI,ORRI)
      EN=MOFGF(1)-(IFF(3,3)-IFF(2,2))*OMFF(2)*OMFF(3)-IFF(1,3)*OMFF(1)*
     %OMFF(2)
      DO 801 I=1,3
      RMI(I)=MF*RPBI(I)+MR*(RLBI(I)+RRBI(I))
      IF(I.EQ.3) GO TO 790
      WFI(I)=0.0D0
      WBI(I)=0.0D0
      WRI(I)=0.0D0
      GO TO 791
  790 WFI(I)=WF
      WBI(I)=WB
      WRI(I)=WR
  791 CONTINUE
      FTI(I)=FBEI(I)+FFGI(I)+FLGI(I)+FRGI(I)+WBI(I)+WFI(I)+2.0D0*WRI(I)
      EF(I)=RFPF(2)*AFI(3,I)-RFPF(3)*AFI(2,I)
  801 EN=EN-(RFPF(2)*AFI(3,I)-RFPF(3)*AFI(2,I))*(MF*ORPI(I)+MF*ORFI(I)
     %-FFGI(I)-WFI(I))
      CALL DBLCRS(OMBI,RMI,ORMI)
      GF(1)=IFF(1,1)
      DO 805 I=1,3
      IF(I.NE.1) GF(I)=0.0D0
      GB(I)=IFF(1,3)*APF(I,3)
      DO 805 L=1,3
      M=L-1+3*((3-L)/2)
      N=L+1-3*((L-1)/2)
      GB(I)=GB(I)+MF*API(I,L)*(EF(M)*RPBI(N)-EF(N)*RPBI(M))
  805 GF(I)=GF(I)+MF*AFI(I,L)*(EF(M)*RFPI(N)-EF(N)*RFPI(M))
      DO 900 I=1,3
      J=I-1+3*((3-I)/2)
      K=I+1-3*((I-1)/2)
C          DEFINE CONSTANTS ON RIGHT HAND SIDE.
      DO 810 N=1,3
      CB(N)=APF(I,2)*IFF(2,2)*APF(N,2)+APF(I,3)*IFF(3,3)*APF(N,3)
      CF(N)=APF(I,2)*(RFPF(3)*AFI(1,N)-RFPF(1)*AFI(3,N))+APF(I,3)*
     %(RFPF(1)*AFI(2,N)-RFPF(2)*AFI(1,N))+RPBP(K)*API(J,N)-RPBP(J)*
     $API(K,N)
      CL(N)=RLBP(K)*API(J,N)-RLBP(J)*API(K,N)
  810 CR(N)=RRBP(K)*API(J,N)-RRBP(J)*API(K,N)
      CN=MOBEP(I)-(IBP(J)-IBP(K))*OMBP(J)*OMBP(K)-APF(I,2)*((IFF(1,1)
     %-IFF(3,3))*OMFF(1)*OMFF(3)+IFF(1,3)*(OMFF(3)**2-OMFF(1)**2)
     $-MOFGF(2))-APF(I,3)*((IFF(2,2)-IFF(1,1))*OMFF(1)*OMFF(2)-IFF(1,3)*
     %OMFF(2)*OMFF(3)-MOFGF(3))
      DN=CN
      DO 812 L=1,3
      M=L-1+3*((3-L)/2)
      N=L+1-3*((L-1)/2)
      DB(L)=MF*(CF(M)*RPBI(N)-CF(N)*RPBI(M))+MR*(CL(M)*RLBI(N)-CL(N)*
     %RLBI(M))+MR*(CR(M)*RRBI(N)-CR(N)*RRBI(M))
      DF(L)=MF*(CF(M)*RFPI(N)-CF(N)*RFPI(M))
  812 DN=DN-CF(L)*(MF*ORPI(L)+MF*ORFI(L)-FFGI(L)-WFI(L))-CL(L)*(MR*
     %ORLI(L)-FLGI(L)-WRI(L))-CR(L)*(MR*ORRI(L)-FRGI(L)-WRI(L))
```

Figure C-8 (continued).

```
C  BEGIN DEFINITION OF COEFFICIENTS IN THE 7-BY-7 MATRIX.
      B(I,I)=MB+MF+2.0D0*MR
      DO 814 L=1,3
      IF(I.NE.L) B(I,L)=0.0D0
      B(I,L+3)=API(L,K)*RMI(J)-API(L,J)*RMI(K)+MF*(APF(L,2)*(AFI(2,K)*
     %RFPI(J)-AFI(2,J)*RFPI(K))+APF(L,3)*(AFI(3,K)*RFPI(J)-AFI(3,J)*
     $RFPI(K)))
      B(I+3,L)=MF*CF(L)+MR*CL(L)+MR*CR(L)
      B(I+3,L+3)=CB(L)
      DO 813 N=1,3
  813 B(I+3,L+3)=B(I+3,L+3)+DF(N)*(AFI(2,N)*APF(L,2)+AFI(3,N)*APF(L,3))
     %+DB(N)*API(L,N)
  814 CONTINUE
      B(7,I)=MF*EF(I)
      B(7,I+3)=GS(I)+GF(2)*APF(I,2)+GF(3)*APF(I,3)
      B(I+3,7)=IFF(1,3)*APF(I,3)+DF(1)*AFI(1,1)+DF(2)*AFI(1,2)+DF(3)*
     %AFI(1,3)
      B(I,7)=MF*(AFI(1,K)*RFPI(J)-AFI(1,J)*RFPI(K))
      B(I+3,I+3)=B(I+3,I+3)+IBP(I)
      IF(I.NE.IAXLE) B(I+3,I+3)=B(I+3,I+3)+2.0D0*IRP(I)
      C(I)=FTI(I)-ORMI(I)-MF*ORFI(I)
      C(I+3)=DN
      IF(I.NE.IAXLE) C(I+3)=C(I+3)+MOLGP(I)+MORGP(I)-(IRP(J)-IRP(K))*
     %(OMLP(J)*OMLP(K)+OMRP(J)*OMRP(K))
      IF(I.EQ.IAXLE) C(I+3)=C(I+3)+RATIOD*TD
  900 CONTINUE
      B(7,7)=GF(1)
      C(7)=EN
C  BEGIN DEFINITION OF ACCELERATION-DEPENDENT VARIABLES.
      CALL SOLVE(7,B,C,X)
      DO 70 I=1,3
      DYDT(I)=X(I)
      DYDT(I+3)=Y(I)
   70 DYDT(I+6)=X(I+3)
      DYDT(18)=X(7)
      DYDT(10)=0.5D0*(-Y(7)*Y(11)-Y(8)*Y(12)-Y(9)*Y(13))
      DYDT(11)=0.5D0*(Y(7)*Y(10)-Y(8)*Y(13)+Y(9)*Y(12))
      DYDT(12)=0.5D0*(Y(8)*Y(10)-Y(9)*Y(11)+Y(7)*Y(13))
      DYDT(13)=0.5D0*(Y(9)*Y(10)-Y(7)*Y(12)+Y(8)*Y(11))
      DYDT(14)=(IR2*(MOLGP(IAXLE)-0.5D0*RATIOD*TD)-IR1*(MORGP(IAXLE)
     %-0.5D0*RATIOD*TD))/IR3
      DYDT(15)=OMLP(IAXLE)
      DYDT(16)=(IR2*(MORGP(IAXLE)-0.5D0*RATIOD*TD)-IR1*(MOLGP(IAXLE)
     %-0.5D0*RATIOD*TD))/IR3
      DYDT(17)=OMRP(IAXLE)
      DYDT(19)=OMFF(1)-OMBF(1)
      DYDT(20)=(TE-TC)/IE
      RETURN
      END
      SUBROUTINE WHEEL(AWI,XBI,VBI,RCBI,OMCI,OMW,RAD,ITR,FWGI,MOWGI)
      IMPLICIT REAL*8(A-H,O-Z)
      COMMON /MW/ SLOPER,SLANR,SLOPEF,SLANF
      COMMON /MSW/ COTR,SWHEEL,FREAR,DREAR,FFRONT,DFRONT,
     %AF,BF,DMPF,AR,BR,DMFR
      COMMON /DOW/ ATI
```

Figure C-8 (continued).

```
      DIMENSION ATI(3,3),AWI(3,3),UWI(3),UGI(3),URI(3),ULI(3),UWGI(3)
      DIMENSION XBI(3),VBI(3),XCI(3),VCI(3),XWI(3),XGI(3),XWGI(3)
      DIMENSION XWPI(3),XGPI(3),UGPI(3),FRPI(3),RWPI(3),RVEC(3)
      DIMENSION URPI(3),XWPII(3)
      REAL*4 FLOAT
      DIMENSION RCBI(3),RWGCI(3),VWGT(3),VWGI(3),OMCI(3)
      DIMENSION VPLANE(3),UDIFF(3),FWGI(3)
      DIMENSION DREAR(5),FREAR(5),DFRONT(5),FFRONT(5),COTR(5),SWHEEL(5)
      DIMENSION SLOPER(5),SLANR(5),SLOPEF(5),SLANF(5)
      REAL*8 MOWGI(3)
C  THIS ROUTINE DETERMINES THE REACTIONS ON THE GIVEN WHEEL.
C  AWI IS THE DIRECTION COSINE MATRIX DEFINING THE WHEEL COORDINATES
C          IN TERMS OF THE INERTIAL (FIXED) COORDINATES, I.E.,
C                     XW = AWI * XI .
C          UNIT VECTOR 2 IS IN THE AXLE DIRECTION (POSITIVE TO RIGHT)
C          UNIT VECTOR 3 IS IN STEER AXIS DIRECTION (POSITIVE DOWN)
C          UNIT VECTOR 1 IS DEFINED BY  UV2 (CROSS) UV3.
C  LOCATE THE POINT BENEATH THE TIRE.
      DO 10 I=1,3
      XCI(I)=XBI(I)+RCBI(I)
      UWI(I)=AWI(2,I)
      XWI(I)=XCI(I)+RAD*AWI(3,I)
   10 XGI(I)=XWI(I)
C  DEFINE THE GROUND ELEVATION AND SLOPE BENEATH THE TIRE.
      CALL SURFAC(XWI,UGI,XGI(3))
C  CHECK TO SEE WHETHER THE WHEEL IS OVER A PLANAR REGION OF THE TERRAIN.
C     ... CHECK THE TERRAIN AHEAD AND BEHIND THE WHEEL.
      DO 108 K=1,2
C          ... DEFINE THE PERIPHERAL POINT.
      DSGN=DBLE(FLOAT(2*K-3))
      DO 101 I=1,3
      XWPI(I)=XCI(I)+RAD*0.70710678D0*(AWI(3,I)-DSGN*AWI(1,I))
  101 XGPI(I)=XWPI(I)
C          ... DETERMINE THE GROUND ELEVATION AND NORMAL VECTOR.
      CALL SURFAC(XWPI,UGPI,XGPI(3))
C          ... CHECK GROUND PLANES TO SEE IF THEY ARE THE SAME.
      IF(DOT(UGI,UGPI).LT.0.999D0) GO TO 110
      DO 102 I=1,3
  102 RVEC(I)=XGI(I)-XGPI(I)
      RVMAG=DSQRT(DOT(RVEC,RVEC))
      IF(DOT(RVEC,UGI)/RVMAG.GT.5.0D-2) GO TO 110
  108 CONTINUE
      GO TO 190
C     *** THE GROUND SURFACE IS IRREGULAR ***
C          ... THE WHEEL IS MODELLED AS A SEGMENTED DISC.
C               ... SELECT 5 DEGREE INCREMENTS.
  110 NCONT=0
      THETR0=-40.0D0/57.2957795D0
      DTHETR=5.00D0/57.2957795D0
      DAREA=0.0D0
      DO 112 I=1,3
  112 FRPI(I)=0.0
      DO 130 ISEG=1,17
C              ... LOCATE A PERIPHERAL POINT.
      THETAR=THETR0+DBLE(FLOAT(ISEG-1))*DTHETR
```

Figure C-8 (continued).

```
      DO 122 I=1,3
      URPI(I)=AWI(3,I)*DCOS(THETAR)+AWI(1,I)*DSIN(THETAR)
      XWPI(I)=XCI(I)+RAD*URPI(I)
  122 XGPI(I)=XWPI(I)
C                  ... CHECK FOR TIRE-GROUND CONTACT.
      CALL SURFAC(XWPI,UGPI,XGPI(3))
      IF(XGPI(3).GE.XWPI(3)) GO TO 130
C                  ... LOCATE THE GROUND INTERSECTION WITH THE RADIAL LINE.
      DR1=2.0D-2*RAD
      DO 123 I=1,3
  123 XWP1I(I)=XCI(I)+(RAD-DR1)*URPI(I)
      CALL SURFAC(XWP1I,UGPI,ELEV1)
C                          ... USE LINEAR INTERPOLATION TO DEFINE THE POINT.
      DEFL=DR1*(XWPI(3)-XGPI(3))/(XWPI(3)-XGPI(3)+ELEV1-XWP1I(3))
C                  ... DETERMINE RADIAL FORCE FOR THIS SEGMENT.
      NCONT=NCONT+1
      IF(ITR.EQ.0) FRAD=-TABLE(DFRONT,FFRONT,DEFL,2,5,1)
      IF(ITR.NE.0) FRAD=-TABLE(DREAR,FREAR,DEFL,2,5,1)
C                  ... DETERMINE RESULTANT RADIAL FORCE.
C                      (UNIT RADIAL VECTOR IS POSITIVE AWAY FROM WHEEL CNTR)
      DAREA=DAREA+DTHETR*(RAD*DEFL-0.5D0*DEFL**2)
      DO 125 I=1,3
  125 FRPI(I)=FRPI(I)+FRAD*URPI(I)
  130 CONTINUE
      FRAD=DSQRT(DOT(FRPI,FRPI))
      IF(FRAD.EQ.0.0D0) GO TO 201
C                  ... DEFINE THE RADIAL FORCE DIRECTION.
  132 DO 133 I=1,3
  133 URI(I)=-FRPI(I)/FRAD
C                  ... AND THE ADJUSTED FORCE MAGNITUDE.
      THETAR=DBLE(FLOAT(NCONT))*DTHETR
      DEFL=2.0D0*(1.D0-DCOS(THETAR/2.D0))*DAREA/(RAD*(THETAR-DSIN(THETAR
     %)))
C            ... LOCATE THE EQUIVALENT GROUND PLANE.
      DO 134 I=1,3
  134 XWGI(I)=XCI(I)+(RAD-DEFL)*URI(I)
C            ... AND THE GROUND NORMAL VECTOR.
      CALL SURFAC(XWGI,UGI,XWPI(3))
      CALL CROSS(UWI,URI,UWGI)
      UNORM=DOT(UGI,UWGI)
      DO 135 I=1,3
  135 UGI(I)=UGI(I)-UNORM*UWGI(I)
      UGMAG=DSQRT(DOT(UGI,UGI))
      DO 136 I=1,3
  136 UGI(I)=UGI(I)/UGMAG
      GO TO 199
C     *** END SECTION FOR IRREGULAR GROUND SURFACE ***
  190 CONTINUE
C     *** BEGIN SECTION FOR SMOOTH TERRAIN ***
C THE GROUND CONTACT POINT IS THE POINT OF INTERSECTION OF 3 PLANES.
C          FIRST EQN FROM DOT OF WHEEL VECTOR AND NORMAL VECTOR = 0.
C          2ND EQN FROM DOT OF GROUND VECTOR AND NORMAL = 0.
C          3RD PLANE HAS THE SOIL NORMAL VECTOR AND THE AXLE IN THIS
C                PLANE; NORMAL VECTOR GIVEN BY CROSS PRODUCT,
      CONST1=DOT(XCI,UWI)
```

Figure C-8 (continued).

```
      A11=UWI(1)
      A12=UWI(2)
      A13=UWI(3)
      A21=UGI(1)
      A22=UGI(2)
      A23=UGI(3)
C                  UWGI = UGI (CROSS) UWI,  SO IT POINTS FORWARD.
      CALL CROSS(UGI,UWI,UWGI)
      A31=UWGI(1)
      A32=UWGI(2)
      A33=UWGI(3)
      CONST2=DOT(XGI,UGI)
      CONST3=DOT(XCI,UWGI)
C         SOLVE FOR THE COMMON POINT IN THESE 3 PLANES. (GROUND CONTACT)
      DETD=A11*A22*A33+A12*A23*A31+A21*A32*A13-A31*A22*A13-A21*A12*A33
     %-A32*A23*A11
      XWGI(1)=(CONST1*A22*A33+CONST2*A32*A13+CONST3*A12*A23
     %-CONST3*A22*A13-CONST2*A12*A33-CONST1*A32*A23)/DETD
      XWGI(2)=(A11*CONST2*A33+A21*CONST3*A13+A31*CONST1*A23
     %-A31*CONST2*A13-A21*CONST1*A33-A11*CONST3*A23)/DETD
      XWGI(3)=(A11*A22*CONST3+A21*A32*CONST1+A12*CONST2*A31
     %-A31*A22*CONST1-A21*A12*CONST3-A11*A32*CONST2)/DETD
C         *** END SECTION FOR SMOOTH TERRAIN ***
  199 CONTINUE
C   DEFINE FORCES ON THE WHEEL.
      DO 20 I=1,3
   20 RWGCI(I)=XWGI(I)-XCI(I)
      RADD=DSQRT(DOT(RWGCI,RWGCI))
      DEFL=RAD-RADD
      IF(DEFL.GT.0.0D0) GO TO 24
      DEFL=0.0D0
  201 DO 21 I=1,3
      FWGI(I)=0.0D0
   21 MOWGI(I)=0.0D0
      RETURN
C         DETERMINE THE WHEEL CENTER VELOCITY AND THE GROUND-CONTACT-
C                POINT VELOCITY: FINAL VALUES OF  VCI & VWGI, RESPECTIVELY.
   24 CALL CROSS(OMCI,RCBI,VCI)
      CALL CROSS(OMCI,RWGCI,VWGI)
      CALL CROSS(UWGI,UGI,ULI)
      DO 25 I=1,3
      VWGI(I)=VBI(I)+VCI(I)+VWGI(I)
   25 VCI(I)=VBI(I)+VCI(I)
C         TIRE SLIP ANGLE = ANGLE BETWEEN THE WHEEL-GROUND-PLANES-LINE-
C                OF-INTERSECTION  AND  THE PROJECTION-OF-THE-GROUND-
C                CONTACT-POINT-VELOCITY-ON-THE-GROUND-PLANE.
C   DEFINE SLIP ANGLE POSITIVE WHEN WHEEL MOVES IN POSITIVE ULI DIRECTION.
      VNORM=DOT(VWGI,UGI)
      DO 26 I=1,3
      URI(I)=RWGCI(I)/RADD
   26 VPLANE(I)=VWGI(I)-VNORM*UGI(I)
      VPMAG=DSQRT(DOT(VPLANE,VPLANE))
C         DEFINE THE SLIP ANGLE (DEGREES).
      IF(VPMAG.NE.0.0D0) GO TO 27
      V1=0.0D0
```

Figure C-8 (continued).

```
      V2=0.0D0
      SLAN=0.0D0
      GO TO 29
   27 V1=DOT(VPLANE,UWGI)/VPMAG
      V2=DOT(VPLANE,ULI)
      IF(DABS(V1).GT.1.0D0) V1=DSIGN(1.0D0,V1)
      SLAN=57.2957795130D0*DSIGN(DARCOS(DABS(V1)),V2)
   29 CONTINUE
      IF(ITR.EQ.0) GO TO 35
C  REAR TIRE FORCES ...
C        RADIAL (URI DIRECTION)
      FRAD=-TABLE(DREAR,FREAR,DEFL,1,5,1)
      DV=DOT(VCI,URI)
      IF(DV.LT.0.0D0) FRAD=FRAD-DV*DMPR
      IF(FRAD.GE.0.0D0) GO TO 201
C        CALCULATE THE REAR WHEEL SLIP (TRAVEL REDUCTION).
      SLIP=0.0D0
      IF(DABS(OMW).GT.1.D-4) SLIP=1.0D0-DOT(VCI,UWGI)/(-RADD*OMW)
      COT=DSIGN(TABLE(SWHEEL,COTR,DABS(SLIP),2,5,1),SLIP)
      IF(DABS(COT).GT.COTR(5)) COT=DSIGN(COTR(5),COT)
      FRATIO=DABS(COT)/COTR(5)
C        LATERAL FORCE (FRICTION ELLIPSE CONCEPT)
      SL=-DSIGN(TABLE(SLANR,SLOPER,DABS(SLAN),2,5,1),SLAN)*DSQRT(1.0D0-
     $FRATIO**2)
C              REDUCE LATERAL FORCE COEF FOR VERY SMALL LATERAL VELOCITY
      IF(DABS(V2).LT.1.0D0) SL=SL*DABS(V2)
C              RECALL THAT FCIR & FLAT ARE FUNCTIONS OF FNORM WHILE
C                     FNORM IS A FUNCTION OF FLAT AND FRAD.
C        FNORM = FORCE NORMAL TO GROUND SURFACE.
      FNORM=FRAD*DOT(UGI,URI)
      FLAT=SL*FNORM
C        CIRCUMFERENTIAL ROLLING RESISTANCE & TRACTION (UWGI DIRECTION)
      FCIR=-DSIGN(FNORM,V1)*(AR+BR*DABS(SLAN))
C              REDUCE ROLLING RESISTANCE FOR SMALL FORWARD VELOCITY.
      IF(VPMAG*DABS(V1).LT.1.0D0) FCIR=FCIR*VPMAG*DABS(V1)
      FCIR=FCIR+COT*FNORM
      GO TO 40
C  FRONT TIRE FORCES  ...
C        RADIAL (URI DIRECTION)
   35 FRAD=-TABLE(DFRONT,FFRONT,DEFL,1,5,1)
      DV=DOT(VCI,URI)
      IF(DV.LT.0.0D0) FRAD=FRAD-DV*DMPF
      IF(FRAD.GE.0.0D0) GO TO 201
C              LATERAL FORCE COEFFICIENT
      SL=-DSIGN(TABLE(SLANF,SLOPEF,DABS(SLAN),2,5,1),SLAN)
C              REDUCE LATERAL FORCE COEF FOR VERY SMALL LATERAL VELOCITY
      IF(DABS(V2).LT.1.0D0) SL=SL*DABS(V2)
C              RECALL THAT FCIR & FLAT ARE FUNCTIONS OF FNORM WHILE
C                     FNORM IS A FUNCTION OF FLAT AND FRAD.
C        FNORM= FORCE NORMAL TO GROUND SURFACE.
      FNORM=FRAD*DOT(UGI,URI)
      FLAT=SL*FNORM
C        CIRCUMFERENTIAL ROLLING RESISTANCE (UWGI DIRECTION)
      FCIR=-DSIGN(FNORM,V1)*(AF+BF*DABS(SLAN))
C              REDUCE ROLLING RESISTANCE FOR VERY SMALL FORWARD VELOCITY.
```

Figure C-8 (continued).

```
      IF(VPMAG*DABS(V1).LT.1.0D0) FCIR=FCIR*VPMAG*DABS(V1)
   40 CONTINUE
C  CALCULATE RESULTANT FORCE AND MOMENT ON THE WHEEL.
      DO 50 I=1,3
   50 FWGI(I)=FNORM*UGI(I)+FCIR*UWGI(I)+FLAT*ULI(I)
      CALL CROSS(RWGCI,FWGI,MOWGI)
      RETURN
      END
      SUBROUTINE TURN(TIME,Y,STEER)
C  THIS ROUTINE DEFINES THE STEER ANGLE(RADIANS) SUCH THAT A ROTATION
C        VECTOR POINTING DOWNWARD (XF3 DIRECTION) IS POSITIVE.
      IMPLICIT REAL*8(A-H,O-Z)
      COMMON /RTURN/ ST1,ST2,ST3,ST4,ST5,IST
      DIMENSION Y(20)
C  IST DEFINES THE TYPE OF STEER ANGLE FUNCTION.
C        IST =  0 - STEER ANGLE IS CONSTANT, DEFINED BY ST1(RADIANS)
C            = -1 - STEER ANGLE=ST1 UNTIL TIME=ST2, THEN STEER
C                       ANGLE=ST3; WHEN TIME=ST4, STEER ANGLE=ST5
      IF(IST.NE.0) GO TO 10
      STEER=ST1
      GO TO 90
   10 IF(IST.NE.-1) GO TO 20
      IF(TIME.LT.ST2) STEER=ST1
      IF(TIME.GE.ST2.AND.TIME.LT.ST4) STEER=ST4
      IF(TIME.GE.ST4) STEER=ST5
   20 CONTINUE
   90 RETURN
      END
      SUBROUTINE POSVEL(ABI,XBI,VBI,RLBB,OMBB,IVEL,XLI,VLI)
      IMPLICIT REAL*8(A-H,O-Z)
      DIMENSION ABI(3,3),XBI(3),VBI(3),RLBB(3),OMBB(3),RLBI(3),VLB(3),
     %XLI(3),VLI(3)
C  THIS ROUTINE CONVERTS THE RELATIVE LOCATION OF A POINT ON A ROTATING
C        AND TRANSLATING BODY TO AN INERTIAL POSITION AND, IF IVEL.NE.0,
C        ALSO TO AN INERTIAL VELOCITY.
      CALL MULT31(ABI,RLBB,-1,RLBI)
      DO 10 I=1,3
   10 XLI(I)=XBI(I)+RLBI(I)
      IF(IVEL.EQ.0) RETURN
      CALL CROSS(OMBB,RLBB,VLB)
      CALL MULT31(ABI,VLB,-1,VLI)
      DO 20 I=1,3
   20 VLI(I)=VBI(I)+VLI(I)
      RETURN
      END
      SUBROUTINE SURFAC(XWI,UGI,ELEV)
C  THIS ROUTINE EVALUATES THE ELEVATION OF THE SURFACE,  ELEV,
C        VERTICALLY ABOVE OR BELOW THE SPECIFIED POINT,  XWI(I).
C        THE UNIT NORMAL VECTOR TO THE GROUND SURFACE AT THE
C        SPECIFIED POINT IS THEN DEFINED AS  UGI(I).
C  THE SURFACE DEFINED IS A 1/12TH SCALE MODEL OF THE SAE-ASAE
C        SIDE OVERTURN RAMP AND BANK.
      IMPLICIT REAL*8(A-H,O-Z)
      DIMENSION XWI(3),UGI(3)
      DATA RTW/6.40D0/
      DATA TAN12,SIN12,COS12,COT50,COS50,SIN50/.21256D0,.20791D0,
```

Figure C-8 (continued).

```
      $.97815D0,.83910D0,.64279D0,.76604D0/
       DATA BNKHT,RMPHT,RMPW,RMPL,RINCL/3.98D0,1.48D0,3.0D0,10.0D0,5.0D0/
C  LOCATE POINT  XWI  RELATIVE TO THE TOP OF THE BANK.
       XBNKT2=-0.4D0*RTW+XWI(1)*TAN12
       IF(XWI(2)-XBNKT2) 10,20,30
C  THE POINT IS DOWN THE BANK.
C          LOCATE THE BOTTOM OF THE BANK.
   10 XBNKB2=-BNKHT*COT50/COS12-0.4D0*RTW+XWI(1)*TAN12
C  LOCATE POINT  XWI  RELATIVE TO THE BOTTOM OF THE BANK.
       IF(XWI(2)-XBNKB2) 11,11,15
C          POINT  XWI  IS BELOW OR AT THE BOTTOM OF THE BANK.
   11 ELEV=BNKHT
       GO TO 99
C          POINT  XWI  IS ON THE BANK SLOPE.
   15 ELEV=-(XWI(2)-XBNKT2)*COS12/COT50
       UGI(1)=SIN12*SIN50
       UGI(2)=-COS12*SIN50
       UGI(3)=-COS50
       GO TO 100
C          POINT  XWI  IS ABOVE THE BANK ON LEVEL GROUND.
   20 ELEV=0.0D0
       GO TO 99
C  LOCATE POINT  XWI  RELATIVE TO THE RAMP.
   30 IF(XWI(2).LT..5D0*RTW-.5D0*RMPW.OR.XWI(2).GT..5D0*RTW+.5D0*RMPW)
      $GO TO 20
C          POINT IS IN LINE WITH THE RAMP; LOCATE THE POSITION RELATIVE
C               TO THE INCLINE.
       IF(XWI(1).LE.0.0D0) GO TO 20
       IF(XWI(1).GE.RINCL+RMPL) GO TO 20
       IF(XWI(1).GE.RINCL) GO TO 40
       ELEV=-RMPHT*XWI(1)/RINCL
       HYP=DSQRT(RMPHT**2+RINCL**2)
       UGI(1)=-RMPHT/HYP
       UGI(2)=0.0D0
       UGI(3)=-RINCL/HYP
       GO TO 100
   40 ELEV=-RMPHT
   99 UGI(1)=0.0D0
       UGI(2)=0.0D0
       UGI(3)=-1.0D0
  100 RETURN
       END
       SUBROUTINE SURFO(XS,YS,ZS,ICON,NCON,NS)
C  THIS ROUTINE EVALUATES THE CHARACTERISTIC FEATURES OF THE TEST
C          TERRAIN FOR PLOTTING.
C          THE TEST TERRAIN IS A 1/12TH SCALE OF THE SAE/ASAE SIDE
C               OVERTURN TEST COURSE.
C  (BECAUSE THE TERRAIN REMAINS FIXED WITH TIME, THIS ROUTINE NEED
C          BE CALLED ONLY ONCE.)
       IMPLICIT REAL*8(A-H,O-Z)
       DIMENSION XS(12),YS(12),ZS(12),ICON(10)
       DIMENSION XMIN(3),XMAX(3),X(12),Y(12),Z(12),ISCON(10)
       DATA RTW/6.40D0/
       DATA X(5),X(6),X(9),X(12)/4*5.0D0/,X(7),X(8)/2*15.0D0/
       DATA X(10),X(11),Z(1),Z(2),Z(10),Z(11)/6*0.0D0/
```

Figure C-8 (continued).

```
      DATA Z(5),Z(6),Z(7),Z(8),Z(9),Z(12)/6*-1.43D0/,Z(3),Z(4)/2*3.98D0/
      DATA ISCON/2,1,4,3,5,12,3,1,4,2/,NSCON,NSURF/10,12/
      DATA XMIN/-15.D0,-20.D0,-15.D0/,XMAX/30.D0,5.D0,5.D0/,WRAMP/3.D0/
      DATA TAN12,COS12,COT50/.21256D0,.97815D0,.83910D0/
C  DEFINE THE BANK BREAK LINES.
      Y(1)=-0.4D0*RTW+XMIN(1)*TAN12
      Y(2)=-0.4D0*RTW+XMAX(1)*TAN12
      Y(3)=-Z(3)*COT50/COS12-0.4D0*RTW+XMIN(1)*TAN12
      Y(4)=-Z(3)*COT50/COS12-0.4D0*RTW+XMAX(1)*TAN12
C  DEFINE THE RAMP OUTLINE.
      DO 12 I=1,2
      X(2*I-1)=XMIN(1)
      X(2*I)=XMAX(1)
      Y(I+7)=0.5D0*(RTW-WRAMP)
      Y(5*I)=0.5D0*(RTW-WRAMP)
      Y(I+5)=0.5D0*(RTW+WRAMP)
   12 Y(I+10)=0.5D0*(RTW+WRAMP)
C  DEFINE NEW ARRAYS THAT ARE ACCEPTABLE FOR ARGUMENTS OF SUBROUTINES.
      NS=NSURF
      NCON=NSCON
      DO 20 I=1,NS
      XS(I)=X(I)
      YS(I)=Y(I)
   20 ZS(I)=Z(I)
      DO 30 I=1,NCON
   30 ICON(I)=ISCON(I)
      RETURN
      END
      SUBROUTINE SOLVE(N,AA,CC,X)
      IMPLICIT REAL*8(A-H,O-Z)
      DIMENSION A(7,7),AA(7,7),C(7),CC(7),X(7)
C A(I,J)*X(J) = C(I)   (SUM ON J = 1,N)   (FOR I = 1,N)
C SUBROUTINE SOLVES BY GAUSSIAN ELIMINATION THE N LINEAR EQUATIONS
C AUTHOR: J.F. BOOKER, CORNELL UNIVERSITY
C BUFFERS ARE USED TO SAVE THE INPUT ARRAYS.
C          DEFINE THE WORKING ARRAYS.
      DO 90 I=1,N
      DO 89 J=1,N
   89 A(I,J)=AA(I,J)
   90 C(I)=CC(I)
C SELECT KTH ROW AS 'PIVOT'
      DO 400 K = 1,N
C FIND LARGEST |A(I,K)| FOR I = K,N
      BIG  = DABS(A(K,K))
      IBIG = K
      DO 100 I = K,N
      SIZE = DABS(A(I,K))
      IF (SIZE.LT.BIG) GO TO 100
      BIG = SIZE
      IBIG = I
  100 CONTINUE
C SWAP ROWS SO |A(K,K)| IS BIGGEST
      IF (K.EQ.IBIG) GO TO 280
      DO 200 J = K,N
      ABIG = A(IBIG,J)
```

Figure C-8 (continued).

```
      A(IBIG,J) = A(K,J)
  200 A(K,J) = ABIG
      CBIG = C(IBIG)
      C(IBIG) = C(K)
      C(K) = CBIG
  280 CONTINUE
C CHECK FOR NULL PIVOT
      IF (A(K,K).EQ.0.0D0) GO TO 600
C DECOUPLE SYSTEM BY SUCCESSIVE SUBTRACTION
C OF FRACTIONS OF K-TH ROW FROM ALL OTHERS
      DO 400 I = 1,N
      IF (I.EQ.K) GO TO 400
      RATIO = A(I,K)/A(K,K)
      DO 300 J = K,N
  300 A(I,J) = A(I,J)-RATIO*A(K,J)
      C(I)   = C(I)   -RATIO*C(K)
  400 CONTINUE
C SOLVE DECOUPLED SYSTEM
      DO 500 K = 1,N
  500 X(K) = C(K)/A(K,K)
      RETURN
C ARRANGE ABORT
  600 WRITE (6,666)
  666 FORMAT(10X,'SINGULAR MATRIX')
      DO 700 I = 1,N
  700 X(I) = 0.0D0
      RETURN
      END
      SUBROUTINE FORTQ(ABI,XCGI,VCGI,OMBI,RHOF,FT,F1,F2,F3,ITYPE,NF,
     %FTOTI,TQTOTI)
      IMPLICIT REAL*8(A-H,O-Z)
      DIMENSION RHOF(5,3),FT(5,3),ABI(3,3),XCGI(3),VCGI(3),OMBI(3)
      DIMENSION F1(5),F2(5),F3(5),FTOTI(3),TQTOTI(3),VECT(3),TQI(3)
      DIMENSION FI(3),RHO(3),RHOI(3),VRELI(3),VI(3),XI(3),UNIT(3)
      DIMENSION ITYPE(5)
C  INITIALIZE FORCES AND MOMENTS.
      DO 5 J=1,3
      FTOTI(J)=0.0D0
    5 TQTOTI(J)=0.0D0
C  BEGIN LOOP FOR ALL FORCES AND MOMENTS ACTING ON THIS BODY.
      DO 50 JF=1,NF
C           DETERMINE TYPE OF REACTION...
      IF(ITYPE(JF)+1) 8,10,12
C               ... CONSTANT MOMENT IN BODY-AXIS DIRECTIONS
    8 DO 9 J=1,3
    9 VECT(J)=FT(JF,J)
      CALL MULT31(ABI,VECT,-1,TQI)
      GO TO 48
C               ... CONSTANT MOMENT IN INERTIAL DIRECTIONS
   10 DO 11 J=1,3
   11 TQI(J)=FT(JF,J)
      GO TO 48
C               ... FORCE TYPE REACTION; DEFINE POINT OF FORCE APPLICATION.
   12 DO 13 J=1,3
   13 RHO(J)=RHOF(JF,J)
```

Figure C-8 (continued).

```
      CALL MULT31(ABI,RHO,-1,RHOI)
      IF(ITYPE(JF)-2) 14,16,18
C              ... CONSTANT FORCE IN INERTIAL COORDINATES.
   14 DO 15 J=1,3
   15 FI(J)=FT(JF,J)
      GO TO 45
C              ... CONSTANT FORCE IN BODY-AXIS COORDINATES.
   16 DO 17 J=1,3
   17 VECT(J)=FT(JF,J)
      CALL MULT31(ABI,VECT,-1,FI)
      GO TO 45
C              ... FORCE DEPENDS UPON POSITION & VELOCITY OF POINT.
   18 CALL CROSS(OMEGI,RHOI,VRELI)
      DO 19 J=1,3
      VI(J)=VCGI(J)+VRELI(J)
      XI(J)=XCGI(J)+RHOI(J)
   19 VECT(J)=XI(J)-FT(JF,J)
      XMAG=DSQRT(DOT(VECT,VECT))
      COMPR=F3(JF)-XMAG
      IF(ITYPE(JF).EQ.4.AND.COMPR.LT.0.0D0) GO TO 50
      IF(ITYPE(JF).EQ.5.AND.COMPR.GT.0.0D0) GO TO 50
      DO 20 J=1,3
   20 UNIT(J)=VECT(J)/XMAG
      DCOMP=DOT(VI,UNIT)
      DO 21 J=1,3
   21 FI(J)=+F1(JF)*COMPR*UNIT(J)-F2(JF)*DCOMP*UNIT(J)
C         CALCULATE MOMENT DUE TO THIS FORCE.
   45 CALL CROSS(RHOI,FI,TQI)
C         ADD THIS FORCE TO THE TOTAL.
      DO 46 J=1,3
   46 FTOTI(J)=FTOTI(J)+FI(J)
C         ADD THIS MOMENT TO THE TOTAL.
   48 DO 49 J=1,3
   49 TQTOTI(J)=TQTOTI(J)+TQI(J)
   50 CONTINUE
      RETURN
      END
      SUBROUTINE DBLCRS(A,B,C)
C  THIS ROUTINE PERFORMS THE DOUBLE CROSS PRODUCT, RETURNING VECTOR C.
C                C = A X (A X B)
      IMPLICIT REAL*8(A-H,O-Z)
      DIMENSION A(3),B(3),C(3),X(3)
      CALL CROSS(A,B,X)
      CALL CROSS(A,X,C)
      RETURN
      END
      SUBROUTINE ROTATE(ATTOLD,THETAR,IAXIS,ATTNEW)
C  THIS ROUTINE CALCULATES THE NEW ATTITUDE(DIRECTION COSINES), ATTNEW,
C         RESULTING FROM ROTATING THE OLD ATTITUDE, ATTOLD, ABOUT ONE OF
C         ITS AXES, IAXIS, BY AN AMOUNT THETAR (RADIANS).
      IMPLICIT REAL*8(A-H,O-Z)
      DIMENSION A(3,3),ATTOLD(3,3),ATTBUF(3,3),ATTNEW(3,3)
      IF(THETAR.EQ.0.0D0) GO TO 11
      SINTH=DSIN(THETAR)
      COSTH=DCOS(THETAR)
```

Figure C-8 (continued).

```
      J=IAXIS-1+3*((3-IAXIS)/2)
      K=IAXIS+1-3*((IAXIS-1)/2)
      A(IAXIS,IAXIS)=1.0
      A(IAXIS,J)=0.0D0
      A(J,IAXIS)=0.0D0
      A(IAXIS,K)=0.0D0
      A(K,IAXIS)=0.0D0
      A(J,J)=COSTH
      A(K,K)=COSTH
      A(J,K)=-SINTH
      A(K,J)=SINTH
      CALL MULT33(A,ATTOLD,1,ATTBUF)
      DO 10 I=1,3
      DO 10 J=1,3
   10 ATTNEW(I,J)=ATTBUF(I,J)
      GO TO 20
   11 DO 15 I=1,3
      DO 15 J=1,3
   15 ATTNEW(I,J)=ATTOLD(I,J)
   20 RETURN
      END
      SUBROUTINE MULT31(AA,X,ITYPE,XOUT)
C  THIS ROUTINE PREMULTIPLIES THE 3-BY-1 VECTOR, X, BY THE 3-BY-3 MATRIX
C          AA.
C          ITYPE DEFINES THE MULTIPLICATION AS DIRECT (ITYPE=1) OR AS
C                 TRANSPOSE-OF-AA TIMES X (ITYPE=-1).
C          THE 3-BY-1 VECTOR, XOUT, IS THE CALCULATED RESULT.
      IMPLICIT REAL*8(A-H,O-Z)
      DIMENSION AA(3,3),X(3),XOUT(3)
      IF(ITYPE.NE.-1) GO TO 30
      DO 20 I=1,3
   20 XOUT(I)=AA(1,I)*X(1)+AA(2,I)*X(2)+AA(3,I)*X(3)
      GO TO 41
   30 DO 40 I=1,3
      XOUT(I)=AA(I,1)*X(1)+AA(I,2)*X(2)+AA(I,3)*X(3)
   40 CONTINUE
   41 CONTINUE
      RETURN
      END
      SUBROUTINE CROSS(A,B,ACROSB)
C  THIS ROUTINE CALCULATES THE CROSS-PRODUCT OF TWO 3-ELEMENT VECTORS.
C          INPUT OF A & B RESULTS IN   ACROSB = A(CROSS)B.
C          THE MAGNITUDE OF  A(CROSS)B  IS STORED AS  ABMAG.
      IMPLICIT REAL*8(A-H,O-Z)
      DIMENSION A(3),B(3),ACROSB(3)
      ACROSB(1)=A(2)*B(3)-A(3)*B(2)
      ACROSB(2)=A(3)*B(1)-A(1)*B(3)
      ACROSB(3)=A(1)*B(2)-A(2)*B(1)
      RETURN
      END
      SUBROUTINE DIRCOS(E0,E1,E2,E3,DCOS)
C  THIS ROUTINE DETERMINES DIRECTION COSINES FROM EULER PARAMETERS.
      IMPLICIT REAL*8(A-H,O-Z)
      DIMENSION DCOS(3,3)
      DCOS(1,1)=E0**2+E1**2-E2**2-E3**2
```

Figure C-8 (continued).

```
      DCOS(1,2)=2.0D0*(E1*E2+E0*E3)
      DCOS(1,3)=2.0D0*(E1*E3-E0*E2)
      DCOS(2,1)=2.0D0*(E1*E2-E0*E3)
      DCOS(2,2)=E0**2+E2**2-E3**2-E1**2
      DCOS(2,3)=2.0D0*(E2*E3+E0*E1)
      DCOS(3,1)=2.0D0*(E3*E1+E0*E2)
      DCOS(3,2)=2.0D0*(E2*E3-E0*E1)
      DCOS(3,3)=E0**2+E3**2-E1**2-E2**2
      RETURN
      END
      SUBROUTINE EULPAR(DCOS,E0,E1,E2,E3)
C CALCULATION OF THE EULER PARAMETERS FROM THE DIRECTION COSINES.
      IMPLICIT REAL*8(A-H,O-Z)
      DIMENSION DCOS(3,3)
      E0=DSQRT((DCOS(1,1)+DCOS(2,2)+DCOS(3,3)+1.0D0)/4.0D0)
      E1=(DCOS(2,3)-DCOS(3,2))/(E0*4.0D0)
      E2=(DCOS(3,1)-DCOS(1,3))/(E0*4.0D0)
      E3=(DCOS(1,2)-DCOS(2,1))/(E0*4.0D0)
      RETURN
      END
      SUBROUTINE MULT33(AA,BB,ITYPE,CC)
C THIS ROUTINE PREMULTIPLIES THE 3-BY-3 MATRIX, BB, BY THE 3-BY-3
C          MATRIX, AA, WITH THE RESULT BEING THE 3-BY-3 MATRIX, CC.
C          ITYPE DEFINES THE TYPE OF MULTIPLICATION DESIRED.
C                 ITYPE=1  -  DIRECT MULTIPLICATION
C                 ITYPE=-1 -  MATRIX BB IS PREMULTIPLIED BY THE TRANSPOSE
C                        OF MATRIX AA.
      IMPLICIT REAL*8(A-H,O-Z)
      DIMENSION AA(3,3),BB(3,3),CC(3,3)
      DO 10 I=1,3
      DO 10 J=1,3
   10 CC(I,J)=0.0D0
      IF(ITYPE.EQ.-1) GO TO 30
      DO 20 I=1,3
      DO 20 J=1,3
      DO 20 K=1,3
   20 CC(I,J)=CC(I,J)+AA(I,K)*BB(K,J)
      GO TO 50
   30 DO 40 I=1,3
      DO 40 J=1,3
      DO 40 K=1,3
   40 CC(I,J)=CC(I,J)+AA(K,I)*BB(K,J)
   50 CONTINUE
      RETURN
      END
      SUBROUTINE EIGVAL(A,NDIAG,NROOTS,ROOT)
      IMPLICIT REAL*8(A-H,O-Z)
      DIMENSION A(3,3),POLY(3,3),ROOT(3)
      DO 100 LAMBDA=1,NROOTS
      KOUNT=0
C ESTABLISH INITIAL GUESSES FOR THE EIGENVALUES.
      PROD=1.0D0
      SUM=0.0D0
      DO 4 I=1,NDIAG
      PROD=PROD*A(I,I)
```

Figure C-8 (continued).

```
    4 SUM=SUM+A(I,I)
      RT1=0.666667D0*SUM
      RT2=0.89D0*SUM
      RT3=SUM
      K=LAMBDA-1
      CALL EIGP3(A,RT1,POLY1)
      CALL EIGP3(A,RT2,POLY2)
      CALL EIGP3(A,RT3,POLY3)
      IF(LAMBDA.EQ.1) GO TO 9
C   DEFLATE THE POLYNOMIAL BY DIVIDING OUT THE DETERMINED FACTORS.
      DO 8 I=1,K
      POLY1=POLY1/(RT1-ROOT(I))
      POLY2=POLY2/(RT2-ROOT(I))
    8 POLY3=POLY3/(RT3-ROOT(I))
    9 DELTA3=(RT3-RT2)/(RT2-RT1)
   15 AZRO=DELTA3**2*(POLY1-POLY2)-DELTA3*(POLY2-POLY3)
      A1=DELTA3**2*POLY1-(1.0D0+DELTA3)**2*POLY2
      A6=(1.0D0+2.0D0*DELTA3)*POLY3
      A1=A1+A6
      A2=(1.0D0+DELTA3)*POLY3
      DISCR=A1*A1-4.0D0*AZRO*A2
      IF(DISCR.LT.0.0D0) DISCR=0.0D0
      KOUNT=KOUNT+1
   10 DEL41=2.0D0*A2/(-A1+DSQRT(DISCR))
      DEL42=2.0D0*A2/(-A1-DSQRT(DISCR))
C   SELECT THE SMALLER ROOT OF THE QUADRATIC EQUATION.
      ABSD41= DABS(DEL41)
      ABSD42= DABS(DEL42)
      IF(ABSD41.LT.ABSD42) DEL4=DEL41
      IF(ABSD41.GE.ABSD42) DEL4=DEL42
      RT4=RT3+DEL4*(RT3-RT2)
      CALL EIGP3(A,RT4,POLY4)
      IF(LAMBDA.EQ.1) GO TO 12
      K=LAMBDA-1
C   DEFLATE THE POLYNOMIAL.
      DO 11 I=1,K
   11 POLY4=POLY4/(RT4-ROOT(I))
   12 ABSP4= DABS(POLY4)
      AR4= DABS(RT4)
      DIF=RT4-RT3
      ADIF= DABS(DIF)
C   CHECK FOR POLYNOMIAL VALUE NEAR ZERO.
      IF(ABSP4.GT.1.0D-4*PROD.AND.ADIF.GT.1.0D-4*AR4) GO TO 13
      ROOT(LAMBDA)=RT4
      PRINT 7, LAMBDA,ROOT(LAMBDA),KOUNT
    7 FORMAT (//' ROOT NO.',I4,' IS', F20.8,20X,I4,' ITERATIONS')
      GO TO 100
   13 IF(KOUNT.LE.20) GO TO 14
      PRINT 1, KOUNT
    1 FORMAT (///' *** ',I3,' ITERATIONS')
      GO TO 101
   14 CONTINUE
C   REDEFINE ROOT AND POLYNOMIAL GUESSES.
      RT1=RT2
      RT2=RT3
```

Figure C-8 (continued).

```
      RT3=RT4
      POLY1=POLY2
      POLY2=POLY3
      POLY3=POLY4
      DELTA3=DEL4
      GO TO 15
  100 CONTINUE
  101 RETURN
      END
      SUBROUTINE EIGP3(A,EIGV,P)
      IMPLICIT REAL*8(A-H,O-Z)
      DIMENSION A(3,3)
      P=(A(1,1)-EIGV)*(A(2,2)-EIGV)*(A(3,3)-EIGV)+A(2,1)*A(3,2)*A(1,3)
     %+A(1,2)*A(2,3)*A(3,1)-A(3,1)*(A(2,2)-EIGV)*A(1,3)-A(2,1)*A(1,2)*
     $(A(3,3)-EIGV)-A(3,2)*A(2,3)*(A(1,1)-EIGV)
      RETURN
      END
      SUBROUTINE VECT33(A,ROOT,X)
C  THIS ROUTINE DETERMINES THE EIGENVECTORS, X(I,LAMBDA), FOR THE 3
C         INPUT EIGENVALUES, ROOT(LAMBDA), AND THE 3-BY-3 MATRIX, A.
C  THE EIGENVECTORS ARE NORMALIZED TO UNIT LENGTH.
C
      IMPLICIT REAL*8(A-H,O-Z)
      DIMENSION A(3,3),X(3,3),ROOT(3)
      DO 99 LAMBDA=1,3
C  CHECK FOR ZERO DETERMINANT IN THE DENOMINATOR.
      DO 20 K=1,3
C  K IS THE COMPONENT OF THE VECTOR ASSUMED TO HAVE A VALUE OF 1.0
      GO TO (11,12,13), K
   11 K2=2
      K3=3
      GO TO 14
   12 K2=1
      K3=3
      GO TO 14
   13 K2=1
      K3=2
   14 DET=(A(K2,K2)-ROOT(LAMBDA))*(A(K3,K3)-ROOT(LAMBDA))-A(K3,K2)*
     %A(K2,K3)
      IF(DET.EQ.0.0D0) GO TO 19
      DTEST=((A(1,1)*A(2,2)*A(3,3))**2)**0.333D0
      IF(DABS(DET).LT.1.0D-5*DTEST) GO TO 19
C  CALCULATE THE COMPONENTS OF THE EIGENVECTOR.
      X(K,LAMBDA)=1.0D0
      X(K2,LAMBDA)=(-A(K2,K)*(A(K3,K3)-ROOT(LAMBDA))+A(K3,K)*A(K2,K3))
     %/DET
      X(K3,LAMBDA)=(-A(K3,K)*(A(K2,K2)-ROOT(LAMBDA))+A(K2,K)*A(K3,K2))
     $/DET
      GO TO 21
   19 IF(K.EQ.3) PRINT 6, LAMBDA
    6 FORMAT (1H0,'******* MATRIX USED IN DETERMINING THE EIGENVECTOR AS
     %SOCIATED WITH EIGENVALUE NO.',I4/5X,'HAS A RANK LESS THAN TWO.')
   20 CONTINUE
C  NORMALIZE THE VECTOR TO UNIT LENGTH.
   21 XLSQ=0.0D0
      DO 22 I=1,3
   22 XLSQ=XLSQ+X(I,LAMBDA)**2
      XL=DSQRT(XLSQ)
      DO 23 I=1,3
   23 X(I,LAMBDA)=X(I,LAMBDA)/XL
      PRINT 7, LAMBDA,ROOT(LAMBDA),(X(I,LAMBDA),I=1,3)
    7 FORMAT (1H0,'EIGENVALUE NO.',I3,' IS',F12.4,';  EIGENVECTOR:',
     %F10.6/(1H ,47X,F10.6))
   99 CONTINUE
      RETURN
      END
```

Figure C-8 (continued).

C.3. Program Use.

The digital simulation of wheel-tractor overturns or simulation of the motions of a wheel tractor over the specified terrain may be obtained by executing the program of Figure C-8 with input data for the desired tractor and terrain conditions. Variations in the terrain profile would require a change in subroutine SURFAC (and subroutine SURFO if graphical output were desired), but variation of most other parameters may be accomplished by changing the input data.

The data which is required by this program, together with an explanation of the program options available through data specification, are provided in the sections which follow.

An explanation of the program options available through data specification is provided in Section C.3.1, a sample set of data is given in Section C.3.2, a discussion of other practical programming considerations is presented in Section C.3.3, and a discussion of program execution statistics is given in Section C.3.4.

C.3.1. Instructions for Data Specification.

Twelve data groupings have been selected according to similarities in variable type or data format. These groups are discussed individually to provide an accurate description of the data required in each group. Although each data block (or group) must be provided to the program in order, the amount of information in each block may vary as different program options are chosen. Table C-4 defines the data format for each of the variables described below.

Data block 1 provides the capability for printing a problem

TABLE C-4. Formats for Program Data.

	Columns	Format	Variable(s)	Units
Block 1				
Cards 1-n	1-80	20A4	DESCR	--
Card n+1	1-4	A4	STOP	--
Block 2				
Card 1	1-5	I5	K1	--
	6-35	3F10.0	XBI	in
Card 2	1-5	I5	K2	--
	6-35	3F10.0	VBI	in/sec
Card 3	1-72	9F8.5	ATI	--
Card 4	1-5	I5	K3	--
	6-35	3F10.0	OMBT	rad/sec
Card 5	1-10	F10.5	THETF	rad
	11-20	F10.5	OMFF1	rad/sec
Card 6	1-5	I5	INIT	--
	6-15	F10.2	SPEEDE	rad/sec
	16-25	F10.2	SPEEDL	rad/sec
	26-35	F10.2	SPEEDR	rad/sec
Block 3				
Card 1	1-72	9F8.0	IBT	lb-in-sec
Card 2	1-72	9F8.0	IFF	lb-in-sec
Card 3	1-30	3F10.2	IRT	lb-in-sec
	31-40	F10.2	ID	lb-in-sec
	41-50	F10.2	IE	lb-in-sec
	51-60	F10.2	WB	lb
Card 4	1-10	F10.2	WR	lb
	11-20	F10.2	WF	lb
Block 4				
Card 1	1-30	3F10.2	RLBT	in
	31-60	3F10.2	RRBT	in
Card 2	1-30	3F10.2	RPBT	in
	31-60	3F10.2	RFPF	in
Card 3	1-30	3F10.2	RLFF	in
	31-60	3F10.2	RRFF	in

TABLE C-4 (continued).

	Columns	Format	Variable(s)	Units
Block 4 (continued)				
Card 4	1-10	F10.2	RADR	in
	11-20	F10.2	RADF	in
	21-30	F10.2	ALENG	in
	31-40	F10.2	TOEIN	rad
	41-50	F10.2	CAMBER	rad
	51-60	F10.2	CASTER	rad
Card 5	1-10	F10.2	THMAX	rad
	11-20	F10.2	SLENG	in
	21-30	F10.2	SK	lb/in
	31-40	F10.2	SC	lb-sec/in
Block 5				
Cards 1-n	1-30	3F10.0	RHOLT	in
	31-50	5A4	WHERE	--
	51-55	I5	MORE	--
Block 6 (repeated for four bodies)				
Card 1	1-5	I5	NFBOD	--
Card 2 (repeated NFBOD times)				
	1-5	I5	ITYPE	--
	6-29	3F8.2	RHOFBT	in
	30-53	3F8.2	PB	in-lb, lb, in
	54-61	F8.2	FB1	lb/in
	62-69	F8.2	FB2	lb-sec/in
	70-77	F8.2	FB3	in
Block 7				
Card 1	1-10	F10.4	AR	--
	11-20	F10.2	BR	deg^{-1}
	21-30	F10.4	DMPR	lb-sec/in
	31-40	F10.4	AF	--
	41-50	F10.4	BF	deg^{-1}
	51-60	F10.4	DMPF	lb-sec/in
Card 2	1-10	F10.4	RATIOD	--
	11-20	F10.4	RATIOT	--
	21-30	F10.4	TEFF	--

TABLE C-4 (continued).

	Columns	Format	Variable(s)	Units
Block 8				
Card 1	1-60	alter-nately	TENG	in-lb
Card 2	1-40	F10.2	SENG	rad/sec
	41-80	10A4	TABDAT	--
Card 3	1-60	alter-nately	TCLUT	in-lb
Card 4	1-40	F10.2	SCLUT	--
	41-80	10A4	TABDAT	--
Card 5	1-60	alter-nately	FREAR	lb
Card 6	1-40	F10.2	DREAR	in
	41-80	10A4	TABDAT	--
Card 7	1-60	alter-nately	FFRONT	lb
Card 8	1-40	F10.2	DFRONT	in
	41-80	10A4	TABDAT	--
Card 9	1-60	alter-nately	COTR	--
Card 10	1-40	F10.2	SWHEEL	--
	41-80	10A4	TABDAT	--
Card 11	1-60	alter-nately	SLOPER	--
Card 12	1-40	F10.2	SLANR	deg
	41-80	10A4	TABDAT	--
Card 13	1-60	alter-nately	SLOPEF	--
Card 14	1-40	F10.2	SLANF	deg
	41-80	10A4	TABDAT	--
Block 9				
Card 1	1-5	I5	IST	--
	6-15	F10.3	ST1	rad
	16-25	F10.3	ST2	sec
	26-35	F10.3	ST3	rad
	36-45	F10.3	ST4	sec
	46-55	F10.3	ST5	rad
Block 10				
Card 1	1-5	I5	IPLOT	--
	6-10	I5	NODB	--
	11-15	I5	NODL	--

TABLE C-4 (continued).

	Columns	Format	Variable(s)	Units
Block 10 (continued)				
Card 1 (continued)				
	16-20	I5	NODR	--
	21-25	I5	NODF	--
	26-30	I5	NODLF	--
	31-35	I5	NODRF	--
Card 2 (repeated for each point)				
	1-5	I5	IDB	--
	6-35	3F10.3	RHODB	in
Block 11				
Card 1	1-5	I5	NLINES	--
Card 2 (repeated, if necessary)				
	1-60	12I5	ICON	--
Block 12				
Card 1	1-10	F10.5	TZERO	sec
	11-20	F10.5	DTMAX	sec
	21-30	F10.5	TFINAL	sec
	31-40	F10.5	ERROR	--
	41-45	I5	NPRINT	--
	46-50	I5	NPUNCH	--
	51-55	I5	IERWT	--
Card 2 (repeated twice, or omitted)				
	1-60	10F6.1	DERY*	--

* The variable name DERY is used only to transfer these values to the integrating subroutine DHPCG, then it assumes its intended identity.

description of the particular simulation at the start of the simulation output. This block may be any number of cards, n , each containing up to 80 columns of character-type input which is to be printed verbatim at the top of the first output page. The end of this block must be specified by a card (after the last card containing information to be printed) containing the four letters 'STOP' in the first four columns.

Data block 2 specifies the state of the tractor at the start of the simulation. Six different cards are required to specify the initial conditions in this block.

Card 1 defines the absolute position of the tractor-body center of mass relative to the origin of the inertial coordinate system. The position vector, however, may be defined by its components in the tractor-axes directions, if desired. the variable K1 indicates whether the position data is in inertial coordinates (K1 = 0) or tractor-axes coordinates (K1 = 1). The three position components (XBI) must be specified in the order of their coordinate axes - XBI(1), XBI(2), XBI(3) if K1 = 0, or XBT(1), XBT(2), XBT(3) if K1 = 1.

Card 2 defines the absolute velocity of the tractor-body center of mass. This vector also may be specified in either inertial or tractor-axes directions (K2 = 0, inertial; K2 = 1, tractor-axes). The velocity components (VBI or VBT must be defined in order as were the positions of card 1.

Card 3 defines the attitude of the tractor-axes in terms of the inertial coordinate directions. The 3-by-3 matrix of direction cosines (ATI) defines the tractor-axes directions by the matrix multiplication: XT = ATI * XI . The direction cosine matrix must be defined by rows, i.e., ATI(1,1), ATI(1,2), ATI(1,3), ATI(2,1),...,ATI(3,3).

Card 4 defines the tractor-body angular velocity, specified either in inertial coordinate directions (K3 = 0) or in tractor-axes directions (K3 = 1). The angular velocity components (OMBT or OMBI) must be defined in order - OMBT(1), OMBT(2), OMBT(3) if K3 = 1, or OMBI(1), OMBI(2), OMBI(3) if K3 = 0.

Card 5 defines the initial values of the front-end angular position and angular velocity. The angular position (THETF) is the angle of rotation of the front end relative to the tractor body with positive being defined by the right-hand direction about the number one tractor axis (i.e., positive motion lowers the right front wheel). The angular velocity (OMFF1) is defined as the component of the absolute angular velocity about the front-end axis $\underline{e}_{F_1}$ (i.e., about the front pin).

Card 6 defines the state of the clutch and speeds for the rear wheels and engine which may, or may not, be used. The clutch may be engaged or disengaged while the tractor conditions may be redefined for a tractor operating on a level terrain having a zero elevation. The clutch is engaged when

INIT = 3 or INIT = 4 and the clutch is disengaged when INIT = 1 or INIT = 2. The initial conditions are redefined when INIT = 2 or INIT = 3, otherwise the tractor velocities and orientations are obtained from the data read previously. SPEEDE is the engine speed to be used in all cases except when INIT = 3. SPEEDL and SPEEDR are, respectively, the absolute values of the left and right rear wheel speeds; they are used only when INIT = 1 or INIT = 4.

Data block 3 defines the inertia properties of the tractor parts. Both moments of inertia and weights are used to describe these properties. The gravitational acceleration is assumed equal to 386 in/sec^2. Three cards are required in this data block.

Card 1 defines the mass moments and products of inertia for the tractor body about its center of mass. The 3-by-3 inertia matrix (IBT) has its elements defined for the directions corresponding to the tractor-axes directions. The inertia elements must be defined by rows, i.e., IBT(1,1), IBT(1,2), ..., IBT(3,2), IBT(3,3).

Card 2 defines the mass moments and products of inertia for the tractor front end. Each element of the 3-by-3 inertia matrix (IFF) is defined about the front-end center of mass with components given for the front-end axes directions. The inertia values include the inertia of all parts which rotate with the front-end. The elements of the inertia matrix must be defined by rows as was done for the tractor body.

Card 3 defines the three tractor-axes moments of inertia for the rear wheels (IRT), the drive-line moment of inertia (ID), the engine moment of inertia at the flywheel (IE), and the weight of the tractor body (WB). Due to rear wheel symmetry the tractor-axes moments of inertia for the rear wheel are also the principal moments of inertia, thus eliminating products of inertia.

Card 4 defines the weights of the rear wheels and the tractor front end. Each rear wheel has the weight specified by WR. The front-end weight (WF) includes the weight of the front wheels and all other parts which rotate with the tractor front end.

Data block 4 defines the geometry required to describe the kinematics of the tractor motion. Five data cards are required in this block.

Card 1 defines the locations of the left rear wheel center (RLBT) and the right rear wheel center (RRBT) relative to the tractor-body center of mass. Each location is expressed as a tractor-axes vector from the tractor-body center of mass to the specified point. The three vector components of each must be given in order.

Card 2 defines the front pin location and the location of the front-end center of mass. The pin location (RPBT) is a tractor-axes vector from the tractor-body center of mass to the front pin. The front-end center-of-mass location (RFPF) is the vector from the pin to the front-end center of mass expressed in front-end coordinates.

Card 3 defines the pivot points of the two front wheels. RLFF is the front-end-axes vector from the front-end center of mass to the point-of-intersection of the left front axle and the steering axis for the left front wheel. RRFF is the front-end-axes vector to the corresponding point for the right front wheel. The components of each vector must be defined in order.

Card 4 defines the rear wheel radius, the front wheel radius, the front axle length, the front wheel toe-in, the front wheel camber, and the front-end caster. The rear wheel radius (RADR) and the front wheel radius (RADF) are defined to be the undeflected radii of those tires. The axle length (ALENG) is the distance from the front wheel center to the point-of-intersection for the axle and the steering axis for that wheel. Toe-in (TOEIN) is defined to be the angle about the steering axis that each front wheel is turned from the condition of parallel planes. CAMBER is the angle of rotation required to move the front wheel plane from a vertical position to the position in which the bottoms of the two front-wheel planes are closer together than the tops. CASTER is the angle of rotation used to move the bottom of the steering axis ahead of the "down" front-end axis.

Card 5 defines the maximum angle which the front end may rotate about the front pin (relative to the tractor body) and the characteristics of the "stop" against which the front end rotates when the limit has been reached. THMAX is the absolute value of the rotation limit for the front end relative to the tractor in either direction. SLENG defines the distance from the front pin to the "stop" measured in the $\underline{e}_{F_2}$ direction (a positive scalar value). SK and SC define, respectively, the spring rate and damping coefficient for the "stop". The spring rate is applied during compression and relaxation, but not extension, of the "stop". The damping coefficient is used only when relaxation (removal of a compression load) occurs at the "stop". (SLENG is shown as ℓ_S and THMAX is shown as θ_{max} in Figure 3-13.)

Data block 5 defines the tractor-axes coordinates of points on the tractor body which are to be monitored throughout the simulation. These points, defined by vectors from the tractor-body center of mass, are located at each printed output cycle and may stop the simulation prematurely if one of them strikes the ground. The number of cards in this block, n , must be at least one. Each card is of the same format.

Each card defines a point location, a literal description of the point, and an indicator to specify if more of these points are to be defined. RHOLT is a tractor-axes vector locating the point to be monitored relative to the tractor-body center of mass. WHERE is a 20-character title which is printed together with the location and velocity of the point during each print cycle. MORE is a flag which indicates that more cards for points to be monitored are to be read (when MORE $\neq 0$) or that no more are to be read (MORE $= 0$).

Data block 6 defines the external reactions which act on each of the tractor parts. Because the same card sequence and same formats are used for reactions on the tractor body, the left rear wheel, the right rear wheel, and the front end, a detailed description is provided for only those reactions on the tractor body. This data block must be repeated four times - for the tractor body, left rear wheel, right rear wheel, and front end in order.

Card 1 defines the number of external reactions acting on this body. NFBOD thus defines the number of cards to be used in defining external reactions on this body. If NFBOD $= 0$, no other cards are needed for this body; begin definition for the next body.

Card 2 defines all the specifications for one reaction on this body. There must be NFBOD of these cards for this body. The reaction type is specified by ITYPE.

If ITYPE = -2, the reaction is a moment which has constant vector components in the body-axes directions (tractor-axes for this example). The point of moment application is given by the body-axes vector RHOFBT and the moment vector components in the body-axes directions are defined by PB.

If ITYPE = -1, the reaction is a moment which has constant vector components in the inertial directions. RHOFBT is defined as above, but PB defines the three components of the inertial-coordinate moment.

If ITYPE = 1, the reaction is a force whose inertial components remain constant. RHOFBT defines the body-axes vector from the body center of mass to the point of force application. PB defines the three components of the inertial-coordinate force.

If ITYPE = 2, the reaction is a force whose body-axes components remain constant. RHOFBT is as for ITYPE = 1, but PB now defines the three components of the body-axes force.

If ITYPE = 3, the reaction is a force which is a linear function of the position and velocity of the point RHOFBT (defined as above) relative to a second point fixed in the inertial reference frame. This reaction may be visualized as the force due to a parallel spring and dashpot connection between the two points specified here. PB defines the inertial coordinates of the second point. FB1 defines the linear spring rate, FB2 defines the dashpot damping rate, and FB3 defines the zero-force length of the spring.

If ITYPE = 4, the reaction is the same as for ITYPE = 3 except that the reaction is limited to conditions when the spring is compressed to lengths less the FB3.

If ITYPE = 5, the reaction is the same as for ITYPE = 3 except that the reaction is nonzero only when the spring is stretched to lengths greater than FB3.

Data block 7 defines individual tire and drive-train parameters. Two data cards are required for this block.

Card 1 defines the two linear equation coefficients for the rolling resistance of the front and rear wheels plus the linear damping coefficients for the same wheels. AR and BR are, respectively, the y-intercept and the slope of the equation expressing the rear wheel coefficient of rolling resistance as a linear function of the wheel slip angle, in degrees. AF and BF are, respectively, the y-intercept and slope of the equation expressing the front wheel coefficient of rolling resistance as a linear function of the wheel slip angle, in degrees. DMPR and DMPF are, respectively, the viscous damping coefficients for the rear and front wheels in radial deformation on the specified terrain.

Card 2 defines the differential ratio, the transmission ratio, and the transmission efficiency for the tractor operating conditions. RATIOD is the ratio of the drive-line speed to the average rear wheel speed. RATIOT is the ratio of the clutch rotational speed to the drive-line speed. The power efficiency of the transmission is defined by TEFF.

Data block 8 defines engine, clutch, and tire-ground characteristic data in tabular form. Seven sets of tabulated data must be defined, each set using two cards. Because the data format for each set of tabulated data is the same, the format for only two cards is described here but it should be used to supply data for each of the seven required tables. Each table must have five data pairs defining five coordinate pairs from the corresponding curve.

Card 1 defines three of the data pairs in alternating order. The order for each table is listed below. Thus for the first table the data order would be TENG(1), SENG(1), TENG(2), SENG(2), TENG(3), SENG(3).

Card 2 defines the remaining two data pairs for this table plus a 40-character definition which will be printed with this table as part of the problem description. Thus the data, again for the first table, would be in the order TENG(4), SENG(4), TENG(5), SENG(5), followed by a 40-character description of this table (TABDAT).

The tables of block 8 must be in the following order with the pairs of data points defined alternately in the order listed below for each table.

TENG-SENG: the engine torque (TENG) at the flywheel as a function of the engine speed (SENG)

TCLUT-SCLUT: the clutch torque (TCLUT) as a function of the clutch slip (SCLUT)

FREAR-DREAR: the radial force on the rear tire (FREAR) as a function of the radial tire deflection (DREAR)

FFRONT-DFRONT: the radial force on the front tire (FFRONT) as a function of the radial tire deflection (DFRONT)

COTR-SWHEEL: the gross coefficient of traction (COTR) for the rear wheel as a function of wheel slip (SWHEEL)

SLOPER-SLANR: the slope (SLOPER) of the rear wheel lateral force-normal force curve for various wheel slip angles (SLANR) in degrees

SLOPEF-SLANF: the slope (SLOPEF) of the front wheel lateral force - normal force curve for various wheel slip angles (SLANF) in degrees.

Data block 9 defines the tractor steering data. This block includes only one card.

Card 1 defines the type of steering control (IST) and five variables which set specific steering inputs (ST1, ST2, ST3, ST4, and ST5). If IST = 0, the steer angle (positive to the driver's right) is defined to remain constant at the level ST1. If IST = -1, the steer angle changes stepwise, being ST1 until time ST2, then being ST3 until time ST4, thereafter being ST5.

Data block 10 defines points which are to be located throughout the simulation for use in graphic display of the tractor motion. This block must contain one card to define the number of such points to be located and the type of output desired for these points, but the number of other cards may be from zero to fifty.

Card 1 defines the type of output to be produced for each point (IPLOT) and the number of such points for the tractor body (NODB), the left rear wheel (NODL), the right rear wheel

(NODR), the front end (NODF), the left front wheel (NODLF), and the right front wheel (NODRF). These numbers specify the number of cards which must be supplied for points on each body. The output options are defined by the value of IPLOT:

-1 = print the point locations

0 = no use of these points

1 = print and punch the locations and other graphic information

2 = punch the locations and other graphic information

Card 2 defines the body (IDB) and the vector location (RHODB) of the point relative to the body center of mass expressed in the unit vector direction of that body. The body options are the tractor body (IDB = 1), the left rear wheel (IDB = 2), the right rear wheel (IDB= 3), the front end (IDB = 4), the left front wheel (IDB = 5), and the right front wheel (IDB = 6). One card contains a body identifier and a vector locating a point so the number of cards described here as "card 2" must equal the number of points to be located. Points locating the wheel circumferences and the ground terrain are automatically defined when IPLOT $\geq$ 1.

Data block 11 defines instructions for using the points located for graphic display. This block must contain one card to define the number of instruction cards. The number of instruction cards may range from zero to nine.

Card 1 defines the number of continuous lines (NLINES) which are to be drawn from the set of points located above. (Drawing a symbol at a point location is equivalent here to one line.) This then defines the number of instructions which must be read from succeeding data cards. Two instructions are required to define one line. The maximum allowable number of instructions (including those defined internally for wheel and terrain features) is 100.

Card 2 defines the specific instructions which can be used together with the point locations and a computer-controlled X-Y plotter to generate graphic displays of the tractor at desired times in the simulation. This card may be repeated, if necessary, to define up to 50 lines (or 100 instructions). If N is the line number and ICON(N) and ICON(N+1) are the instructions for line number N, then line number N is defined as follows:

If ICON(N) = ICON(N+1), locate the point whose subscript is ICON(N) with a symbol.

If ICON(N) < ICON(N+1), draw a line from the point whose subscript is ICON(N) consecutively through points of increasing subscript numbers up to that point whose subscript is ICON(N+1).

If ICON(N) > ICON(N+1), draw a line from the point whose subscript is ICON(N) to the point whose subscript is ICON(N+1).

The subscripts are assigned to the points defined in block 10 in the order that they were defined, the starting subscript being 1. Other useful subscripts for points defined by the program are 0 (for the inertial reference frame origin, -1 (for the right front wheel center), -2 (for the left front wheel center), -3 (for the front-end center of mass), -4 (for the right rear wheel center), -5 (for the left rear wheel center), and -6 (for the tractor-body center of mass).

Data block 12 defines the parameters which control the integration of the differential equations. Either one or three cards are required in this data block.

Card 1 defines the integration time limits, the acceptable limit for the local integration error, indicators for printing and punching frequencies, and an indicator for weighting the state variables in the calculation of the local integration error. TZERO defines the starting time for the simulation and TFINAL defines the time at which integration should terminate. DTMAX specifies the maximum time step size which may be used in the integration. ERROR defines the maximum allowable local error that may occur before the integration time step is reduced in size. This local error is calculated as the sum of weighted differences between predicted and corrected state variable values at each point in time. Each state variable difference is weighted equally when IERWT = 1, otherwise the relative weighting factors must be defined on cards 2 described below. NPRINT defines the number of DTMAX-sized integration steps desired per print cycle (NPRINT $\geq$ 1). NPUNCH defines the number of print outputs per punch-type cycle (NPUNCH $\geq$ 1). NPUNCH is not used if IPLOT of data block 10 is less than or equal to zero.

Card 2 defines the relative weights used in calculating the total local truncation error encountered in integrating the twenty state variables. (See Table C-1 for the state variable definitions.) When IERWT $\neq$ 1, all twenty relative error weights must be specified on cards 2 (two cards). When IERWT = 1, the program defines all the error weights equal to one, thus making ERROR the average of all the state variable errors, so cards 2 may be omitted.

C.3.2. Sample Input Data.

The input data was described previously in Section C.3.1. A complete sample set of data which was used for a simulation corresponding to test 1, run 1 of the experimental overturns is provided in Figure C-9. Note that the characters "STOP" in the eighth line are in the first four columns of a data card.

C.3.3. Practical Programming Considerations.

The digital computer program was developed to simulate tractor responses to a wide variety of tractor and terrain conditions. Because parameter studies of the tractor response to changing tractor and terrain conditions are desirable, this program has been designed

```
EXAMPLE RUN TO SHOW OUTPUT GENERATED FOR TEST 1, RUN 1 OF OVERTURNS
   TRACTOR INITIALLY ON LEVEL, ZERO-ELEVATION SURFACE
   TRACTOR SPEED: 38 IN/SEC
   FRONT-END ROTATION LIMIT: 10 DEGREES
   CLUTCH DISENGAGED
   STEERING ANGLE FIXED AT ZERO DEGREES
   PUNCHED OUTPUT REQUESTED FOR SUBSEQUENT PLOTTING
STOP
   0  -8.80      0.10      -4.224                                          XBI
   0  38.0       0.0        0.0                                            VBI
  1.0     0.0    0.0       0.0      1.0      0.0      0.0      0.0      1.0      ATI
   1    0.0       0.0        0.0                                           OMBI
  0.0       0.0                                                       THETF,OMFF1
   2  250.       0.0        0.0                                       INIT,SPE,SPL,SPR
 0.0260     0.0  -.000447  0.0     0.0840     0.0  -.000447  0.0   0.0788    IBT
 0.0128     0.0  -.000136  0.0     0.0788     0.0  -.000136  0.0   0.0125    IFF
 0.00825    0.0132    0.00825      0.0      0.001       3.69           IRT,ID,IE,WB
    0.985     0.76                                                     WR,WF
  -2.80      -3.20       1.35      -2.80       3.20      1.35          RLBT,RRBT
   5.65       0.00       1.75       0.0        0.0       0.90          RPBT,RFPF
   0.0       -1.80       0.35       0.0        1.85      0.35          RLFF,RRFF
   2.75       1.50       0.90       0.0        0.0       0.0      RR,RF,AL,TOI,CAM,CAS
 0.1745       1.20     1000.        0.5                             THMAX,SLENG,SK,SC
  -4.23      -1.52      -5.90  LEFT REAR POINT           1             RHOLT,WHERE
  -4.23       1.43      -5.90  RIGHT REAR POINT          1             RHOLT,WHERE
   6.87      -3.35      -0.90  LEFT FRONT POINT          1             RHOLT,WHERE
   7.20       3.35      -0.90  RIGHT FRONT POINT         0             RHOLT,WHERE
   0                                                                   NFBOD
   0                                                                   NFLR
   0                                                                   NFRR
   0                                                                   NFFE
 0.0174     0.00242      0.500     0.0199    0.00210     0.150  AR,BR,DMPR,AF,BF,DMF
  10.0       10.0        0.90                                     RATIOD,RATIOT,TEFF
   1.04      180.        1.45      200.        1.60      230.          TENG,SENG
   1.45      260.        1.27      290.   ENGINE TORQUE(IN.LB)-ENGINE SPEED(RAD/S)
   0.00      0.0000      1.56     0.0300       2.64     0.0700         TCLUT,SCLUT
   3.13      0.1000      3.47     0.2000  CLUTCH TORQUE(IN.LB)-SLIP
   0.0       0.00000     2.0      0.00545      4.0      0.00887        FREAR,DREAR
   6.0       0.01220     8.0      0.01560 REAR TIRE FORCE(LB)-DEFLECTION(IN)
```

Figure C-9. Sample Input Data.

```
 0.0      0.00000     2.0     0.0128      4.0     0.0203        FFRONT,DFRONT
 6.0      0.0275      8.0     0.0344  FRONT TIRE FORCE(LB)-DEFLECTION(IN)
 0.02       0.00      0.29      0.05      0.44      0.10        COTR,SWHEEL
 0.52       0.20      0.60      0.40  COEF OF GROSS TRACTION-REAR WHEEL SLIP
0.0       0.0        1.07      5.0      1.85      10.0          SLOPER,SLANR
2.22      15.0       2.87      25.0   REAR WHEEL LAT FORCE COEF-SLIP ANGLE(D)
0.0       0.0        0.466     5.0      0.863     10.0          SLOPEF,SLANF
1.27      15.0       1.65      25.0   FRONT WHEEL LAT FORCE COEF-SLIP ANGLE(D)
 0  0.0                                                  IST,ST1,ST2,ST3,ST4,ST5
 2   21     0     0     4     0     0                  IPLOT,NB,NL,NR,NF,NLF,NRF
 1  -4.30      -0.65       2.50                                   IDB,RHODB
 1   6.20      -0.85       1.30                                   IDB,RHODB
 1   6.50      -0.65      -1.85                                   IDB,RHODB
 1   0.60      -0.60      -2.00                                   IDB,RHODB
 1   1.00      -0.75      -0.10                                   IDB,RHODB
 1  -3.75      -0.60      -0.10                                   IDB,RHODB
 1  -3.75       0.60      -0.10                                   IDB,RHODB
 1   1.00       0.75      -0.10                                   IDB,RHODB
 1   0.60       0.60      -2.00                                   IDB,RHODB
 1   6.50       0.65      -1.85                                   IDB,RHODB
 1   6.20       0.85       1.30                                   IDB,RHODB
 1  -4.30       0.65       2.50                                   IDB,RHODB
 1   5.65       0.00       1.75                                   IDB,RHODB
 1  -2.55      -1.52      -0.10                                   IDB,RHODB
 1  -4.23      -1.52      -5.90                                   IDB,RHODB
 1  -2.55       1.43      -0.10                                   IDB,RHODB
 1  -4.23       1.43      -5.90                                   IDB,RHODB
 1   6.35      -0.80      -1.15                                   IDB,RHODB
 1   6.87      -3.35      -0.90                                   IDB,RHODB
 1   6.35       0.80      -1.15                                   IDB,RHODB
 1   7.20       3.35      -0.90                                   IDB,RHODB
 4   0.00       1.85       0.35                                   IDB,RHODB
 4   0.00       1.85      -0.90                                   IDB,RHODB
 4   0.00      -1.80      -0.90                                   IDB,RHODB
 4   0.00      -1.80       0.35                                   IDB,RHODB
18                                                                NLINES
 1   12   12    1   12    7    8    5    9    4   10    3         ICON
11    2   -4   -5   13   11   13    2   13   -3   22   25         ICON
22   -1   25   -2   15   14   17   16   19   18   21   20         ICON
 1.50    0.003525    2.50       0.01          4    1    0   TZ,DT,TF,ER,NPR,NPU,IER
0.05   0.2    0.2    0.2    0.2    0.2    1.0    1.0    1.0    2.0
 2.0   2.0    2.0    0.1    0.2    0.1    0.2    0.5    5.0  0.003
```

Figure C-9 (continued).

to allow easy modification of simulation conditions through changes in the input data. Some of these program features are cited in the paragraphs which follow.

Frequently when parameter studies are being conducted, it is desirable to generate a control simulation, then repeat the final part of this simulation several times, using different parameter values each time, to determine the effect of this one parameter on the tractor response. This programming feature has been provided through the initial condition indicator, INIT, and the other initial position and velocity specifications. After the first simulation has been completed, setting INIT equal to 1 or 4 in succeeding simulations enables the program user to specify the tractor initial conditions exactly, thus the initial conditions for these simulations may be defined to match the tractor conditions printed for an intermediate time in the first simulation. This feature adds versatility for changing the operating conditions during various periods of the simulation. It also saves time by eliminating the need for repeating the initial parts of simulations having identical beginnings. An interesting example would be to simulate one complete tractor overturn while the clutch is engaged, then in succeeding simulations select various intermediate points in time after which the simulation would continue with the clutch disengaged.

The tractor mathematical model was developed to predict motions of wide-front-end wheel tractors, but data specification may be used to constrain motion to that of a tricycle-type tractor. Because the front-end rotation limit (THMAX) and the front-end geometry are defined by input data, the tractor model may be made to conform to a tricycle-type tractor having either two closely-spaced front wheels or a "thick" single front wheel. Setting THMAX equal to zero forces the front wheels to be fixed to the tractor body except for the steering motion and minor deflections at the "stops". Locating the axle pivot points (RLFF and RRFF) on the steering axis and defining the appropriate TOEIN, CAMBER, CASTER, and axle length (ALENG) values, should enable the program user to model a tricycle-type tractor with two front tires. The "thick" single front wheel may be designated by two closely-spaced tires, each having half the stiffness and damping properties of the real tire, while the TOEIN and CAMBER are zero. Note that the inertia properties of the front end are now defined equal to those of the front wheel(s) and yoke.

Digital computer simulation of the tractor motion continues from the initial time (TZERO) until the final time (TFINAL) unless a flag stops the integration prematurely. Because the time span required for a completion of a desired motion often is unknown, it is advantageous to define those conditions which indicate completion of the desired motion. Then these conditions can set the flag (set PRMT(5) $\neq 0$ in subroutine OUTPUT) to terminate integration. The flag conditions for this program are specified within the "SET FLAG" block in subroutine OUTPUT. Presently conditions for terminating integration are the intrusion of any of the monitored points (each being read as data) into the ground at the bottom of the bank. ($XI(3) \geq 4.0$ indicates penetration into the ground.) The points being monitored are easily changed by the data cards, but requesting a flag for any but the above condition would require a change in the "SET FLAG" block.

Flexibility in the introduction of external reactions acting on the tractor allows a variety of interesting simulations to be considered. The influence of gravity or different gravitational fields can be determined by applying forces constant in the vertical direction to the centers of mass for the tractor parts. If the weights of the tractor parts have been negated in this manner, individual application of other reactions to the tractor parts enables the program user to determine the tractor motion sensitivity to individual inputs and check tractor motions against conditions of known response. The use of compression-type springs (ITYPE = 4) enables studies of the tractor motion to collision-type forces which exist only when point(s) on the tractor intrude into a defined area. The use of tension-type springs (ITYPE = 5) allows observations of tractor motions when parts of the tractor are tied down or when a trailed implement strikes an immovable object.

Tractor steering options which are provided include constant values of incrementally-stepped values for steering angles. Other steering options which may be functions of any of the state variables or time may be added as options. Because the tractor orientation and position relative to a path fixed in the inertial reference frame can be expressed in terms of the state variables, a "wagon tongue" (McHenry, et al., 1968) or similar steering control scheme could be defined as another option to be chosen by the value of IST.

Although the particular tractor motion being considered in this dissertation is that on the tractor overturn test course, specification of other tractor initial conditions could send the tractor across the zero-elevation surface defined everywhere above the bank, in any direction down the bank, in any direction up the bank, or across the lower-elevation level surface below the bank. Changes in the terrain would require programming changes in subroutine SURFAC and, if graphic output were desired, in subroutine SURFO.

The graphic display option provides capabilities for generating position information for many points on the tractor at each selected output time. A person could manually use the coordinate information (requested as printed or punched output) in tracing the path of particular points on the tractor or in sketching the tractor at particular times of interest, but this becomes laborious. Instead, computer processing of the point locations and connecting instructions (requested as punched output) could produce sequential plots of the tractor traversing the overturn course, or, if appropriate equipment is available, cathode-ray displays of the tractor motion. (Figure 3-19 shows a sample computer-generated plot.) With either of these two computer-produced graphic displays, the predicted tractor motion could be recorded on motion picture film for subsequent comparison with filmed experimental overturns.

The error weighting option (IERWT) enables the program user to respond to sensitivities of the mathematical model and avoid excessive computer execution time resulting from unnecessary bisections of the integration time step. Because the error value used in interval-bisection decisions is the weighted sum of the error calculated for for each state variable, an abrupt change in any of the state variables may greatly increase the calculated local error and trigger multiple interval bisections. Also, because the state variables have a wide range of magnitudes between them, the same magnitude error contribution by each variable may be a negligibly small error for one variable but a dangerously large error for another variable. The relative error weights should be defined inversely proportional to the expected magnitudes of the individual state variables if the value of ERROR is desired to represent 100 times the average percentage error for the variables at any one time.

Many of the above-mentioned applications of the digital computer program have been suggested to demonstrate generality which was incorporated in the program to make it useful in extensions of the reported work. Some of the options suggested have not been tested fully by the author. Only those options used in the two overturn simulations have been tested thoroughly.

C.3.4. Program Execution Statistics

The digital computer simulations of tractor overturns were run on an IBM 360/65 computer at Cornell University. Double precision constants were used throughout the program to reduce round-off errors inherent in the short word length of this computer. Input and output, however, were usually performed with F-formatted constants to simplify interpretation and to make punched output compatible with a digital incremental plotter used for graphic display of the tractor motions.

The simulation program was compiled with the Fortran H compiler using level 2 optimization. This optimizing compiler increased compilation time but reduced execution time requirements from those of other compilers, thus encouraging a single compilation to create an object program deck and thus eliminate the compilation step from successive simulations. The program statistics for time and central-processing-unit core space for the steps of this program are indicated by the experiences summarized in Table C-5.

TABLE C-5. Core and Time Requirements of the Digital Simulation Program Steps.

Program step	Core (bytes)	CPU time (sec)	I/O time (sec)
Compile (FORTH, OPT = 2)	220K	140	20
Link	98K	5	12
Go (simulation of test 1)	98K	200	17
Go (simulation of test 4)	98K	215	21

C.4. Sample Program Output.

The digital computer program provides printed output at equally-spaced time increments throughout the simulations of tractor motions in addition to the printed definition of the input conditions for the simulation. Figure C-10 shows the input condition printout and the first of the time-spaced printouts generated by the computer program when the input data of Figure C-9 was used. The first four pages of Figure C-9 show the input data description while the last two pages show the output which would be printed at each specified time interval.

Punched output is provided by the program if it is requested. The interval for punched output is specified by the input data. The information shown in Figure C-11 is a listing of some of the punched output generated by the program when the data in Figure C-9 was used. The first card defines the number of points whose inertial coordinates are punched each time punched output is produced and the number of connecting instructions which are punched only once. Cards two through seven give the instruction pairs which define the connections to be used with the point coordinates to draw the tractor and terrain.

Card 8 begins the section of punched output which is produced at a specific simulation time. The block of data previous to the next time card is the coordinate definitions for the points which are located. A partial list of the punched output for time 1.51410 is provided as well in this figure.

The punched output shown in Figure C-11 was used to generate the line drawing of the tractor and terrain shown in Figure 5-19.

```
EXAMPLE RUN TO SHOW OUTPUT GENERATED FOR TEST 1, RUN 1 OF OVERTURNS
   TRACTOR INITIALLY ON LEVEL, ZERO-ELEVATION SURFACE
   TRACTOR SPEED: 38 IN/SEC
   FRONT-END ROTATION LIMIT: 10 DEGREES
   CLUTCH DISENGAGED
   STEERING ANGLE FIXED AT ZERO DEGREES
   PUNCHED OUTPUT REQUESTED FOR SUBSEQUENT PLOTTING


        MOMENTS OF INERTIA (LB.SEC**2.IN.) IN TRACTOR-AXIS DIRECTIONS:

                  TRACTOR BODY                                        FRONT-END
        --                                --         --                                --
        | 0.260D-01 0.000     -0.447D-03 |          | 0.128D-01 0.000     -0.136D-03 |
        | 0.000     0.840D-01 0.000      |          | 0.000     0.788D-01 0.000      |
        |-0.447D-03 0.000     0.788D-01  |          |-0.136D-03 0.000     0.125D-01  |
        --                                --         --                                --

            REAR WHEEL
           --         --
           | 0.825D-02|
           | 0.132D-01|
           | 0.825D-02|
           --         --

            ENGINE        DRIVE TRAIN
           0.100D-02        0.000

        WEIGHTS (LB.):

          TRACTOR BODY       FRONT-END       REAR WHEEL
             3.69              0.760            0.985

        LOCATIONS OF POINTS (IN.) AS TRACTOR-AXIS VECTORS:
           L.R. WHEEL          R.R. WHEEL       FRONT-END PIN
           --       --         --       --        --       --
           |   -2.80|          |   -2.80|         |     5.65|
           |   -3.20|          |    3.20|         |     0.00|
           |    1.35|          |    1.35|         |     1.75|
           --       --         --       --        --       --
```

Figure C-10. Sample Printed Output.

```
FRONT-END C.G.        L.F. --WHEEL PIVOTS-- R.F.
 --     --           --     --        --     --
 |    0.00|          |    0.00|       |    0.00|
 |    0.00|          |   -1.80|       |    1.85|
 |    0.90|          |    0.35|       |    0.35|
 --     --           --     --        --     --
```

FRONT AXLE LENGTHS(IN.): 0.90

FRONT-END ROTATION LIMIT(RADIANS): 0.1745

DISTANCE FROM FRONT PIN TO "STOP"(IN): 1.20

"STOP" STIFFNESS(LB/IN): 1000.0

"STOP" DAMPING(LB-SEC/IN): 0.500

CASTER(RAD): 0.0000

CAMBER(RADIANS): 0.0000

TOEIN(RADIANS): 0.0000

WHEEL RADII (IN.):

REAR	FRONT
2.75	1.50

TIRE ROLLING RESISTANCE COEF. AND RADIAL DAMPING COEF.:
(ROLLING RESISTANCE COEF.= A + B * SLIP ANGLE(DEG))
(DAMPING COEF. UNITS ARE LB.SEC/IN)

	A	B	DAMP
FRONT	0.0199	0.00210	0.1500
REAR	0.0174	0.00242	0.5000

DIFFERENTIAL RATIO = 10.000

TRANSMISSION RATIO = 10.000

TRANSMISSION EFFICIENCY = 0.900

Figure C-10 (continued).

TABULATED INPUT DATA: ENGINE TORQUE(IN.LB)-ENGINE SPEED(RAD/S)

1.0400	180.0000
1.4500	200.0000
1.6000	230.0000
1.4500	260.0000
1.2700	290.0000

TABULATED INPUT DATA: CLUTCH TORQUE(IN.LB)-SLIP

0.0000	0.0000
1.5600	0.0300
2.6400	0.0700
3.1300	0.1000
3.4700	0.2000

TABULATED INPUT DATA: REAR TIRE FORCE(LB)-DEFLECTION(IN)

0.0000	0.0000
2.0000	0.0055
4.0000	0.0089
6.0000	0.0122
8.0000	0.0156

TABULATED INPUT DATA: FRONT TIRE FORCE(LB)-DEFLECTION(IN)

0.0000	0.0000
2.0000	0.0128
4.0000	0.0203
6.0000	0.0275
8.0000	0.0344

TABULATED INPUT DATA: COEF OF GROSS TRACTION-REAR WHEEL SLIP

0.0200	0.0000
0.2900	0.0500
0.4400	0.1000
0.5200	0.2000
0.6000	0.4000

TABULATED INPUT DATA: REAR WHEEL LAT FORCE COEF-SLIP ANGLE(D)

0.0000	0.0000
1.0700	5.0000
1.8500	10.0000
2.2200	15.0000
2.8700	25.0000

Figure C-10 (continued).

```
TABULATED INPUT DATA:     FRONT WHEEL LAT FORCE COEF-SLIP ANGLE(D)
                    0.0000         0.0000
                    0.4660         5.0000
                    0.8630        10.0000
                    1.2700        15.0000
                    1.6500        25.0000


ROOT NO.   1 IS          0.08400226                    8 ITERATIONS


ROOT NO.   2 IS          0.07880378                    2 ITERATIONS


ROOT NO.   3 IS          0.02599621                    2 ITERATIONS

EIGENVALUE NO.  1 IS      0.0840;  EIGENVECTOR:  0.000000
                                                 1.000000
                                                 0.000000

EIGENVALUE NO.  2 IS      0.0788;  EIGENVECTOR: -0.008465
                                                 0.000000
                                                 0.999964

EIGENVALUE NO.  3 IS      0.0260;  EIGENVECTOR:  0.999964
                                                 0.000000
                                                 0.008465

          INTEGRATION PARAMETERS:  TZERO, DTMAX, TFINAL, ERROR
                    1.50000      0.00353       2.50000        0.01000
           PRINT EVERY   4 DTMAX TIME STEPS
           PUNCH EVERY   1 PRINT CYCLES

            THE EQUATION VARIABLES HAVE THE FOLLOWING ERROR WEIGHTS:
             0.0025  0.0100  0.0100  0.0100  0.0100  0.0100  0.0500  0.0500  0.0500  0.1000
             0.1000  0.1000  0.1000  0.0050  0.0100  0.0050  0.0100  0.0250  0.2500  0.0002
```

Figure C-10 (continued).

```
      |<-------------- TRACTOR BODY (LESS REAR WHEELS AND FRONTEND) --------------->|<--REAR WHEELS & FRONTEND -->|

 TIME    C.G. POSITION    C.G. VELOCITY       TRACTOR ORIENTATION        ANGULAR VELOCITY   ANGULAR SPEEDS    ANGULAR POS.
 (SEC)   (IN--FIXED CS)  (IN/SEC--FIXED)  (DIRECTION COSINES--FIXED)  (1/SEC--TR AXES)    (RADIAN/SEC)       (RADIANS)


          --       --     --       --     --                     --      --       --
          |   -8.800|     |    38.000|    | 0.9988  0.0000 -0.0480|      |  0.0000|          -13.864   LEFT        0.00
 1.5000  <|    0.100|>   <|     0.000|>   |-0.0000  1.0000  0.0000|     <|  0.0000|>           0.000   FR.END     0.000
          |   -4.224|     |     0.000|    | 0.0480 -0.0000  0.9988|      |  0.0000|          -13.864   RIGHT       0.00
          --       --     --       --     --                     --      --       --
             LEFT REAR POINT
            -13.308         38.000
             -1.420          0.000
             -9.914          0.000
             RIGHT REAR POINT
            -13.308         38.000
              1.530          0.000
             -9.914          0.000
             LEFT FRONT POINT
             -1.981         38.000
             -3.250          0.000
             -5.453          0.000
             RIGHT FRONT POINT
             -1.651         38.000
              3.450          0.000
             -5.468          0.000

  ENGINE SPEED:      250. RAD/SEC  OR     2387. RPM

  THE INITIAL INTEGRATION TIME INTERVAL WAS HALVED   0 TIMES FOR THIS TIME STEP

  THE TRACTOR STEER ANGLE IS   0.0000 RADIANS.

  THE RESULTANT FORCE ON THE L.R., R.R., L.F., & R.F. TIRE IS,  RESPECTIVELY (LBS, INERTIAL DIRECTIONS):
                -0.152         -0.152         -0.003         -0.003
                -0.000         -0.000         -0.000         -0.000
                -4.075         -4.075         -0.147         -0.147
```

Figure C-10 (continued).

TRANSLATIONAL MOMENTA (LB.SEC) - INERTIAL DIRECTIONS

TRACTOR	L.R. WHEEL	R.R. WHEEL	FRONTEND	TOTAL
0.363	0.097	0.097	0.075	0.632
0.000	0.000	0.000	0.000	0.000
0.000	0.000	0.000	0.000	0.000

ROTATIONAL MOMENTA (LB.IN.SEC) - INERTIAL DIRECTIONS

0.000	0.000	0.000	0.000	0.000
0.000	-0.183	-0.183	0.000	-0.366
0.000	-0.000	-0.000	0.000	-0.000

POTENTIAL ENERGIES (IN.LB)

15.586	2.700	2.700	1.405	22.390

TRANSLATIONAL KINETIC ENERGIES (IN.LB.)

6.902	1.842	1.842	1.422	12.008

ROTATIONAL KINETIC ENERGIES (IN.LB)

0.000	1.269	1.269	0.000	2.537

				36.936

Figure C-10 (continued).

```
116   62                                                                    NPTS,NINST
  8   19   19    8   19   14   15   12   16   11   17   10                 INSTR PAIRS
 18    9    3    2   20   18   20    9   20    4   29   32                 INSTR PAIRS
 29    6   32    5   22   21   24   23   26   25   28   27                 INSTR PAIRS
 33   50   50   33   51   68   68   51   69   86   86   69                 INSTR PAIRS
 87  104  104   87  106  105  108  107  109  116  107  105                 INSTR PAIRS
108  106
 1.50000                                                             TIME
  1     -8.800      0.100     -4.224    2    -11.532     -3.100     -2.741
  3    -11.532      3.300     -2.741    4     -3.029      0.100     -1.848
  5     -3.013     -2.600     -1.498    6     -3.013      2.850     -1.498
  7      0.000      0.000      0.000    8    -12.975     -0.550     -1.520
  9     -2.545     -0.750     -3.223   10     -2.396     -0.550     -6.384
 11     -8.297     -0.500     -6.250   12     -7.806     -0.650     -4.372
 13    -12.550     -0.500     -4.144   14    -12.550      0.700     -4.144
 15     -7.806      0.850     -4.372   16     -8.297      0.700     -6.250
 17     -2.396      0.750     -6.384   18     -2.545      0.950     -3.223
 19    -12.975      0.750     -1.520   20     -3.073      0.100     -2.747
 21    -11.352     -1.420     -4.201   22    -13.308     -1.420     -9.914
 23    -11.352      1.530     -4.201   24    -13.308      1.530     -9.914
 25     -2.513     -0.700     -5.677   26     -1.981     -3.250     -5.453
 27     -2.513      0.900     -5.677   28     -1.651      3.450     -5.468
 29     -3.013      1.950     -1.498   30     -3.073      1.950     -2.747
 31     -3.073     -1.700     -2.747   32     -3.013     -1.700     -1.498
 33    -11.400     -3.100      0.006   34    -10.469     -3.100     -0.204
 35     -9.665     -3.100     -0.722   36     -9.087     -3.100     -1.482
 37     -8.803     -3.100     -2.393   38     -8.849     -3.100     -3.349
 39     -9.219     -3.100     -4.229   40     -9.867     -3.100     -4.930
 41    -10.717     -3.100     -5.368   42    -11.664     -3.100     -5.488
 43    -12.595     -3.100     -5.278   44    -13.399     -3.100     -4.760
 45    -13.977     -3.100     -4.000   46    -14.261     -3.100     -3.089
 47    -14.215     -3.100     -2.133   48    -13.845     -3.100     -1.253
 49    -13.197     -3.100     -0.552   50    -12.347     -3.100     -0.114
 51    -11.400      3.300      0.006   52    -10.469      3.300     -0.204
 53     -9.665      3.300     -0.722   54     -9.087      3.300     -1.482
 55     -8.803      3.300     -2.393   56     -8.849      3.300     -3.349
 57     -9.219      3.300     -4.229   58     -9.867      3.300     -4.930
 59    -10.717      3.300     -5.368   60    -11.664      3.300     -5.488
 61    -12.595      3.300     -5.278   62    -13.399      3.300     -4.760
 63    -13.977      3.300     -4.000   64    -14.261      3.300     -3.089
 65    -14.215      3.300     -2.133   66    -13.845      3.300     -1.253
 67    -13.197      3.300     -0.552   68    -12.347      3.300     -0.114
 69     -2.941     -2.600     -0.000   70     -2.432     -2.600     -0.115
 71     -1.994     -2.600     -0.397   72     -1.679     -2.600     -0.812
```

Figure C-11. Sample Punched Output.

73	-1.524	-2.600	-1.309	74	-1.549	-2.600	-1.830
75	-1.751	-2.600	-2.310	76	-2.104	-2.600	-2.692
77	-2.568	-2.600	-2.931	78	-3.085	-2.600	-2.997
79	-3.593	-2.600	-2.882	80	-4.031	-2.600	-2.600
81	-4.346	-2.600	-2.185	82	-4.501	-2.600	-1.688
83	-4.476	-2.600	-1.167	84	-4.274	-2.600	-0.687
85	-3.921	-2.600	-0.304	86	-3.457	-2.600	-0.065
87	-2.941	2.850	-0.000	88	-2.432	2.850	-0.115
89	-1.994	2.850	-0.397	90	-1.679	2.850	-0.812
91	-1.524	2.850	-1.309	92	-1.549	2.850	-1.830
93	-1.751	2.850	-2.310	94	-2.104	2.850	-2.692
95	-2.568	2.850	-2.931	96	-3.085	2.850	-2.997
97	-3.593	2.850	-2.882	98	-4.031	2.850	-2.600
99	-4.346	2.850	-2.185	100	-4.501	2.850	-1.688
101	-4.476	2.850	-1.167	102	-4.274	2.850	-0.687
103	-3.921	2.850	-0.304	104	-3.457	2.850	-0.065
105	-15.000	-5.748	0.000	106	30.000	3.817	0.000
107	-15.000	-9.163	3.980	108	30.000	0.403	3.980
109	5.000	1.700	-1.480	110	5.000	4.700	-1.480
111	15.000	4.700	-1.480	112	15.000	1.700	-1.480
113	5.000	1.700	-1.480	114	0.000	1.700	0.000
115	0.000	4.700	0.000	116	5.000	4.700	-1.480

1.51410 TIME

1	-8.263	0.100	-4.223	2	-10.997	-3.100	-2.745
3	-10.997	3.300	-2.745	4	-2.496	0.100	-1.837
5	-2.480	-2.600	-1.487	6	-2.480	2.850	-1.487
7	0.000	0.000	0.000	8	-12.443	-0.550	-1.527
9	-2.009	-0.750	-3.211	10	-1.855	-0.550	-6.371
11	-7.756	-0.500	-6.249	12	-7.268	-0.650	-4.369
13	-12.013	-0.500	-4.150	14	-12.013	0.700	-4.150
15	-7.268	0.850	-4.369	16	-7.756	0.700	-6.249
17	-1.855	0.750	-6.371	18	-2.009	0.950	-3.211
19	-12.443	0.750	-1.527	20	-2.538	0.100	-2.736
21	-10.815	-1.420	-4.205	22	-12.761	-1.420	-9.922
23	-10.815	1.530	-4.205	24	-12.761	1.530	-9.922
25	-1.973	-0.700	-5.665	26	-1.442	-3.250	-5.439
27	-1.973	0.900	-5.665	28	-1.112	3.450	-5.454
29	-2.480	1.950	-1.487	30	-2.538	1.950	-2.736
31	-2.538	-1.700	-2.736	32	-2.480	-1.700	-1.487
33	-11.405	-3.100	-0.026	34	-10.451	-3.100	-0.049
35	-9.561	-3.100	-0.400	36	-8.846	-3.100	-1.032

•
•
•

Figure C-11 (continued).

APPENDIX D

EXPERIMENTAL OVERTURN DATA

The four tractor-body reference points define the position of the tractor at any time. The locations of these points, defined in the three inertial-coordinate directions $(\underline{e}_{I_1}$, $\underline{e}_{I_2}$, and $\underline{e}_{I_3})$, and the film-frame times for each of the ten filmed overturns are given in Tables D-1 through D-10. Each table presents the coordinate and time data for one scale-model overturn.

TABLE D-1. Tractor-Body Reference-Point Coordinates and Times for Overturn Test 1, Run 1.

	TIME		XLRI			XRRI			XLFI			XRFI	
1	1.48	-13.55	-1.26	-10.07	-13.71	1.64	-10.16	-2.32	-3.22	-5.57	-1.94	3.34	-5.43
2	1.50	-13.17	-1.26	-10.07	-13.13	1.64	-10.07	-1.67	-3.21	-5.66	-1.65	3.33	-5.43
3	1.51	-12.51	-1.26	-10.07	-12.56	1.63	-10.07	-1.11	-3.20	-5.66	-0.97	3.32	-5.53
4	1.53	-12.04	-1.25	-10.07	-12.08	1.62	-10.07	-0.65	-3.20	-5.66	-0.48	3.31	-5.43
5	1.54	-11.37	-1.37	-10.06	-11.50	1.62	-10.07	0.00	-2.95	-5.67	0.19	3.30	-5.43
6	1.55	-11.00	-1.37	-10.06	-10.93	1.62	-10.07	0.37	-3.18	-5.75	0.78	3.41	-5.34
7	1.57	-10.34	-1.37	-10.06	-10.45	1.62	-10.07	0.93	-3.17	-5.57	1.16	3.28	-5.43
8	1.58	-9.96	-1.36	-10.06	-9.87	1.61	-10.07	1.48	-3.28	-5.66	1.65	3.27	-5.43
9	1.59	-9.40	-1.36	-9.96	-9.49	1.61	-9.97	1.86	-3.27	-5.66	2.13	3.38	-5.53
10	1.61	-9.12	-1.36	-9.96	-9.01	1.60	-9.97	2.32	-3.26	-5.84	2.71	3.26	-5.62
11	1.62	-8.46	-1.35	-9.87	-8.44	1.72	-9.98	1.85	-3.39	-5.93	3.20	3.25	-5.72
12	1.64	-8.18	-1.35	-9.96	-8.06	1.72	-9.98	3.15	-3.37	-5.93	3.77	3.01	-5.71
13	1.65	-7.71	-1.35	-9.96	-7.57	1.59	-9.97	3.80	-3.59	-6.10	4.16	2.89	-5.71
14	1.66	-7.33	-1.35	-9.96	-7.09	1.59	-9.97	3.88	-3.81	-6.19	4.64	2.76	-5.90
15	1.67	-7.05	-1.47	-9.86	-6.90	1.59	-9.97	4.35	-3.81	-6.19	5.02	2.76	-6.09
16	1.69	-6.67	-1.46	-9.77	-6.52	1.59	-9.87	4.72	-3.80	-6.37	5.41	2.75	-6.19
17	1.70	-6.39	-1.34	-9.78	-6.13	1.58	-9.87	5.36	-3.78	-6.56	5.79	2.63	-6.38
18	1.72	-5.92	-1.46	-9.77	-5.94	1.58	-9.87	5.55	-3.90	-6.64	6.27	2.63	-6.57
19	1.73	-5.64	-1.46	-9.77	-5.27	1.58	-9.78	6.01	-3.89	-6.83	6.66	2.62	-6.67
20	1.74	-5.07	-1.45	-9.77	-4.98	1.57	-9.87	6.56	-3.99	-6.73	7.04	2.61	-6.57
21	1.76	-4.69	-1.57	-9.76	-4.60	1.45	-9.87	6.74	-4.10	-6.72	7.53	2.61	-6.57
22	1.77	-4.41	-1.57	-9.76	-4.12	1.45	-9.87	7.19	-4.20	-6.72	7.91	2.49	-6.56
23	1.78	-3.76	-1.56	-9.76	-3.73	1.32	-9.86	7.66	-4.19	-6.72	8.29	2.48	-6.56
24	1.80	-3.47	-1.68	-9.66	-3.35	1.20	-9.75	8.03	-4.07	-6.63	8.77	2.37	-6.66
25	1.82	-3.00	-1.80	-9.65	-2.96	1.08	-9.75	8.49	-4.06	-6.54	9.14	2.25	-6.55
26	1.83	-2.62	-2.15	-9.63	-2.43	0.84	-9.83	8.94	-4.28	-6.44	9.63	2.35	-6.66
27	1.84	-2.05	-2.38	-9.61	-1.91	0.71	-9.82	9.50	-4.26	-6.44	9.91	2.24	-6.65
28	1.86	-1.77	-2.74	-9.59	-1.43	0.24	-9.98	9.87	-4.25	-6.16	10.28	2.01	-6.54
29	1.87	-1.30	-3.09	-9.47	-1.14	-0.24	-9.94	10.11	-4.70	-5.78	10.65	1.78	-6.44
30	1.88	-0.83	-3.67	-9.52	-0.66	-0.83	-9.90	10.84	-4.79	-5.50	11.03	1.67	-6.53
31	1.90	-0.28	-4.02	-9.50	-0.19	-1.18	-10.07	11.08	-5.23	-5.20	11.59	1.44	-6.52
32	1.92	0.09	-4.60	-9.18	0.28	-1.53	-9.95	11.62	-5.32	-4.74	11.86	1.33	-6.42
33	1.93	0.64	-5.06	-9.15	0.75	-2.23	-9.90	11.98	-5.42	-4.38	12.31	0.88	-6.40
34	1.94	1.19	-5.63	-8.93	1.21	-2.70	-9.96	12.50	-5.74	-3.91	12.66	0.55	-6.29
35	1.96	1.73	-6.08	-8.54	1.85	-3.62	-9.89	12.95	-5.83	-3.45	13.12	0.33	-6.09

TABLE D-1 (continued).

36	1.97	2.45	-6.64	-8.41	2.49	-3.96	-9.78	13.41	-5.82	-3.00	13.48	0.11	-5.89
37	1.98	2.98	-7.20	-7.93	2.94	-4.53	-9.46	13.78	-5.81	-2.55	13.92	-0.22	-5.78
38	2.00	3.42	-7.76	-7.54	3.48	-5.21	-9.41	14.31	-5.90	-2.09	14.38	-0.44	-5.77
39	2.02	3.86	-8.09	-7.34	3.83	-5.90	-9.18	14.54	-6.33	-1.81	14.82	-0.76	-5.75
40	2.03	4.30	-8.54	-6.96	4.36	-6.57	-8.96	14.92	-6.21	-1.54	15.17	-0.98	-5.65
41	2.04	4.73	-8.98	-6.58	4.79	-7.13	-8.47	15.47	-6.19	-1.09	15.51	-1.41	-5.63
42	2.06	5.33	-9.75	-6.01	5.31	-7.69	-8.25	15.83	-6.17	-0.73	15.94	-1.73	-5.52
43	2.07	5.75	-10.30	-5.63	5.74	-8.24	-7.86	16.28	-6.27	-0.54	16.40	-1.84	-5.52
44	2.08	6.26	-10.62	-5.09	6.25	-8.90	-7.38	16.74	-6.25	-0.18	16.71	-2.37	-5.40
45	2.10	6.78	-10.81	-4.65	6.77	-9.33	-7.00	17.28	-6.23	0.18	17.08	-2.47	-5.31
46	2.11	7.37	-11.46	-3.93	7.27	-9.99	-6.52	17.56	-6.22	0.54	17.57	-3.00	-5.19
47	2.13	8.06	-11.64	-3.31	8.03	-10.52	-6.06	17.92	-6.21	1.00	17.91	-3.32	-4.90
48	2.14	8.57	-11.84	-2.78	8.61	-11.27	-5.41	18.48	-6.08	1.36	18.41	-3.74	-4.89
49	2.16	9.05	-12.59	-1.99	9.17	-12.02	-4.69	18.84	-6.18	1.81	18.79	-4.37	-4.59
50	2.17	9.55	-12.90	-1.12	9.49	-12.45	-4.07	19.39	-6.16	2.18	19.29	-4.78	-4.39
51	2.18	9.79	-13.22	-0.26	9.97	-13.09	-3.19	19.75	-6.14	2.54	19.88	-5.19	-4.01
52	2.20	10.36	-13.62	1.03	10.37	-13.51	-2.15	19.93	-6.14	2.99	20.33	-5.91	-3.54
53	2.22	10.96	-13.69	1.98	11.04	-13.79	-1.11	20.30	-6.12	3.45	20.79	-6.53	-2.98
54	2.23	10.96	-13.69	2.41	11.25	-14.33	-0.60	20.39	-6.12	3.63	21.15	-7.15	-2.60
55	2.24	11.03	-13.91	2.40	11.32	-14.55	-0.60	20.62	-6.43	3.62	21.36	-7.56	-2.68

TABLE D-2. Tractor-Body Reference-Point Coordinates and Times for Overturn Test 1, Run 2.

	TIME		XLRI			XRRI			XLFI			XRFI	
1	1.47	-13.94	-1.01	-10.08	-13.76	2.15	-10.00	-2.61	-2.75	-5.31	-2.23	3.70	-5.35
2	1.49	-13.30	-0.88	-10.09	-13.36	2.02	-9.99	-1.96	-2.74	-5.68	-1.85	3.81	-5.35
3	1.50	-12.92	-0.88	-10.09	-12.88	2.01	-9.99	-1.58	-2.74	-5.59	-1.26	3.80	-5.35
4	1.52	-12.25	-1.00	-10.08	-12.30	2.01	-9.99	-1.40	-2.73	-5.59	-0.68	3.79	-5.35
5	1.53	-11.78	-1.00	-10.08	-11.71	1.88	-9.99	-0.56	-2.60	-5.59	-0.10	3.66	-5.35
6	1.54	-11.21	-1.00	-9.99	-11.34	2.00	-10.09	0.00	-2.71	-5.59	0.29	3.65	-5.35
7	1.56	-10.65	-1.00	-10.08	-10.67	1.99	-10.09	0.47	-2.71	-5.59	0.68	3.76	-5.35
8	1.57	-10.27	-0.99	-10.08	-10.28	1.99	-10.09	1.12	-2.70	-5.68	1.26	3.87	-5.35
9	1.58	-9.71	-0.99	-10.08	-9.70	1.98	-10.09	1.49	-2.69	-5.68	1.85	3.86	-5.55
10	1.60	-9.33	-0.99	-10.08	-9.33	2.10	-10.10	1.96	-2.80	-5.86	2.24	3.73	-5.64
11	1.62	-8.76	-0.99	-9.99	-8.74	1.97	-10.09	2.33	-2.80	-5.86	2.82	3.84	-5.74
12	1.63	-8.48	-0.98	-9.89	-8.46	2.09	-10.00	2.98	-2.90	-5.95	3.40	3.71	-5.74
13	1.64	-8.10	-0.98	-9.89	-7.88	2.09	-10.00	3.25	-3.13	-6.03	3.88	3.58	-5.83
14	1.65	-7.63	-0.98	-9.89	-7.50	2.08	-10.00	3.81	-3.24	-6.03	4.36	3.34	-5.82
15	1.67	-7.26	-0.98	-9.89	-7.12	2.08	-9.91	4.18	-3.23	-6.21	4.94	3.33	-6.11
16	1.68	-6.88	-0.98	-9.89	-6.73	2.07	-10.00	4.55	-3.34	-6.30	5.13	3.22	-6.11
17	1.69	-6.50	-0.98	-9.89	-6.34	1.95	-9.90	4.82	-3.34	-6.49	5.52	3.09	-6.30
18	1.71	-6.31	-0.97	-9.71	-6.06	2.07	-9.81	5.38	-3.33	-6.58	6.00	3.09	-6.49
19	1.72	-5.74	-1.09	-9.70	-5.67	2.06	-9.81	5.75	-3.32	-6.76	6.38	2.97	-6.58
20	1.74	-5.37	-0.97	-9.71	-5.28	1.94	-9.80	6.22	-3.31	-6.76	6.77	3.07	-6.59
21	1.75	-4.80	-1.09	-9.70	-4.80	1.81	-9.89	6.68	-3.42	-6.66	7.45	2.95	-6.58
22	1.76	-4.52	-1.09	-9.70	-4.51	1.61	-9.89	7.13	-3.52	-6.66	7.64	2.95	-6.58
23	1.77	-4.05	-1.20	-9.69	-3.84	1.68	-9.79	7.41	-3.52	-6.57	8.02	2.94	-6.58
24	1.79	-3.67	-1.20	-9.69	-3.55	1.68	-9.79	7.78	-3.62	-6.75	8.51	3.04	-6.59
25	1.80	-3.29	-1.20	-9.69	-3.16	1.68	-9.79	8.15	-3.62	-6.56	8.89	2.81	-6.58
26	1.82	-2.73	-1.32	-9.68	-2.68	1.55	-9.87	8.70	-3.61	-6.65	9.38	3.03	-6.59
27	1.83	-2.25	-1.55	-9.67	-2.20	1.55	-9.87	9.16	-3.71	-6.56	9.76	2.80	-6.68
28	1.84	-1.88	-1.67	-9.75	-1.72	1.31	-9.86	9.53	-3.70	-6.46	10.04	2.68	-6.57
29	1.86	-1.59	-2.14	-9.81	-1.34	0.95	-10.02	9.62	-3.81	-6.27	10.32	2.57	-6.47
30	1.87	-0.93	-2.37	-9.89	-0.86	0.71	-10.20	10.44	-3.91	-6.08	10.62	2.68	-6.48
31	1.89	-0.56	-2.60	-9.78	-0.38	0.35	-10.17	10.89	-4.12	-5.80	11.46	2.33	-6.46
32	1.90	0.00	-2.95	-9.85	0.00	-0.12	-10.14	11.34	-4.22	-5.61	11.74	2.22	-6.46
33	1.92	0.37	-3.18	-9.74	0.66	-0.35	-10.31	11.70	-4.32	-5.33	12.20	1.99	-6.45
34	1.93	0.74	-3.76	-9.61	0.94	-0.82	-10.28	12.05	-4.65	-5.04	12.47	1.77	-6.34
35	1.94	1.11	-3.99	-9.78	1.32	-1.29	-10.25	12.50	-4.75	-4.76	12.84	1.54	-6.43

TABLE D-2 (continued).

36	1.96	1.66	-4.44	-9.65	1.78	-1.52	-10.32	12.87	-4.74	-4.49	13.31	1.43	-6.33
37	1.97	2.11	-4.90	-9.16	2.34	-2.10	-10.28	13.32	-4.83	-4.21	13.59	1.32	-6.22
38	1.99	2.56	-5.24	-8.96	2.80	-2.44	-10.25	13.67	-4.93	-3.84	14.04	1.09	-6.12
39	2.00	3.11	-5.46	-8.67	3.26	-2.78	-10.04	14.30	-5.14	-3.47	14.50	0.87	-6.01
40	2.02	3.65	-5.79	-8.46	3.81	-3.24	-9.92	14.56	-5.24	-3.10	14.97	0.76	-5.91
41	2.03	4.27	-6.34	-8.43	4.25	-3.81	-9.88	15.09	-5.44	-2.64	15.31	0.43	-5.80
42	2.04	4.71	-6.79	-8.04	4.70	-4.37	-9.65	15.37	-5.43	-2.46	15.66	0.11	-5.79
43	2.06	5.24	-7.35	-7.65	5.23	-4.94	-9.43	15.90	-5.52	-2.00	16.12	0.00	-5.69
44	2.07	5.58	-7.68	-7.36	5.67	-5.50	-9.30	16.35	-5.62	-1.82	16.37	-0.32	-5.68
45	2.09	6.02	-8.00	-7.07	6.10	-6.06	-8.99	16.72	-5.60	-1.55	16.84	-0.43	-5.67
46	2.10	6.54	-8.43	-6.60	6.54	-6.38	-8.69	17.18	-5.59	-1.18	17.27	-0.75	-5.66
47	2.12	7.05	-8.98	-6.31	6.98	-6.82	-8.48	17.53	-5.69	-1.00	17.62	-0.97	-5.56
48	2.13	7.56	-9.41	-5.84	7.49	-7.48	-8.08	18.08	-5.67	-0.64	18.06	-1.28	-5.54
49	2.14	8.16	-9.83	-5.47	8.09	-7.91	-7.79	18.54	-5.65	-0.27	18.52	-1.39	-5.35
50	2.16	8.68	-10.14	-4.93	8.68	-8.56	-7.39	18.91	-5.64	0.09	18.86	-1.60	-5.15
51	2.17	9.27	-10.56	-4.56	9.20	-8.88	-6.84	19.38	-5.52	0.55	19.29	-1.91	-4.96
52	2.18	9.85	-11.08	-4.11	9.59	-9.64	-6.62	19.79	-5.83	0.82	19.80	-2.33	-4.94
53	2.20	10.09	-11.41	-3.49	10.18	-10.17	-6.16	20.19	-5.60	1.00	20.20	-2.85	-4.83
54	2.22	10.61	-11.48	-2.88	10.58	-10.71	-5.52	20.50	-6.01	1.45	20.68	-3.37	-4.53
55	2.23	10.85	-11.80	-2.26	10.99	-11.13	-5.06	20.77	-6.00	1.81	21.10	-3.68	-4.43
56	2.24	11.43	-12.21	-1.91	11.58	-11.42	-4.44	21.21	-6.09	2.08	21.66	-4.30	-4.04
57	2.26	11.75	-12.52	-0.86	11.87	-12.18	-3.72	21.67	-6.08	2.72	22.14	-4.81	-3.75
58	2.27	12.15	-12.94	0.00	12.45	-12.47	-2.94	22.11	-6.17	3.17	22.59	-5.42	-3.37
59	2.28	12.56	-13.24	0.86	12.76	-12.89	-1.98	22.44	-5.84	3.54	23.06	-5.92	-2.81
60	2.30	13.23	-13.41	1.63	13.31	-13.51	-1.46	22.65	-6.25	3.62	23.35	-6.43	-2.62

TABLE D-3. Tractor-Body Reference-Point Coordinates and Times for Overturn Test 1, Run 3.

	TIME		XLRI			XRRI			XLFI			XRFI	
1	1.45	-14.12	-1.14	-10.07	-14.09	1.65	-9.97	-2.97	-3.11	-5.57	-2.62	3.59	-5.44
2	1.46	-13.64	-1.26	-10.07	-13.52	1.64	-10.07	-2.23	-2.98	-5.58	-1.94	3.34	-5.43
3	1.48	-13.26	-1.26	-9.97	-13.04	1.64	-9.97	-1.67	-3.09	-5.57	-1.36	3.33	-5.33
4	1.49	-12.51	-1.26	-10.07	-12.56	1.63	-10.07	-1.21	-3.09	-5.57	-0.78	3.43	-5.43
5	1.50	-12.03	-1.38	-10.06	-11.98	1.63	-10.07	-0.65	-3.20	-5.66	-0.39	3.31	-5.33
6	1.52	-11.48	-1.25	-9.97	-11.41	1.62	-10.07	-0.19	-3.19	-5.66	0.19	3.30	-5.43
7	1.53	-10.91	-1.25	-9.97	-10.93	1.62	-9.97	0.37	-3.18	-5.66	0.68	3.29	-5.33
8	1.54	-10.35	-1.24	-9.97	-10.35	1.62	-9.97	0.93	-3.17	-5.57	1.16	3.40	-5.34
9	1.56	-9.97	-1.24	-9.97	-9.97	1.61	-9.97	1.30	-3.05	-5.67	1.65	3.39	-5.43
10	1.57	-9.41	-1.24	-9.97	-9.40	1.73	-9.98	1.76	-3.16	-5.57	2.23	3.26	-5.53
11	1.58	-9.02	-1.36	-9.96	-8.92	1.73	-9.98	2.32	-3.15	-5.85	2.71	3.37	-5.63
12	1.60	-8.47	-1.23	-9.88	-8.44	1.72	-9.88	2.78	-3.26	-5.84	3.20	3.25	-5.72
13	1.62	-8.19	-1.23	-9.88	-7.96	1.72	-9.88	3.06	-3.48	-5.83	3.87	3.12	-5.72
14	1.63	-7.71	-1.35	-9.96	-7.48	1.59	-9.97	3.61	-3.70	-5.92	4.35	3.00	-5.81
15	1.64	-7.43	-1.35	-10.06	-7.00	1.59	-9.97	3.98	-3.70	-6.19	4.74	2.99	-6.00
16	1.66	-7.05	-1.47	-9.77	-6.80	1.59	-9.87	4.44	-3.80	-6.46	5.02	2.76	-6.09
17	1.67	-6.58	-1.46	-9.77	-6.52	1.59	-9.87	4.81	-3.80	-6.46	5.60	2.63	-6.28
18	1.69	-6.39	-1.34	-9.68	-6.23	1.58	-9.78	5.08	-3.91	-6.64	5.69	2.63	-6.47
19	1.70	-5.92	-1.46	-9.67	-5.65	1.58	-9.78	5.55	-3.78	-6.74	6.27	2.63	-6.57
20	1.72	-5.55	-1.33	-9.68	-5.27	1.58	-9.78	5.92	-3.77	-6.74	6.75	2.62	-6.67
21	1.73	-5.07	-1.45	-9.67	-4.89	1.57	-9.78	6.48	-3.76	-6.74	7.13	2.50	-6.56
22	1.74	-4.60	-1.45	-9.67	-4.40	1.45	-9.77	6.83	-4.10	-6.63	7.81	2.49	-6.56
23	1.76	-4.22	-1.57	-9.67	-3.93	1.44	-9.77	7.38	-4.08	-6.63	8.00	2.49	-6.56
24	1.77	-3.76	-1.56	-9.76	-3.54	1.44	-9.87	7.66	-4.19	-6.44	8.39	2.60	-6.57
25	1.78	-3.38	-1.56	-9.67	-3.15	1.20	-9.75	8.02	-4.18	-6.53	8.87	2.48	-6.56
26	1.80	-2.81	-1.91	-9.64	-2.68	1.20	-9.75	8.58	-4.17	-6.53	9.25	2.36	-6.56
27	1.81	-2.53	-2.03	-9.63	-2.29	0.95	-9.83	9.03	-4.27	-6.44	9.63	2.35	-6.56
28	1.83	-1.96	-2.26	-9.62	-1.81	0.71	-9.82	9.40	-4.26	-6.25	10.20	2.23	-6.55
29	1.84	-1.58	-2.62	-9.59	-1.43	0.24	-9.88	9.48	-4.49	-6.06	10.28	2.01	-6.35
30	1.85	-1.12	-2.97	-9.66	-0.76	-0.24	-10.04	10.38	-4.80	-5.77	10.84	1.78	-6.44
31	1.87	-0.65	-3.55	-9.62	-0.47	-0.71	-10.10	10.75	-4.79	-5.40	11.31	1.56	-6.43
32	1.88	-0.18	-3.90	-9.42	-0.09	-0.94	-10.08	11.19	-5.00	-5.12	11.68	1.44	-6.42
33	1.90	0.28	-4.48	-9.19	0.47	-1.53	-10.04	11.72	-5.21	-4.75	12.04	1.11	-6.41
34	1.91	0.92	-4.81	-9.08	1.03	-1.99	-10.01	12.07	-5.42	-4.28	12.49	0.77	-6.20
35	1.92	1.37	-5.39	-8.86	1.58	-2.69	-9.96	12.52	-5.52	-3.92	12.87	0.77	-6.10

TABLE D-3 (continued).

36	1.94	1.92	-5.84	-8.65	2.04	-3.15	-9.93	12.96	-5.72	-3.55	13.30	0.22	-5.99
37	1.95	2.46	-6.29	-8.44	2.50	-3.73	-9.79	13.42	-5.71	-2.91	13.67	0.11	-5.89
38	1.96	2.99	-6.85	-8.22	3.04	-4.30	-9.66	13.96	-5.80	-2.64	14.21	-0.22	-5.68
39	1.98	3.61	-7.29	-7.83	3.67	-4.98	-9.43	14.31	-5.90	-2.09	14.58	-0.33	-5.68
40	1.99	4.04	-7.97	-7.43	4.20	-5.54	-9.30	14.74	-6.21	-1.81	15.01	-0.76	-5.66
41	2.01	4.48	-8.30	-7.06	4.55	-6.11	-9.08	15.19	-6.20	-1.54	15.36	-0.98	-5.65
42	2.02	5.00	-8.96	-6.49	4.99	-6.67	-9.58	15.65	-6.18	-1.09	15.79	-1.41	-5.54
43	2.04	5.51	-9.51	-6.20	5.49	-7.68	-8.25	16.10	-6.27	-0.82	16.22	-1.73	-5.52
44	2.05	6.03	-9.83	-5.65	6.03	-7.89	-7.97	16.45	-6.37	-0.45	16.67	-1.94	-5.33
45	2.06	6.46	-10.26	-5.19	6.45	-8.44	-7.58	16.92	-6.24	0.00	17.09	-2.37	-5.22
46	2.08	6.97	-10.58	-4.66	7.05	-8.98	-7.19	17.47	-6.22	0.18	17.54	-2.47	-5.03
47	2.09	7.64	-11.22	-4.02	7.54	-9.86	-6.44	17.90	-6.42	0.63	17.95	-3.00	-4.92
48	2.11	8.23	-11.63	-3.40	8.12	-10.51	-6.23	18.37	-6.30	0.91	18.37	-3.31	-4.81
49	2.12	8.56	-12.06	-2.78	8.62	-11.05	-5.51	18.75	-6.18	1.18	18.76	-3.94	-4.60
50	2.13	9.34	-12.13	-2.00	9.29	-11.57	-4.70	19.20	-6.16	1.63	19.35	-4.35	-4.40
51	2.14	9.90	-12.87	-1.29	9.83	-12.54	-4.06	19.66	-6.15	2.27	19.85	-4.76	-4.12
52	2.16	10.23	-13.07	-0.34	10.33	-12.95	-3.19	19.93	-6.14	2.45	20.23	-5.28	-3.92
53	2.18	10.79	-13.70	0.77	10.80	-13.59	-2.06	20.38	-6.23	2.99	20.74	-5.58	-3.45
54	2.19	11.21	-13.78	1.72	11.47	-13.76	-1.37	20.76	-6.11	3.45	21.11	-6.20	-2.89
55	2.21	11.45	-13.98	2.06	11.78	-14.18	-0.85	20.83	-6.21	3.71	21.58	-6.71	-2.61

TABLE D-4. Tractor-Body Reference-Point Coordinates and Times for Overturn Test 2, Run 1.

	TIME		XLRI			XRRI			XLFI			XRFI	
1	1.22	-14.40	-1.14	-10.07	-14.30	1.77	-9.98	-3.16	-2.88	-5.58	-2.81	3.47	-5.34
2	1.23	-13.84	-1.14	-10.07	-13.72	1.77	-9.98	-2.51	-2.87	-5.58	-2.14	3.70	-5.35
3	1.25	-13.09	-1.13	-9.98	-13.15	1.76	-9.98	-1.95	-2.86	-5.68	-1.65	3.57	-5.44
4	1.27	-12.52	-1.13	-9.98	-12.47	1.76	-10.07	-1.12	-2.73	-5.59	-0.87	3.67	-5.35
5	1.28	-11.86	-1.13	-9.98	-11.80	1.75	-9.98	-0.65	-2.84	-5.58	-0.19	3.42	-5.34
6	1.29	-11.19	-1.25	-9.97	-11.23	1.75	-9.98	0.09	-2.83	-5.58	0.39	3.53	-5.34
7	1.31	-10.55	-1.12	-9.98	-10.55	1.74	-10.07	0.65	-3.06	-5.57	1.07	3.52	-5.34
8	1.32	-9.98	-1.12	-9.98	-9.98	1.74	-10.07	1.30	-3.05	-5.57	1.65	3.63	-5.35
9	1.33	-9.32	-1.11	-9.98	-9.40	1.73	-10.07	1.77	-3.04	-5.67	2.23	3.38	-5.53
10	1.35	-8.76	-1.11	-9.98	-8.84	1.97	-10.09	2.32	-3.15	-5.85	2.91	3.49	-5.63
11	1.37	-8.38	-1.11	-9.98	-8.25	1.72	-9.98	2.97	-3.14	-5.94	3.58	3.24	-5.72
12	1.38	-7.82	-1.10	-9.98	-7.68	1.84	-9.89	3.43	-3.24	-6.03	3.97	3.00	-5.91
13	1.39	-7.34	-1.10	-9.89	-7.10	1.71	-9.88	3.89	-3.47	-6.11	4.74	3.11	-6.01
14	1.41	-6.87	-1.22	-9.88	-6.62	1.71	-9.88	4.36	-3.34	-6.30	5.12	2.76	-6.09
15	1.42	-6.40	-1.22	-9.88	-6.14	1.70	-9.88	4.91	-3.68	-6.47	5.69	2.63	-6.47
16	1.43	-5.93	-1.22	-9.78	-5.66	1.70	-9.79	5.46	-3.67	-6.65	6.09	2.86	-6.58
17	1.45	-5.55	-1.33	-9.68	-5.18	1.70	-9.79	6.11	-3.66	-6.75	6.66	2.73	-6.67
18	1.47	-4.89	-1.33	-9.68	-4.79	1.57	-9.78	6.57	-3.76	-6.74	7.44	2.84	-6.68
19	1.48	-4.42	-1.33	-9.68	-4.31	1.57	-9.78	7.12	-3.75	-6.65	7.81	2.60	-6.67
20	1.49	-3.76	-1.44	-9.67	-3.55	1.56	-9.78	7.67	-3.85	-6.55	8.39	2.48	-6.47
21	1.51	-3.29	-1.56	-9.67	-3.16	1.44	-9.77	8.05	-3.73	-6.56	8.87	2.59	-6.57
22	1.53	-2.72	-1.56	-9.76	-2.49	1.31	-9.86	8.59	-3.95	-6.55	9.54	2.47	-6.56
23	1.54	-1.97	-1.91	-9.83	-1.81	0.95	-9.93	9.23	-4.16	-6.35	10.31	2.46	-6.56
24	1.55	-1.50	-2.26	-9.81	-1.33	0.71	-10.01	10.05	-4.25	-6.16	10.59	2.34	-6.66
25	1.57	-0.84	-2.72	-9.77	-0.57	0.24	-10.17	10.39	-4.69	-5.78	11.05	2.00	-6.54
26	1.58	-0.28	-3.19	-9.65	-0.09	-0.35	-10.22	10.93	-4.79	-5.50	11.71	1.77	-6.44
27	1.59	0.28	-3.77	-9.52	0.47	-0.82	-10.19	11.58	-4.77	-5.22	12.06	1.44	-6.42
28	1.61	0.92	-4.34	-9.29	1.03	-1.41	-10.14	12.09	-5.20	-4.75	12.61	1.10	-6.41
29	1.63	1.47	-4.80	-9.17	1.59	-1.99	-10.10	12.52	-5.52	-4.28	12.97	0.88	-6.30
30	1.64	2.01	-5.25	-8.96	2.14	-2.68	-9.96	13.08	-5.39	-3.83	13.60	0.44	-6.09
31	1.65	2.64	-5.93	-8.73	2.88	-3.25	-9.92	13.80	-5.59	-3.37	14.07	0.33	-5.89
32	1.67	3.36	-6.61	-8.32	3.51	-3.82	-9.78	14.23	-5.79	-2.91	14.61	0.00	-5.88
33	1.68	4.07	-7.16	-7.75	4.14	-4.50	-9.46	14.67	-5.77	-2.45	15.25	-0.22	-5.68
34	1.69	4.59	-7.72	-7.45	4.58	-5.30	-9.22	15.31	-5.98	-2.00	15.62	-0.33	-5.58
35	1.70	5.11	-8.27	-7.06	5.19	-6.08	-8.90	15.95	-5.95	-1.54	16.03	-0.87	-5.65

TABLE D-4 (continued).

36	1.72	5.81	-8.81	-6.41	5.72	-6.53	-8.41	16.56	-6.15	-1.18	16.47	-1.19	-5.55
37	1.73	6.31	-9.47	-5.93	6.31	-7.53	-7.99	17.02	-6.13	-0.82	17.10	-1.40	-5.54
38	1.75	7.01	-9.89	-5.38	6.92	-7.96	-7.52	17.57	-6.11	-0.45	17.52	-1.82	-5.24
39	1.76	7.69	-10.31	-4.66	7.60	-8.73	-7.21	18.11	-6.20	0.00	17.96	-2.14	-5.13
40	1.77	8.36	-10.95	-4.12	8.19	-9.38	-6.73	18.85	-6.07	0.73	18.48	-2.45	-4.94
41	1.78	9.03	-11.47	-3.58	8.77	-10.02	-6.34	19.29	-6.16	0.82	18.97	-2.98	-4.92
42	1.80	9.69	-12.10	-2.78	9.50	-10.99	-5.42	19.75	-6.14	1.27	19.49	-3.29	-4.72
43	1.81	10.27	-12.51	-1.90	10.34	-11.61	-4.70	20.22	-6.02	1.63	20.15	-3.91	-4.51
44	1.83	10.93	-13.02	-1.03	11.06	-12.46	-4.06	20.77	-6.00	2.09	20.66	-4.22	-4.32
45	1.84	11.60	-13.31	-0.26	11.54	-12.98	-3.10	21.23	-5.99	2.54	21.29	-4.93	-4.02
46	1.85	12.26	-13.59	0.94	12.29	-13.26	-2.32	21.69	-5.97	3.08	21.77	-5.44	-3.55
47	1.87	12.83	-13.99	1.54	12.65	-14.11	-1.54	21.87	-5.96	3.45	22.33	-5.95	-2.72
48	1.88	13.15	-14.29	1.96	13.45	-14.71	-1.10	22.04	-6.06	3.81	22.80	-6.45	-2.53

TABLE D-5. Tractor-Body Reference-Point Coordinates and Times for Overturn Test 2, Run 2.

	TIME		XLRI			XRRI			XLFI			XRFI	
1	1.25	-14.11	-1.27	-10.07	-14.09	1.65	-10.07	-2.88	-3.11	-5.57	-2.62	3.35	-5.43
2	1.27	-13.45	-1.26	-10.07	-13.42	1.64	-10.07	-1.95	-3.10	-5.67	-1.84	3.33	-5.43
3	1.28	-12.79	-1.26	-10.07	-12.85	1.64	-10.07	-1.58	-3.09	-5.57	-1.26	3.32	-5.43
4	1.29	-12.23	-1.25	-10.07	-12.27	1.63	-10.07	-0.93	-2.96	-5.58	-0.68	3.31	-5.33
5	1.31	-11.57	-1.25	-10.07	-11.60	1.63	-10.07	-0.28	-3.07	-5.67	0.00	3.30	-5.43
6	1.32	-11.01	-1.25	-10.07	-10.93	1.62	-10.07	0.19	-2.95	-5.58	0.58	3.53	-5.34
7	1.33	-10.25	-1.37	-10.06	-10.26	1.61	-10.07	0.74	-3.17	-5.57	1.16	3.40	-5.34
8	1.35	-9.88	-1.24	-10.07	-9.78	1.61	-10.07	1.49	-3.04	-5.57	1.84	3.51	-5.44
9	1.36	-9.31	-1.36	-9.96	-9.20	1.61	-10.07	2.04	-3.15	-5.66	2.42	3.38	-5.63
10	1.37	-8.74	-1.36	-9.96	-8.53	1.60	-9.97	2.60	-3.26	-5.75	3.00	3.25	-5.72
11	1.39	-8.19	-1.23	-9.97	-8.05	1.60	-9.97	3.06	-3.48	-5.92	3.78	3.12	-5.72
12	1.41	-7.61	-1.35	-9.96	-7.38	1.59	-9.87	3.61	-3.59	-6.01	4.26	3.11	-5.81
13	1.42	-7.24	-1.35	-9.87	-7.00	1.59	-9.87	3.98	-3.70	-6.19	4.84	2.99	-6.10
14	1.44	-6.87	-1.22	-9.78	-6.52	1.59	-9.87	4.63	-3.68	-6.47	5.21	2.75	-6.09
15	1.45	-6.39	-1.34	-9.78	-6.04	1.58	-9.78	5.18	-3.79	-6.56	5.71	2.98	-6.49
16	1.46	-5.92	-1.46	-9.77	-5.56	1.58	-9.68	5.55	-3.78	-6.74	6.46	2.62	-6.67
17	1.47	-5.45	-1.46	-9.67	-5.08	1.57	-9.68	6.20	-3.77	-6.74	6.86	2.84	-6.68
18	1.49	-4.80	-1.33	-9.68	-4.60	1.57	-9.68	6.66	-3.87	-6.74	7.43	2.61	-6.67
19	1.51	-4.32	-1.57	-9.67	-4.12	1.45	-9.77	7.12	-3.86	-6.74	7.91	2.60	-6.67
20	1.52	-3.66	-1.56	-9.67	-3.54	1.32	-9.76	7.66	-4.08	-6.45	8.58	2.48	-6.47
21	1.53	-3.10	-1.56	-9.76	-2.97	1.32	-9.76	8.21	-4.18	-6.44	8.97	2.59	-6.76
22	1.55	-2.62	-2.03	-9.63	-2.39	1.19	-9.75	8.86	-4.17	-6.44	9.61	2.02	-6.54
23	1.57	-2.06	-2.15	-9.63	-1.72	0.83	-9.83	9.30	-4.38	-6.25	10.10	2.12	-6.55
24	1.58	-1.49	-2.62	-9.59	-1.24	0.36	-9.98	9.49	-4.38	-5.97	10.48	2.01	-6.35
25	1.59	-0.84	-2.96	-9.66	-0.66	0.00	-10.15	10.38	-4.80	-5.68	11.14	1.89	-6.54
26	1.61	-0.28	-3.43	-9.45	-0.19	-0.47	-10.12	11.02	-4.78	-5.40	11.59	1.44	-6.52
27	1.62	0.28	-3.89	-9.32	0.38	-1.18	-10.07	11.65	-4.99	-4.85	12.06	1.44	-6.52
28	1.63	0.92	-4.58	-9.09	1.03	-1.88	-10.02	12.18	-5.20	-4.47	12.51	0.99	-6.40
29	1.65	1.56	-5.15	-8.96	1.59	-2.34	-9.98	12.62	-5.40	-4.01	13.06	0.77	-6.10
30	1.66	2.10	-5.83	-8.65	2.33	-2.91	-9.94	13.34	-5.60	-3.55	13.59	0.33	-5.99
31	1.67	2.81	-6.51	-8.42	2.96	-3.72	-9.88	13.79	-5.70	-2.82	14.13	0.00	-5.79
32	1.69	3.44	-7.07	-8.03	3.59	-4.52	-9.46	14.32	-5.79	-2.45	14.59	-0.22	-5.68
33	1.70	4.23	-7.73	-7.45	4.21	-5.42	-9.31	14.85	-5.99	-2.00	15.12	-0.54	-5.67
34	1.72	4.67	-8.17	-7.07	4.56	-5.76	-9.01	15.40	-5.97	-1.63	15.56	-0.87	-5.65
35	1.73	5.18	-8.84	-6.50	5.17	-6.66	-8.41	15.93	-6.17	-1.18	16.00	-1.19	-5.64

36	1.74	5.87	-9.49	-6.02	5.87	-7.32	-8.18	16.46	-6.26	-0.82	16.62	-1.51	-5.44
37	1.76	6.38	-10.04	-5.56	6.37	-8.21	-7.77	17.01	-6.24	-0.36	17.04	-1.94	-5.33
38	1.77	7.15	-10.45	-4.92	7.06	-8.75	-7.21	17.47	-6.22	0.00	17.57	-2.25	-4.94
39	1.78	7.83	-11.09	-4.29	7.73	-9.63	-6.80	18.01	-6.21	0.63	18.09	-2.57	-4.93
40	1.80	8.59	-11.50	-3.58	8.50	-10.15	-6.16	18.56	-6.19	1.09	18.60	-2.99	-4.64
41	1.81	9.01	-11.81	-2.87	9.16	-10.90	-5.51	19.20	-6.16	1.63	19.18	-3.51	-4.53
42	1.83	9.67	-12.44	-1.99	9.74	-11.43	-4.79	19.65	-6.25	1.90	19.68	-3.92	-4.33
43	1.84	10.17	-12.74	-1.38	10.20	-12.29	-4.07	19.90	-6.35	2.44	20.24	-4.54	-3.94
44	1.86	10.67	-13.04	-0.34	10.70	-12.59	-3.20	20.53	-6.43	2.98	20.77	-5.37	-3.55
45	1.87	11.15	-13.45	0.69	11.25	-13.33	-2.41	20.79	-6.53	3.34	21.32	-5.98	-3.17
46	1.88	11.47	-13.76	1.54	11.81	-13.85	-1.63	21.15	-6.52	3.89	21.88	-6.49	-2.62

TABLE D-6. Tractor-Body Reference-Point Coordinates and Times for Overturn Test 3, Run 1.

	TIME		XLRI			XRRI			XLFI			XRFI	
1	2.23	-15.05	-1.27	-10.07	-15.05	1.65	-9.87	-3.90	-3.25	-5.57	-3.58	3.24	-5.43
2	2.27	-14.12	-1.14	-10.07	-14.00	1.64	-9.97	-2.97	-3.11	-5.57	-2.52	3.35	-5.43
3	2.31	-13.09	-1.13	-10.07	-13.13	1.64	-9.97	-2.04	-3.22	-5.57	-1.55	3.33	-5.43
4	2.35	-12.22	-1.38	-10.06	-12.18	1.63	-9.97	-1.11	-3.20	-5.57	-0.68	3.31	-5.43
5	2.39	-11.38	-1.25	-9.97	-11.22	1.62	-9.87	-0.19	-2.95	-5.58	0.19	3.30	-5.43
6	2.44	-10.53	-1.37	-9.96	-10.26	1.61	-9.97	0.37	-3.18	-5.57	1.16	3.28	-5.33
7	2.48	-9.69	-1.24	-10.07	-9.49	1.61	-9.97	1.58	-3.16	-5.57	1.65	3.16	-5.43
8	2.53	-8.94	-1.23	-9.97	-8.82	1.60	-9.97	2.13	-3.27	-5.84	2.71	3.14	-5.62
9	2.57	-8.18	-1.35	-9.87	-7.96	1.60	-9.87	2.96	-3.60	-5.83	3.58	3.13	-5.72
10	2.61	-7.71	-1.35	-9.87	-7.38	1.59	-9.87	3.42	-3.82	-5.82	4.06	2.89	-5.80
11	2.65	-7.23	-1.47	-9.86	-7.00	1.59	-9.87	4.07	-3.81	-6.19	4.73	2.65	-6.09
12	2.69	-6.76	-1.46	-9.67	-6.52	1.59	-9.78	4.53	-3.80	-6.46	5.31	2.64	-6.28
13	2.73	-6.39	-1.46	-9.67	-6.13	1.58	-9.78	4.99	-3.79	-6.56	5.69	2.63	-6.47
14	2.77	-6.11	-1.46	-9.67	-5.94	1.58	-9.87	5.36	-3.90	-6.55	6.08	2.63	-6.47
15	2.82	-5.64	-1.46	-9.67	-5.46	1.46	-9.77	5.73	-4.01	-6.64	6.46	2.62	-6.57
16	2.87	-5.35	-1.58	-9.67	-5.08	1.45	-9.77	6.00	-4.00	-6.64	6.74	2.39	-6.56
17	2.91	-4.98	-1.45	-9.67	-4.69	1.45	-9.77	6.28	-4.11	-6.63	7.12	2.27	-6.55
18	2.95	-4.60	-1.57	-9.67	-4.50	1.33	-9.76	6.74	-4.10	-6.63	7.42	2.50	-6.47
19	2.98	-4.41	-1.57	-9.67	-4.12	1.45	-9.77	7.11	-4.09	-6.54	7.80	2.38	-6.46
20	3.03	-4.04	-1.57	-9.67	-3.83	1.44	-9.77	7.38	-4.20	-6.53	8.00	2.37	-6.56
21	3.07	-3.76	-1.56	-9.67	-3.54	1.44	-9.77	7.56	-4.19	-6.63	8.39	2.48	-6.56
22	3.11	-3.47	-1.92	-9.64	-3.25	1.20	-9.75	7.84	-4.19	-6.53	8.57	2.25	-6.46
23	3.15	-3.09	-1.92	-9.64	-2.96	1.08	-9.75	8.21	-4.18	-6.44	8.86	2.25	-6.55
24	3.20	-2.90	-2.04	-9.63	-2.67	0.96	-9.74	8.49	-4.17	-6.44	9.24	2.25	-6.55
25	3.24	-2.53	-2.03	-9.63	-2.38	0.84	-9.83	8.76	-4.17	-6.26	9.61	2.02	-6.64
26	3.33	-1.86	-2.74	-9.59	-1.62	0.24	-9.98	9.48	-4.49	-5.97	10.18	1.90	-6.54
27	3.37	-1.58	-2.85	-9.49	-1.23	0.00	-10.05	9.93	-4.70	-5.78	10.56	1.90	-6.54
28	3.41	-1.02	-3.44	-9.35	-0.85	-0.59	-9.92	10.29	-4.80	-5.50	10.72	1.45	-6.42
29	3.45	-0.65	-4.02	-9.32	-0.47	-1.06	-9.98	10.82	-5.01	-5.12	11.20	1.44	-6.42
30	3.49	-0.09	-4.48	-9.10	0.09	-1.65	-9.94	11.27	-5.22	-4.75	11.66	1.11	-6.31
31	3.53	0.64	-5.06	-8.79	0.75	-2.35	-9.89	11.97	-5.53	-4.19	12.19	0.66	-6.19
32	3.58	1.37	-5.86	-8.46	1.49	-3.16	-9.93	12.50	-5.74	-3.55	12.74	0.33	-5.99
33	3.62	2.27	-6.76	-8.23	2.30	-4.31	-9.75	12.31	-5.85	-2.82	13.47	0.00	-5.88
34	3.66	3.06	-7.78	-7.63	3.11	-5.46	-9.40	13.95	-5.91	-1.91	14.17	-0.66	-5.76
35	3.70	4.02	-8.89	-6.76	3.99	-6.70	-8.95	14.59	-5.89	-1.36	14.83	-0.65	-5.76
36	3.74	5.05	-10.00	-5.91	5.03	-7.93	-8.24	15.33	-5.76	-0.64	15.31	-1.52	-5.63
37	3.78	5.98	-10.97	-4.64	6.05	-9.37	-7.35	16.16	-5.73	0.00	16.08	-2.16	-5.60
38	3.83	6.83	-11.61	-3.66	6.79	-10.59	-6.32	16.86	-5.92	0.73	16.83	-3.02	-5.29
39	3.87	7.38	-12.82	-1.99	7.62	-11.67	-4.96	17.45	-6.33	1.63	17.66	-4.61	-4.58
40	3.92	8.05	-13.34	0.17	8.31	-13.21	-2.76	17.86	-6.75	2.89	18.64	-6.29	-3.53
41	3.95	8.27	-13.89	1.98	8.76	-14.42	-1.11	18.31	-6.73	3.88	19.11	-7.55	-2.60

TABLE D-7. Tractor-Body Reference-Point Coordinates and Times for Overturn Test 3, Run 2.

	TIME		XLRI			XRRI			XLFI			XRFI	
1	2.33	-14.70	-1.02	-9.99	-14.59	1.78	-9.88	-2.97	-3.23	-5.57	-3.02	3.95	-5.35
2	2.38	-13.84	-1.14	-9.98	-13.63	1.77	-9.88	-2.23	-2.86	-5.58	-2.04	3.70	-5.44
3	2.42	-12.80	-1.13	-9.98	-12.76	1.76	-9.98	-1.49	-2.85	-5.58	-1.26	3.68	-5.35
4	2.46	-11.96	-1.13	-9.98	-11.80	1.75	-9.98	-0.56	-2.84	-5.58	-0.29	3.66	-5.44
5	2.50	-11.11	-1.12	-9.98	-10.84	1.74	-9.88	0.09	-2.95	-5.58	0.49	3.65	-5.44
6	2.54	-10.17	-1.12	-9.98	-10.17	1.74	-9.98	1.02	-3.05	-5.57	1.26	3.28	-5.33
7	2.58	-9.60	-1.11	-9.98	-9.40	1.73	-9.98	1.67	-3.16	-5.66	2.13	3.38	-5.53
8	2.63	-8.95	-0.99	-9.99	-8.63	1.73	-9.98	2.41	-3.26	-5.84	3.00	3.25	-5.62
9	2.68	-8.19	-1.11	-9.98	-7.97	1.84	-9.89	3.06	-3.25	-5.84	3.68	3.12	-5.72
10	2.72	-7.63	-1.10	-9.98	-7.39	1.84	-9.89	3.70	-3.59	-6.01	4.26	3.11	-5.91
11	2.75	-7.24	-1.22	-9.88	-7.00	1.71	-9.88	4.07	-3.70	-6.19	4.93	2.87	-6.10
12	2.79	-6.86	-1.34	-9.87	-6.52	1.71	-9.88	4.63	-3.68	-6.19	5.42	3.10	-6.30
13	2.84	-6.40	-1.22	-9.78	-6.14	1.70	-9.79	5.00	-3.68	-6.56	5.70	2.86	-6.48
14	2.88	-6.21	-1.22	-9.88	-5.95	1.70	-9.79	5.27	-3.79	-6.65	6.08	2.63	-6.57
15	2.92	-5.83	-1.34	-9.78	-5.46	1.58	-9.78	5.55	-3.78	-6.65	6.47	2.85	-6.48
16	2.97	-5.45	-1.46	-9.77	-5.08	1.57	-9.78	5.83	-3.78	-6.65	6.86	2.73	-6.48
17	3.01	-5.17	-1.45	-9.77	-4.79	1.57	-9.78	6.29	-3.77	-6.56	7.04	2.61	-6.47
18	3.05	-4.70	-1.45	-9.77	-4.60	1.57	-9.78	6.66	-3.76	-6.65	7.43	2.61	-6.57
19	3.09	-4.51	-1.45	-9.77	-4.41	1.57	-9.78	6.66	-3.76	-6.56	7.62	2.61	-6.57
20	3.13	-4.32	-1.45	-9.77	-4.02	1.57	-9.87	7.12	-3.75	-6.56	7.91	2.60	-6.57
21	3.18	-4.04	-1.45	-9.77	-3.74	1.56	-9.78	7.30	-3.86	-6.55	8.10	2.60	-6.57
22	3.22	-3.76	-1.56	-9.76	-3.55	1.56	-9.78	7.68	-3.74	-6.56	8.40	2.71	-6.57
23	3.27	-3.57	-1.56	-9.76	-3.45	1.56	-9.78	7.67	-3.85	-6.55	8.59	2.59	-6.57
24	3.31	-3.47	-1.56	-9.76	-3.16	1.56	-9.78	8.04	-3.84	-6.55	8.78	2.59	-6.57
25	3.36	-3.10	-1.56	-9.67	-2.97	1.44	-9.77	8.40	-4.06	-6.54	8.96	2.36	-6.56
26	3.40	-2.91	-1.56	-9.67	-2.68	1.32	-9.86	8.59	-3.95	-6.45	9.26	2.58	-6.57
27	3.44	-2.72	-1.67	-9.75	-2.58	1.31	-9.86	8.87	-3.94	-6.55	9.55	2.58	-6.57
28	3.48	-2.53	-1.91	-9.74	-2.29	0.95	-9.83	8.76	-4.17	-6.44	9.64	2.47	-6.56
29	3.53	-2.34	-2.03	-9.73	-2.20	0.95	-9.83	8.96	-4.05	-6.26	9.82	2.24	-6.55
30	3.57	-2.15	-2.27	-9.62	-1.91	0.71	-9.82	9.41	-4.15	-6.26	9.82	2.35	-6.56
31	3.61	-1.87	-2.50	-9.70	-1.71	0.48	-9.99	9.67	-4.37	-6.16	10.20	2.23	-6.55
32	3.64	-1.68	-2.62	-9.59	-1.43	0.36	-10.08	9.86	-4.37	-6.06	10.38	2.01	-6.54
33	3.68	-1.49	-2.73	-9.59	-1.23	0.24	-10.07	9.67	-4.37	-5.97	10.38	2.01	-6.45
34	3.74	-1.02	-2.73	-9.59	-0.85	0.00	-10.05	10.39	-4.69	-5.59	10.84	1.78	-6.44
35	3.78	-0.74	-3.32	-9.55	-0.57	-0.35	-10.03	10.67	-5.80	-5.36	11.12	1.67	-6.43

TABLE D-1. Tractor-Body Reference-Point Coordinates and Times for Overturn Test 1, Run 1.

	TIME		XLRI			XRRI			XLFI			XRFI	
1	1.48	-13.55	-1.26	-10.07	-13.71	1.64	-10.16	-2.32	-3.22	-5.57	-1.94	3.34	-5.43
2	1.50	-13.17	-1.26	-10.07	-13.13	1.64	-10.07	-1.67	-3.21	-5.66	-1.65	3.33	-5.43
3	1.51	-12.51	-1.26	-10.07	-12.56	1.63	-10.07	-1.11	-3.20	-5.66	-0.97	3.32	-5.53
4	1.53	-12.04	-1.25	-10.07	-12.08	1.63	-10.07	-0.65	-3.20	-5.66	-0.48	3.31	-5.43
5	1.54	-11.37	-1.37	-10.06	-11.50	1.62	-10.07	0.00	-2.95	-5.67	0.19	3.30	-5.43
6	1.55	-11.00	-1.37	-10.06	-10.93	1.62	-10.07	0.37	-3.18	-5.75	0.78	3.41	-5.34
7	1.57	-10.34	-1.37	-10.06	-10.45	1.62	-10.07	0.93	-3.17	-5.57	1.16	3.28	-5.43
8	1.58	-9.96	-1.36	-10.06	-9.87	1.61	-10.07	1.48	-3.28	-5.66	1.65	3.27	-5.43
9	1.59	-9.40	-1.36	-9.96	-9.49	1.61	-9.97	1.86	-3.27	-5.66	2.13	3.38	-5.53
10	1.61	-9.12	-1.36	-9.96	-9.01	1.60	-9.97	2.32	-3.26	-5.84	2.71	3.26	-5.62
11	1.62	-8.46	-1.35	-9.87	-8.44	1.72	-9.98	1.85	-3.39	-5.93	3.20	3.25	-5.72
12	1.64	-8.18	-1.35	-9.96	-8.06	1.72	-9.98	3.15	-3.37	-5.93	3.77	3.01	-5.71
13	1.65	-7.71	-1.35	-9.96	-7.57	1.59	-9.97	3.80	-3.59	-6.10	4.16	2.89	-5.71
14	1.66	-7.33	-1.35	-9.96	-7.09	1.59	-9.97	3.88	-3.81	-6.19	4.64	2.76	-5.90
15	1.67	-7.05	-1.47	-9.86	-6.90	1.59	-9.97	4.35	-3.81	-6.19	5.02	2.76	-6.09
16	1.69	-6.67	-1.46	-9.77	-6.52	1.59	-9.87	4.72	-3.80	-6.37	5.41	2.75	-6.19
17	1.70	-6.39	-1.34	-9.78	-6.13	1.58	-9.87	5.36	-3.78	-6.56	5.79	2.63	-6.38
18	1.72	-5.92	-1.46	-9.77	-5.94	1.58	-9.87	5.55	-3.90	-6.64	6.27	2.63	-6.57
19	1.73	-5.64	-1.46	-9.77	-5.27	1.58	-9.78	6.01	-3.89	-6.83	6.66	2.62	-6.67
20	1.74	-5.07	-1.45	-9.77	-4.98	1.57	-9.87	6.56	-3.99	-6.73	7.04	2.61	-6.57
21	1.76	-4.69	-1.57	-9.76	-4.60	1.45	-9.87	6.74	-4.10	-6.72	7.53	2.61	-6.57
22	1.77	-4.41	-1.57	-9.76	-4.12	1.45	-9.87	7.19	-4.20	-6.72	7.91	2.49	-6.56
23	1.78	-3.76	-1.56	-9.76	-3.73	1.32	-9.86	7.66	-4.19	-6.72	8.29	2.48	-6.56
24	1.80	-3.47	-1.68	-9.66	-3.35	1.20	-9.75	8.03	-4.07	-6.63	8.77	2.37	-6.66
25	1.82	-3.00	-1.80	-9.65	-2.96	1.08	-9.75	8.49	-4.06	-6.54	9.14	2.25	-6.55
26	1.83	-2.62	-2.15	-9.63	-2.48	0.84	-9.83	8.94	-4.28	-6.44	9.63	2.35	-6.66
27	1.84	-2.05	-2.38	-9.61	-1.91	0.71	-9.82	9.50	-4.26	-6.44	9.91	2.24	-6.65
28	1.86	-1.77	-2.74	-9.59	-1.43	0.24	-9.98	9.87	-4.25	-6.16	10.28	2.01	-6.54
29	1.87	-1.30	-3.09	-9.47	-1.14	-0.24	-9.94	10.11	-4.70	-5.78	10.65	1.78	-6.44
30	1.88	-0.83	-3.67	-9.52	-0.66	-0.83	-9.90	10.84	-4.79	-5.50	11.03	1.67	-6.53
31	1.90	-0.28	-4.02	-9.50	-0.19	-1.18	-10.07	11.08	-5.23	-5.20	11.59	1.44	-6.52
32	1.92	0.09	-4.60	-9.18	0.28	-1.53	-9.95	11.62	-5.32	-4.74	11.86	1.33	-6.42
33	1.93	0.64	-5.06	-9.15	0.75	-2.23	-9.90	11.98	-5.42	-4.38	12.31	0.88	-6.40
34	1.94	1.19	-5.63	-8.93	1.21	-2.70	-9.96	12.50	-5.74	-3.91	12.66	0.55	-6.29
35	1.96	1.73	-6.08	-8.54	1.85	-3.62	-9.89	12.95	-5.83	-3.45	13.12	0.33	-6.09

TABLE D-1 (continued).

36	1.97	2.45	-6.64	-8.41	2.49	-3.96	-9.78	13.41	-5.82	-3.00	13.48	0.11	-5.89
37	1.98	2.98	-7.20	-7.93	2.94	-4.53	-9.46	13.78	-5.81	-2.55	13.92	-0.22	-5.78
38	2.00	3.42	-7.76	-7.54	3.48	-5.21	-9.41	14.31	-5.90	-2.09	14.38	-0.44	-5.77
39	2.02	3.86	-8.09	-7.34	3.83	-5.90	-9.18	14.54	-6.33	-1.81	14.82	-0.76	-5.75
40	2.03	4.30	-8.54	-6.96	4.36	-6.57	-8.96	14.92	-6.21	-1.54	15.17	-0.98	-5.65
41	2.04	4.73	-8.98	-6.58	4.79	-7.13	-8.47	15.47	-6.19	-1.09	15.51	-1.41	-5.63
42	2.06	5.33	-9.75	-6.01	5.31	-7.69	-8.25	15.83	-6.17	-0.73	15.94	-1.73	-5.52
43	2.07	5.75	-10.30	-5.63	5.74	-8.24	-7.86	16.28	-6.27	-0.54	16.40	-1.84	-5.52
44	2.08	6.26	-10.62	-5.09	6.25	-8.90	-7.38	16.74	-6.25	-0.18	16.71	-2.37	-5.40
45	2.10	6.78	-10.81	-4.65	6.77	-9.33	-7.00	17.28	-6.23	0.18	17.08	-2.47	-5.31
46	2.11	7.37	-11.46	-3.93	7.27	-9.99	-6.52	17.56	-6.22	0.54	17.57	-3.00	-5.19
47	2.13	8.06	-11.64	-3.31	8.03	-10.52	-6.06	17.92	-6.21	1.00	17.91	-3.32	-4.90
48	2.14	8.57	-11.84	-2.78	8.61	-11.27	-5.41	18.48	-6.08	1.36	18.41	-3.74	-4.89
49	2.16	9.05	-12.59	-1.99	9.17	-12.02	-4.69	18.84	-6.18	1.81	18.79	-4.37	-4.59
50	2.17	9.55	-12.90	-1.12	9.49	-12.45	-4.07	19.39	-6.16	2.18	19.29	-4.78	-4.39
51	2.18	9.79	-13.22	-0.26	9.97	-13.09	-3.19	19.75	-6.14	2.54	19.88	-5.19	-4.01
52	2.20	10.36	-13.62	1.03	10.37	-13.51	-2.15	19.93	-6.14	2.99	20.33	-5.91	-3.54
53	2.22	10.96	-13.69	1.98	11.04	-13.79	-1.11	20.30	-6.12	3.45	20.79	-6.53	-2.98
54	2.23	10.96	-13.69	2.41	11.25	-14.33	-0.60	20.39	-6.12	3.63	21.15	-7.15	-2.60
55	2.24	11.03	-13.91	2.40	11.32	-14.55	-0.60	20.62	-6.43	3.62	21.36	-7.56	-2.68

TABLE D-2. Tractor-Body Reference-Point Coordinates and Times for Overturn Test 1, Run 2.

	TIME		XLRI			XRRI			XLFI			XRFI	
1	1.47	-13.94	-1.01	-10.08	-13.76	2.15	-10.00	-2.61	-2.75	-5.31	-2.23	3.70	-5.35
2	1.49	-13.30	-0.88	-10.09	-13.36	2.02	-9.99	-1.96	-2.74	-5.68	-1.85	3.81	-5.35
3	1.50	-12.92	-0.88	-10.09	-12.88	2.01	-9.99	-1.58	-2.74	-5.59	-1.26	3.80	-5.35
4	1.52	-12.25	-1.00	-10.08	-12.30	2.01	-9.99	-1.40	-2.73	-5.59	-0.68	3.79	-5.35
5	1.53	-11.78	-1.00	-10.08	-11.71	1.88	-9.99	-0.56	-2.60	-5.59	-0.10	3.66	-5.35
6	1.54	-11.21	-1.00	-9.99	-11.34	2.00	-10.09	0.00	-2.71	-5.59	0.29	3.65	-5.35
7	1.56	-10.65	-1.00	-10.08	-10.67	1.99	-10.09	0.47	-2.71	-5.59	0.68	3.76	-5.35
8	1.57	-10.27	-0.99	-10.08	-10.28	1.99	-10.09	1.12	-2.70	-5.68	1.26	3.87	-5.35
9	1.58	-9.71	-0.99	-10.08	-9.70	1.98	-10.09	1.49	-2.69	-5.68	1.85	3.86	-5.55
10	1.60	-9.33	-0.99	-10.08	-9.33	2.10	-10.10	1.96	-2.80	-5.86	2.24	3.73	-5.64
11	1.62	-8.76	-0.99	-9.99	-8.74	1.97	-10.09	2.33	-2.80	-5.86	2.82	3.84	-5.74
12	1.63	-8.48	-0.98	-9.89	-8.46	2.09	-10.00	2.98	-2.90	-5.95	3.40	3.71	-5.74
13	1.64	-8.10	-0.98	-9.89	-7.88	2.09	-10.00	3.25	-3.13	-6.03	3.88	3.58	-5.83
14	1.65	-7.63	-0.98	-9.89	-7.50	2.08	-10.00	3.81	-3.24	-6.03	4.36	3.34	-5.82
15	1.67	-7.26	-0.98	-9.89	-7.12	2.08	-9.91	4.18	-3.23	-6.21	4.94	3.33	-6.11
16	1.68	-6.88	-0.98	-9.89	-6.73	2.07	-10.00	4.55	-3.34	-6.30	5.13	3.22	-6.11
17	1.69	-6.50	-0.98	-9.89	-6.34	1.95	-9.90	4.82	-3.34	-6.49	5.52	3.09	-6.30
18	1.71	-6.31	-0.97	-9.71	-6.06	2.07	-9.81	5.38	-3.33	-6.58	6.00	3.09	-6.49
19	1.72	-5.74	-1.09	-9.70	-5.67	2.06	-9.81	5.75	-3.32	-6.76	6.38	2.97	-6.58
20	1.74	-5.37	-0.97	-9.71	-5.28	1.94	-9.80	6.22	-3.31	-6.76	6.77	3.07	-6.59
21	1.75	-4.80	-1.09	-9.70	-4.80	1.81	-9.89	6.68	-3.42	-6.66	7.45	2.95	-6.58
22	1.76	-4.52	-1.09	-9.70	-4.51	1.61	-9.89	7.13	-3.52	-6.66	7.64	2.95	-6.58
23	1.77	-4.05	-1.20	-9.69	-3.84	1.68	-9.79	7.41	-3.52	-6.57	8.02	2.94	-6.58
24	1.79	-3.67	-1.20	-9.69	-3.55	1.68	-9.79	7.78	-3.62	-6.75	8.51	3.04	-6.59
25	1.80	-3.29	-1.20	-9.69	-3.16	1.68	-9.79	8.15	-3.62	-6.56	8.89	2.81	-6.58
26	1.82	-2.73	-1.32	-9.68	-2.68	1.55	-9.87	8.70	-3.61	-6.65	9.38	3.03	-6.59
27	1.83	-2.25	-1.55	-9.67	-2.20	1.55	-9.87	9.16	-3.71	-6.56	9.76	2.80	-6.68
28	1.84	-1.88	-1.67	-9.75	-1.72	1.31	-9.86	9.53	-3.70	-6.46	10.04	2.68	-6.57
29	1.86	-1.59	-2.14	-9.81	-1.34	0.95	-10.02	9.62	-3.81	-6.27	10.32	2.57	-6.47
30	1.87	-0.93	-2.37	-9.89	-0.86	0.71	-10.20	10.44	-3.91	-6.08	10.62	2.68	-6.48
31	1.89	-0.56	-2.60	-9.78	-0.38	0.35	-10.17	10.89	-4.12	-5.80	11.46	2.33	-6.46
32	1.90	0.00	-2.95	-9.85	0.00	-0.12	-10.14	11.34	-4.22	-5.61	11.74	2.22	-6.46
33	1.92	0.37	-3.18	-9.74	0.66	-0.35	-10.31	11.70	-4.32	-5.33	12.20	1.99	-6.45
34	1.93	0.74	-3.76	-9.61	0.94	-0.82	-10.28	12.05	-4.65	-5.04	12.47	1.77	-6.34
35	1.94	1.11	-3.99	-9.78	1.32	-1.29	-10.25	12.50	-4.75	-4.76	12.84	1.54	-6.43

TABLE D-2 (continued).

36	1.96	1.66	-4.44	-9.65	1.78	-1.52	-10.32	12.87	-4.74	-4.49	13.31	1.43	-6.33
37	1.97	2.11	-4.90	-9.16	2.34	-2.10	-10.28	13.32	-4.83	-4.21	13.59	1.32	-6.22
38	1.99	2.56	-5.24	-8.96	2.80	-2.44	-10.25	13.67	-4.93	-3.84	14.04	1.09	-6.12
39	2.00	3.11	-5.46	-8.67	3.26	-2.78	-10.04	14.30	-5.14	-3.47	14.50	0.87	-6.01
40	2.02	3.65	-5.79	-8.46	3.81	-3.24	-9.92	14.56	-5.24	-3.10	14.97	0.76	-5.91
41	2.03	4.27	-6.34	-8.43	4.25	-3.81	-9.88	15.09	-5.44	-2.64	15.31	0.43	-5.80
42	2.04	4.71	-6.79	-8.04	4.70	-4.37	-9.65	15.37	-5.43	-2.46	15.66	0.11	-5.79
43	2.06	5.24	-7.35	-7.65	5.23	-4.94	-9.43	15.90	-5.52	-2.00	16.12	0.00	-5.69
44	2.07	5.58	-7.68	-7.36	5.67	-5.50	-9.30	16.35	-5.62	-1.82	16.37	-0.32	-5.68
45	2.09	6.02	-8.00	-7.07	6.10	-6.06	-8.99	16.72	-5.60	-1.55	16.84	-0.43	-5.67
46	2.10	6.54	-8.43	-6.60	6.54	-6.38	-8.69	17.18	-5.59	-1.18	17.27	-0.75	-5.66
47	2.12	7.05	-8.98	-6.31	6.98	-6.82	-8.48	17.53	-5.69	-1.00	17.62	-0.97	-5.56
48	2.13	7.56	-9.41	-5.84	7.49	-7.48	-8.06	18.08	-5.67	-0.64	18.06	-1.28	-5.54
49	2.14	8.16	-9.83	-5.47	8.09	-7.91	-7.79	18.54	-5.65	-0.27	18.52	-1.39	-5.35
50	2.16	8.68	-10.14	-4.93	8.68	-8.56	-7.39	18.91	-5.64	0.09	18.86	-1.60	-5.15
51	2.17	9.27	-10.56	-4.56	9.20	-8.88	-6.84	19.38	-5.52	0.55	19.29	-1.91	-4.96
52	2.18	9.85	-11.08	-4.11	9.59	-9.64	-6.62	19.79	-5.83	0.82	19.80	-2.33	-4.94
53	2.20	10.09	-11.41	-3.49	10.18	-10.17	-6.16	20.19	-5.60	1.00	20.20	-2.85	-4.83
54	2.22	10.61	-11.48	-2.88	10.58	-10.71	-5.52	20.50	-6.01	1.45	20.68	-3.37	-4.53
55	2.23	10.85	-11.80	-2.26	10.99	-11.13	-5.06	20.77	-6.00	1.81	21.10	-3.68	-4.43
56	2.24	11.43	-12.21	-1.91	11.58	-11.42	-4.44	21.21	-6.09	2.08	21.66	-4.30	-4.04
57	2.26	11.75	-12.52	-0.86	11.87	-12.18	-3.72	21.67	-6.08	2.72	22.14	-4.81	-3.75
58	2.27	12.15	-12.94	0.00	12.45	-12.47	-2.94	22.11	-6.17	3.17	22.59	-5.42	-3.37
59	2.28	12.56	-13.24	0.86	12.76	-12.89	-1.98	22.44	-5.84	3.54	23.06	-5.92	-2.81
60	2.30	13.23	-13.41	1.63	13.31	-13.51	-1.46	22.65	-6.25	3.62	23.35	-6.43	-2.62

TABLE D-3. Tractor-Body Reference-Point Coordinates and Times for Overturn Test 1, Run 3.

	TIME		XLRI			XRRI			XLFI			XRFI	
1	1.45	-14.12	-1.14	-10.07	-14.09	1.65	-9.97	-2.97	-3.11	-5.57	-2.62	3.59	-5.44
2	1.46	-13.64	-1.26	-10.07	-13.52	1.64	-10.07	-2.23	-2.98	-5.58	-1.94	3.34	-5.43
3	1.48	-13.26	-1.26	-9.97	-13.04	1.64	-9.97	-1.67	-3.09	-5.57	-1.36	3.33	-5.33
4	1.49	-12.51	-1.26	-10.07	-12.56	1.63	-10.07	-1.21	-3.09	-5.57	-0.78	3.43	-5.43
5	1.50	-12.03	-1.38	-10.06	-11.98	1.63	-10.07	-0.65	-3.20	-5.66	-0.39	3.31	-5.33
6	1.52	-11.48	-1.25	-9.97	-11.41	1.62	-10.07	-0.19	-3.19	-5.66	0.19	3.30	-5.43
7	1.53	-10.91	-1.25	-9.97	-10.93	1.62	-9.97	0.37	-3.18	-5.66	0.68	3.29	-5.33
8	1.54	-10.35	-1.24	-9.97	-10.35	1.62	-9.97	0.93	-3.17	-5.57	1.16	3.40	-5.34
9	1.56	-9.97	-1.24	-9.97	-9.97	1.61	-9.97	1.30	-3.05	-5.67	1.65	3.39	-5.43
10	1.57	-9.41	-1.24	-9.97	-9.40	1.73	-9.98	1.76	-3.16	-5.57	2.23	3.26	-5.53
11	1.58	-9.02	-1.36	-9.96	-8.92	1.73	-9.98	2.32	-3.15	-5.85	2.71	3.37	-5.63
12	1.60	-8.47	-1.23	-9.88	-8.44	1.72	-9.88	2.78	-3.26	-5.84	3.20	3.25	-5.72
13	1.62	-8.19	-1.23	-9.88	-7.96	1.72	-9.88	3.06	-3.48	-5.83	3.87	3.12	-5.72
14	1.63	-7.71	-1.35	-9.96	-7.48	1.59	-9.97	3.61	-3.70	-5.92	4.35	3.00	-5.81
15	1.64	-7.43	-1.35	-10.06	-7.00	1.59	-9.97	3.98	-3.70	-6.19	4.74	2.99	-6.00
16	1.66	-7.05	-1.47	-9.77	-6.80	1.59	-9.87	4.44	-3.80	-6.46	5.02	2.76	-6.09
17	1.67	-6.58	-1.46	-9.77	-6.52	1.59	-9.87	4.81	-3.80	-6.46	5.60	2.63	-6.28
18	1.69	-6.39	-1.34	-9.68	-6.23	1.58	-9.78	5.08	-3.91	-6.64	5.69	2.63	-6.47
19	1.70	-5.92	-1.46	-9.67	-5.65	1.58	-9.78	5.55	-3.78	-6.74	6.27	2.63	-6.57
20	1.72	-5.55	-1.33	-9.68	-5.27	1.58	-9.78	5.92	-3.77	-6.74	6.75	2.62	-6.67
21	1.73	-5.07	-1.45	-9.67	-4.89	1.57	-9.78	6.48	-3.76	-6.74	7.13	2.50	-6.56
22	1.74	-4.60	-1.45	-9.67	-4.40	1.45	-9.77	6.83	-4.10	-6.63	7.81	2.49	-6.56
23	1.76	-4.22	-1.57	-9.67	-3.93	1.44	-9.77	7.38	-4.08	-6.63	8.00	2.49	-6.56
24	1.77	-3.76	-1.56	-9.76	-3.54	1.44	-9.87	7.66	-4.19	-6.44	8.39	2.60	-6.57
25	1.78	-3.38	-1.56	-9.67	-3.15	1.20	-9.75	8.02	-4.18	-6.53	8.87	2.48	-6.56
26	1.80	-2.81	-1.91	-9.64	-2.68	1.20	-9.75	8.58	-4.17	-6.53	9.25	2.36	-6.56
27	1.81	-2.53	-2.03	-9.63	-2.29	0.95	-9.83	9.03	-4.27	-6.44	9.63	2.35	-6.56
28	1.83	-1.96	-2.26	-9.62	-1.81	0.71	-9.82	9.40	-4.26	-6.25	10.20	2.23	-6.55
29	1.84	-1.58	-2.62	-9.59	-1.43	0.24	-9.88	9.48	-4.49	-6.06	10.28	2.01	-6.35
30	1.85	-1.12	-2.97	-9.66	-0.76	-0.24	-10.04	10.38	-4.80	-5.77	10.84	1.78	-6.44
31	1.87	-0.65	-3.55	-9.62	-0.47	-0.71	-10.10	10.75	-4.79	-5.40	11.31	1.56	-6.43
32	1.88	-0.18	-3.90	-9.42	-0.09	-0.94	-10.08	11.19	-5.00	-5.12	11.68	1.44	-6.42
33	1.90	0.28	-4.48	-9.19	0.47	-1.53	-10.04	11.72	-5.21	-4.75	12.04	1.11	-6.41
34	1.91	0.92	-4.81	-9.08	1.03	-1.99	-10.01	12.07	-5.42	-4.28	12.49	0.77	-6.20
35	1.92	1.37	-5.39	-8.86	1.58	-2.69	-9.96	12.52	-5.52	-3.92	12.87	0.77	-6.10

TABLE D-3 (continued).

36	1.94	1.92	-5.84	-8.65	2.04	-3.15	-9.93	12.96	-5.72	-3.55	13.30	0.22	-5.99
37	1.95	2.46	-6.29	-8.44	2.50	-3.73	-9.79	13.42	-5.71	-2.91	13.67	0.11	-5.89
38	1.96	2.99	-6.85	-8.22	3.04	-4.30	-9.66	13.96	-5.80	-2.64	14.21	-0.22	-5.68
39	1.98	3.61	-7.29	-7.83	3.67	-4.98	-9.43	14.31	-5.90	-2.09	14.58	-0.33	-5.68
40	1.99	4.04	-7.97	-7.43	4.20	-5.54	-9.30	14.74	-6.21	-1.81	15.01	-0.76	-5.66
41	2.01	4.48	-8.30	-7.06	4.55	-6.11	-9.08	15.19	-6.20	-1.54	15.36	-0.98	-5.65
42	2.02	5.00	-8.96	-6.49	4.99	-6.67	-9.58	15.65	-6.18	-1.09	15.79	-1.41	-5.54
43	2.04	5.51	-9.51	-6.20	5.49	-7.68	-8.25	16.10	-6.27	-0.82	16.22	-1.73	-5.52
44	2.05	6.03	-9.83	-5.65	6.03	-7.89	-7.97	16.45	-6.37	-0.45	16.67	-1.94	-5.33
45	2.06	6.46	-10.26	-5.19	6.45	-8.44	-7.58	16.92	-6.24	0.00	17.09	-2.37	-5.22
46	2.08	6.97	-10.58	-4.66	7.05	-8.98	-7.19	17.47	-6.22	0.18	17.54	-2.47	-5.03
47	2.09	7.64	-11.22	-4.02	7.54	-9.86	-6.44	17.90	-6.42	0.63	17.95	-3.00	-4.92
48	2.11	8.23	-11.63	-3.40	8.12	-10.51	-6.23	18.37	-6.30	0.91	18.37	-3.31	-4.81
49	2.12	8.56	-12.06	-2.78	8.62	-11.05	-5.51	18.75	-6.18	1.18	18.76	-3.94	-4.60
50	2.13	9.34	-12.13	-2.00	9.29	-11.57	-4.70	19.20	-6.16	1.63	19.35	-4.35	-4.40
51	2.14	9.90	-12.87	-1.29	9.83	-12.54	-4.06	19.66	-6.15	2.27	19.85	-4.76	-4.12
52	2.16	10.23	-13.07	-0.34	10.33	-12.95	-3.19	19.93	-6.14	2.45	20.23	-5.28	-3.92
53	2.18	10.79	-13.70	0.77	10.80	-13.59	-2.06	20.38	-6.23	2.99	20.74	-5.58	-3.45
54	2.19	11.21	-13.78	1.72	11.47	-13.76	-1.37	20.76	-6.11	3.45	21.11	-6.20	-2.89
55	2.21	11.45	-13.98	2.06	11.78	-14.18	-0.85	20.83	-6.21	3.71	21.58	-6.71	-2.61

TABLE D-4. Tractor-Body Reference-Point Coordinates and Times for Overturn Test 2, Run 1.

	TIME		XLRI			XRRI			XLFI			XRFI	
1	1.22	-14.40	-1.14	-10.07	-14.30	1.77	-9.98	-3.16	-2.88	-5.58	-2.81	3.47	-5.34
2	1.23	-13.84	-1.14	-10.07	-13.72	1.77	-9.98	-2.51	-2.87	-5.58	-2.14	3.70	-5.35
3	1.25	-13.09	-1.13	-9.98	-13.15	1.76	-9.98	-1.95	-2.86	-5.68	-1.65	3.57	-5.44
4	1.27	-12.52	-1.13	-9.98	-12.47	1.76	-10.07	-1.12	-2.73	-5.59	-0.87	3.67	-5.35
5	1.28	-11.86	-1.13	-9.98	-11.80	1.75	-9.98	-0.65	-2.84	-5.58	-0.19	3.42	-5.34
6	1.29	-11.19	-1.25	-9.97	-11.23	1.75	-9.98	0.09	-2.83	-5.58	0.39	3.53	-5.34
7	1.31	-10.55	-1.12	-9.98	-10.55	1.74	-10.07	0.65	-3.06	-5.57	1.07	3.52	-5.34
8	1.32	-9.98	-1.12	-9.98	-9.98	1.74	-10.07	1.30	-3.05	-5.57	1.65	3.63	-5.35
9	1.33	-9.32	-1.11	-9.98	-9.40	1.73	-10.07	1.77	-3.04	-5.67	2.23	3.38	-5.53
10	1.35	-8.76	-1.11	-9.98	-8.84	1.97	-10.09	2.32	-3.15	-5.85	2.91	3.49	-5.63
11	1.37	-8.38	-1.11	-9.98	-8.25	1.72	-9.98	2.97	-3.14	-5.94	3.58	3.24	-5.72
12	1.38	-7.82	-1.10	-9.98	-7.68	1.84	-9.89	3.43	-3.24	-6.03	3.97	3.00	-5.91
13	1.39	-7.34	-1.10	-9.89	-7.10	1.71	-9.88	3.89	-3.47	-6.11	4.74	3.11	-6.01
14	1.41	-6.87	-1.22	-9.88	-6.62	1.71	-9.88	4.36	-3.34	-6.30	5.12	2.76	-6.09
15	1.42	-6.40	-1.22	-9.88	-6.14	1.70	-9.88	4.91	-3.68	-6.47	5.69	2.63	-6.47
16	1.43	-5.93	-1.22	-9.78	-5.66	1.70	-9.79	5.46	-3.67	-6.65	6.09	2.86	-6.58
17	1.45	-5.55	-1.33	-9.68	-5.18	1.70	-9.79	6.11	-3.66	-6.75	6.66	2.73	-6.67
18	1.47	-4.89	-1.33	-9.68	-4.79	1.57	-9.78	6.57	-3.76	-6.74	7.44	2.84	-6.68
19	1.48	-4.42	-1.33	-9.68	-4.31	1.57	-9.78	7.12	-3.75	-6.65	7.81	2.60	-6.67
20	1.49	-3.76	-1.44	-9.67	-3.55	1.56	-9.78	7.67	-3.85	-6.55	8.39	2.48	-6.47
21	1.51	-3.29	-1.56	-9.67	-3.16	1.44	-9.77	8.05	-3.73	-6.56	8.87	2.59	-6.57
22	1.53	-2.72	-1.56	-9.76	-2.49	1.31	-9.86	8.59	-3.95	-6.55	9.54	2.47	-6.56
23	1.54	-1.97	-1.91	-9.83	-1.81	0.95	-9.93	9.23	-4.16	-6.35	10.31	2.46	-6.56
24	1.55	-1.50	-2.26	-9.81	-1.33	0.71	-10.01	10.05	-4.25	-6.16	10.59	2.34	-6.66
25	1.57	-0.84	-2.72	-9.77	-0.57	0.24	-10.17	10.39	-4.69	-5.78	11.05	2.00	-6.54
26	1.58	-0.28	-3.19	-9.65	-0.09	-0.35	-10.22	10.93	-4.79	-5.50	11.71	1.77	-6.44
27	1.59	0.28	-3.77	-9.52	0.47	-0.82	-10.19	11.58	-4.77	-5.22	12.06	1.44	-6.42
28	1.61	0.92	-4.34	-9.29	1.03	-1.41	-10.14	12.09	-5.20	-4.75	12.61	1.10	-6.41
29	1.63	1.47	-4.80	-9.17	1.59	-1.99	-10.10	12.52	-5.52	-4.28	12.97	0.88	-6.30
30	1.64	2.01	-5.25	-8.96	2.14	-2.68	-9.96	13.08	-5.39	-3.83	13.60	0.44	-6.09
31	1.65	2.64	-5.93	-8.73	2.88	-3.25	-9.92	13.80	-5.59	-3.37	14.07	0.33	-5.89
32	1.67	3.36	-6.61	-8.32	3.51	-3.82	-9.78	14.23	-5.79	-2.91	14.61	0.00	-5.88
33	1.68	4.07	-7.16	-7.75	4.14	-4.50	-9.46	14.67	-5.77	-2.45	15.25	-0.22	-5.68
34	1.69	4.59	-7.72	-7.45	4.58	-5.30	-9.22	15.31	-5.98	-2.00	15.62	-0.33	-5.58
35	1.70	5.11	-8.27	-7.06	5.19	-6.08	-8.90	15.95	-5.95	-1.54	16.03	-0.87	-5.65

TABLE D-4 (continued).

36	1.72	5.81	-8.81	-6.41	5.72	-6.53	-8.41	16.56	-6.15	-1.18	16.47	-1.19	-5.55
37	1.73	6.31	-9.47	-5.93	6.31	-7.53	-7.99	17.02	-6.13	-0.82	17.10	-1.40	-5.54
38	1.75	7.01	-9.89	-5.38	6.92	-7.96	-7.52	17.57	-6.11	-0.45	17.52	-1.82	-5.24
39	1.76	7.69	-10.31	-4.66	7.60	-8.73	-7.21	18.11	-6.20	0.00	17.96	-2.14	-5.13
40	1.77	8.36	-10.95	-4.12	8.19	-9.38	-6.73	18.85	-6.07	0.73	18.48	-2.45	-4.94
41	1.78	9.03	-11.47	-3.58	8.77	-10.02	-6.34	19.29	-6.16	0.82	18.97	-2.98	-4.92
42	1.80	9.69	-12.10	-2.78	9.50	-10.99	-5.42	19.75	-6.14	1.27	19.49	-3.29	-4.72
43	1.81	10.27	-12.51	-1.90	10.34	-11.61	-4.70	20.22	-6.02	1.63	20.15	-3.91	-4.51
44	1.83	10.93	-13.02	-1.03	11.06	-12.46	-4.06	20.77	-6.00	2.09	20.66	-4.22	-4.32
45	1.84	11.60	-13.31	-0.26	11.54	-12.98	-3.10	21.23	-5.99	2.54	21.29	-4.93	-4.02
46	1.85	12.26	-13.59	0.94	12.29	-13.26	-2.32	21.69	-5.97	3.08	21.77	-5.44	-3.55
47	1.87	12.83	-13.99	1.54	12.65	-14.11	-1.54	21.87	-5.96	3.45	22.33	-5.95	-2.72
48	1.88	13.15	-14.29	1.96	13.45	-14.71	-1.10	22.04	-6.06	3.81	22.80	-6.45	-2.53

TABLE D-5. Tractor-Body Reference-Point Coordinates and Times for Overturn Test 2, Run 2.

	TIME		XLRI			XRRI			XLFI			XRFI	
1	1.25	-14.11	-1.27	-10.07	-14.09	1.65	-10.07	-2.88	-3.11	-5.57	-2.62	3.35	-5.43
2	1.27	-13.45	-1.26	-10.07	-13.42	1.64	-10.07	-1.95	-3.10	-5.67	-1.84	3.33	-5.43
3	1.28	-12.79	-1.26	-10.07	-12.85	1.64	-10.07	-1.58	-3.09	-5.57	-1.26	3.32	-5.43
4	1.29	-12.23	-1.25	-10.07	-12.27	1.63	-10.07	-0.93	-2.96	-5.58	-0.68	3.31	-5.33
5	1.31	-11.57	-1.25	-10.07	-11.60	1.63	-10.07	-0.28	-3.07	-5.67	0.00	3.30	-5.43
6	1.32	-11.01	-1.25	-10.07	-10.93	1.62	-10.07	0.19	-2.95	-5.58	0.58	3.53	-5.34
7	1.33	-10.25	-1.37	-10.06	-10.26	1.61	-10.07	0.74	-3.17	-5.57	1.16	3.40	-5.34
8	1.35	-9.88	-1.24	-10.07	-9.78	1.61	-10.07	1.49	-3.04	-5.57	1.84	3.51	-5.44
9	1.36	-9.31	-1.36	-9.96	-9.20	1.61	-10.07	2.04	-3.15	-5.66	2.42	3.38	-5.63
10	1.37	-8.74	-1.36	-9.96	-8.53	1.60	-9.97	2.60	-3.26	-5.75	3.00	3.25	-5.72
11	1.39	-8.19	-1.23	-9.97	-8.05	1.60	-9.97	3.06	-3.48	-5.92	3.78	3.12	-5.72
12	1.41	-7.61	-1.35	-9.96	-7.38	1.59	-9.87	3.61	-3.59	-6.01	4.26	3.11	-5.81
13	1.42	-7.24	-1.35	-9.87	-7.00	1.59	-9.87	3.98	-3.70	-6.19	4.84	2.99	-6.10
14	1.44	-6.87	-1.22	-9.78	-6.52	1.59	-9.87	4.63	-3.68	-6.47	5.21	2.75	-6.09
15	1.45	-6.39	-1.34	-9.78	-6.04	1.58	-9.78	5.18	-3.79	-6.56	5.71	2.98	-6.49
16	1.46	-5.92	-1.46	-9.77	-5.56	1.58	-9.68	5.55	-3.78	-6.74	6.46	2.62	-6.67
17	1.47	-5.45	-1.46	-9.67	-5.08	1.57	-9.68	6.20	-3.77	-6.74	6.86	2.84	-6.68
18	1.49	-4.80	-1.33	-9.68	-4.60	1.57	-9.68	6.66	-3.87	-6.74	7.43	2.61	-6.67
19	1.51	-4.32	-1.57	-9.67	-4.12	1.45	-9.77	7.12	-3.86	-6.74	7.91	2.60	-6.67
20	1.52	-3.66	-1.56	-9.67	-3.54	1.32	-9.76	7.66	-4.08	-6.45	8.58	2.48	-6.47
21	1.53	-3.10	-1.56	-9.76	-2.97	1.32	-9.76	8.21	-4.18	-6.44	8.97	2.59	-6.76
22	1.55	-2.62	-2.03	-9.63	-2.39	1.19	-9.75	8.86	-4.17	-6.44	9.61	2.02	-6.54
23	1.57	-2.06	-2.15	-9.63	-1.72	0.83	-9.83	9.30	-4.38	-6.25	10.10	2.12	-6.55
24	1.58	-1.49	-2.62	-9.59	-1.24	0.36	-9.98	9.49	-4.38	-5.97	10.48	2.01	-6.35
25	1.59	-0.84	-2.96	-9.66	-0.66	0.00	-10.15	10.38	-4.80	-5.68	11.14	1.89	-6.54
26	1.61	-0.28	-3.43	-9.45	-0.19	-0.47	-10.12	11.02	-4.78	-5.40	11.59	1.44	-6.52
27	1.62	0.28	-3.89	-9.32	0.38	-1.18	-10.07	11.65	-4.99	-4.85	12.06	1.44	-6.52
28	1.63	0.92	-4.58	-9.09	1.03	-1.88	-10.02	12.18	-5.20	-4.47	12.51	0.99	-6.40
29	1.65	1.56	-5.15	-8.96	1.59	-2.34	-9.98	12.62	-5.40	-4.01	13.06	0.77	-6.10
30	1.66	2.10	-5.83	-8.65	2.33	-2.91	-9.94	13.34	-5.60	-3.55	13.59	0.33	-5.99
31	1.67	2.81	-6.51	-8.42	2.96	-3.72	-9.88	13.79	-5.70	-2.82	14.13	0.00	-5.79
32	1.69	3.44	-7.07	-8.03	3.59	-4.52	-9.46	14.32	-5.79	-2.45	14.59	-0.22	-5.68
33	1.70	4.23	-7.73	-7.45	4.21	-5.42	-9.31	14.85	-5.99	-2.00	15.12	-0.54	-5.67
34	1.72	4.67	-8.17	-7.07	4.56	-5.76	-9.01	15.40	-5.97	-1.63	15.56	-0.87	-5.65
35	1.73	5.18	-8.84	-6.50	5.17	-6.66	-8.41	15.93	-6.17	-1.18	16.00	-1.19	-5.64

36	1.74	5.87	-9.49	-6.02	5.87	-7.32	-8.18	16.46	-6.26	-0.82	16.62	-1.51	-5.44
37	1.76	6.38	-10.04	-5.56	6.37	-8.21	-7.77	17.01	-6.24	-0.36	17.04	-1.94	-5.33
38	1.77	7.15	-10.45	-4.92	7.06	-8.75	-7.21	17.47	-6.22	0.00	17.57	-2.25	-4.94
39	1.78	7.83	-11.09	-4.29	7.73	-9.63	-6.80	18.01	-6.21	0.63	18.09	-2.57	-4.93
40	1.80	8.59	-11.50	-3.58	8.50	-10.15	-6.16	18.56	-6.19	1.09	18.60	-2.99	-4.64
41	1.81	9.01	-11.81	-2.87	9.16	-10.90	-5.51	19.20	-6.16	1.63	19.18	-3.51	-4.53
42	1.83	9.67	-12.44	-1.99	9.74	-11.43	-4.79	19.65	-6.25	1.90	19.68	-3.92	-4.33
43	1.84	10.17	-12.74	-1.38	10.20	-12.29	-4.07	19.90	-6.35	2.44	20.24	-4.54	-3.94
44	1.86	10.67	-13.04	-0.34	10.70	-12.59	-3.20	20.53	-6.43	2.98	20.77	-5.37	-3.55
45	1.87	11.15	-13.45	0.69	11.25	-13.33	-2.41	20.79	-6.53	3.34	21.32	-5.98	-3.17
46	1.88	11.47	-13.76	1.54	11.81	-13.85	-1.63	21.15	-6.52	3.89	21.88	-6.49	-2.62

TABLE D-6: Tractor-Body Reference-Point Coordinates and Times for Overturn Test 3, Run 1.

	TIME		XLRI			XRRI			XLFI			XRFI	
1	2.23	-15.05	-1.27	-10.07	-15.05	1.65	-9.87	-3.90	-3.25	-5.57	-3.58	3.24	-5.43
2	2.27	-14.12	-1.14	-10.07	-14.00	1.64	-9.97	-2.97	-3.11	-5.57	-2.52	3.35	-5.43
3	2.31	-13.09	-1.13	-10.07	-13.13	1.64	-9.97	-2.04	-3.22	-5.57	-1.55	3.33	-5.43
4	2.35	-12.22	-1.38	-10.06	-12.18	1.63	-9.97	-1.11	-3.20	-5.57	-0.68	3.31	-5.43
5	2.39	-11.38	-1.25	-9.97	-11.22	1.62	-9.87	-0.19	-2.95	-5.58	0.19	3.30	-5.43
6	2.44	-10.53	-1.37	-9.96	-10.26	1.61	-9.97	0.37	-3.18	-5.57	1.16	3.28	-5.33
7	2.48	-9.69	-1.24	-10.07	-9.49	1.61	-9.97	1.58	-3.16	-5.57	1.65	3.16	-5.43
8	2.53	-8.94	-1.23	-9.97	-8.82	1.60	-9.97	2.13	-3.27	-5.84	2.71	3.14	-5.62
9	2.57	-8.18	-1.35	-9.87	-7.96	1.60	-9.87	2.96	-3.60	-5.83	3.58	3.13	-5.72
10	2.61	-7.71	-1.35	-9.87	-7.38	1.59	-9.87	3.42	-3.82	-5.82	4.06	2.89	-5.80
11	2.65	-7.23	-1.47	-9.86	-7.00	1.59	-9.87	4.07	-3.81	-6.19	4.73	2.65	-6.09
12	2.69	-6.76	-1.46	-9.67	-6.52	1.59	-9.78	4.53	-3.80	-6.46	5.31	2.64	-6.28
13	2.73	-6.39	-1.46	-9.67	-6.13	1.58	-9.78	4.99	-3.79	-6.56	5.69	2.63	-6.47
14	2.77	-6.11	-1.46	-9.67	-5.94	1.58	-9.87	5.36	-3.90	-6.55	6.08	2.63	-6.47
15	2.82	-5.64	-1.46	-9.67	-5.46	1.46	-9.77	5.73	-4.01	-6.64	6.46	2.62	-6.57
16	2.87	-5.35	-1.58	-9.67	-5.08	1.45	-9.77	6.00	-4.00	-6.64	6.74	2.39	-6.56
17	2.91	-4.98	-1.45	-9.67	-4.69	1.45	-9.77	6.28	-4.11	-6.63	7.12	2.27	-6.55
18	2.95	-4.60	-1.57	-9.67	-4.50	1.33	-9.76	6.74	-4.10	-6.63	7.42	2.50	-6.47
19	2.98	-4.41	-1.57	-9.67	-4.12	1.45	-9.77	7.11	-4.09	-6.54	7.80	2.38	-6.46
20	3.03	-4.04	-1.57	-9.67	-3.83	1.44	-9.77	7.38	-4.20	-6.53	8.00	2.37	-6.56
21	3.07	-3.76	-1.56	-9.67	-3.54	1.44	-9.77	7.56	-4.19	-6.63	8.39	2.48	-6.56
22	3.11	-3.47	-1.92	-9.64	-3.25	1.20	-9.75	7.84	-4.19	-6.53	8.57	2.25	-6.46
23	3.15	-3.09	-1.92	-9.64	-2.96	1.08	-9.75	8.21	-4.18	-6.44	8.86	2.25	-6.55
24	3.20	-2.90	-2.04	-9.63	-2.67	0.96	-9.74	8.49	-4.17	-6.44	9.24	2.25	-6.55
25	3.24	-2.53	-2.03	-9.63	-2.38	0.84	-9.83	8.76	-4.17	-6.26	9.61	2.02	-6.64
26	3.33	-1.86	-2.74	-9.59	-1.62	0.24	-9.98	9.48	-4.49	-5.97	10.18	1.90	-6.54
27	3.37	-1.58	-2.85	-9.49	-1.23	0.00	-10.05	9.93	-4.70	-5.78	10.56	1.90	-6.54
28	3.41	-1.02	-3.44	-9.35	-0.85	-0.59	-9.92	10.29	-4.80	-5.50	10.72	1.45	-6.42
29	3.45	-0.65	-4.02	-9.32	-0.47	-1.06	-9.98	10.82	-5.01	-5.12	11.20	1.44	-6.42
30	3.49	-0.09	-4.48	-9.10	0.09	-1.65	-9.94	11.27	-5.22	-4.75	11.66	1.11	-6.31
31	3.53	0.64	-5.06	-8.79	0.75	-2.35	-9.89	11.97	-5.53	-4.19	12.19	0.66	-6.19
32	3.58	1.37	-5.86	-8.46	1.49	-3.16	-9.93	12.50	-5.74	-3.55	12.74	0.33	-5.99
33	3.62	2.27	-6.76	-8.23	2.30	-4.31	-9.75	12.31	-5.85	-2.82	13.47	0.00	-5.88
34	3.66	3.06	-7.78	-7.63	3.11	-5.46	-9.40	13.95	-5.91	-1.91	14.17	-0.66	-5.76
35	3.70	4.02	-8.89	-6.76	3.99	-6.70	-8.95	14.59	-5.89	-1.36	14.83	-0.65	-5.76
36	3.74	5.05	-10.00	-5.91	5.03	-7.93	-8.24	15.33	-5.76	-0.64	15.31	-1.52	-5.63
37	3.78	5.98	-10.97	-4.64	6.05	-9.37	-7.35	16.16	-5.73	0.00	16.08	-2.16	-5.60
38	3.83	6.83	-11.61	-3.66	6.79	-10.59	-6.32	16.86	-5.92	0.73	16.83	-3.02	-5.29
39	3.87	7.38	-12.82	-1.99	7.62	-11.67	-4.96	17.45	-6.33	1.63	17.66	-4.61	-4.58
40	3.92	8.05	-13.34	0.17	8.31	-13.21	-2.76	17.86	-6.75	2.89	18.64	-6.29	-3.53
41	3.95	8.27	-13.89	1.98	8.76	-14.42	-1.11	18.31	-6.73	3.88	19.11	-7.55	-2.60

TABLE D-7. Tractor-Body Reference-Point Coordinates and Times for Overturn Test 3, Run 2.

	TIME		XLRI			XRRI			XLFI			XRFI	
1	2.33	-14.70	-1.02	-9.99	-14.59	1.78	-9.88	-2.97	-3.23	-5.57	-3.02	3.95	-5.35
2	2.38	-13.84	-1.14	-9.98	-13.63	1.77	-9.88	-2.23	-2.86	-5.58	-2.04	3.70	-5.44
3	2.42	-12.80	-1.13	-9.98	-12.76	1.76	-9.98	-1.49	-2.85	-5.58	-1.26	3.68	-5.35
4	2.46	-11.96	-1.13	-9.98	-11.80	1.75	-9.98	-0.56	-2.84	-5.58	-0.29	3.66	-5.44
5	2.50	-11.11	-1.12	-9.98	-10.84	1.74	-9.88	0.09	-2.95	-5.58	0.49	3.65	-5.44
6	2.54	-10.17	-1.12	-9.98	-10.17	1.74	-9.98	1.02	-3.05	-5.57	1.26	3.28	-5.33
7	2.58	-9.60	-1.11	-9.98	-9.40	1.73	-9.98	1.67	-3.16	-5.66	2.13	3.38	-5.53
8	2.63	-8.95	-0.99	-9.99	-8.63	1.73	-9.98	2.41	-3.26	-5.84	3.00	3.25	-5.62
9	2.68	-8.19	-1.11	-9.98	-7.97	1.84	-9.89	3.06	-3.25	-5.84	3.68	3.12	-5.72
10	2.72	-7.63	-1.10	-9.98	-7.39	1.84	-9.89	3.70	-3.59	-6.01	4.26	3.11	-5.91
11	2.75	-7.24	-1.22	-9.88	-7.00	1.71	-9.88	4.07	-3.70	-6.19	4.93	2.87	-6.10
12	2.79	-6.86	-1.34	-9.87	-6.52	1.71	-9.88	4.63	-3.68	-6.19	5.42	3.10	-6.30
13	2.84	-6.40	-1.22	-9.78	-6.14	1.70	-9.79	5.00	-3.68	-6.56	5.70	2.86	-6.48
14	2.88	-6.21	-1.22	-9.88	-5.95	1.70	-9.79	5.27	-3.79	-6.65	6.08	2.63	-6.57
15	2.92	-5.83	-1.34	-9.78	-5.46	1.58	-9.78	5.55	-3.78	-6.65	6.47	2.85	-6.48
16	2.97	-5.45	-1.46	-9.77	-5.08	1.57	-9.78	5.83	-3.78	-6.65	6.86	2.73	-6.48
17	3.01	-5.17	-1.45	-9.77	-4.79	1.57	-9.78	6.29	-3.77	-6.56	7.04	2.61	-6.47
18	3.05	-4.70	-1.45	-9.77	-4.60	1.57	-9.78	6.66	-3.76	-6.65	7.43	2.61	-6.57
19	3.09	-4.51	-1.45	-9.77	-4.41	1.57	-9.78	6.66	-3.76	-6.56	7.62	2.61	-6.57
20	3.13	-4.32	-1.45	-9.77	-4.02	1.57	-9.87	7.12	-3.75	-6.56	7.91	2.60	-6.57
21	3.18	-4.04	-1.45	-9.77	-3.74	1.56	-9.78	7.30	-3.86	-6.55	8.10	2.60	-6.57
22	3.22	-3.76	-1.56	-9.76	-3.55	1.56	-9.78	7.68	-3.74	-6.56	8.40	2.71	-6.57
23	3.27	-3.57	-1.56	-9.76	-3.45	1.56	-9.78	7.67	-3.85	-6.55	8.59	2.59	-6.57
24	3.31	-3.47	-1.56	-9.76	-3.16	1.56	-9.78	8.04	-3.84	-6.55	8.78	2.59	-6.57
25	3.36	-3.10	-1.56	-9.67	-2.97	1.44	-9.77	8.40	-4.06	-6.54	8.96	2.36	-6.56
26	3.40	-2.91	-1.56	-9.67	-2.68	1.32	-9.86	8.59	-3.95	-6.45	9.26	2.58	-6.57
27	3.44	-2.72	-1.67	-9.75	-2.58	1.31	-9.86	8.87	-3.94	-6.55	9.55	2.58	-6.57
28	3.48	-2.53	-1.91	-9.74	-2.29	0.95	-9.83	8.76	-4.17	-6.44	9.64	2.47	-6.56
29	3.53	-2.34	-2.03	-9.73	-2.20	0.95	-9.83	8.96	-4.05	-6.26	9.82	2.24	-6.55
30	3.57	-2.15	-2.27	-9.62	-1.91	0.71	-9.82	9.41	-4.15	-6.26	9.82	2.35	-6.56
31	3.61	-1.87	-2.50	-9.70	-1.71	0.48	-9.99	9.67	-4.37	-6.16	10.20	2.23	-6.55
32	3.64	-1.68	-2.62	-9.59	-1.43	0.36	-10.08	9.86	-4.37	-6.06	10.38	2.01	-6.54
33	3.68	-1.49	-2.73	-9.59	-1.23	0.24	-10.07	9.67	-4.37	-5.97	10.38	2.01	-6.45
34	3.74	-1.02	-2.73	-9.59	-0.85	0.00	-10.05	10.39	-4.69	-5.59	10.84	1.78	-6.44
35	3.78	-0.74	-3.32	-9.55	-0.57	-0.35	-10.03	10.67	-5.80	-5.36	11.12	1.67	-6.43

TABLE D-7 (continued).

36	3.83	-0.46	-3.78	-9.42	-0.28	-0.83	-10.09	11.03	-5.90	-5.18	11.49	1.44	-6.42
37	3.87	0.09	-4.24	-9.30	0.19	-1.41	-10.05	11.47	-6.10	-4.81	11.78	1.44	-6.42
38	3.91	0.64	-4.59	-9.00	0.75	-2.00	-9.91	11.82	-5.21	-4.57	12.34	1.33	-6.42
39	3.95	1.19	-5.28	-8.77	1.31	-2.46	-9.88	12.54	-5.30	-4.01	12.68	0.77	-6.30
40	3.99	1.91	-5.96	-8.55	2.04	-3.38	-9.91	13.05	-5.72	-3.46	13.31	0.33	-6.09
41	4.04	2.72	-6.86	-8.31	2.95	-4.30	-9.84	13.60	-5.70	-2.64	13.95	0.11	-5.79
42	4.07	3.51	-7.76	-7.63	3.65	-5.67	-9.38	14.32	-5.79	-1.91	14.47	-0.44	-5.77
43	4.12	4.38	-8.88	-6.85	4.53	-6.68	-8.95	14.97	-5.77	-1.36	15.00	-0.87	-5.84
44	4.17	5.33	-9.64	-6.02	5.39	-8.14	-8.23	15.71	-5.64	-0.64	15.69	-1.41	-5.73
45	4.22	6.35	-10.61	-5.01	6.24	-9.25	-7.36	16.45	-5.51	-0.18	16.20	-1.95	-5.70
46	4.26	7.18	-11.59	-3.75	7.07	-10.34	-6.33	17.06	-5.81	0.55	16.93	-2.91	-5.48
47	4.30	7.92	-12.56	-1.99	7.87	-11.88	-4.87	17.77	-6.00	1.54	17.79	-4.29	-4.87
48	4.33	8.24	-12.99	-0.60	8.43	-12.75	-3.63	18.20	-6.20	2.08	18.32	-5.23	-4.38
49	4.36	8.89	-13.73	1.12	9.05	-13.83	-1.80	18.38	-6.19	2.99	18.90	-6.39	-3.52
50	4.38	9.06	-13.72	3.01	9.35	-14.48	0.00	18.47	-6.19	3.90	19.47	-7.53	-2.42

TABLE D-8. Tractor-Body Reference-Point Coordinates and Times for Overturn Test 4, Run 1.

	TIME		XLRI			XRRI			XLFI			XRFI	
1	1.61	-15.33	-1.27	-9.97	-15.15	1.65	-9.87	-4.00	-3.01	-5.58	-3.69	3.49	-5.43
2	1.64	-14.39	-1.27	-10.07	-14.20	1.77	-9.88	-2.97	-3.23	-5.57	-2.72	3.71	-5.35
3	1.67	-13.45	-1.26	-10.07	-13.24	1.76	-9.98	-2.14	-3.22	-5.57	-1.74	3.33	-5.33
4	1.69	-12.42	-1.26	-10.07	-12.37	1.63	-9.97	-1.21	-3.32	-5.56	-0.78	3.32	-5.43
5	1.72	-11.57	-1.25	-9.97	-11.50	1.62	-9.97	-0.28	-3.19	-5.57	0.10	3.30	-5.43
6	1.75	-10.63	-1.24	-10.07	-10.45	1.62	-9.97	0.65	-3.29	-5.56	1.07	3.28	-5.43
7	1.77	-9.68	-1.36	-9.96	-9.68	1.61	-9.97	1.58	-3.39	-5.56	1.84	3.27	-5.43
8	1.80	-9.12	-1.36	-9.96	-8.91	1.60	-9.97	2.23	-3.26	-5.93	2.71	3.26	-5.82
9	1.83	-8.47	-1.23	-9.97	-8.44	1.72	-9.88	2.88	-3.25	-6.21	3.48	3.13	-6.10
10	1.86	-7.81	-1.23	-9.78	-7.86	1.60	-9.87	3.53	-3.24	-6.49	4.16	3.12	-6.40
11	1.89	-7.34	-1.22	-9.78	-7.19	1.59	-9.78	4.36	-3.23	-6.77	4.84	3.11	-6.59
12	1.92	-6.77	-1.34	-9.68	-6.52	1.59	-9.78	4.92	-3.33	-7.04	5.52	3.09	-6.88
13	1.95	-6.11	-1.34	-9.68	-5.94	1.58	-9.59	5.47	-3.44	-7.13	6.10	3.20	-6.98
14	1.97	-5.35	-1.45	-9.67	-5.18	1.57	-9.68	6.39	-3.54	-7.12	6.87	3.07	-6.98
15	2.00	-4.70	-1.45	-9.67	-4.60	1.57	-9.59	6.95	-3.41	-7.13	7.45	3.06	-6.98
16	2.03	-4.04	-1.45	-9.67	-3.93	1.56	-9.59	7.69	-3.51	-7.12	8.13	3.16	-6.98
17	2.06	-3.48	-1.44	-9.67	-3.35	1.56	-9.68	8.25	-3.50	-7.03	8.81	3.15	-6.98
18	2.08	-2.63	-1.67	-9.66	-2.58	1.31	-9.76	9.07	-3.71	-6.83	9.67	3.03	-6.98
19	2.11	-1.87	-2.26	-9.62	-1.81	0.71	-9.82	9.44	-3.70	-6.46	10.14	2.68	-6.86
20	2.14	-1.21	-2.73	-9.68	-1.14	0.12	-9.97	10.43	-4.02	-6.17	10.79	2.45	-6.85
21	2.17	-0.46	-3.31	-9.55	-0.28	-0.35	-10.12	11.04	-4.56	-5.78	11.35	2.11	-6.84
22	2.20	0.28	-3.89	-9.23	0.28	-0.94	-9.99	11.78	-4.54	-5.50	12.00	1.88	-6.83
23	2.23	1.11	-4.34	-9.02	1.03	-1.53	-10.04	12.50	-4.75	-5.04	12.64	1.43	-6.80
24	2.26	1.74	-5.03	-8.88	1.77	-2.45	-9.88	13.13	-4.84	-4.49	13.20	1.32	-6.80
25	2.29	2.56	-5.70	-8.47	2.51	-3.26	-9.82	13.84	-5.15	-3.93	13.93	0.88	-6.59
26	2.32	3.54	-6.60	-8.14	3.42	-3.94	-9.78	15.47	-5.32	-3.28	14.54	0.33	-6.37
27	2.35	4.42	-7.38	-7.56	4.40	-4.96	-9.43	15.39	-5.21	-2.28	15.38	0.11	-6.17
28	2.38	5.47	-8.37	-7.05	5.46	-6.19	-9.16	16.02	-5.30	-1.64	16.10	-0.22	-5.87
29	2.41	6.24	-9.25	-6.30	6.24	-7.08	-8.47	16.73	-5.50	-1.09	16.68	-0.97	-5.84
30	2.43	6.82	-10.01	-5.38	6.81	-8.42	-7.67	17.44	-5.69	-0.64	17.26	-1.72	-5.62
31	2.47	7.77	-10.53	-4.48	7.59	-8.84	-7.02	18.03	-6.10	0.00	18.01	-2.46	-5.49
32	2.49	8.50	-11.62	-3.31	8.57	-10.49	-6.15	18.67	-6.08	0.73	18.73	-3.41	-5.27
33	2.52	9.25	-12.13	-2.34	9.30	-11.45	-4.97	19.36	-6.37	1.54	19.61	-4.45	-4.77
34	2.54	9.72	-13.00	-0.60	10.09	-12.64	-3.46	19.97	-6.56	2.53	20.37	-5.59	-3.82
35	2.57	10.38	-13.40	1.12	10.79	-13.70	-1.80	20.41	-6.65	3.79	21.14	-6.62	-2.79

TABLE D-9. Tractor-Body Reference-Point Coordinates and Times for Overturn Test 4, Run 2.

	TIME		XLRI			XRRI			XLFI			XRFI	
1	1.73	-12.87	-1.51	-10.05	-12.75	1.63	-10.07	-1.58	-3.21	-5.66	-1.26	3.21	-5.43
2	1.75	-11.93	-1.50	-10.05	-11.78	1.50	-10.06	-0.74	-3.32	-5.56	-0.39	3.07	-5.42
3	1.78	-10.99	-1.50	-9.96	-11.02	1.50	-10.06	0.09	-3.30	-5.56	0.58	3.29	-5.33
4	1.81	-10.15	-1.37	-10.06	-10.06	1.49	-10.06	1.02	-3.29	-5.56	1.45	3.28	-5.43
5	1.84	-9.49	-1.48	-9.96	-9.30	1.61	-10.07	1.67	-3.63	-5.64	2.32	3.15	-5.62
6	1.86	-8.83	-1.48	-9.96	-8.81	1.48	-9.87	2.59	-3.49	-6.20	3.00	3.25	-5.92
7	1.88	-8.17	-1.48	-9.86	-8.04	1.47	-9.77	3.24	-3.48	-6.48	3.78	3.24	-6.11
8	1.92	-7.60	-1.59	-9.85	-7.47	1.47	-9.87	3.98	-3.58	-6.57	4.55	3.11	-6.49
9	1.95	-7.13	-1.59	-9.76	-7.09	1.47	-9.87	4.54	-3.69	-6.84	5.13	3.10	-6.69
10	1.97	-6.48	-1.58	-9.67	-6.22	1.46	-9.77	5.19	-3.56	-7.12	5.71	3.09	-6.88
11	2.01	-5.91	-1.58	-9.67	-5.65	1.46	-9.67	5.83	-3.78	-7.11	6.39	3.08	-6.98
12	2.03	-5.26	-1.58	-9.67	-5.07	1.33	-9.67	6.48	-3.76	-7.11	7.06	2.96	-6.97
13	2.06	-4.51	-1.57	-9.67	-4.59	1.33	-9.67	7.22	-3.75	-7.11	7.73	2.83	-6.97
14	2.08	-3.75	-1.68	-9.66	-3.83	1.32	-9.67	7.86	-3.73	-7.02	8.40	2.71	-6.96
15	2.12	-3.28	-1.92	-9.55	-3.15	1.08	-9.75	8.05	-3.73	-6.93	8.89	2.93	-6.78
16	2.15	-2.52	-2.15	-9.53	-2.38	0.72	-9.72	9.07	-3.71	-6.74	9.47	2.92	-6.97
17	2.17	-1.77	-2.74	-9.49	-1.81	0.36	-9.89	9.78	-4.14	-6.44	10.60	2.45	-6.76
18	2.20	-1.11	-3.20	-9.55	-1.04	-0.36	-9.94	10.59	-4.46	-5.97	10.85	1.89	-6.83
19	2.24	-0.37	-3.90	-9.23	-0.28	-1.18	-9.97	11.12	-4.67	-5.59	11.52	1.89	-6.83
20	2.27	0.37	-4.59	-8.91	0.28	-1.53	-9.85	11.84	-4.87	-5.13	11.96	1.33	-6.90
21	2.29	1.19	-5.28	-8.68	1.21	-2.58	-9.69	12.66	-4.96	-4.57	12.61	1.10	-6.69
22	2.32	2.10	-5.83	-8.37	2.04	-3.27	-9.64	13.38	-5.16	-3.93	13.25	0.77	-6.68
23	2.34	2.99	-6.85	-7.95	2.95	-4.30	-9.57	14.10	-5.25	-3.19	14.07	0.33	-6.47
24	2.37	4.05	-7.62	-7.54	3.94	-5.20	-9.41	14.90	-5.55	-2.19	14.78	-0.22	-5.97
25	2.40	5.10	-8.50	-6.87	4.90	-6.55	-8.96	15.55	-5.42	-1.55	15.41	-0.54	-5.95
26	2.43	5.60	-9.51	-6.11	5.59	-7.45	-8.27	16.26	-5.62	-1.09	16.08	-1.30	-5.92
27	2.46	6.62	-6.72	-5.33	6.43	-8.78	-7.65	16.88	-5.82	-0.55	16.86	-1.94	-5.70
28	2.49	7.21	-11.02	-4.38	7.12	-9.43	-7.08	17.48	-6.12	0.18	17.54	-2.47	-5.49
29	2.52	7.88	-11.66	-3.40	7.94	-10.63	-6.23	18.29	-6.20	0.82	18.25	-3.53	-5.26
30	2.54	8.53	-12.52	-2.16	8.67	-11.72	-4.96	18.81	-6.39	1.72	19.06	-4.47	-4.68
31	2.57	9.18	-13.15	-0.60	9.39	-12.68	-3.54	19.33	-6.58	2.71	19.81	-5.72	-3.90
32	2.60	9.94	-13.43	1.29	10.36	-13.62	-1.72	19.86	-6.67	3.70	20.56	-6.85	-2.70

TABLE D-10. Tractor-Body Reference-Point Coordinates and Times for Overturn Test 5.

	TIME		XLRI			XRRI			XLFI			XRFI	
1	1.64	-12.48	-1.63	-10.04	-11.73	0.88	-10.02	-2.00	-6.08	-5.37	-0.29	0.35	-5.32
2	1.67	-11.88	-2.13	-10.01	-11.16	0.87	-10.02	-1.28	-5.94	-5.46	0.28	0.24	-5.32
3	1.70	-11.22	-2.12	-10.01	-10.48	0.75	-10.01	-0.73	-6.28	-5.45	1.04	0.12	-5.32
4	1.72	-10.56	-2.24	-10.00	-9.81	0.62	-10.00	-0.18	-6.49	-5.44	1.61	-0.23	-5.30
5	1.75	-9.98	-2.48	-9.98	-9.13	0.37	-9.98	0.27	-6.71	-5.34	2.18	-0.35	-5.30
6	1.77	-9.23	-2.60	-9.98	-8.55	0.25	-9.98	1.09	-6.92	-5.33	2.93	-0.46	-5.29
7	1.80	-8.75	-2.84	-9.96	-7.87	0.00	-9.96	1.63	-6.90	-5.42	3.49	-0.81	-5.28
8	1.83	-8.26	-3.20	-9.93	-7.48	-0.25	-9.94	2.17	-7.23	-5.32	4.05	-0.92	-5.28
9	1.85	-7.70	-3.31	-9.93	-6.91	-0.37	-9.94	2.88	-7.55	-5.22	4.61	-1.27	-5.36
10	1.83	-7.11	-4.04	-9.60	-6.41	-0.97	-9.89	3.33	-7.88	-5.11	5.26	-1.49	-5.35
11	1.92	-6.71	-4.64	-9.28	-5.90	-1.82	-9.65	3.86	-8.32	-4.47	5.80	-2.06	-5.33
12	1.94	-6.22	-5.36	-8.96	-5.40	-2.67	-9.50	4.47	-8.64	-4.01	6.25	-2.63	-5.31
13	1.97	-5.45	-6.31	-8.54	-4.73	-3.50	-9.35	5.16	-9.30	-3.20	6.88	-3.07	-4.92
14	2.00	-4.61	-7.13	-8.13	-3.86	-4.57	-9.19	5.77	-9.84	-2.21	7.68	-3.74	-4.34
15	2.03	-3.59	-8.17	-7.53	-2.83	-5.63	-8.76	6.46	-10.15	-1.15	8.57	-4.40	-3.68
16	2.06	-2.94	-9.10	-6.86	-2.18	-6.68	-8.42	7.33	-10.56	-0.62	9.17	-5.06	-3.57
17	2.08	-2.57	-9.92	-6.02	-2.07	-7.63	-7.74	8.19	-10.96	-0.26	9.78	-5.60	-3.92
18	2.11	-2.02	-11.08	-5.27	-1.52	-8.56	-7.15	8.94	-11.48	-0.26	10.36	-6.36	-4.17
19	2.14	-1.32	-11.40	-5.26	-0.71	-9.23	-7.20	9.80	-11.76	0.09	11.22	-7.00	-4.15
20	2.17	-0.61	-11.95	-4.97	0.09	-9.79	-7.08	10.45	-12.39	0.17	11.98	-7.64	-4.21
21	2.20	0.17	-12.37	-4.87	0.71	-10.46	-7.13	11.32	-12.44	0.43	12.75	-8.15	-4.20
22	2.23	0.87	-12.92	-4.76	1.41	-10.89	-6.93	11.96	-13.06	0.43	13.52	-8.56	-4.27
23	2.26	1.47	-13.23	-4.66	2.19	-11.43	-6.90	12.72	-13.34	0.60	14.27	-9.07	-4.34
24	2.29	2.33	-13.64	-4.56	2.89	-11.85	-6.88	13.45	-13.83	0.60	15.02	-9.58	-4.32
25	2.32	3.01	-14.05	-4.54	3.58	-12.04	-6.78	14.21	-13.99	0.68	15.69	-9.97	-4.31
26	2.34	3.61	-14.35	-4.45	4.18	-12.58	-6.66	14.76	-14.49	0.68	16.34	-10.48	-4.29
27	2.37	4.20	-14.77	-4.43	4.94	-12.99	-6.64	15.49	-14.87	0.76	16.98	-10.98	-4.27
28	2.40	4.79	-15.07	-4.33	5.45	-13.41	-6.62	16.04	-15.26	0.85	17.64	-11.37	-4.26
29	2.43	5.37	-15.37	-4.24	6.04	-13.71	-6.51	16.61	-15.53	0.93	18.19	-11.86	-4.32
30	2.46	5.95	-15.78	-3.97	6.45	-14.25	-6.40	17.14	-16.02	1.09	18.75	-12.25	-4.31
31	2.48	6.36	-16.20	-3.79	7.02	-14.78	-6.20	17.61	-16.30	1.26	19.26	-12.96	-4.28
32	2.52	6.84	-16.73	-3.60	7.43	-15.09	-6.19	18.14	-16.79	1.25	19.71	-13.46	-4.26
33	2.54	7.27	-18.05	-3.48	7.99	-15.83	-5.98	18.66	-17.27	1.41	20.23	-14.05	-4.16
34	2.57	7.65	-18.81	-3.13	8.39	-16.14	-5.71	19.13	-17.54	1.82	20.74	-14.64	-4.05
35	2.59	8.03	-19.34	-2.71	8.66	-17.24	-5.33	19.55	-18.14	1.89	21.05	-15.46	-4.02
36	2.63	8.33	-19.87	-2.21	8.93	-18.23	-4.96	19.92	-18.41	2.22	21.43	-16.26	-3.83